Biological Role of Conceptus Derived Factors

During Early Pregnancy in Ruminants

A dissertation submitted in partial fulfillment of
the requirements for the degree of

DOCTOR OF PHILOSOPHY IN ANIMAL SCIENCES

UNIVERSITY OF MISSOURI- COLUMBIA
Division of Animal Science

By

KELSEY BROOKS

Dr. Thomas Spencer, Dissertation Supervisor

August 2016

The undersigned have examined the dissertation entitled,

BIOLOGICAL ROLE OF CONCEPTUS DERIVED FACTORS

DURING EARLY PREGNANCY IN RUMINANTS

presented by Kelsey Brooks,

a candidate for the degree of doctor of philosophy, and hereby certify that, in their opinion, it is worthy of acceptance.

_____

Chair, Dr. Thomas Spencer

_____

Dr. Rodney Geisert

_____

Dr. Randall Prather

_____

Dr. Laura Schulz

ACKNOWLEDGMENTS

I would like to acknowledge all the students, faculty and staff at Washington State University and the University of Missouri for their help and support throughout my doctoral program. I am grateful for the opportunity to work with Dr. Thomas Spencer, and thank him for his input and guidance not only in planning experiments and completing projects but for helping me turn my love of science into a career in research. I would also like to acknowledge the members of my graduate committee at Washington State University for their help and input during the first 3 years of my studies. A special thanks to Dr. Jim Pru and Cindy Pru for providing unlimited entertainment, and the occasional missing reagent. Thank you to my committee members at the University of Missouri for adopting me late in my program and helping shape my future as an independent scientist. Thanks are also extended to members of the Prather lab and Wells lab for letting me in on the secrets of success using the CRISPR/Cas9 system.

None of this work would have been possible without support from my fellow graduate students in the Spencer lab. In particular, I thank Greg Burns for his unwavering support throughout our time together as Team Uterus. A million thank yous to the current Spencer lab; Andrew Kelleher, Joao Moraes, Wang Peng, and Eleanore O'Neil. As well as past members; Carolyn Allen, Piotr Dorniak and Justyna Filant.

Finally, special thanks to my family and friends for understanding that in the fall, the sheep always come first.

TABLE OF CONTENTS

LIST OF FIGURES AND TABLES

SECTION I:

SECTION II:

SECTION III:

SECTION IV:

SECTION V:

SECTION VI:

ABSTRACT

In cycling domestic animals, pregnancy loss during early gestation is a major cause of infertility. The majority of pregnancy loss during this time is due to errors in mitotic division early in development, or occurs later in gestation and is characterized by endometrial dysfunction, or asynchrony between the conceptus (embryo and trophectoderm) and uterus. During early pregnancy in sheep, endometrial functions are primarily regulated by ovarian progesterone (P4) and interferon tau (IFNT) from the conceptus trophectoderm. In addition to IFNT, the conceptus as well as the endometrium synthesize prostaglandins (PGs) via prostaglandin synthase two (PTGS2) and cortisol via hydroxysteroid (11-beta) dehydrogenase 1 (HSD11B1). The central hypothesis is that factors from the ovary (progesterone), the conceptus (interferon tau, prostaglandins, and cortisol) and endometrium (prostaglandins and cortisol) regulate endometrial function and conceptus survival and development in ruminants. This work tested that hypothesis that conceptus derived factors regulate gene expression changes in the trophectoderm which are essential for trophectoderm development and conceptus elongation in sheep. The hypothesis was addressed by determining the physiological roles of: (1) IFNT and interferon receptors 1 and 2 (IFNAR1 and IFNAR2) in conceptus development; (2) PG signaling through peroxisome proliferator activator receptors delta (PPARD) and gamma (PPARG) in the elongating conceptus; (3) the cortisol converting enzymes HSD11B1 and HSD11B2 in conceptus development; (4) the role of the glucocorticoid receptor (GR) in cortisol signaling during conceptus elongation. Gene knockout studies

utilizing osmotic pumps to deliver morpholino antisense oligonucleotides, lentiviral transduction of shRNAs, and CRISPR/Cas9 based genome editing were used to target the conceptus during elongation. Results of the studies established that: (1) IFNT is not only the maternal recognition of pregnancy signal, but is also required for conceptus elongation; (2) the IFN receptors IFNAR1 and IFNAR2 are not important for autocrine based signaling to the conceptus trophectoderm during development; (3) PPARG, but not PPARD is essential for conceptus elongation; (4) PPARG regulated pathways are involved in lipid uptake and metabolism in the day 14 conceptus; (5) Regulation of intracellular cortisol levels by HSD11B1 is important for conceptus development; (6) inactivation of bioactive cortisol by the enzyme HSD11B2 is not essential for conceptus elongation, but is important for proper conceptus development; and (7) signaling through GR is not essential for conceptus development up to day 14 of pregnancy. Collectively, results of these studies support the idea that IFNT, PGs and cortisol are all important regulators of conceptus elongation during early pregnancy in ruminants. Knowledge gained from these studies provides new insight into the physiological pathways governing conceptus development and elongation. Information from these studies provides a foundation for future translational research that is necessary to increase fertility of domestic ruminants.

SECTION I:

LITERATURE REVIEW

Early Pregnancy

Uterine Histoarchitecture

The mature uterus is comprised of three histological layers; (1) the endometrium, (2) myometrium, consisting of both an inner circular layer and surrounding longitudinal layer of smooth muscle, and (3) perimetrium (Figure 1). The uterine lumen is lined by the endometrial epithelium and surrounded by the myometrium. In domestic animals the uterine mesenchyme is differentiated at birth, whereas in rodents, postnatal development of the uterus involves differentiation of the mesenchyme into endometrial stroma and myometrium. Morphological events common in postnatal uterine development across mammals include organization and stratification of endometrial stroma, differentiation and growth of the myometrium, and development of endometrial glands [1-3]. The endometrium of adult sheep and cattle consists of numerous caruncles, which are dense stromal protrusions covered by luminal epithelium (LE), and glandular intercaruncular areas [4, 5]. Cross sections of the sheep uterus reveal hundreds of glands in these regions. Endometrial glands develop from budding of the LE, followed by growth into the underlying endometrium and subsequent coiling and branching [3].

The caruncular areas are the sites of superficial implantation and placentation, while intercaruncular glandular areas synthesize, secrete or transport a variety of substances, collectively termed histotroph [6, 7]. Histotroph contains a variety of transport proteins, enzymes, adhesion molecules, cytokines, amino acids, lipids, ions, and growth factors [7-12]. Histotroph produced by the uterine epithelia is especially important for conceptus elongation and implantation.

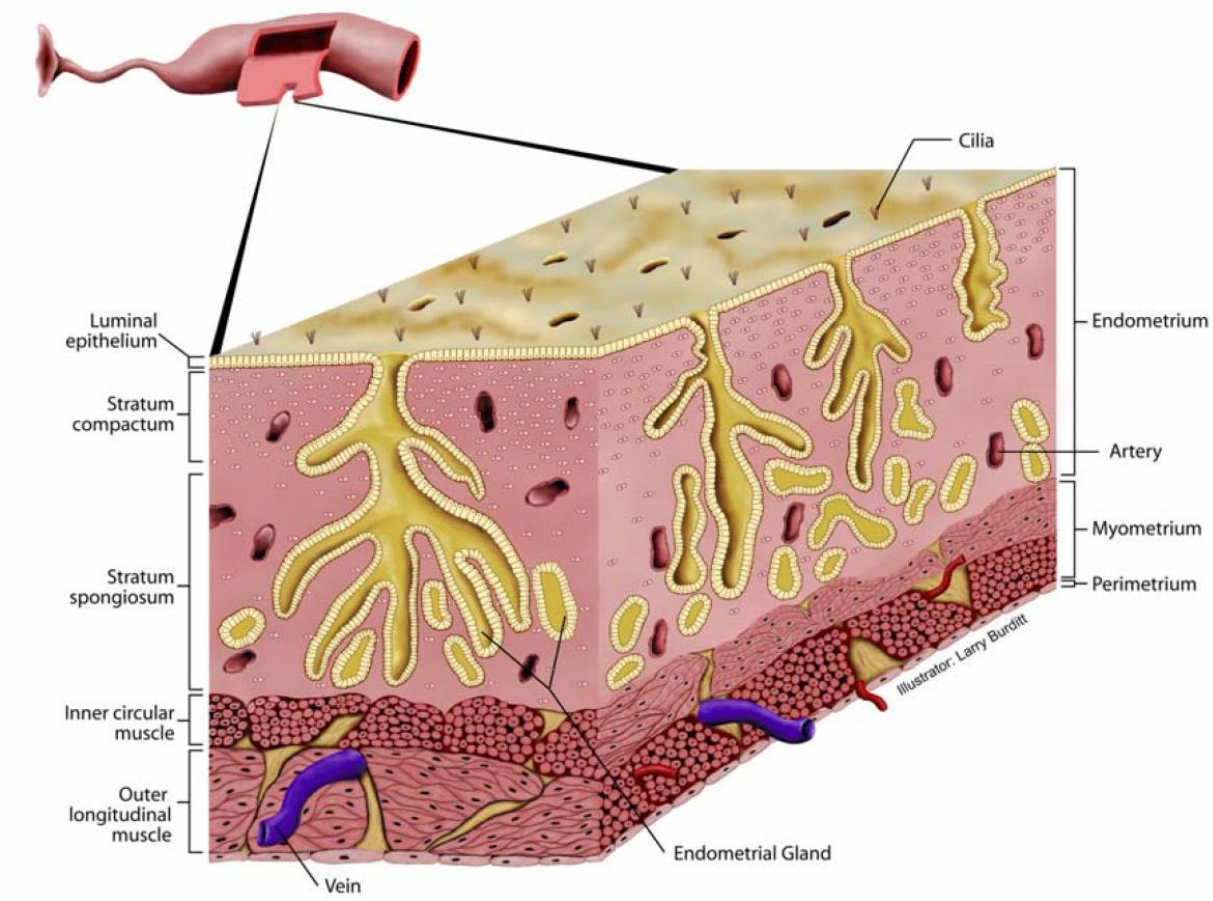

Figure 1. Illustration of uterine histoarchitecture. The uterus is composed of 3 distinct layers, the endometrium, myometrium and perimetrium. The endometrium contains both luminal and glandular epithelia, as well as underlying stromal cells. The myometrium consists of an inner circular and outer longitudinal smooth muscle layers. In ruminants, caruncles are readily visible in the non-pregnant uterus and are formed from thickenings in the uterine mucosa resulting from proliferation of subepithelial connective tissue. (Graphic courtesy of Rodney Geisert and Larry Burdett, Oklahoma State University, Stillwater, USA)

Conceptus Development

Formation of ICM and Trophoblast:

Following fertilization the zygote undergoes a series of mitotic divisions without changing size, resulting in an increase in number of progressively smaller cells. Mitosis continues until the embryo undergoes compaction to form a morula. Increased cell to cell contact within the morula allows for intracellular polarization to occur. Subsequent cell divisions after the morula stage are influenced by the orientation of the cleavage axis in relation to the polarity of the dividing cells. Symmetrical versus asymmetrical cleavage division result in the generation of two distinct cell populations; the cells on the inside becoming part of the inner cell mass (ICM) while the cells on the outside contribute to the trophectoderm [13, 14].

In sheep, the morula stage embryo enters the uterus between gestational days 4 and 5, and by day 6 has begun to form a blastocoel surrounded by a monolayer of trophectoderm cells [15]. The zona pellucida is shed between days 8 and 9. Before conceptus elongation is initiated, the extraembryonic endoderm originates from the ICM and migrates under the trophectoderm as the blastocoel expands. The mesoderm originates from the ICM and migrates between the endoderm and trophectoderm. Because the extraembryonic membranes form prior to implantation in ruminants, it is plausible that their development may assist in elongation of the surrounding trophectoderm.

Elongation of trophectoderm:

Conceptus elongation occurs in sheep, cattle, pigs and goats [16]. The elongation processes encompasses exponential lengthening and morphological transition of the extraembryonic tissues from a spherical to ovoid to tubular to filamentous form (Figure 2). In the ewe, the elongation process is initiated around day 12, and the transition from ovoid to filamentous form is complete by day 16. After transitioning from a tubular or ovoid form, the elongated embryo is then termed a conceptus (embryo and associated extraembryonic membranes). Coincident with elongation of the trophoblast is the growth and differentiation of the inner cell mass to an embryonic disc (i.e., onset of gastrulation). In the ovine ovoid conceptus, the mesoderm is already migrating extra-embryonically and by the filamentous stage the primitive streak is apparent in most embryonic discs of ungulates. Cellular proliferation, gastrulation and movement as well as redistribution of cells within the trophectoderm contributes to the increase in length of the developing conceptus [17]. Substantial increases in dry weight, glycogen content and DNA synthesis occur between days 13 to 19 [18]. Interestingly, ovine conceptus elongation is not dependent on the ICM, as terminal portions of the trophectoderm continue to elongate *in utero* when separated from the embryonic disk [19].

The cellular and molecular mechanism involved in conceptus elongation are not completely understood although it is accepted that conceptus elongation is dependent on the uterine environment, as fertilized embryos may be cultured to the blastocyst stage *in vitro* but must be transferred into the uterus to undergo

elongation [19-21]. It is hypothesized that conceptus elongation requires not only histotrophic nutrients provided by secretions from the luminal (LE) and glandular epithelium (GE), but also requires interaction between the trophectoderm and the LE of the uterus. Elongation is essential for production of the maternal recognition of pregnancy signal, interferon tau (IFNT), and for implantation. Based on studies by Guillomot and colleagues [15], the phases of implantation include: (1) shedding of the zona pellucida; (2) pre-contact with the LE and orientation of the blastocyst; (3) apposition between trophectoderm and LE and superficial GE (sGE); (4) adhesion of the trophectoderm to the LE/sGE; and (5) limited to extensive endometrial invasion depending on the species (Figure 3).

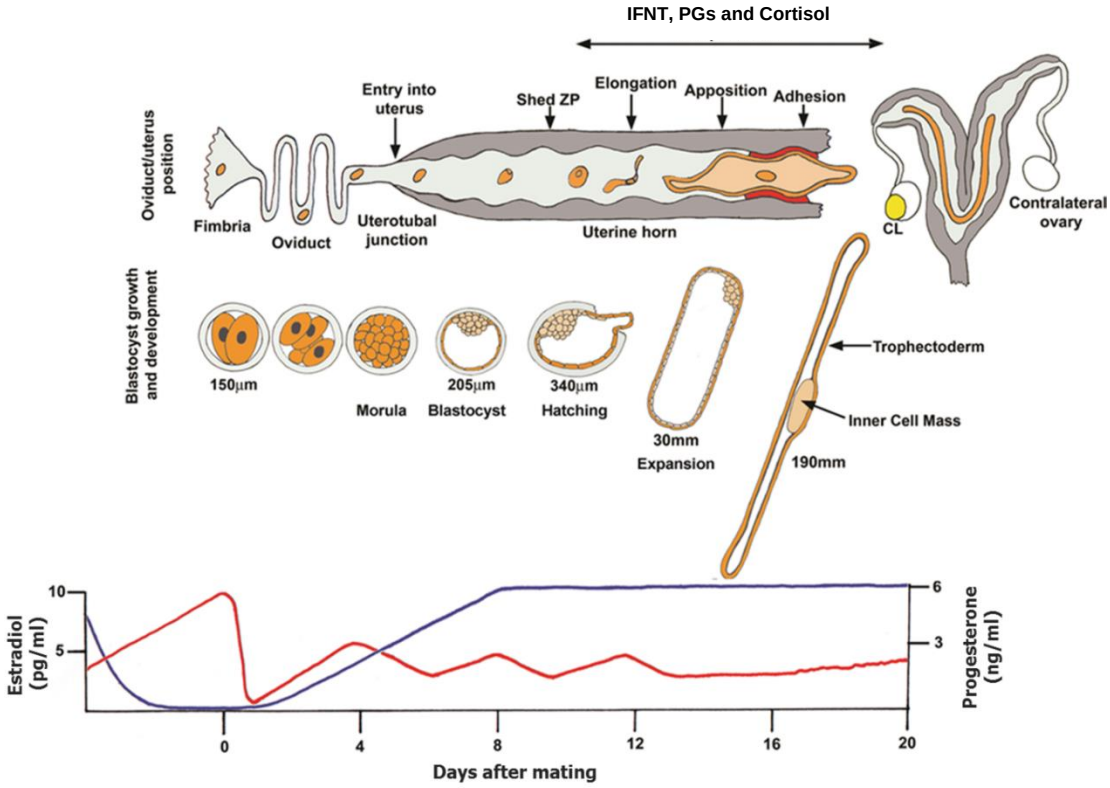

Figure 2. Early pregnancy events in ruminants. Prior to implantation in sheep, the developing embryo undergoes extensive remodeling to transition from a spherical to tubular to filamentous form. Fertilization occurs in the oviduct and a morula stage embryo enters the uterus on day 4, forms a blastocyst by day 6 and which then hatches from the zona pellucida by day 8. Between day 10 and 12 the embryo begins to transition from a spherical to tubular form, and continues to elongate to its filamentous form by day 14. By day 14 the embryo can reach up to 19 cm or more, and is now termed a conceptus to include both the ICM and surround extra-embryonic trophectoderm. Conceptus elongation marks the beginning of implantation, which involves apposition and transient attachment of the trophectoderm to the LE from days 12–15 followed by firm adhesion on day 16. The elongating conceptus synthesizes and secretes substances such as IFNT, PGs and cortisol which act on the P4 primed endometrium to regulate gene expression important for conceptus growth and development. Figure from [22].

Phases of implantation in sheep

(1) Shedding of the zona pellucida

Following formation of a blastocyst on day 6, the zona pellucida (ZP) is shed between days 8 and 9. The loss of the ZP is thought to be due to rupture by the expanding blastocyst, and by enzymatic lysis by uterine or embryonic proteases. *In vitro* produced and *in vivo* cultured embryos can be cultured to the blastocyst stage and hatch from the ZP *in vitro*. Traditionally, the ZP is thought to protect the developing embryo from attaching to the LE prior to implantation, as well as provide structural support during blastomere division prior to compaction. In the sheep, the blastocyst is spherical on day 8, contains approximately 300 cells and measures 200 μm in diameter. The blastocyst continues to proliferate, and by day 10 contains approximately 3000 cells and is 900 μm in diameter. Following day 10, elongation of the blastocyst begins, first by development into an ovoid, tubular and then filamentous form [23].

(2) Pre-contact and orientation

From days 9 to 14, the developing conceptus is not in immediate contact with the uterine epithelium, and can easily be recovered by flushing the uterine lumen without structure damage to the conceptus. Around day 11, the spherical conceptus begins to grow and by day 12 is 10-22 mm in length. Significant growth occurs following day 12, and the conceptus reaches 10 cm or more in length by day 14. By day 17, the conceptus is 25 cm or more in length and is composed mainly of trophectoderm, resembling a long thin filament or shoe string.

Down regulation of the progesterone receptor in the LE/sGE during following 8-10 days of progesterone exposure is associated with the loss of high molecular weight mucin O-linked glycoproteins such as mucin 1 which acts to prevent premature attachment of the trophectoderm to the uterine lumen in multiple species [24, 25]. As conceptus development continues, the spatial and temporal actions of P4 on the LE/sGE allow for synchronized alterations in the LE extracellular matrix exposing attachment factors such as transmembrane integrin heterodimer receptors and release of the secreted phosphoprotein 1 (SPP1) or osteopontin important for initiation of attachment of the trophectoderm to the LE [17, 26].

While the developing embryo is initially located centrally in the uterine horn ipsilateral to the corpus luteum, as is characteristic of species which undergo large expansion of the blastocyst, the developing conceptus elongates into the contralateral horn around day 13. In pregnancies where only one ovulation has occurred, the conceptus may fill both the ipsilateral, and half of the contralateral, horn [27].

(3) Apposition

Apposition of the conceptus involves the trophectoderm becoming closely associated with the LE followed by incomplete/unstable adhesion. Following day 14, the developing conceptus appears to be immobilized in the uterine lumen. Analyses of histological sections at this time show close association of the apical membranes of both cell types to be in close association with each other; however,

the conceptus can still be recovered from the uterine lumen by flushing at this time point. As seen in most species, apposition of the embryo with the LE is accompanied by reduction in microvilli on the trophectoderm. In sheep, this occurs between days 13 and 15 [28, 29]. Apposition of the blastocyst to the LE is enhanced by interdigitation of cytoplasmic projections of the trophectoderm cells and uterine epithelial microvilli. In sheep this apposition occurs beginning at the ICM and progresses towards the outer end of the elongating conceptus.

Uterine glands are also sites for apposition in the sheep [28, 30]. The trophoblast develops finger-like projections, which migrate into the mouths of superficial glands between days 15 and 18 [28, 31]. Although these projections do not remain past day 20, they are thought to anchor the preimplantation conceptus, assist in development of more permanent interactions between the trophoblast and the LE, and increase absorption of histotrophic secretions from the uterine glands [31].

(4) Adhesion

The trophoblast begins to firmly adhere to the endometrial LE on day 16. Interdigitation between the trophectoderm and endometrial LE occurs in both caruncular and intercaruncular areas of the endometrium. Adhesion progresses along the uterine horn, and appears to be complete around day 22 [32]. By day 16 trophoblast binucleate cells (BNC) have differentiated from the mononuclear trophectoderm; although, only the mononuclear cells are thought to adhere to the endometrial LE. The formation of BNCs is thought to fulfill two main functions. The

first function is formation of a hybrid fetal maternal interface important for initial implantation, and subsequent placentation. The second function of BNC is to synthesize and secrete placental proteins and hormones into the maternal system which are important for regulation of maternal metabolism and other physiological functions [33-35]. BNC are thought to arise from consecutive nuclear division of mononuclear trophoblast cells without cytokinesis [36, 37]. Following formation, BNC cells fuse with the LE to form syncytium of trinucleate cells. This process replaces the endometrial LE with cells of trophectoderm origin. These trinucleate cells continue to enlarge as BNC migration and continued fusion form plaques of multinucleated syncytia. The number of nuclei present in a single plaque appears to be limited in size to 20-25 nuclei in the sheep [38]. The growing syncytial plaques eventually cover the surface of the caruncles, and help to establish formation of the placentomes. The definitive placental type for sheep is defined as synepitheliochorial, as it is neither entirely syndesmochorial without uterine epithelium, or entirely epitheliochorial with two adjacent but intact cells layers.

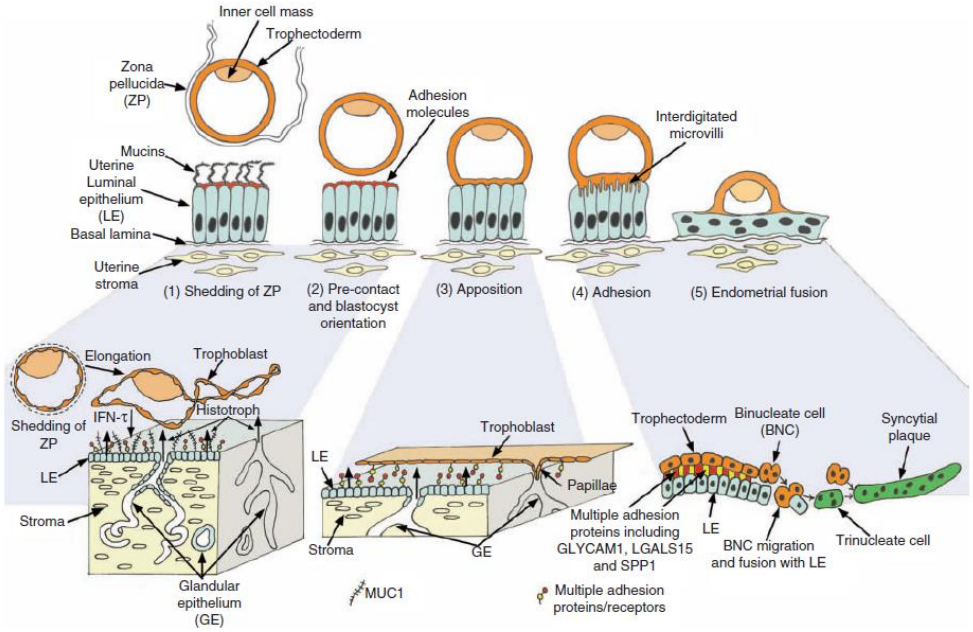

Figure 3. Initiation of conceptus implantation during early pregnancy. Implantation in sheep involves pre-attachment, apposition, and adhesion of the conceptus trophectoderm to the uterine LE. **(A)** Pre-attachment involves shedding of the zona pellucida and orientation of the blastocyst within the uterine horn. The presence of the antiadhesive mucin, MUC1 on the LE prevents premature contact of the trophectoderm with adhesive receptors such as integrins. **(B)** During the transition of the conceptus from a tubular to filamentous form, expression of MUC1 decreases, exposing the presence of integrins on the LE allows for apposition between the trophectoderm and LE, and between the trophoblast papillae and GE ducts. Apposition and transient attachment of the trophectoderm to the LE is likely required for conceptus elongation. **(C)** Adhesion between the conceptus trophectoderm and LE is in part mediated by secretory proteins for the epithelium, such as GlyCAM-1, SPP1, LGALS15 interacting with receptors on the trophectoderm. Differentiation of trophoblast binucleate cells, and their migration and fusion with the LE to form syncytial plaques marks the beginning of placentome formation. Figure from [39].

Progesterone

Actions of Progesterone on the Endometrium

In ruminants, progesterone (P4) is the unequivocal hormone of pregnancy. During early embryo development, P4 acts to stimulate and maintain uterine functions important for conceptus growth, implantation and development to term [40, 41]. In sheep, P4 levels are low at estrus, increase with formation of the corpus luteum, and reach maximal level after days 8 to 9 [42]. If pregnancy is not established, the uterine luteolytic mechanism develops to cause the CL to regress resulting in a decline in P4 levels [43, 44].

P4 acts through the progesterone receptor (PGR), a nuclear receptor and transcription factor that regulates gene expression [45]. In sheep, the endometrial epithelium and stroma of the uterus express PGR after estrus, and initiation of P4 induced gene expression is temporarily associates with the loss of PGR [46, 47]. PGR is lost in the LE between days 10 and 12, and in the GE between days 12 and 16 following estrus [40, 47]. Interestingly, PGR expression is maintained in the uterine stroma and myometrium throughout gestation [40]. Spatially restricted expression of PGR throughout the cycle allows for direct induction or repression of P4 responsive genes in specifically in the epithelia and stroma (Figure 4). The loss of PGR immediately prior to implantation is common to domestic ruminants and other studied mammals [9], which supports the hypothesis that the loss of PGR is responsible for gene expression changes in the LE and GE that act to modulate uterine receptivity.

The postovulatory rise in P4 during early pregnancy has been shown to positively influence conceptus growth and development in both sheep and cattle [48-50]. In heifers, increasing concentrations of P4 from days 2-5 stimulated conceptus elongation when evaluated on day 14 [51, 52]. In contrast, animals with low levels of P4 during the early luteal phase displayed retarded embryonic development and decreased production of IFNT [51, 53]. Exposing bovine embryos to P4 *in vitro* did not affect the number of embryos which develop to the blastocyst stage, cell number within the blastocyst or conceptus elongation after synchronized transfer into the uterus. Therefore, in cattle, and likely sheep, the effect of P4 on embryonic development is mediated by the endometrium.

Between days 10 and 12 post estrus, P4 induces the expression of multiple genes in the endometrial LE and superficial GE which have been investigated as potential mediators of conceptus elongation and development [54]. These genes include secreted attachment and migration factors (galectin-15 or LGALS15, insulin-like growth factor binding protein one or IGFBP1) [55, 56], intracellular enzymes (prostaglandin G/H synthase and cyclooxygenase 2 or PTGS2 and HSD11B1) [57-59], secreted proteases (cathepsin L or CTSL) [60], secreted protease inhibitors (cystatin C or CST3 and CST6) [61], secreted cell proliferation factor (gastrin releasing peptide or GRP) [62, 63], glucose transporters (SLC2A1, SLC2A5, SLC5A1), and a cationic amino acid (arginine, lysine and ornithine) transporter (SLC7A2) [64-66]. In the endometrial GE, P4 induces genes that encode for a secreted cell proliferation factor (GRP), a glucose transporter (SLC5A11), secreted adhesion protein (secreted phosphoprotein one or SPP1)

[67], a regulator of calcium/phosphate homeostasis (stanniocalcin one or STC1) [68], and an immunomodulatory factor (uterine milk protein or UTMP) [69, 70].

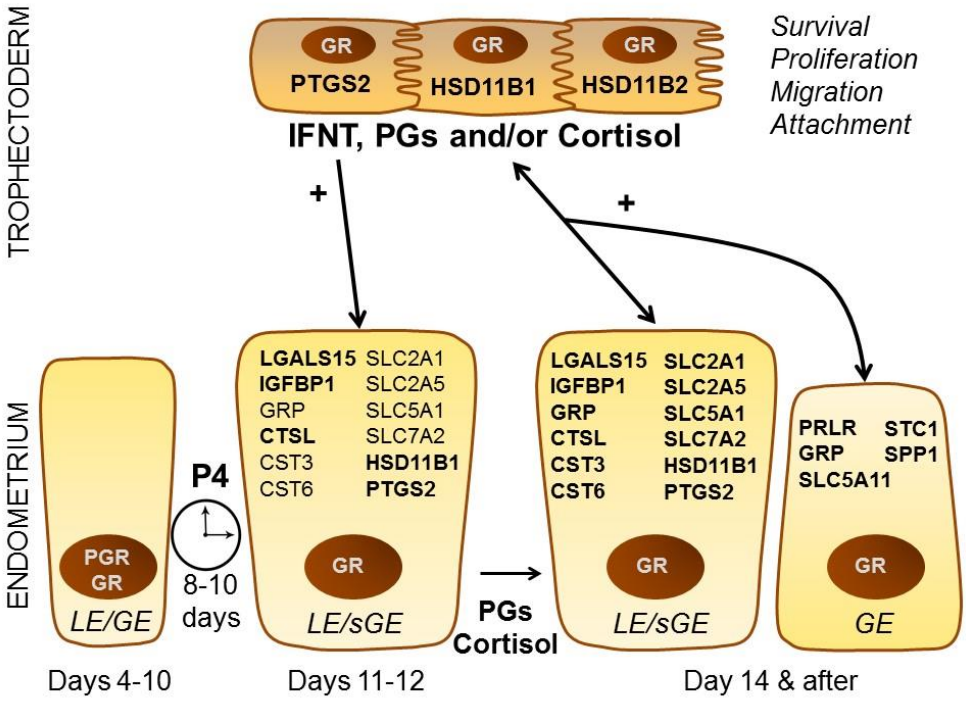

Figure 4. Working hypothesis on the regulation of conceptus development and endometrial function in sheep. Following 8 to 10 days of progesterone exposure, PGR is lost in the endometrial LE between days 10 and 12, and in the GE between days 12 and 16. Loss of PGR is concurrent with induction of expression of multiple P4 regulated genes. Expression of these genes is further stimulated by factors from the developing conceptus including IFNT, PGs and cortisol. Many of these endometrial genes encode secreted factors which contribute to the uterine luminal fluid and promote survival, proliferation, migration and attachment of the conceptus trophectoderm.

Interferon Tau

Actions of IFNT on the Endometrium

A subset of genes initially induced by P4 have been found to be further stimulated by factors secreted by the elongating conceptus. The trophectoderm of the elongating ruminant conceptus synthesizes and secretes IFNT as well as prostaglandins (PGs) and cortisol. IFNT is the maternal recognition of pregnancy signal that acts on the endometrium to inhibit production of luteolytic pulses of PGF2α by the LE [19, 20], thereby ensuring continued P4 production by the corpus luteum [71]. IFNT also acts on the endometrium to stimulate transcription of classical Type I IFN-stimulated genes (ISGs) in the stroma as well as a number of P4-induced elongation and implantation related genes in the LE and GE [72-74].

In both sheep and cattle, the uterus and conceptus synthesize and secrete numerous prostaglandins, including PGE2, PGF2α, PGI2, PGD2 [75-77]. Prostaglandins have been shown to be important for conceptus elongation, as pharmaceutical inhibition of prostaglandin G/H synthase and cyclooxygenase (PTGS2) inhibited conceptus elongation [57]. Interestingly, uterine infusion of PGE2, PGF2α or PGI2 during early pregnancy in sheep increased expression of multiple endometrial genes hypothesized to be involved in conceptus elongation including GRP, IGFBP1, LGALS15, HEXB, CTSL, CST3, ANGPTL3, HIF1A, SLC2A1, SLC2A12, and SLC5A1 [78].

The elongating conceptus and endometrium also produce cortisol via hydroxysteroid (11-β) dehydrogenase 1 (HSD11B1). Ovarian P4 induces endometrial HSD11B1 expression and keto-reductase activity as well as many

epithelial genes that govern trophectoderm proliferation, migration, and attachment during elongation [58, 59]. HSD11B1 was found to play a biological role in endometrial function and conceptus development as infusion of PF915275, a selective inhibitor of HSD11B1, in utero prevented conceptus elongation [59]. These results support the hypothesis that HSD11B1-derived cortisol mediates, in part, actions of ovarian P4 in regulation of endometrial functions important for conceptus elongation and implantation during early pregnancy in sheep.

Collectively, the actions of P4 as well as IFNT, PGs and cortisol act to modulate gene expression during early pregnancy important for conceptus growth and implantation. The capacity of the uterus to stimulate conceptus elongation is thought to dependent primarily on changes in genes products and their subsequent secretion from the LE and GE. These secretions from the uterine epithelium are a critical component for conceptus survival, as they contain amino acids, ions, glucose, enzymes, growth factors, hormones, transport proteins and others substances required by the developing conceptus before implantation [79]. This mixture is collectively termed uterine histotroph [7]. Evidence from studies using the uterine gland knockout (UGKO) ewe supports the hypothesis that ULF secretions are necessary for the growth, survival and development of the elongating conceptus [80, 81]. Although the cellular and molecular mechanisms regulating conceptus elongation are not yet defined, they are hypothesized to require both histotrophic secretions, as well as apposition and transient attachment of the trophectoderm to the LE.

Interferon Tau (IFNT)

IFNT is a type I IFN expressed and secreted by the elongating ruminant conceptus. IFNT has potent antiviral [82], antiproliferative [83, 84], antitumor [85], and immunomodulatory biological activities [83, 86]. Conceptus-derived IFNT functions in ruminants by serving as the signal for maternal recognition of pregnancy and may also inhibit viral infection of the conceptus or uterus as well as modulate the maternal immune response [39, 82, 87, 88]. In domestic ruminant species (cow, sheep, goat), IFNT displays conserved sequence homology as well as mechanism of action [89-92]. IFNT most resembles IFN-omega, but is also structurally similar to IFN-alpha and IFN-beta [93]. Genes for IFNT have been identified in cattle, sheep, musk oxen, goats, gazelle, giraffe and deer. The expression of IFNT is unique compared to other interferons as it is not produced in response to viral infection, its expression is restricted to the trophectoderm, and it is produced at high levels for multiple days.

Pregnancy Recognition in Ruminants

IFNT is the maternal recognition of pregnancy signal secreted by the elongating conceptus which acts to maintain the CL, thereby preventing luteolysis and sustaining P4 levels [86]. Onset of maximal IFNT secretion by the ovine trophoblast is directly related to morphological transition of the conceptus from a spherical to filamentous form [53, 94, 95]. The ruminant conceptus produces IFNT from days 10 to 21 with the highest amount produced on day 14. Indeed, day 14 ovine filamentous conceptuses produce approximately 25–500 ng of IFNT per hour over a 48 hour period [95].

In sheep the estrous cycle is uterine dependent, as the endometrium releases PGF2α in a pulsatile manner to induce luteolysis during late diestrus. The endometrial LE and sGE produce PGF2α in response to binding of oxytocin to its receptor on those cells [96]. Expression of oxytocin receptor (OXTR) is regulated by both P4 and estrogen (E2). The negative regulation of ESR1 by PGR results in a 'P4 block' in the LE and sGE between days 5 and 11 preventing the expression of both ER and subsequently OXTR. With continuous P4 exposure, PR is downregulated in the LE/sGE between days 10 and 12 in cycling ewes allowing for increased expression of ESR1 on day 12-13, followed by OXTR on day 14. IFNT acts on the endometrium LE/sGE to inhibit transcription of ESR1, and therefore OXTR, which prevents production of luteolytic pulses of PGF2α [97]. This anti-luteolytic action of IFNT sustains P4 production by the CL, and maintains the endometrium in a receptive state.

IFNT stimulated genes in the endometrium

IFNT induces or stimulates expression of a number of classical IFN stimulated genes (ISGs) in the endometrium, which are hypothesized to be important for uterine receptivity to implantation as well as conceptus development (Figure 4). *In vitro* studies determined IFNT activates the classical JAK/STAT (janus kinase/signal transduce and activator of transcription) signaling pathway used by other Type I IFNs [98]. In the ovine endometrium, IFNT produced by the developing conceptus binds to its receptor, IFNAR, which is a heterodimeric receptor composed of IFNAR1 and IFNAR2 subunits. IFNAR1 and IFNAR2 are expressed in all endometrial cell types with highest expression in endometrial LE

[99]. However, IFNT does not induce ISG expression in these cells. The LE/sGE expresses IRF2, a potent and stable transcriptional repressor whose expression in the LE and sGE increases during early pregnancy [100]. The presence of IRF2 in the LE/sGE is thought to bind IFN stimulated response element (ISRE) and IFN regulatory factory response element (IRFE) in the promoter/enhancer regions of classical ISGs, resulting in their inability to be activated by IFNT. Furthermore, critical factors (STAT1, STAT2, IRF9) required for JAK/STAT signaling are not present in the LE/sGE, as they are ISGs themselves [101, 102]. IRF2 is not expressed in the cells of the stroma and middle to deep GE. Thus, in these cells lines IFNT can induce classical ISGs including STAT1, STAT2, ISGF3G, B2M, ISG15, MIC and OAS [103].

IFNT is likely transported or passively diffuses across the LE into the stroma. Work done by Guillomot and coworkers [28, 104] showed that injection of horseradish peroxidase into the uterine lumen of pregnant sheep and cattle accumulated in the endometrial stroma beneath the basement membrane of the LE. They found that this transport was mediated by both transepithelial endocytosis as well as passage through intercellular spaces between tight junctions. The accumulation of HRP in these areas was especially apparent when P4 concentrations were high during late diestrus.

Effects of IFNT on the LE/sGE

IFNT also acts on the endometrial LE to induce expression of non-classical interferon stimulated genes (Figure 4). Transcriptional profiling of human U3A (STAT1 null) cells, ovine endometrium, as well as candidate gene analyses

revealed that the expression of *CST3*, *CST6*, *CTSL*, *GRP*, *HSD11B1*, *IGFBP1*, *LGALS15*, *SLC2A1*, *SLC2A5*, *SLC5A11*, *SLC7A2,* and *WNT7A* are also regulated by IFNT [39, 54, 60, 61, 103, 105-108]. Transcriptomic and candidate genes studies found that IFNT further stimulates expression of these elongation- and implantation-related genes after initial induced by P4 specifically in the endometrial LE, sGE, and/or GE. Many of these genes have been investigated, and found to promote trophectoderm proliferation, migration, attachment and/or adhesion.

It is hypothesized that IFNT uses a non-canonical, STAT1-independent signaling pathway to regulate expression of non-classical ISGs, as the critical signaling components of the JAK-STAT signaling system are not expressed in endometrial LE or sGE [100]. The non-canonical pathway mediating IFNT stimulation of genes in the LE and sGE has yet to be identified, but other Type I IFN use mitogen-activated protein kinase (MAPK) and phosphatidylinositol 3-kinase (PI3K) cascades [109]. There is evidence indicating that IFNT activates distinct epithelial and stromal cell-specific JAK, epidermal growth factor receptor, MAPK (ERK1/2), PI3K-AKT, and/or Jun N-terminal kinase (JNK) signaling modules to regulate expression of PGE2 receptors in the endometrium of the ovine uterus or in ovine uterine LE cells *in vitro* [110, 111]. Identification and characterization of the role of both classical and non-classical ISGs in the LE and sGE is important for understanding their function in promoting conceptus development.

Prostaglandins

Prostaglandin synthesis

During early pregnancy in the sheep, both the conceptus and endometrium synthesize and secrete a variety of prostaglandins (PGs) (Figure 5) [75, 76, 112]. Prostaglandins are hormonally active oxygenated fatty acids that are formed via multiple enzymatic reactions [113-116]. Arachidonic acid (AA) is the major precursor of prostaglandin biosynthesis, and is derived from the phospholipids of the cell membrane by phospholipase A2 (PLA2) [117]. Arachidonic acid is first converted into prostaglandin G2 and then reduced to prostaglandin H2 (PGH2) [113, 114, 118]. PGH2 can then be metabolized to the five primary prostaglandins, including prostaglandin D2 (PGD2), prostaglandin E2 (PGE2), prostaglandin F2α (PGF2α), prostacyclin (PGI2) and thromboxane A2 (TXA2) by different cell-specific prostaglandin isomerases and synthases (Figure 5) [119-121]. In sheep, the dominant cyclooxygenase expressed in both the endometrium and trophectoderm of the elongating conceptus is prostaglandin-endoperoxide synthase 2 (prostaglandin G/H synthase and cyclooxygenase) or PTGS2 [76, 112].

Two prostaglandin synthases isoforms exist, PTGS1 and PTGS2, which are encoded by distinct genes [122]. *PTGS2* activity can be induced by several cytokines, growth factors and mechanical stress, while *PTGS1* is expressed at a relatively constant level in most tissues [122, 123]. This differential activity is perhaps due to the numerous regulatory elements present in the promoter region of *PTGS2*, compared to the few cis-acting response elements and no TATA box in the 5' flanking region of *PTGS1* [113, 124, 125]. Nonetheless, both isoforms act as

the rate limiting enzyme in the production of PGs. PTGS1 and PTGS2 share high similarity with respect to the primary structure of the active site and kinetic properties [114, 126-128]. However, distinct differences exist aside from tissue specificity and expression level between PTGS1 and PTGS2. The cyclooxygenase active site of PTGS2 is approximately 20% larger than that of PTGS1, which has been exploited in developing PTGS2–specific non-steroidal anti-inflammatory drugs (NSAID) [129]. PTGS2 also competes more effectively for newly released arachidonate when both isoenzymes are co-expressed in the same cell, because PTGS1 exhibits negative allosterism at low arachidonate concentrations [130, 131].

Prostaglandin production during early pregnancy is essential for conceptus development in sheep, as infusion of the selective inhibitor of PTGS2, meloxicam, into the uterine lumen during early pregnancy prevented conceptus elongation [57]. The conceptus synthesizes and secretes more PG than the underlying endometrium in both sheep and cattle; therefore, PG levels are much greater in the uterine lumen of pregnant as compared with cyclic animals [132-135]. When cultured *in vitro,* day 14 sheep conceptuses release the cyclooxygenase metabolites TXB2 (22.5%), PGF2α (21%), 6-keto-PGF1α (18.2%) a stable metabolite of PGHI2, PGE2 (14.5%) and PGD2 (2.7%) [75-77].

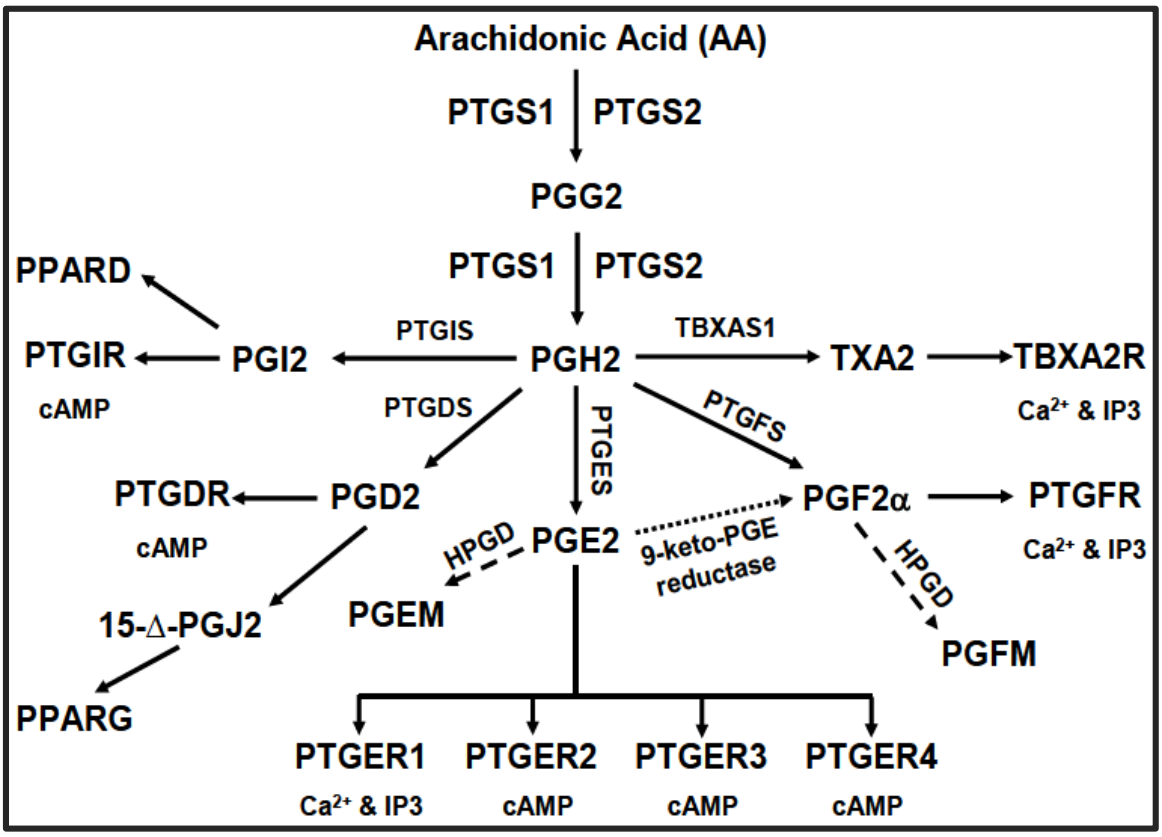

Figure 5. Prostaglandin biosynthesis. Arachidonic acid is cleaved from membrane phospholipids by A2 (PLA2) and then converted to prostaglandin H2 (PGH2) by prostaglandin synthase (PTGS). Next, PGH2 is metabolized to five primary prostaglandins by specific synthases and isomerases. Figure modified from [136].

Prostaglandin Receptors

Membrane and nuclear PG receptors are expressed in both the endometrium and conceptus during early pregnancy [57, 137]. In addition to G-protein coupled cell membrane receptors for PGE2, PGF2α, and PGI2, select PGs can also activate the nuclear receptors peroxisome proliferator activator receptor delta (PPARD) and gamma (PPARG) [138]. PGI2 is a ligand for PPARD, and PGD2 spontaneously forms 15-deoxy-delta-PGJ2 within cells, which is a ligand for PPARG [139-142]. The expression of prostacyclin (PGI2) synthase (PTGIS), PGI2 receptors (PTGIR), PPARs and RXRs in the uterus and conceptuses of sheep during early pregnancy has been previously documented [137]. *PTGIS* mRNA and protein is mainly localized to the LE of the endometrium, and decreases in expression between day 12 and 17. Expression of PTGIR, PPARA, PPARG and RXRG in the endometrium varies during the peri-implantation period, while PPARD, RXRA and RXRB are consistently expressed in the LE. In the trophectoderm, the expression of PTGIS, PPARD and PPARG increases from day 12 to day 17 [137].

PPAR mechanisms of action

The PPARs belong to a family of nuclear hormone receptors that regulate development and differentiation, and govern cellular processes by modulating fat and glucose metabolism as well as inflammatory response [143, 144]. PPARs, like other nuclear receptors, are composed of multiple distinct functional domains [145]. The DNA binding domain (DBD) and the ligand binding domain (LBD) are highly conserved across all PPAR receptor isoforms. The DBD consists of two zinc

fingers that specifically bind peroxisome proliferator response elements (PPRE) in the regulatory region of PPAR-responsive genes. The LBD, located towards the C-terminus, has been shown by crystallography to be composed of 13 α-helices and a small 4-stranded β-sheet. The ligand binding region of PPARs is large in comparison to other nuclear receptors, which may be what allows PPARs to interact with a broad range of structurally distinct natural and synthetic ligands [146, 147]. Located at the C terminus of the LBD is the ligand-dependent activation domain (AF-2) which is involved in the generation of the receptors' coactivator binding pocket [148]. Additionally, a ligand-independent activation function (AF-1) is found in close proximity to the N terminus of the receptor [149]. Unlike the steroid hormone receptors, which function as homodimers, PPARs form heterodimers with the retinoid X receptor (RXR) (Figure 6) [150]. Like PPARs, RXR exists as three distinct isoforms (alpha, beta and gamma), which are activated by the endogenous agonist 9-*cis* retinoic acid [151]. No specific role has been elucidated for the different isoform pairings within the PPAR:RXR complex.

The PPAR:RXR complex influences transcription of responsive genes by binding PPREs which consist of two repeated AGGTCA consensus sequences separated by a single nucleotide spacer. PPREs have been found in a number of PPAR-inducible genes including acyl-CoA oxidase and adipocyte fatty acid-binding protein [152]. The cis elements adjacent to the PPRE appear to play a role in defining the binding selectivity of these response elements [152]. Several cofactors, coactivators, and corepressors which mediate the ability of nuclear receptors to initiate (or suppress) the transcription process have been identified

(Figure 6) [153]. Coactivators interact with nuclear receptors in an agonist-dependent manner through a conserved LXXLL amino acid motif [154, 155]. Several coactivators, including CBP/p300 and steroid receptor coactivator (SRC)-1 [156], possess histone acetylase activity that can remodel chromatin structure. A second group of coactivators, represented by the members of the DRIP/TRAP complex, such as PPAR binding protein (PBP)/TRAP220 [157], form a bridge between the nuclear receptor and the transcription initiation machinery. The role of the third coactivator group, which includes PGC-1 [158], RIP140 [159] and ARA70 [160], is not well understood. It is thought that coactivators with histone acetylase activity complex with ligand activated, PPRE-bound PPAR/RXR receptors, disrupt nucleosomes and help to open chromatin structure in the vicinity of the regulatory region of a gene. Complexes such as DRIP/TRAP are then recruited and provide a direct link to the basal transcription machinery. Together this hypothesized cascade is thought to promote transcription initiation. The use of a partial PPARG agonist was shown to cause the receptor to interact with CBP or SRC-1 in a less efficacious manner than a full agonist [161], suggesting that distinct PPAR:cofactor interactions may be a critical for transmitting signals that result in unique gene regulatory activity and could therefore prove useful in identifying and characterizing selective PPAR modulators with novel physiological actions.

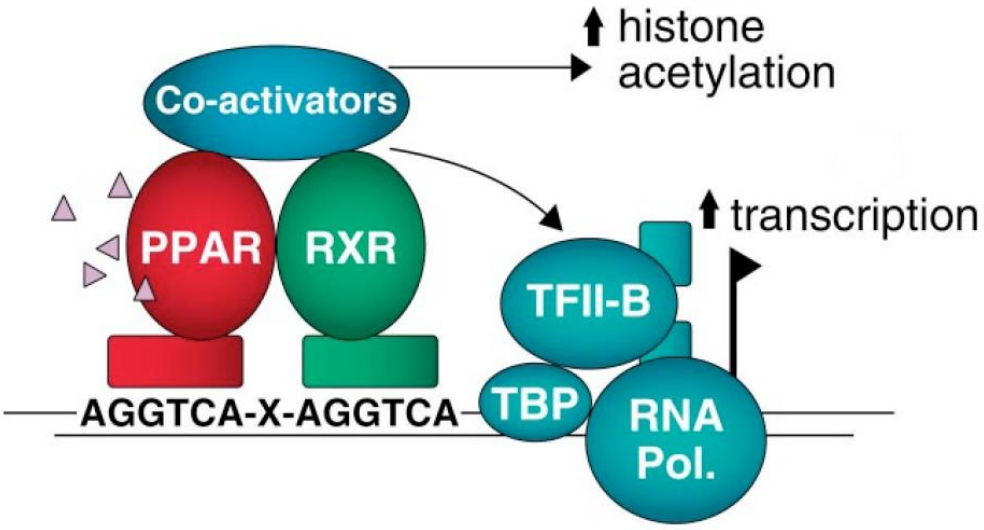

Figure 6. Mechanism of transcriptional activation by PPAR isoforms. PPARs heterodimerize with RXRs and bind PPREs in the promoter regions of PPAR responsive genes. Recruitment of co-activators allows for regulation of gene transcription through acetylation of histones and recruitment of transcriptional machinery. Figure adapted from [162].

Peroxisome Proliferator Activator Gamma

PPARG is naturally activated by thiazolidinediones and the 15-deoxy-delta-PGJ2, as well as several types of fatty acids, fatty acid derivatives, oxidized LDL, oxidized alkyl-phospholipids and nitro linoleic acid [139, 140, 143, 163, 164]. The effects of PPARs on target gene expression depends not only on ligand, but also DNA allosteric constraints, promoter context and availability of transcriptional co-regulators [144, 148, 165]. PPARG plays a pivotal role in adipocyte biology, where it is essential for adipogenesis, survival of mature adipocytes and expression of genes that govern fatty acid uptake, lipid storage and systemic energy homeostasis [166-168]. *PPARG* may also play a role in placental fatty acid accumulation and transport as trophoblasts of null murine embryos lack lipid droplets that are normally present in wild-type placentas [166]. In mink, treatment of trophoblast cells PGJ2 attenuated cell proliferation, increased expression of *ADRP* (adipose differentiation related protein), a protein involved in lipid homeostasis, and *SPP1* (secreted phosphoprotein 1 or osteopontin) [169]. Importantly, several proteins that modulate fatty acid uptake and accumulation, including fatty acid transport proteins (FATP/SLC27A), PAT proteins (perilipin, adipophilin and Tip47) and fatty acid binding proteins (FABP) are expressed in the mouse and human placenta [170-174]. Therefore, PPARG is also thought to play a regulatory role in the uptake and accumulation of lipids in trophoblast cells.

Peroxisome Proliferator Activator Delta

Similar to other PPARs, PPARD is activated by both saturated and unsaturated fatty acids. Additionally, PPARD interacts with palmitic acid, 2-

bromopalmitic acid, PGA1, PGI2 and PGD2 [175-177]. PPARD, along with PPARA and PPARG, has been identified as a key regulators of lipid homeostasis and energy metabolism. Use of a synthetic PPARD agonist demonstrated that PPARD can induce cholesterol transport and normalize lipoprotein profiles and triglyceride levels in obese monkeys, categorizing it as a regulator of lipid metabolism like the other PPAR isoforms [178]. PPARD appears to be involved in the regulation of fatty acid burning capacities in skeletal muscles and adipose tissue by controlling the expression of genes involved in fatty acid uptake, β-oxidation and energy uncoupling. PPARD is also hypothesized to be a regulator of adiposity, and metabolic adaptations to environmental change [179, 180]. Based on the spatial and temporal expression patterns of PPARD expression and necessity of its natural ligand PGI2, PPARD has also been proposed as a critical mediator of embryo implantation [142, 175]. Collectively, these observations implicate PPARD as a versatile regulator of distinct biological processes relating to lipid metabolism, cellular differentiation, and pregnancy.

To investigate the role of PPARD in placental differentiation, genetically modified mouse models were used. PPARD was found to be expressed in implantation sites within the uterus, and was strongly upregulated during the decidualization process in a manner similar to PTGS2 [142]. Mice deficient in *Ppard* exhibited severe placental defects and reduced or inhibited trophoblast giant cell differentiation [181] [182, 183]. Treatment of rat trophoblast cells with a specific PPARD agonist triggered early differentiation of giant cells that expressed chorionic somatomammotropin hormone one (CSH1, Prl3d1 or placental lactogen)

and reduced expression of inhibitor of differentiation two (ID2), which is an inhibitor of several basic helix-loop-helix (bHLH) transcription factors, such as HAND1, that promote giant cell differentiation [183]. *PTGS2* null mice display decreased fecundity in part due to decreased blastocyst implantation and decidualization [184]. Treatment with carboprostacyclin or the PPARD agonist L-165041 restored implantation in *PTGS2* null mice [142]. Such results support the conclusion that PPARD may play a role in maintaining reproductive capacity in females. Further, PPARD stimulates expression of ADRP. In the skin, PPARD potentiates cell chemotaxis, polarization and migration [185], which are all cellular activities implicated in conceptus elongation.

Therefore, it is hypothesized that the regulation of PG signaling through PPARD and PPARG may be important for the development and differentiation of the ruminant conceptus due to intrinsic actions of PGI2 and PGJ2, or through regulation of other cellular processes. These include regulation of genes such as fatty acid binding proteins (FABP) and fatty acid transport proteins (FATP and SLC27As) required for lipid uptake and triacylglycerol synthesis, which is undoubtedly important in rapidly growing and elongating ruminant conceptuses producing large amounts of PGs (Figure 7).

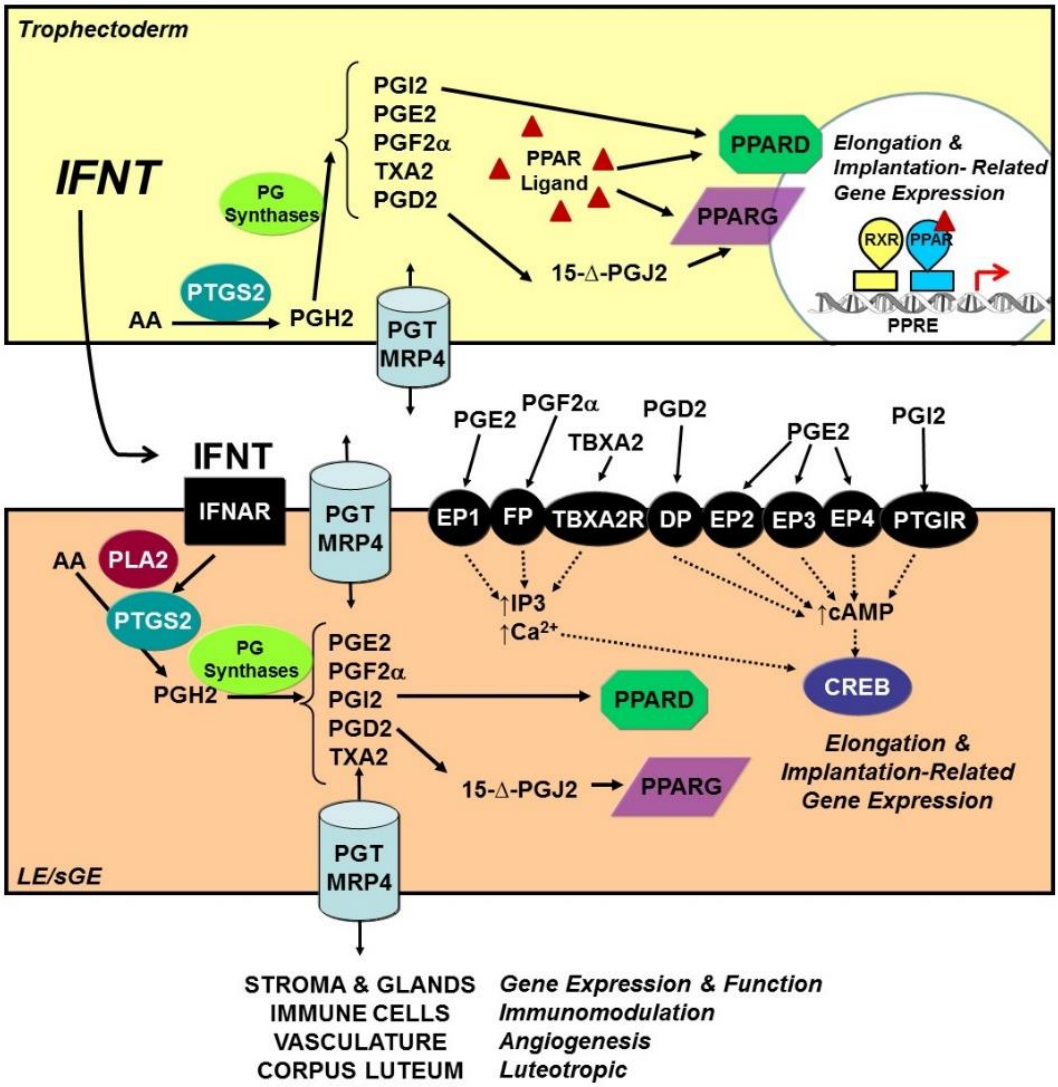

Figure 7. Schematic of PG signaling in the LE/sGE and conceptus trophectoderm during early pregnancy. PGs synthesized by PTGS2 in the LE/sGE and trophectoderm can be converted to multiple different PG metabolites including PGE2, PGF2α, PGI2, and PGD2. These PGs can act via nuclear (PPARG and PPARD) or cell surface receptors to regulate expression of genes important for conceptus elongation and implantation in the endometrium and trophectoderm.

Glucocorticoids

Glucocorticoid Synthesis

Glucocorticoids (GC) regulate a variety of physiological processes primarily due to their actions as transcription factors. Synthesized in response to activation of the hypothalamic-pituitary-adrenal (HPA) axis, GCs are hormones that function to maintain homeostasis during inflammatory and immune responses and also have roles in development and reproduction [186, 187]. The cortex of the adrenal gland produces multiple steroid hormones, including cortisol, cortisone, aldosterone and the adrenal androgens. The GCs, cortisol and cortisone, characterized by their ability to bind and activate the glucocorticoid receptor (GR), are produced in the zona fasciculata, the middle cortical layer of the adrenal gland [188]. GC secretion by the adrenal gland is regulated by adrenocorticotropin (ACTH) from the anterior pituitary. Episodic production of ACTH is regulated by circadian rhythms, and further stimulated by stress. Production of corticotrophin-releasing hormone (CRH) and arginine-vasopressin (AVP) in the paraventricular nuclei (PVN) of the hypothalamus act synergistically to stimulate ACTH production and release from the anterior pituitary [189, 190]. ACTH binds plasma membrane receptors on the adrenal gland, and activates pathways important for the synthesis and secretion of steroids. The adrenal cortex of ruminants secretes both cortisol and cortisone. The ratio of cortisol to cortisone in the adrenal venous blood in bovine is 1:1, and 15-20:1 in sheep [191]. Biologically active cortisol is secreted in an unbound state; however, it binds plasma proteins, usually corticosteroid binding globulin, upon entering the circulation. Therefore, both cortisol and cortisone

originate from the adrenal gland, are present in the circulation and readily diffuse into target tissues to elicit effects. Metabolism of these steroids in the liver renders them inactive by increasing their water solubility, allowing for eventual excretion and clearance by the kidneys.

GC interconversion by hydroxysteroid (11-beta) dehydrogenases

The 11-beta-hydroxysteroid dehydrogenase enzymes regulate the intracellular level of bioactive glucocorticoids within tissues. The type I isozyme (HSD11B1) has both 11-beta-dehydrogenase (cortisol to cortisone) and 11-oxoreductase (cortisone to cortisol) activities. The type II isozyme (HSD11B2) has only 11-beta-dehydrogenase activity. The direction of the HSD11B1-catalyzed reaction is determined by the relative abundance of NADP+ and NADPH within the cell (Figure 8). In the presence of a high NADPH/NADP+ ratio, generated *in vivo* by hexose-6- phosphate dehydrogenase (H6PD), HSD11B1 functions predominately as a ketoreductase that converts inactive cortisone to active cortisol. In contrast, HSD11B2 is a high affinity NAD-dependent unidirectional dehydrogenase that inactivates cortisol to cortisone.

Using a model of P4 accelerated blastocyst growth, *HSD11B1* was identified as a candidate P4 and conceptus stimulated gene in the ovine endometrium that was hypothesized to influence conceptus development and elongation [192]. *HSD11B1* was found to be expressed specifically in the endometrial LE and superficial GE of the uterus and is further stimulated by IFNT after initial induction by P4 [192]. *HSD11B1* is also expressed and active in the conceptus trophectoderm. Inhibition of the actions of HSD11B1 in the ovine uterus

through infusion of the selective pharmacological inhibitor, PF 915275, from day 10 to 14 prevented conceptus elongation [59]. Inhibition of HSD11B1 by PF 915275 also decreased expression of a number of conceptus elongation and implantation related genes, including *CTSL, CST3, CST6, CXCL10, IGFBP1, LGALS15* and *SPP1* [59].

During the estrous cycle and early pregnancy *HSD11B2* expression was most abundant in the conceptus trophectoderm but is also detectable at lower levels in all endometrial cell types of the ovine uterus [192]. Biologically active GCs can also act through the mineralocorticoid receptor (MR), to regulate gene expression within the cell. In cells where binding of GCs to MR would inhibit binding of aldosterone to MR, HSD11B2 catalyzes conversion of the cortisol to the inactive metabolite cortisone, to prevent activation of MR. In tissues that do not express MR, such as the placenta and testis, HSD11B2 is thought to protect cells from the growth-inhibiting and/or pro-apoptotic effects of cortisol. In the placenta, HSD11B2 expression is thought to protect the fetus from high levels of maternal GCs, as fetal exposure to excessive GCs is linked to lower birth weight [193]. Additionally, intrauterine growth restriction models in both humans and animals report reduced HSD11B2 expression/activity in the placenta [194, 195]. Of note, MR is not expressed in the uterus or conceptus during the peri-implantation period of pregnancy in the sheep [196].

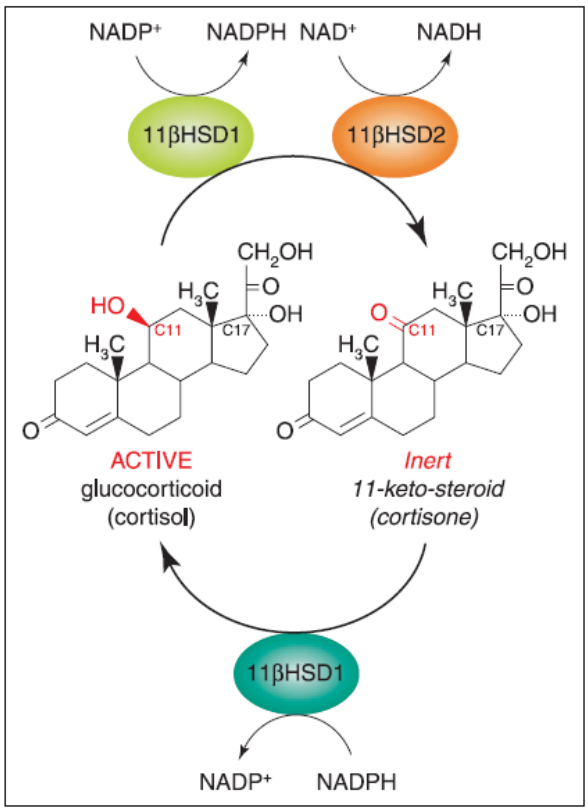

Figure 8. Cortisol-cortisone inter-conversion by hydroxysteroid (11-beta) dehydrogenases within target tissues. The conversion of inert cortisone to active cortisol, which can bind and activate GR, is catalyzed by HSD11B1. The metabolism of cortisol to inert cortisone is predominately mediated via type II hydroxysteroid (11-beta) dehydrogenases. Modified from [197]

Structure and function of GR

The GR (NR3C1) is a nuclear hormone receptor with three major domains, an N-terminal transactivation domain, a DNA-binding domain, and a C-terminal ligand-binding domain (Figure 9A) [198, 199]. The N-terminal transactivation domain contains the transcriptional activation function (AF-1) that interacts with co-regulators and transcriptional machinery [200, 201]. The central DNA-binding domain is composed of two highly conserved zinc fingers important for receptor dimerization, target site binding, and transcriptional regulation [201-203]. The C-terminal ligand-binding domain contains a nuclear localization signal and is the binding site for hormones, chaperone proteins and coactivators [201, 203]. In the absence of ligand, the inactive GR resides in the cytoplasm complexed with multiple chaperone proteins [203-206]. Following ligand binding, the chaperone proteins are released exposing the nuclear localization signal, and GR is translocated to the nucleus (Figure 9B).

In most tissues the molecular actions of GCs are mediated by intracellular signaling through GR. Following activation by ligand binding, GR acts predominantly as a homodimer to bind glucocorticoid responsive elements (GREs) in the promoter regions of target genes acting either as a trans-activator or trans-repressor of gene expression [207]. GR can also regulate gene expression through physical interactions with other transcription factors at GREs (Figure 9B). Binding of GR to GREs induces a conformational change in the receptor, allowing for recruitment of several coactivator complexes important for chromatin remodeling [207]. The GR interacts with coactivators such as CBP/p300 and p/CAF, both of

which acetylate lysine residues in core histones to induce nucleosome rearrangement and open heterochromatic regions [208-210]. GR binding to GREs can also inhibit gene transcription, primarily via two mechanisms. In the first mechanism, GR acts on the GRE that overlaps another transcription factor site, thereby preventing the binding of that site or displacing another transcription factor. GR regulates expression of bone gamma-carboxyglutamate protein (*BGLAP*) and prolactin (*PRL*) through this mechanism [211, 212]. The second mechanism involves genes repressed by GR mediated through interactions with other transcription factors on adjacent binding sites [213]. For example, GR interplays with activation protein 1 (AP-1) to repress transcription of genes encoding proopiomelanocortin (*POMC*) and *CRH* [214-216]. GR can also interact directly with other transcription factors to regulate expression of genes without the use of GREs [217]. GR interacts directly with the c-Jun subunit of the AP-1 to inhibit expression of matrix metallopeptidase 2 (*MMP2*) [218, 219]. Similarly, GR represses the transcriptionally active p65 (RelA) subunit of nuclear factor-κB (NF-κB) to inhibit interleukin-1B (*IL1B*) expression [220].

(A)

(B)

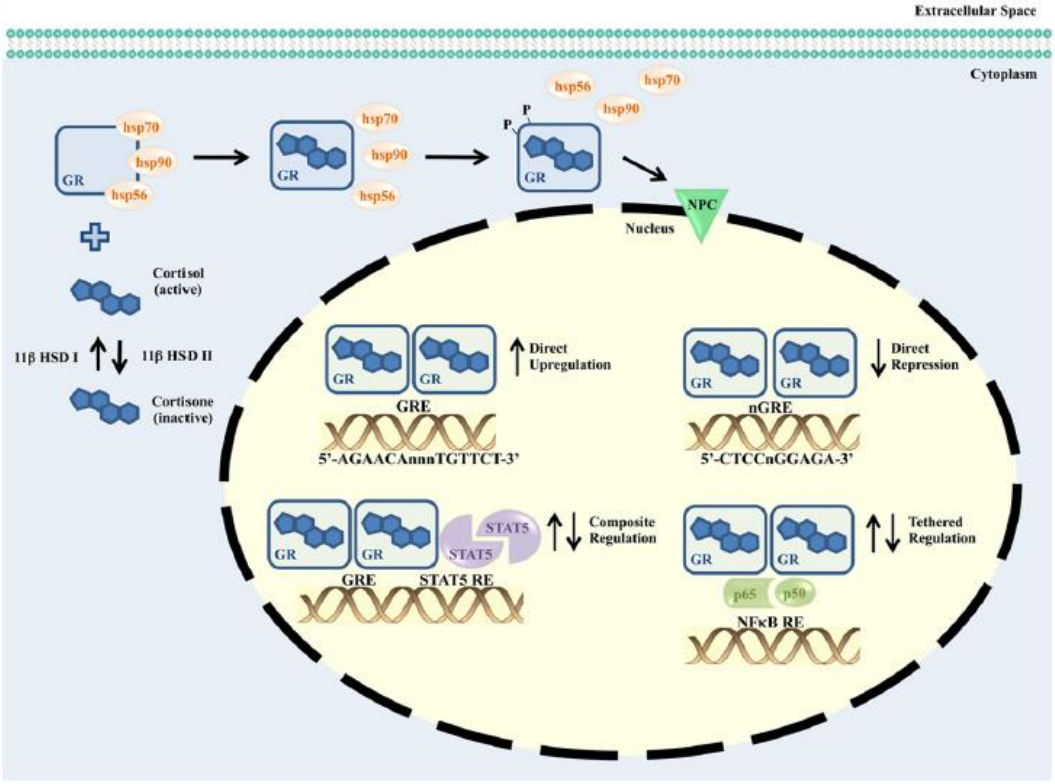

Figure 9. (A) Molecular structure of GR. The N-terminal region contains an activation function (AF-1) motif which interacts with transcriptional machinery. The DNA-binding domain contains two zinc fingers involved in dimerization and interactions with DNA. The hinge region contains a nuclear localization sequence. The C-terminal domain contains the ligand-binding motif and an AF-2 motif which is involved in interactions with various transcriptional regulatory factors. **(B) GR signaling**. Ligand binding to GR allows for translocation to the nucleus, binding to responsive DNA elements and regulation of gene expression by direct DNA binding or interactions with other transcription factors. From [186].

GCs during pregnancy

Glucocorticoids regulate many processes that are thought to both negatively and positively impact key aspects of early pregnancy. GC actions assist in regulation of the maternal immune system [221, 222], embryo attachment and invasion, stimulation of placental transport of glucose, lactate and amino acids [223, 224], as well as growth and development of the fetus [225, 226]. GCs have also been linked to adverse effects that would be expected to compromise pregnancy including inhibition of cytokine-prostaglandin signaling [227, 228], restriction of trophoblast invasion following up-regulation of serpin peptidase inhibitor (SERPINE1) [229], induction of apoptosis [225, 230], and inhibition of embryonic and placental growth [231, 232]. Administration of GCs has been used with success to increase pregnancy rates in women undergoing assisted reproductive technologies and pregnancy outcomes in women with a history of recurrent miscarriage: although these findings require additional verification [221, 233, 234]. In contrast, negative effects on pregnancy following GC treatment have been seen in studies using sheep. These studies found that administration of synthetic glucocorticoids reduced placental growth and development, and decreased binucleate cell number and circulating levels of placental lactogen (CSH1) [235].

The actions of GC are primarily mediated through GR signaling, and GR stimulates a number of genes implicated in regulation of cell growth, differentiation, and apoptosis as well cellular metabolism, signal transduction, and membrane transport [236-238]. Indeed, in the ovine uterus, intrauterine infusion of cortisol

stimulated the expression of a number of elongation- and implantation-related genes in the endometrium that are implicated in regulation of conceptus elongation via effects on the trophectoderm [59]. Recent characterization of the uterine GR knockout mouse showed GR to be important for blastocyst implantation and proper stromal cell differentiation [239]. Therefore, it is thought that homeostatsis of cortisol and its actions via GR are important for successful establishment of pregnancy and proper development to term in many species.

Gene Knockdown Approaches

Gene knockdown is a technique that refers to the reduction of gene expression either through genetic modification or treatment with a reagent that reduces mRNA abundance or translation. Genetic modification (CRISPRs) often results in production of a knockout animal, while temporary gene expression inhibition (MAOs or siRNAs) is often referred to as transient knockdown. Both techniques may be utilized to examine the function of a gene of interest.

Morpholino antisense oligonucleotides (MAO)

Oligonucleotides, oligonucleotide analogs, and other sequence-specific binding polymers designed to block translation of selected mRNA are commonly called "antisense oligos" [240]. Morpholino antisense oligonucleotides (MAOs) are distinct from other blocking peptides as the normal 5-membered-ring sugars of the nucleic acid backbone are replaced by 6- membered morpholine rings. Additionally, the negatively-charged phosphate intersubunit linkages of DNA and RNA are replaced by non-ionic phosphorodiamidate intersubunit linkages in MAOs

[240]. These two structural changes increase MAO's stability and binding affinity for complementary RNA sequences.

MAOs use Watson/Crick base pairing to bind selected target sites on mRNAs, and physically inhibit access of cellular components to that site. This technique can be used to design MAOs that block translation, splicing, miRNAs, miRNA targets, or ribozyme activity. Use of MAOs to block translation commonly results in targeting of the 5' untranslated region or areas surrounding the start codon of the RNA transcript. Through continuous steric blocking of the translation initiation complex, MAOs inhibit expression of the target so that after existing proteins have degraded, the target protein is no longer present. Unlike other transient knockdown methods, MAOs do not cause degradation of RNA targets; instead, they block the biological activity of the target RNA until it is degraded through normal cellular processes. Additionally, MAO are water soluble and are inexpensive to produce [241].

MAOs must be actively delivered into most cells, which can be achieved by scrape-loading adherent cells, electroporation, or through use of Endo-Porter delivery reagent [242]. Endo-Porter is an amphiphilic peptide with a hydrophobic face which associates with cell membranes once added to culture medium [243]. Endo-Porter delivers content into the cytosol of cells through internal budding of the cell membrane and uptake of components of the surrounding fluid (Figure 10). Following endosome formation and subsequent acidification (a natural process), the Endo-Porter contained within that endosome is converted to its poly-cationic form, which acts to permeabilize the endosomal membrane. This acid-induced

permeabilization of the endosomal membrane allows any co-endocytosed cargo to pass from the endosome into the cytosol of the cell. Because Endo-Porter is a peptide-based reagent which uses endocytosis for delivery, it is less toxic than other delivery mechanisms as it does not disrupt the plasma membrane. Infusion of fluorescently labeled MAOs, along with Endo-Porter, into the uterine lumen of pregnant ewes showed uptake primarily by the conceptus trophectoderm and significant effects on targeted protein abundance [244, 245].

MAOs along with Endo-Porter can easily be mixed and loaded into an osmotic pump for direct delivery into the uterine lumen during early pregnancy. ALZET osmotic pumps (Cupertino, CA, http://www.alzet.com) are miniature, implantable pumps that can be attached to a catheter to deliver liquid reagents at continuous and controlled rates. ALZET pumps operate through utilization of osmotic pressure differences between the pump and the tissue environment. The high osmolality within the salt sleeve of the pump causes water to flux inward through a semipermeable membrane which forms the outer surface of the pump. As the water enters the salt sleeve, it compresses the flexible reservoir, displacing the reagent from the pump at a controlled, predetermined rate [246]. Therefore, the rate of delivery by an ALZET pump is controlled by the water permeability of the pump's outer membrane and can be regulated to deliver controlled amounts of reagent over a set time period [247].

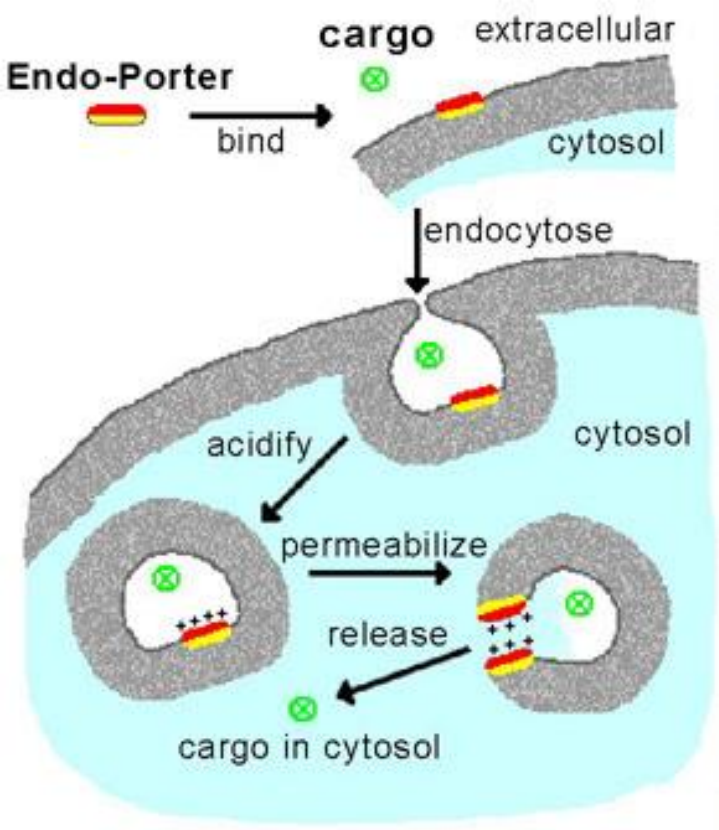

Figure 10. Use of Endo-Porter reagent for delivery of MAOs. Delivery of substances into the cytosol of cells by endocytosis-mediated processes that avoid damaging the plasma membrane of the cells. Use of this mechanism prevents the loss of cellular content, and its associated toxicity [248].

Short interfering RNA (siRNA)

RNA interference (RNAi) was first recognized as a natural antiviral defense mechanism in plants where long double-stranded RNAs generated during viral replication are cleaved by the enzyme Dicer into short 21–23 nucleotide double-stranded RNA molecules called small interfering RNAs (siRNAs) [249, 250]. These siRNAs function by inhibiting expression of specific genes through degradation of their mRNA after transcription. To achieve this, siRNAs associate with a multiprotein complex called the RNA-induced silencing complex (RISC), during which the siRNA sense strand is cleaved by the enzyme, Argonaute 2 (Ago2) [251]. The complimentary, antisense strand is contained within the activated RISC and guides RISC to the corresponding mRNA based on sequence homology. The Ago2 nuclease then cuts the target mRNA, resulting in specific gene silencing (Figure 11). RNAi can be used to target genes of interested through introduction of synthetic siRNA or by intracellular generation of siRNA from vector driven expression of the precursor small hairpin RNAs (shRNAs).

siRNAs have a well-defined structure of 20-24 base pair double stranded RNA molecules. Multiple bioinformatics tools are available to assist in design of siRNAs to target genes of interest. Typically more than half of randomly designed siRNAs provide at least a 50% reduction in target mRNA levels and approximately 1 of 4 siRNAs provide a 75-95% reduction [252]. Design of effective siRNAs can be increased by designing siRNAs with 3’ overhanging UU dinucleotides, keeping G/C between 30-50%, avoiding poly(T) sequence areas, designing siRNAs at different areas along the gene sequence, and by evaluating possible off target sites

[253]. Design of proper controls for siRNA induced knock down is also critical to ensure confidence in RNAi results. Combating off target effects in siRNA is challenging, as genes with incomplete complementary sequences to the siRNA are inadvertently down regulated.

Gene knockdown using siRNAs is limited due to their transient nature. Therefore siRNAs are often incorporated into expression vectors as shRNAs, which can later be processed into siRNAs in the cytoplasm. To achieve optimal delivery, shRNA vectors can be introduced via transient transfection, or through transduction with non-replicating recombinant viral vectors (Figure 11). Adeno viruses, adeno-associated viruses and lentiviruses are often used because they can infect actively dividing as well as resting and differentiated cells [254]. Lentiviruses are more favorable for long-term shRNA expression and gene silencing since their viral DNA is incorporated in the host genome. Although viral vectors can efficiently deliver shRNA leading to persistent siRNA expression [255], they also have potential toxicities associated with unregulated expression of large amounts siRNA, unexpected gene silencing due to promoter driven shRNA expression, and require additional training and proper facilities. Therefore significant time and effort has gone into optimizing recombinant viral vectors for regulated shRNA expression in different tissues.

Of particular note, the trophoblast lineage of the developing embryo can be selectively transfected via a lentiviral based approach due to the structure of the blastocyst and the tight epithelium formed by the outer trophectoderm, effectively restricting viral particle access to the inner cell mass (Figure 12). Developing

embryos can be exposed to the lentivirus either through extended incubation of blastocysts with their zonas removed in a lentiviral concentrate [256], or through micro-injection of lentivirus into the perivitelline space of zygotes or oocytes prior to hatching [257, 258].

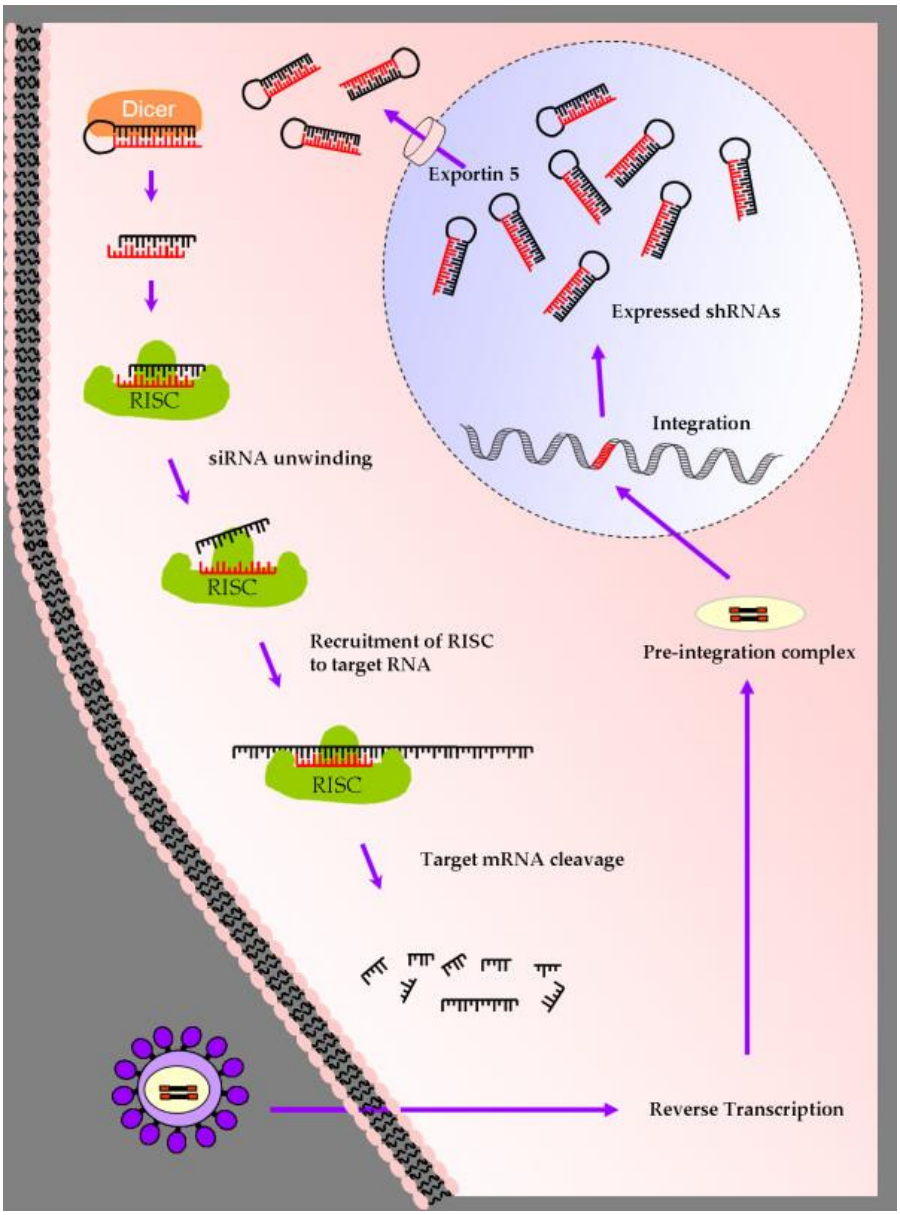

Figure 11. Mechanism of viral siRNA delivery, expression and targeting. Retroviruses can be used to deliver vectors containing targeting shRNAs that will integrate into the genome, and results in stable shRNA expression. Processing of these shRNA to siRNAs by DICER is followed by incorporation into the activated RNA-induced silencing complex (RISC) which uses the siRNA sequence to target complementary mRNA which is subsequently cleaved and degraded. Figure from [259].

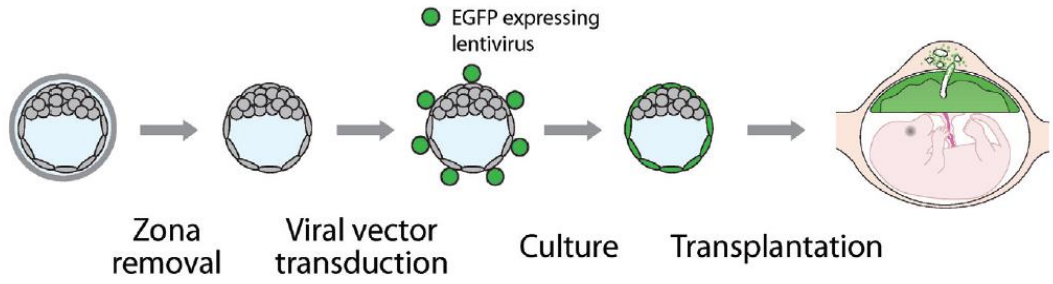

Figure 12. Select lentiviral transduction of the trophectoderm. Following zona removal, blastocysts transduced with lentiviral vectors display infection limited infection to the outermost cells, the trophectoderm. Select trophoblast infection is directly related to the structure of the blastocyst and the tight epithelium formed by the outer trophectoderm which restricts viral particle access to the inner cell mass. Lentiviral delivery of vectors containing constitutive promoters driving enhanced green fluorescence protein (EGFP) have been used to demonstrate the feasibility of using lentiviral transduction of shRNA for ‘‘loss-of-function’’ studies specifically in the trophoblast lineage. Image modified from [260].

Clustered Regularly Interspaced Short Palindromic Repeats (CRISPRs)

Similar to the use of siRNAs in plants, prokaryotes have developed a viral defense mechanism involving loci called 'Clustered Regularly Interspaced Short Palindromic Repeats', or CRISPRs. When invaded by a virus, one of the initial stages of the prokaryotic immune response is to capture a portion of the viral DNA and insert it into a CRISPR locus as a spacer [261]. CRISPR loci are composed of short, palindromic repeats that occur at regular intervals composed of alternate CRISPR repeats and variable CRISPR spacers [262]. These CRISPR loci are usually accompanied by adjacent CRISPR-associated (Cas) genes, specifically the endonuclease Cas9. Arrays within the CRISPR loci are transcribed by the host RNA polymerase and then cleaved by Cas proteins into smaller pieces containing a single spacer and a partial repeat [263]. Spacer with strong complementarity to incoming foreign DNA initiates a cleavage event using the Cas proteins. This DNA cleavage interferes with viral replication thereby providing immunity to the host organism.

The controlled use of endonucleases for genome editing had been proposed prior to characterization of the CRISPR/Cas9 system and included the use of zinc-finger nucleases (ZFNs) and transcription activator–like effector nucleases (TALENs) [264-267]. ZFN and TALENS act by tethering endonucleases to DNA-binding proteins to allow for targeted DNA double-stranded breaks (DSBs) at specific genomic loci. In contrast, the Cas9 protein in CRISPRs is a nuclease guided by small RNAs through Watson/Crick base pairing with target DNA [268, 269]. This key difference makes CRISPRs easier to design with greater target

specificity, as well as efficient and suitable for gene editing in a variety of cell types and organisms. The mechanism of action is similar between ZFNs, TALENs, and CRISPR/Cas9 as they all promote genome editing by stimulating a DSB at a target genomic locus [270]. In the CRISPR/Cas9 system, the target locus typically undergoes one of two major pathways for DNA damage repair: the error-prone NHEJ or the high-fidelity HDR pathway. Both pathways can be manipulated to achieve a desired editing outcome (Figure 14). In the absence of a repair template, DSBs are re-ligated through the NHEJ process, which leaves errors in the form of base pair insertions and deletions.

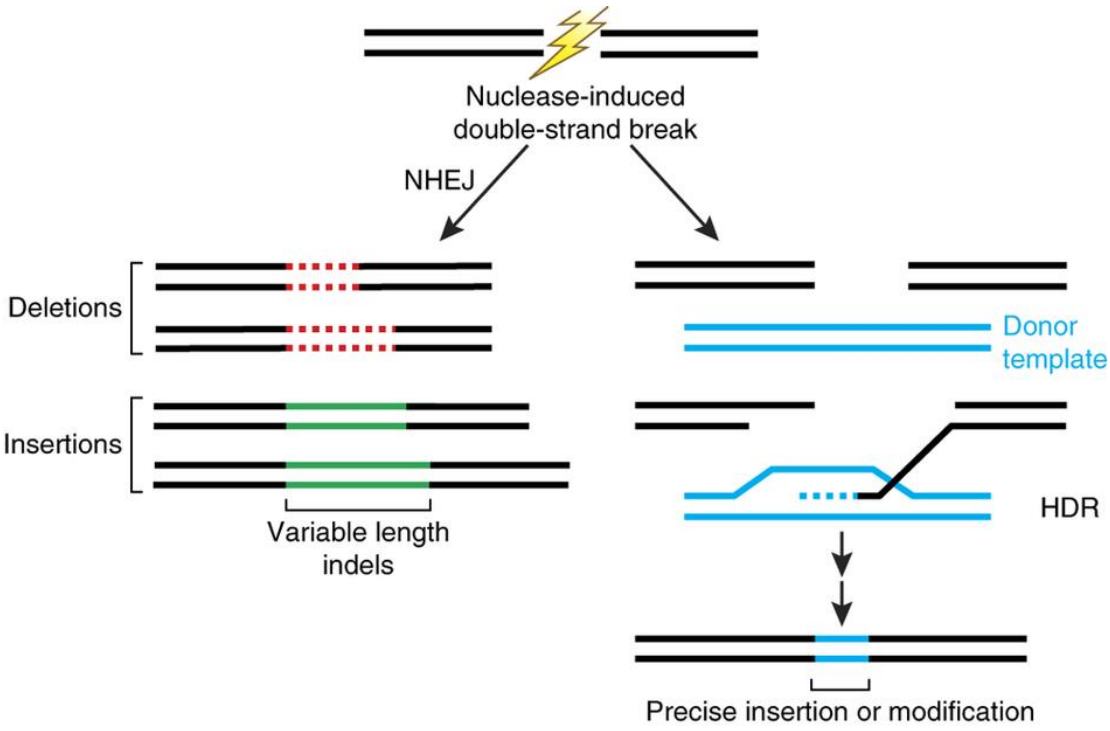

Figure 13. DNA repair mechanism following CRISPR/Cas9 mediated DSBs. Following Cas9 induced DSB, genomic DNA can undergo two different mechanisms of repair. NHEJ is error prone, and often results in insertions or deletions. These errors often result in differential codon usage and production of a premature stop codon. DNA can also undergo repair through HDR when template DNA is present. This repair mechanism occurs less frequently but can be utilized for insertions of specific DNA sequence into the area surrounding the DSB. Image from [271].

Therefore, NHEJ can be used to create gene knockouts, as insertions or deletions occurring within a coding exon can lead to frameshift mutations and premature stop codons [272]. Induction of multiple DSBs can be exploited to mediate larger deletions in the genome [273, 274]. Alternatively, HDR can be used, as an alternative major DNA repair pathway, to generate precise, defined modifications at a target locus or knock-in modifications when used in conjunction with a specific repair template [275].

Multiple CRISPR systems exist, although the best characterized and most widely used is the Type II, consisting of the nuclease Cas9, the crRNA array that encodes the guide RNAs and a required auxiliary trans-activating crRNA (tracrRNA) that facilitates the processing of the crRNA array into discrete units (Figure 14) [269, 276]. Each crRNA unit contains a 20-nucleotide guide sequence (gRNA) which directs Cas9 to a 20-bp DNA target via Watson/Crick base pairing. In the Type II CRISPR/Cas9 system the target DNA must immediately precede the sequence 5′-NGG-3’ also known as a protospacer adjacent motif (PAM) [263]. The specificity of the Cas9 nuclease is determined by the 20-nt guide sequence within the crRNA and cleaves the DNA 3 bp upstream of the PAM (Figure 15). Therefore, there are only two main criteria for the selection of a 20-nt guide sequence for gene targeting: the 5′-NGG PAM and minimizing off-target activity [277, 278]. On average, PAM sequences (NGG) occur every 10-12nt in the genome so targeting can be fairly sequence specific within a gene of interest. Multiple software programs are available provide optimize gRNA sequences to a region of interest, which can then be inserted into a synthesized tracerRNA sequence and delivered

into the cell via several methods. The CRISPR/Cas9 system can be used *in vitro* through transfections of a single plasmid containing both the gRNA and Cas9 protein components. Additionally, for generation of knockout animals CRISPRs can be injected into single cell zygotes as mRNA, or CRISPR edited cells can be used for traditional cloning using nuclear transfer techniques. The efficiency of gRNAs and editing across different organisms varies widely and optimization is key. The CRISPR/Cas9 system has been successfully utilized in multiple mammalian species including large animals (pigs, cattle, sheep, chickens, non-human primates) and smaller animals (mice, rats, guinea pigs) [279, 280]. Animal models created using the CRISPR/Cas9 system are important for furthering our understanding of gene function and often serve as important biomedical research models.

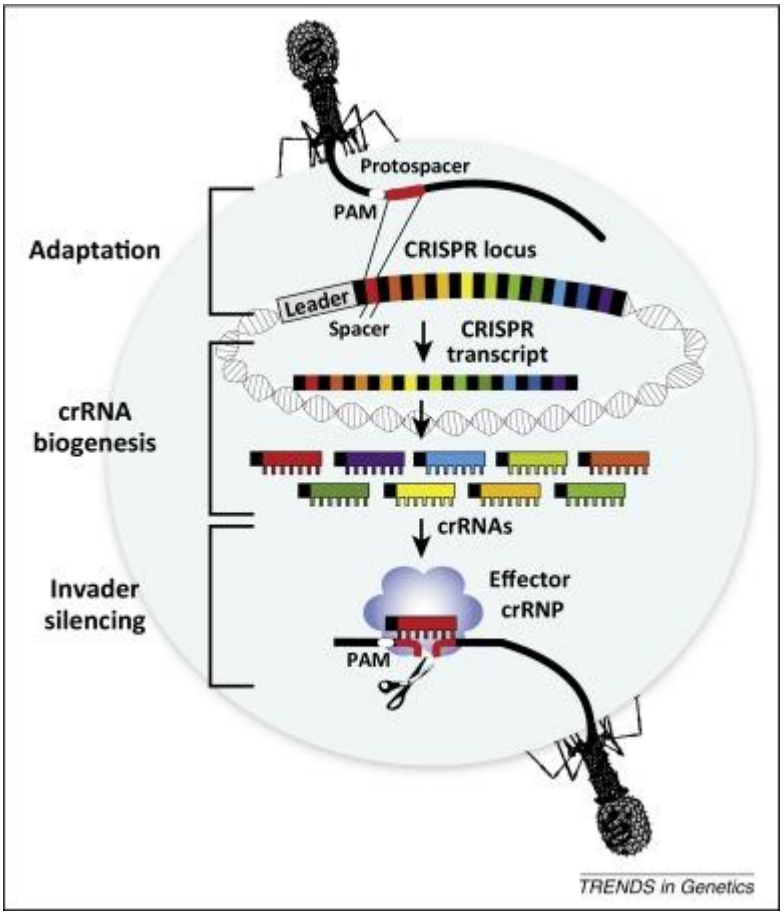

Figure 14. Overview of the CRISPR-Cas pathway for viral defense. For prokaryotes to recognize and silence a specific virus or other foreign genetic element, a short fragment of invader DNA is integrated into the host CRISPR locus. The CRISPR locus contains copies of a short direct repeat sequence (black) that separate the invader-derived sequences (multiple colors). Cas genes encoding the protein components of the system are typically located adjacent to CRISPR loci (not shown). Protospacer adjacent motifs (PAMs) are found immediately adjacent to viral sequences selected for CRISPR integration (protospacers). CRISPR locus transcripts are processed to generate multiple individual crRNAs. The crRNAs associate with Cas proteins to specifically recognizes foreign DNA via base-pairing of the crRNA and cleave the region of hybridization. PAMs provide important auxiliary signals for the recognition and silencing of invaders for some Type I and II DNA-targeting systems. Figure from [281].

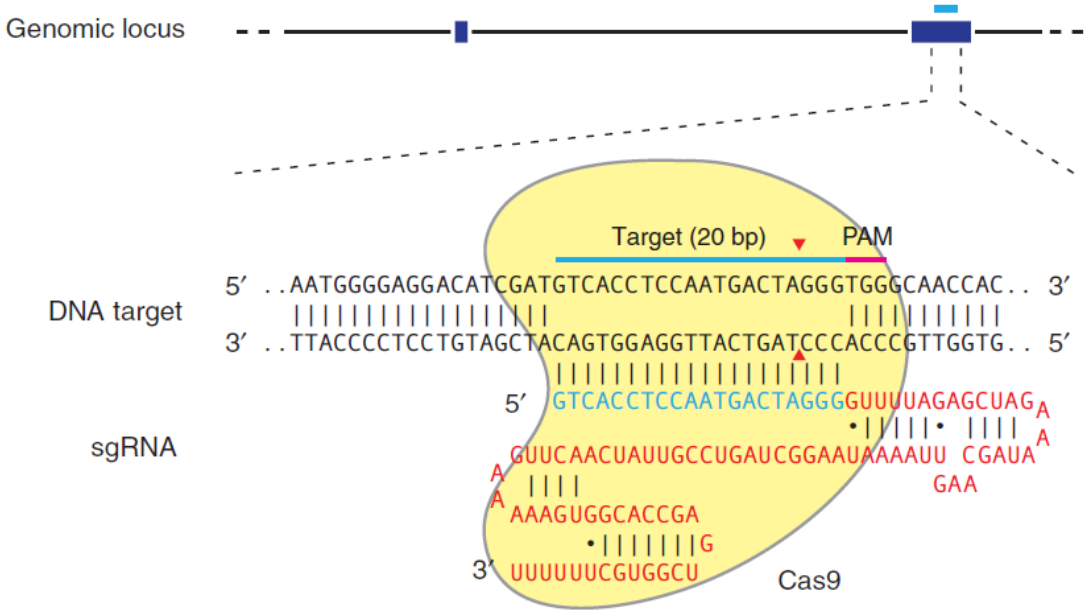

Figure 15. Schematic of the RNA-guided Cas9 nuclease. The Cas9 nuclease is targeted to specific genomic DNA regions by a sgRNA consisting of a 20-nt guide sequence (blue) and a scaffold (red). The guide sequence pairs with the DNA target (blue bar on top strand), directly upstream of a requisite 5′-NGG adjacent motif (PAM; pink). Cas9 mediates a DSB ~3 bp upstream of the PAM (red triangle). From [282]

SECTION II:

Biological roles of interferon tau (IFNT) and Type I IFN receptors in elongation of the ovine conceptus

Kelsey Brooks and Thomas E. Spencer

This work has been published in:

Biol Reprod. 2015 Feb;92(2):47. doi: 10.1095/biolreprod.114.124156. Epub 2014 Dec 10.

ABSTRACT

Interferon tau (IFNT) is produced by the elongating conceptus in ruminants and is the maternal recognition of pregnancy signal. Available evidence supports the idea that IFNT acts in a paracrine and autocrine manner to modulate expression of genes in the endometrium and trophectoderm, respectively, which promote conceptus elongation. The actions of IFNT are mediated by the interferon (alpha and beta) receptor (IFNAR), which is comprised of two subunits, IFNAR1 and IFNAR2. To test the hypothesis that IFNT and its receptor have biological roles in conceptus elongation, an *in vivo* loss of function study was conducted by inhibiting *IFNT or IFNAR1/2* mRNA translation in the trophectoderm of the ovine conceptus using morpholino antisense oligonucleotides (MAO) delivered via osmotic pumps from Days 8 to 14 post-mating. Elongating, filamentous type conceptuses were recovered from Day 14 ewes receiving a control morpholino or IFNAR MAOs. In contrast, severely growth-retarded and malformed conceptuses were recovered from IFNT MAO-infused ewes. Those conceptuses contained abnormal trophectoderm cells that were apoptotic based on TUNEL analyses. IFNT concentrations were reduced in the uterine lumen of IFNT MAO-infused ewes, as was the expression of classical Type I IFN-stimulated genes in the endometrium. IFNT concentrations were also lower in the uterine lumen of IFNAR1/2 MAO-infused ewes. These studies provide *in vivo* evidence that IFNT is a critical regulator of conceptus elongation and that it's embryotrophic actions are primarily mediated by paracrine effects on the endometrium.

INTRODUCTION

The ovine blastocyst hatches from the zona pellucida on Day 8 and develops into an ovoid or tubular conceptus (embryo and associated extraembryonic membranes) that grows and elongates into a filamentous form between Days 12 and 16 [15]. The mononuclear trophectoderm cells in the elongating ruminant conceptus synthesize and secrete interferon tau (IFNT) and prostaglandins (PGs). A significant increase in IFNT and PG production occurs after Day 12 as the conceptus develops from a spherical to filamentous form [132, 283-285]. Interferon tau is a member of the Type I IFN family [90] and is the maternal recognition of pregnancy signal in ruminants [72, 286]. As a pregnancy recognition signal, IFNT acts in a paracrine manner on the endometrium to inhibit development of the luteolytic mechanism, thereby ensuring continued production of progesterone by the corpus luteum (CL) of the ovary [72, 287].

Available evidence supports the idea that conceptus-derived IFNT and PGs are also embryotrophic, as they both act in a paracrine manner to modulate expression of progesterone-induced elongation- and implantation-related genes in the endometrial epithelia that, in turn, are hypothesized to promote conceptus elongation via effects on the trophectoderm [35, 39, 72-74, 103, 288-290]. Of note, IFNT and PGs from the elongating conceptus stimulate a number of progesterone-induced genes in the endometrial luminal epithelium (LE) and superficial glandular epithelium (sGE) of the ovine uterus that encode enzymes (*HSD11B1*) and secreted proteins (*CST3, CTSL1, GRP, IGFBP1, LGALS15*), as well as transporters for glucose (*SLC2A1, SLC2A5, SLC5A11*) and amino acids

(*SLC7A2*). In the endometrial GE and stroma, IFNT induces or substantially stimulates expression of a large number of classical Type I IFN stimulated genes (ISGs), including *ISG15,* chemokine (C-X-C motif) ligand 10 *(CXCL10),* and the radical S-adenosyl-containing domain 2 (*RSAD2*) that may also have biological roles in conceptus elongation [290]. Of note, PGs are particularly important for conceptus elongation in sheep, because intrauterine infusion of meloxicam, a selective PTGS2 inhibitor, into the uterine lumen from Days 8 to 14 post-mating completely inhibited conceptus elongation [57]. The biological role of IFNT in conceptus elongation has not been studied using a loss-of-function approach, however our recent data supports the idea that IFNT has an embryotrophic effect on conceptus elongation [59].

Like other Type I IFNs, IFNT signals via the interferon (alpha and beta) receptor (IFNAR), which is a cell membrane receptor comprised of two subunits, IFNAR1 and IFNAR2 [98, 291]. Ligand-induced dimerization of the subunits results in activation of canonical and non-canonical signaling pathways. The canonical Type I IFN and IFNT signaling pathway involves janus kinase-signal transducer and activator of transcription-interferon regulatory factor (JAK-STAT-IRF) signaling that results in induction of a large number of classical ISGs [100, 102, 292]. The non-canonical Type I IFN signaling pathway involves mitogen-activated protein kinase (MAPK) and phosphatidylinositol 3-kinase thymoma viral proto-oncogene 1 (PI3K-AKT1) cascades [109]. Recent evidence indicates that IFNT activates MAPK (ERK1/2), PI3K-AKT1, and Jun N-terminal kinase (JNK) signaling in the endometrium of the ovine uterus as well as in ovine uterine cells *in vitro* [110, 111].

Ovine and bovine *IFNAR1* and *IFNAR2* mRNAs were cloned from the endometrium, and both were found to be expressed in cyclic and pregnant endometrium, but not in Day 15 ovine conceptuses using RT-PCR analysis [293]. In contrast, Imakawa and coworkers [294] observed immunoreactive IFNAR1 protein in Day 14 and 16 ovine conceptuses using an antibody against human IFNAR1. Further, Wang and coworkers [295] detected *IFNAR1* mRNA in both Day 15 and 20 ovine conceptuses by RT-PCR and found that expression of several classical ISGs (*BST2, ISG15, OAS1*) could be induced in ovine trophectoderm cells treated with recombinant bovine IFNT *in vitro.* Similar to IFNT, the biological role of IFNAR in conceptus elongation has not been studied using a loss of function approach.

Collectively, available studies support the hypothesis that the embryotrophic actions of IFNT are mediated by paracrine as well as autocrine actions that promote conceptus elongation in ruminants. In order to test this hypothesis, an *in vivo* morpholino loss of function study was conducted by specifically inhibiting *IFNT* or *IFNAR1/2* mRNA translation in the trophectoderm of the developing ovine conceptus.

MATERIALS AND METHODS

Morpholino Design and Validation

Design. Morpholino oligonucleotides were designed and synthesized by Gene Tools (Philomath, OR) to specifically target only one mRNA. The IFNT morpholino antisense oligonucleotide (MAO)

(TCAGTAGAGAGAGCACGAAGGCCAT) targets the first 25 bp of the ovine *IFNT* mRNA coding sequence (CDS) (GenBank accession no. X56343.1). The *IFNAR1* MAO (CGGCAGCCCTCCAGTCACATCTTTC) targets 86 to 110 bp of the 5' untranslated region (UTR) of the ovine *IFNAR1* mRNA that is only 15 bp upstream of the ATG (GenBank accession no. U65978.1). The *IFNAR2* MAO (CTGACACATTCTGACTCAAAAGCAT) targets the first 25 bp of the ovine *IFNAR2* mRNA CDS (GenBank accession no. NM_001009342.1). In Study One, a standard control morpholino (MO) (CCTCTTACCTCAGTTACAATTTATA) was used that targets a splice site mutant of *Homo sapiens hemoglobin beta-chain (HBB)* gene (GenBank accession no. AY605051) that is not present in the *Ovis aries* genome. For Study Two, a random oligo 25-N morpholino was used as a control, as it is synthesized with a random base at every position and does not target any known mRNAs (Gene Tools).

Validation of IFNT MAO. The complete CDS for ovine *IFNT* (GenBank accession no. X56343.1), along with additional 5' and 3' restriction sites, was synthesized as a gBlock Gene Fragment by Integrated DNA Technologies (IDT, Coralville, IA). The resulting gBlock fragments were assembled using a Gibson assembly cloning kit (New England Biolabs, Ipswich, MA), and ligated into the pCMV6-A-Puro (Origene, Rockville, MD) mammalian expression vector using T4 DNA ligase (Invitrogen, Carlsbad, CA). The resulting vectors were sequenced for verification purposes. Human 293T cells were transfected with pCMV6-A-Puro-IFNT with Lipofectamine 2000 (Invitrogen). After 24 h, cells were incubated with Endo-Porter delivery reagent (GeneTools) (6 µl per 1 ml) and 2 µM, 4 µM or 8 µM

of IFNT MAO. After 48 h, the media from the cells was harvested, and protein concentration determined. Equal amounts of protein were mixed with Laemmli sample buffer (31.5 mM Tris-HCl (pH 6.8), 10% glycerol, 5% β-mercaptoethanol, 1% SDS, 0.01% bromophenol blue), denatured at 95°C for 5 min, and separated by SDS-PAGE at a constant voltage of 150 V for approximately 90 minutes in 1X running buffer (25 mM Tris, 192 mM glycine, 0.1% SDS). Proteins were transferred to 0.45 µm Protran BA 85 nitrocellulose membrane (GE Healthcare, Buckinghamshire, UK) in Towbin transfer buffer (25 mM Tris, 192 mM glycine, 20% methanol) at 100 V for 60 minutes. Membranes were placed in blocking buffer (TBS, 5% non-fat milk, 0.1% Tween 20) for 1 hour at room temperature and then incubated in primary rabbit anti-ovine IFNT serum [105] at 1:1000 dilution in blocking buffer overnight at 4°C. Membranes were then washed with TBS containing 0.1% Tween 20 (TBST) before incubation with goat anti-rabbit HRP conjugated secondary antibody (Thermo Scientific) at 1:10,000 dilution for 1 hour at room temperature. Membranes were washed with excess TBST and incubated with SuperSignal West Pico Chemiluminescent Substrate (Thermo Scientific) for 3 minutes prior to imaging with a ChemiDoc MP system and Image Lab 4.1 software (BioRad, Hercules, CA).

Validation of IFNAR1, IFNAR2 and IFNT MAO using an in vitro translational inhibition assay. Oligos analogous to the partial ovine *IFNAR1*, *IFNAR2* and *IFNT* mRNA coding sequences (CDS) were synthesized by Integrated DNA Technologies (Supplementary Table 1). Oligos were designed to include a 5' *NheI* overhang, portion of the mRNA to be targeted and bound by the MAO, and a 3'

NheI overhang. The psiCHECK2 dual luciferase (LUC) reporter plasmid (Promega, Madison, WI) was digested with the restriction enzyme *NheI*, and subsequently treated with antarctic phosphatase (NEB). Oligos were annealed and ligated into psiCHECK2 using T4 DNA ligase (Life Technologies, Carlsbad, CA), upstream and in-frame with LUC. The resulting vectors were sequenced (Washington State University Molecular Biology and Genomics Core) for verification. Human 293T cells were transfected with psiCHECK2:IFNAR1 CDS LUC or psiCHECK2:IFNAR2 CDS LUC vectors using Lipofectamine 2000 (Life Technologies). After 6 h, cells were incubated with Endo-Porter delivery reagent (GeneTools) (6 µl per 1 ml) and 2, 4 or 8 µM of IFNAR1 MAO, IFNAR2 MAO, IFNT MAO or Control MO. After 48 h, cell lysates were analyzed for luciferase activity using dual luciferase reporter assay system (Promega).

Experimental Designs

All experimental and surgical procedures were approved by the Institutional Animal Care and Use Committee of Washington State University. For both studies, mature Columbia Rambouillet crossbred ewes (*Ovis aries*) were observed for onset of estrus (designated Day 0). Ewes were mated to an intact ram of proven fertility on Days 0 and 1.

Study One. On Day 8 post-mating, ewes were subjected to a midventral laparotomy. Ewes were then randomly assigned to the following groups ($n \geq 5$ ewes per group): (1) no uterine horn ligation; (2) uterine horn ligation but no intrauterine injection; (3) uterine horn ligation followed by single intrauterine injection of

standard control MO; or (4) uterine horn ligation and constant intrauterine infusion of standard control MO using an osmotic pump. Using methods described previously [57, 244, 296], ewes in Groups 2-4 had the base of the uterine horn ipsilateral to the CL double ligated using non-absorbable, sterile polyester umbilical tape to prevent migration and growth of the conceptus through the uterine body into the contralateral uterine horn. For group 3, the standard control MO (100 nmol) was complexed with Gene Tools Endo-Porter Aqueous delivery reagent (50 µl) and diluted to a 1 ml final volume with Opti-MEM (Catalog number 31985-062; Life Technologies, Grand Island, NY). The MO solution was then introduced into the lumen of the ligated uterine horn via the uterotubal junction using a 1 cc syringe fitted with a Tom Cat Catheter. After the MO solution was discharged into the uterine lumen, the catheter was withdrawn, and the uterine horn was gently massaged to distribute the MO throughout the uterine lumen. For group 4, a vinyl catheter (Item no. 0007760, Durect Corporation, Cupertino, CA), connected to a preloaded and equilibrated Alzet 2ML1 Osmotic Pump (Durect Corporation), was inserted 1 cm distal to the uterotubal junction into the lumen of the ligated uterine horn. The Alzet 2ML1 Osmotic Pump is factory calibrated to constantly deliver 10 µl per h (240 µl/day) for 7 days. The pumps were loaded with standard control MO (100 nmol) complexed with 50 µl of Gene Tools Endo-Porter Aqueous delivery reagent in 2 ml sterile PBS (Hyclone, Logan, UT). The Alzet pump was then affixed to the mesosalpinx supporting the oviduct using cyanoacrylate glue (SUPER GLUE, Bentonville, AR) and secured by suturing the mesosalpinx to the perimetrium of the uterine horn using 0 Coated Vicryl suture (Ethicon, Somerville,

NJ). After ligation and/or pump implantation, the outside of the uterus was rinsed with sterile 5% (vol/vol) glycerol in saline to prevent the formation of adhesions and placed back in the body cavity prior to closing the body cavity and skin. All ewes were necropsied on Day 14 post-mating. The female reproductive tract was recovered, and the uterine horn(s) gently flushed with 20 ml of sterile PBS. If present, the morphology of the conceptus was recorded (spherical, tubular, or elongated) and length carefully measured using a ruler and stereomicroscope.

Study Two. On Day 8 post-mating, ewes were subjected to a mid-ventral laparotomy. Using procedures described above in Study One, a uterine horn ipsilateral to the CL was ligated and fitted with an osmotic pump containing either: (1) random oligo 25-N control MO; (2) IFNT MAO; or (3) an equal mixture of IFNAR1 and IFNAR2 MAOs. Each pump contained a total of 100 nmol of the indicated morpholino complexed with 50 µl of Gene Tools Endo-Porter Aqueous delivery reagent in 2 ml sterile PBS (Hyclone, Logan, UT). All ewes ($n \geq 5$ per treatment) were necropsied on Day 14 post-mating. The female reproductive tract was recovered, and the ligated uterine horn gently flushed with 10 ml of sterile PBS (pH 7.2). If present, the state of conceptus development was assessed using a Nikon SMZ1000 stereomicroscope (Nikon Instruments Inc., Lewisville, TX) fitted with a Nikon DS-Fi1 digital camera. The volume of the uterine flush was measured, and the flush clarified by centrifugation (3000 x g at 4°C for 15 min). The supernatant was carefully removed with a pipet, mixed, aliquoted, frozen in liquid nitrogen, and stored at -80°C. Portions of the conceptus were fixed in fresh 4% paraformaldehyde in PBS (pH 7.2). After 24 h, fixed tissues were changed to 70%

ethanol for 24 h and then dehydrated and embedded in Paraplast-Plus (Oxford Labware, St. Louis, MO). The endometrium was physically dissected from the remainder uterine horn using curved scissors. Endometrial samples as well as any remaining conceptus tissue were frozen in liquid nitrogen, and stored at -80°C for subsequent RNA extraction.

Study Three. On Day 8 post-mating, ewes (n=8) were subjected to a mid-ventral laparotomy. Using procedures described above, a uterine horn ipsilateral to the CL was ligated and fitted with an osmotic pump containing 100 nmol of IFNT MAO complexed with 50 µl of Gene Tools Endo-Porter Aqueous delivery reagent in 2 ml sterile PBS (Hyclone). The uterus was recovered from all ewes on Day 12. The uterus was also recovered from an additional group of bred, unligated ewes (n=8) on Day 12 post-mating as a control. The female reproductive tract was recovered, and the ligated uterine horn gently flushed with 10 ml of sterile PBS (pH 7.2). If present, the state of conceptus development was assessed using a Nikon SMZ1000 stereomicroscope Uterine flush and tissues were processed as described in Study Two.

Quantification of IFNT in Uterine Flush

The amount of IFNT in the uterine flush of ewes from Studies Two and Three was quantified using previously described methods [105]. A sample of the uterine flush (100 µl) from each ewe was diluted to 200 µl final volume with 10 mM Tris buffered saline (TBS). A nitrocellulose membrane (GE Healthcare-Life Sciences, Pittsburgh, PA), presoaked with TBS, was loaded into a BioRad dot blot

apparatus (Hercules, CA) backed by Whatman filter paper. Wells were subsequently washed with 200 µl TBS prior to addition of the diluted uterine flush sample, and then rinsed with 200 µl TBS. The membrane was allowed to air dry and then blocked in 5% (wt/vol) milk/TBS-tween (TBST) for 1 h at room temperature. The membrane was then incubated in primary rabbit anti-ovine IFNT serum at 1:1000 dilution in 5% milk/TBST overnight at 4°C. The membrane was then washed for 30 min in TBST followed by incubation with goat anti-rabbit IgG horseradish peroxidase conjugate (Thermo Scientific) at 1:5,000 diluted in 5% milk/TBST for 1 h at room temperature. The membrane was washed again for 30 min in TBST. Immunoreactive IFNT was detected using SuperSignal West Pico Chemiluminescent Substrate (Thermo Scientific) and quantified with a ChemiDoc MP system and Image Lab 4.1 software (BioRad). The data are expressed as total relative amount of IFNT in the uterine flush determined by adjusting for the recovered volume of uterine flushing.

Quantification of PGs in the Uterine Flush

Prostaglandins in the uterine flush from Studies Two and Three were measured by sensitive enzyme immunoassay (EIA) from Cayman Chemical (catalog no. 514012; Ann Arbor, MI). The antiserum used in this assay exhibits high cross reactivity for most PGs, which allows quantification of all the PGs in a given sample with a single assay (Cayman Chemical). Total PGs in the uterine flush were measured according to the manufacturer's recommendations in a single assay with a sensitivity of 15.6 pg/ml. The data are expressed as total amounts of

PGs in the uterine flush determined by adjusting for the recovered volume of uterine flushing.

Total RNA Isolation and Real-Time PCR Analysis

Total RNA was isolated from endometrial samples using Isol-RNA lysis reagent (5 Prime, Gaithersburg, MD) according to the manufacturer's protocol. To eliminate genomic DNA contamination, extracted RNA was treated with DNase I and purified using RNeasy MinElute cleanup kit (Qiagen, Valencia, CA). The quantity and quality of total RNA were determined by spectrometry. Total RNA (1 µg) from each sample was reverse transcribed in a total reaction volume of 20 µl using iScript RT supermix (BioRad, Hercules, CA). Reverse transcription was performed as follows: 5 min at 25°C; 30 min at 42°C; and 5 min at 85°C. Control reactions in the absence of reverse transcriptase were prepared for each sample to test for genomic DNA contamination. The resulting cDNA was stored at -20°C for further analysis.

Real-time PCR was performed using BioRad CFX384 Touch Real Time System (BioRad, Hercules, CA) with SsoAdvanced Universal SYBR Green Supermix (BioRad, Hercules, CA). Previously published primers for *CXCL10, CTSL1, GAPDH, ISG15, IGFBP1, RSAD2, SLC2A1, SLC5A1* and *SLC7A2* were used [57], and primers for ovine *GRP* and *LGALS15* were designed and synthesized by IDT (Supplementary Table 1). Each individual sample was analyzed in duplicate with the following conditions for 40 cycles: 95°C for 30 sec; 95°C for 5 sec; and 60°C for 30 sec. A dissociation curve was generated at the

end of amplification to ensure that a single product was amplified. PCR reactions without template and template substituted with total RNA were used as a negative control to verify experimental results. The threshold line was set in the linear region of the amplification plot above the baseline noise, and quantification cycle (Cq) values were determined as the cycle number in which the threshold line intersected the amplification curve. Ovine *GAPDH* was used as the reference gene.

Immunohistochemistry

Fixed conceptuses from Study Two were embedded in paraffin wax and sectioned (6 µm). Sections were mounted on slides, deparaffinized in xylene substitute, and rehydrated in a graded alcohol series. Sections were then submitted to hematoxylin and eosin staining (Scytek, Logan, UT), immunohistochemistry, or TUNEL apoptosis assay. For immunohistochemistry, antigen retrieval was performed by incubating sections for 10 min in boiling 10 mM citrate buffer (pH 6.0). After cooling to room temperature, sections were incubated with 10% normal goat serum in PBS (pH 7.5) for 10 min at room temperature and then overnight at 4°C with rabbit anti-Ki67 IgG (1.2 µg/ml of 1% BSA in PBS, pH 7.5; cat. no. ab66155, Abcam, Cambridge, MA, USA). Sections were washed in PBS and incubated with biotinylated secondary antibody (5 µg/ml; PK-4001; Vector Laboratories, Burlingame, CA, USA) for 1 h at 37°C. Immunoreactive Ki67 protein was visualized using Vectastain ABC kit (Vector Laboratories) using diamino-benzidine tetrahydrochloride as the chromagen. Sections were counterstained with hematoxylin, and coverslips were affixed to slides with Permount mounting medium (Fisher Scientific, Fairlawn, NJ, USA). Images of

representative fields were recorded using a Nikon Eclipse 90i model photomicroscope fitted with a Nikon DS-Ri1 digital camera.

TUNEL apoptosis assay

Terminal deoxynucleotidyl transferase (TdT)-mediated dUTP nick-end labeling (TUNEL) assay (Catalog No. G3250; Promega Corporation, Madison, Wisconsin) was performed according to the manufacturer's instructions for paraffin-embedded tissue, with slight modification. Briefly, sections from conceptuses in Study Two were rehydrated and fixed in 4% methanol free paraformaldehyde (PFA) in PBS for 15 min at room temperature. The tissue was permeabilized with Proteinase K for 8 minutes then washed with PBS and fixed in PFA. Slides were then covered with equilibration buffer for 5-10 minutes at room temperature followed by incubation with the TdT incubation buffer (containing TdT and nucleotide mix) for 1 hour at 37 °C, in a humidified chamber. The reaction was terminated by submersion of slides in 2x SSC for 15 minutes at room temperature. The sections were washed with PBS and cover slips applied using Vectashield mounting media with DAPI (Vector laboratories). Images of representative fields were recorded using a Nikon Eclipse 90i model photomicroscope fitted with a Nikon DS-Ri1 digital camera. Brightfield and epifluorescent (DAPI and FITC) images were collected using NIS Elements BR 3.2 software. Background fluorescence was corrected based on FITC intensity in positive control slides produced by DNase I (Qiagen) treatment according to manufacturer's instructions.

Statistical Analysis

All quantitative data were subjected to least-squares analyses of variance (ANOVA) using the General Linear Models (GLM) procedures of the Statistical Analysis System (SAS Institute Inc., Cary, NC). For analyses of real-time PCR data, *GAPDH* values were used as a covariate. Error terms used in test of significance were identified according to the expectation of the mean squares for error. Significance ($P<0.05$) was determined by probability differences of least-squares means (LSM).

RESULTS

Study One: Effects of Uterine Ligation on Conceptus Elongation

Pregnancy rates averaged 90% and were not different ($P>0.10$) between unligated control and ligated ewes (data not shown). Elongating conceptuses were recovered from all pregnant ewes (Figure 1). Conceptus length was not different ($P>0.10$) in bred ewes without uterine horn ligation (Unligated Control) as compared to ewes with one uterine horn ligated and no intrauterine injection of morpholino (Ligated Control). In uterine horn ligated ewes, conceptus length was 2.4-fold shorter ($P<0.01$) in ewes receiving a bolus injection of standard control MO in Opti-MEM on Day 8 post-mating as compared to those receiving no MO (Ligated Control) or constantly infused with the standard control MO in PBS using an osmotic pump. Of note, no difference in conceptus length ($P>0.10$) was observed in uterine horn ligated ewes constantly infused with the standard control MO in PBS as compared to those receiving no morpholino (Ligated Control).

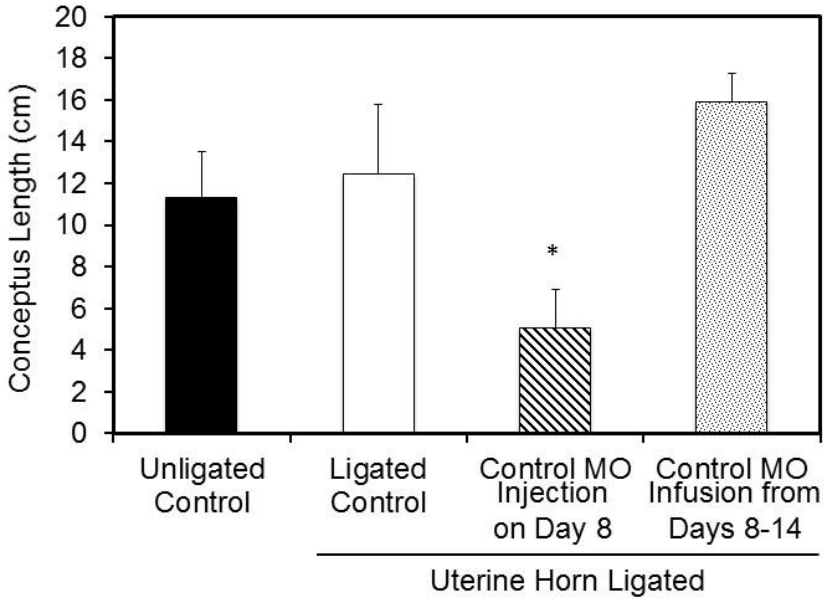

FIGURE 1. Effects of uterine ligation and morpholino delivery procedure on conceptus elongation in sheep. On Day 8 post-mating, ewes were randomly assigned to one of the following groups ($n \geq 4$-5 ewes per group): (1) unligated control; (2) uterine horn ligated control (no intrauterine injection); (3) uterine horn ligation and single bolus intrauterine injection of standard control MO in 1 ml of Opti-MEM; or (4) uterine horn ligation and constant intrauterine infusion of standard control MO in PBS using an implanted osmotic pump. Length of the recovered conceptuses was determined on Day 14 for all ewes. The asterisk (*) denotes a difference ($P<0.01$) in conceptus length.

Studies Two and Three: Inhibition of IFNT Inhibits Conceptus Elongation

Morpholinos are short chains of morpholino subunits comprised of a nucleic acid base, a morpholine ring, and a non-ionic phosphorodiamidate intersubunit linkage and not sensitive to nucleases [240]. They act through RNase H-independent steric interference to block translation of target mRNAs [297]. Morpholinos were designed to specifically inhibit translation of ovine *IFNT, IFNAR1*

or *IFNAR2* mRNA. Effectiveness of MAO translation inhibition was assessed *in vitro* using transiently transfected HEK 293T cells. Increasing amounts of IFNT MAO decreased the amount of IFNT in the media from cells transfected with an ovine IFNT expression vector (Figure 2). The Control MO had no effect (data not shown). As illustrated in Figure 3, treatment of cells transfected with ovine IFNAR1 CDS-LUC, IFNAR2 CDS-LUC, or IFNT CDS-LUC vectors with the appropriate IFNAR MAO inhibited ($P<0.01$) luciferase activity, whereas the Control MO had no effect ($P>0.10$).

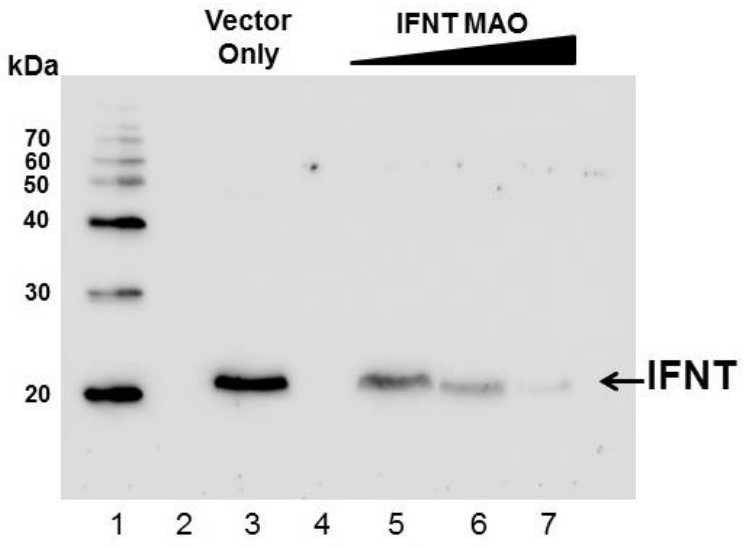

FIGURE 2. Validation of IFNT morpholino antisense oligonucleotides (MAO). HEK 293T cells were transfected with an expression vector encoding ovine IFNT, and cells were treated with nothing (lane 3) or increasing amounts of IFNT MAO at 2 µM (lane 5), 4 µM (lane 6) or 8 µM (lane 7). After 48 h, the abundance of IFNT in the culture media was determined by Western blot analysis. Results are representative of three different transfection experiments.

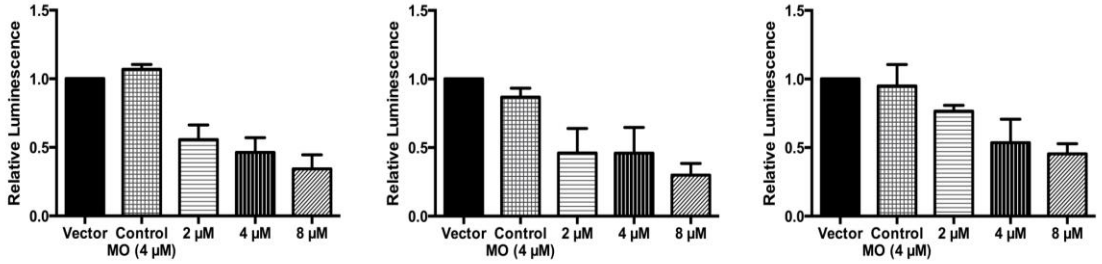

FIGURE 3. *In vitro* validation of IFNAR1, IFNAR2 and IFNT morpholinos. HEK 293T cells were transfected with psiCHECK2, a luciferase reporter vector, containing a portion of the coding sequence (CDS) for either ovine *IFNAR1*, *IFNAR2* or *IFNT* upstream and in frame with the luciferase (LUC) gene. After 6 h, cells were treated with nothing (Vector only), a Control morpholino (MO; 4 µM) or specific MAO (2, 4 or 8 µM) along with the Endo-porter delivery reagent. After 24 h, luciferase activity was assayed in lysed cells. Data for the morpholinos is presented as relative to the vector only. Differences (P<0.01; MAO vs Control MO) are denoted with an asterisk (*).

In vivo loss of function studies were then conducted to determine the effect of IFNT and IFNAR MAO on conceptus elongation in sheep. This approach is based on previous studies demonstrating that *in utero* administration of labeled morpholinos results in their delivery primarily to the conceptus trophectoderm [244, 298]. Pregnancy rates averaged 85% and were not different (P>0.10) between ewes receiving Control MO, IFNT MAO, or IFNAR1/2 MAO (data not shown). Conceptuses recovered on Day 14 from ewes receiving Control MO and IFNAR1/2 MAO from Day 8 were elongated and filamentous (Figure 4 and Table 1), consistent with normal conceptus morphology in Day 14 pregnant ewes [18, 35]. However, conceptuses collected on Day 14 from IFNT MAO infused ewes were small and malformed. Histological examination found that conceptuses recovered from ewes infused with Control MO or IFNAR1/2 MAO were normal containing many mononuclear trophectoderm cells lined with endoderm (Figure 4). In

contrast, conceptuses from IFNT MAO infused ewes contained almost no distinct mononuclear trophectoderm cells or endoderm.

Elongation of the conceptus primarily involves proliferation of the mononuclear trophectoderm cells [15, 18]. Cell proliferation was assessed by immunostaining conceptuses for Ki67, a nuclear protein that is associated with cellular proliferation [299]. Nuclear Ki67 protein was observed in all cells of the conceptuses regardless of treatment group (Figure 4). Apoptosis was assessed using a fluorometric TUNEL assay [300, 301]. Apoptotic cells were particularly prevalent in conceptuses recovered from IFNT MAO infused ewes, but were very low in conceptuses from Control MO or IFNAR1/2 MAO infused ewes (Figure 4).

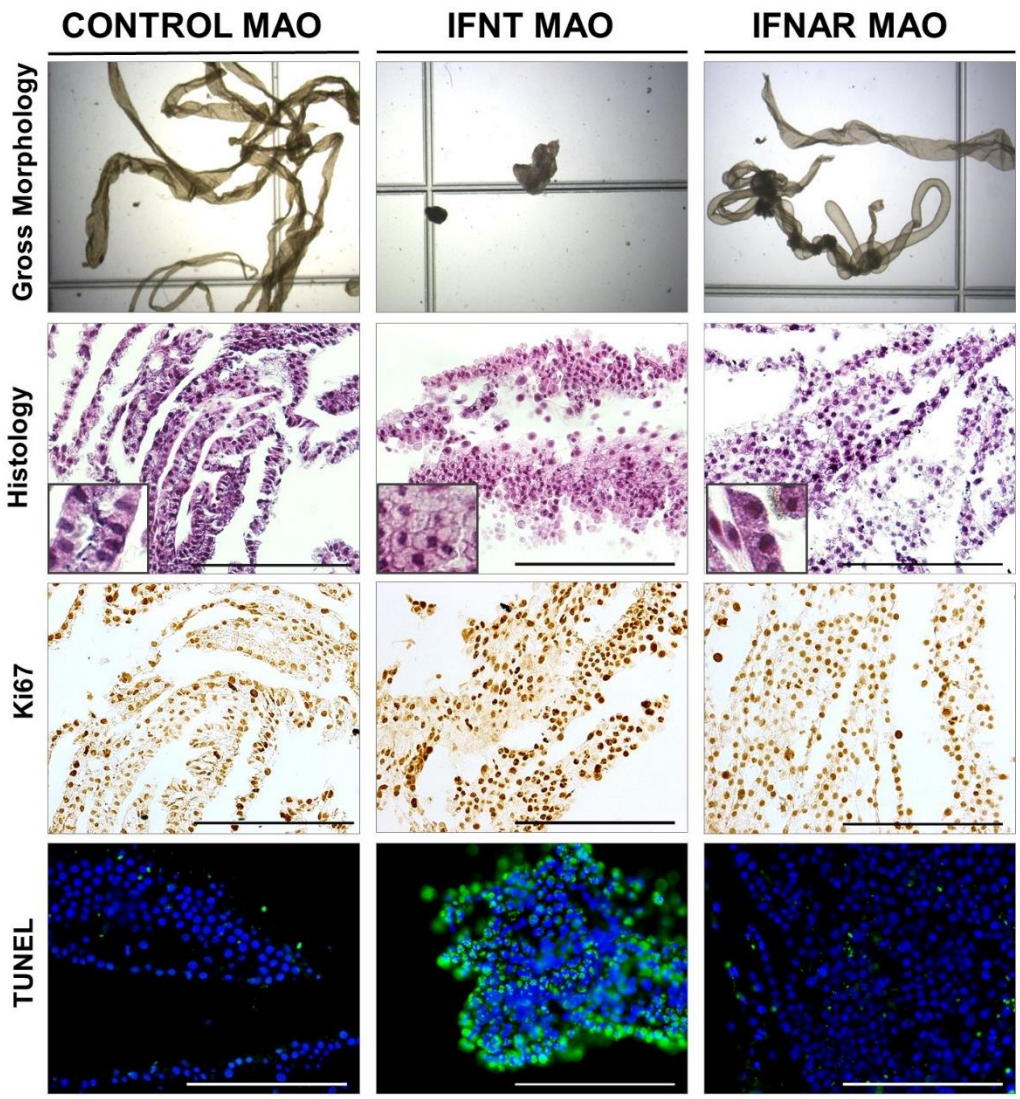

FIGURE 4. Effect of morpholino treatment on conceptus morphology, histology, proliferation and apoptosis. Control MO, IFNT MAO or IFNAR MAOs (IFNAR1 MAO and IFNAR2 MAO) was infused into the uterine lumen of uterine horn ligated ewes on Day 7 post-mating (n≥7 per morpholino type). Conceptuses were recovered on Day 14. Conceptus morphology was examined using a stereomicroscope; all photomicrographs of gross morphology are at the same magnification. Portions of the conceptuses were then fixed in paraformaldehyde, embedded in paraffin, sectioned and stained with hematoxylin and eosin (H&E). The inset in the left lower portion is a higher magnification (40x) photomicrograph of the conceptus. Cell proliferation was assessed by immunostaining for Ki67 protein, and sections were lightly counterstained with hematoxylin. A fluorometric TUNEL assay was performed to detect apoptotic cells in sections of the conceptus. Data are representative of conceptuses from all ewes. Scale bars represent 100 μm.

Given that the trophectoderm cells of the elongating conceptus synthesize and secrete IFNT and PGs, the abundance of those factors in the uterine lumen can be used as an indirect measure of conceptus development and viability as well as trophectoderm cell number [57, 90, 132, 285]. Consistent with retarded conceptus growth, the total amount of IFNT and PGs in the uterine lumen was substantially lower ($P<0.01$) in ewes infused with IFNT MAO as compared to those receiving the Control MO (Table 1). Total PGs in the uterine lumen of IFNAR1/2 MAO infused ewes was not different ($P>0.10$) from Control MO ewes, although IFNT levels were lower ($P<0.05$).

A number of elongation- and implantation-related genes are induced by progesterone in the LE and/or GE of the endometrium between Days 10 and 14 post-estrus/mating and further stimulated by conceptus-derived IFNT and/or PGs after Day 12 [74]. The majority of progesterone-induced elongation- and implantation-related genes (*CTSL1, GRP, IGFBP1, LGALS15, SLC2A1, SLC5A1, SLC7A2*) were not different ($P>0.10$) in the endometria from IFNT MAO or IFNAR1/2 MAO as compared to Control MO infused ewes (data not shown). The abundance of *SLC2A5* mRNA was greater ($P<0.001$) in the endometrium of ewes infused with IFNT MAO as compared to Control MO (Figure 5). In contrast, *SLC2A5* mRNA was not different ($P>0.10$) in the endometria of IFNAR1/2 MAO as compared to Control MO infused ewes. As illustrated in Figure 5, classical Type I ISGs (*CXCL10, ISG15, RSAD2*) were substantially lower ($P<0.001$; 31-, 34-, and 11-fold, respectively) in the endometrium from ewes receiving IFNT MAO as compared to those infused with Control MO. In contrast, *ISG* expression was not

different (P>0.10) in the endometria of ewes from Control MO as compared to IFNAR1/2 MAO infused ewes.

TABLE 1. Effect of morpholino treatment on Day 14 ovine conceptus morphology and total amounts of interferon tau (IFNT) and prostaglandins (PGs) in the uterine lumen

	Conceptus		Uterine Lumen	
Morpholino Type	**Number**	**Morphology**	**Total IFNT** (RU x 10^3 ± SE)	**Total PGs** (ng ± SE)
Control MO	13	Elongated & Filamentous	125.5 ± 21	1934.3 ± 679
IFNT MAO	7	Very small & Malformed	21.5 ± 23*	319.9 ± 775*
IFNAR MAO	7	Elongated & Filamentous	53.1 ± 26$^+$	589.1 ± 824

***MAO vs. Control MO (P< 0.01)**

$^+$MAO vs. Control MO (P< 0.05)

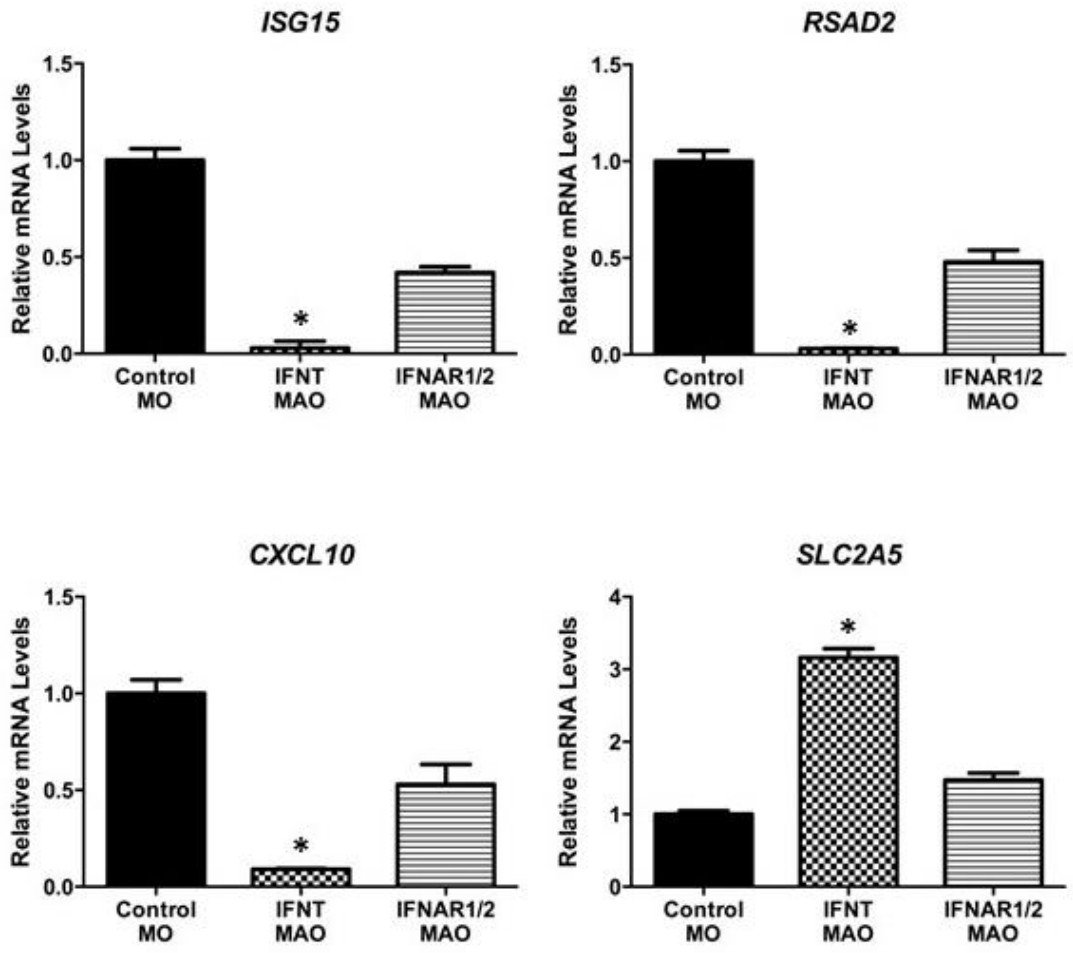

FIGURE 5. Expression of classical IFN-stimulated genes (ISGs) and elongation- and implantation-related genes in the endometrium from morpholino-treated ewes. Control MO, IFNT MAO or IFNAR MAOs (IFNAR1 MAO and IFNAR2 MAO) was infused into the uterine lumen of uterine horn ligated ewes on Day 7 post-mating (n≥7 per morpholino type). Conceptuses were recovered on Day 14, and endometrium frozen for RNA extraction. The relative abundance of mRNA was determined by qPCR using only samples of endometrium from ewes whose uterine flush contained a conceptus. Data are expressed as fold change relative to endometria from Control MO infused sheep. The asterisk (*) denotes differences ($P<0.05$) in mRNA abundance of Control MO vs MAO ewes.

Study Three: IFNT MAO does not affect blastocyst survival or growth into an ovoid conceptus

Conceptuses recovered from ewes infused with the IFNT MAO collected on Day 12 were ovoid or slightly tubular, which was consistent with conceptus morphology observed in Day 12 bred ewes. As expected, IFNT levels in the uterine lumen were very low and not different (P>0.10) (data not shown). Total PG levels were also not different (P>0.10) in the uterine lumen of unligated control bred ewes (214.1±62 ng) as compared to ewes with a uterine horn ligation and infusion of IFNT MAO (261.5±62 ng). Expression of ISGs and elongation- and implantation-related genes (*CXCL10, CTSL1, GRP, IGFBP1, ISG15, LGALS15, RSAD2, SLC2A1, SLC5A1, SLC7A2*) were also not different (P>0.10) in the endometrium of IFNT MAO infused ewes and untreated Day 12 pregnant ewes (data not shown).

DISCUSSION

The unilateral pregnant ewe model was originally reported by Bazer and coworkers [296] as a method to obtain uterine secretions by restricting the fetus to one uterine horn. This surgical procedure was reported to not affect conceptus implantation or fetal development. Based on that report, several studies have used that surgical approach to maintain higher levels of infused or injected substances within the ligated horn containing the conceptus given the long length of each bicornuate horn [57, 244, 298, 302]. The results of Study One confirm the assertion that ligation of the uterine horn ipsilateral to the CL on Day 8 post-mating does not affect pregnancy rate nor growth of the conceptus as assessed on Day 14 post-mating (Figure 1). Similarly, implantation of osmotic pumps that infuse morpholinos

or chemical inhibitors into the uterine lumen also do not affect pregnancy rate in ewes with ligated or unligated uterine horns based on this study and others [57, 59]. Conversely, Study One found that a bolus injection of 1 ml of a cell culture medium (Opti-MEM) into the lumen of a ligated uterine horn on Day 8 post-mating, followed by manipulation of the horn, negatively affected growth of the conceptus contained within that uterine horn (Figure 1). Although conceptus length was shorter on Day 14 in the present study, similar studies reported morphologically normal and elongated conceptuses present on Day 16 or 20 using the same experimental design [244, 298, 302]. Thus, decreased conceptus length observed on Day 14 does not appear to affect continued elongation into a filamentous conceptus by Day 16 or establishment of pregnancy by Day 20. This result could be in part due to manipulation of the horn following bolus injection, and variation in conceptus development due to differences in surgical manipulation of the horn. Opti-MEM Reduced Serum Media (Life Technologies) is a modification of Eagle's Minimum Essential Media, buffered with HEPES and sodium bicarbonate, and supplemented with hypoxanthine, thymidine, sodium pyruvate, L-glutamine, trace elements, and growth factors. The components of the media are proprietary, but undoubtedly are different than the intrinsic luminal environment of the early pregnant uterus in terms of amino acids, glucose, and growth factors [64, 65, 103]. Available results support the idea that exposure of the Day 8 hatching ovine blastocyst to nonphysiological factors present in the Opti-MEM modifies its growth trajectory, resulting in decreased growth observed on Day 14. This idea is supported by studies demonstrating effects of cell culture conditions (serum, amino

acids, glucose and growth factors) on embryo metabolism and developmental outcomes [303-305]. The effects of abnormal embryo culture conditions includes altered gene expression [304] and aberrant epigenetic modifications [306] in a number of different species including ruminants. Given the results of Study One, subsequent studies were conducted using a constant intrauterine infusion of morpholinos in PBS via implanted osmotic pumps (10 µl per hour for a total of 240 µl per day) into the lumen of the ligated uterine horn, since that approach did not alter conceptus growth as assessed on Day 14 post-mating (Figure 1).

A major finding of Study Two was that inhibition of *IFNT* mRNA translation in the trophectoderm compromises conceptus elongation, as Day 14 conceptuses recovered from ewes infused with IFNT MAOs from Day 8 post-mating were severely growth retarded as evidenced by lower levels of IFNT and PGs in the uterine lumen. The TUNEL analysis detected significant levels of DNA fragmentation in those growth-retarded conceptuses, which is due to activation of apoptotic signaling cascades [307, 308]. The induction of apoptosis in the conceptus is likely the cause of growth retardation and malformation observed in conceptuses from ewes infused with IFNT MAO. IFNT can be readily detected in the medium of cultured bovine blastocysts [309, 310], although peak secretion does not occur until several days later around the time of implantation [311]. Given that IFNT production by the conceptus is a surrogate marker of trophectoderm number and viability, studies have attempted to link IFNT with morphological quality and developmental competence of blastocysts in cattle [310, 312]. However, the levels of IFNT secretion are low and differ markedly between

individual blastocysts [312]. Further studies asserted that IFNT secretion by the blastocyst may be a useful tool to predict pregnancy outcome in cattle, but only within certain developmental stages [313]. The results of Study Three suggest that IFNT secretion by the hatching blastocyst may not be a good predictor of pregnancy outcome, as morphologically normal conceptuses (spherical or ovoid) were found on Day 12 in ewes infused with IFNT MAOs from Day 8 post-mating. Collectively, the results of Studies Two and Three suggest that the embryotrophic effects of IFNT occurs after Day 12, even though *IFNT* mRNA by the developing embryo is detectable much earlier, at the blastocyst stage, in sheep and cattle [283, 309].

Available studies support the ideas that the embryotrophic effects of IFNT are via: (1) paracrine effects on the endometrium to induce expression of ISGs that have reciprocal effects on trophectoderm survival and proliferation; and/or (2) autocrine effects on the trophectoderm. Although IFNT certainly inhibits development of the endometrial luteolytic mechanism to maintain the CL, progesterone levels are not different in cyclic or nonpregnant and pregnant ewes until after Day 14 post-estrus/mating [47]. The paracrine effects of IFNT to modify endometrial gene expression within the endometrium are well documented in sheep and cattle [74, 314]. Between Days 12 and 16 of pregnancy in sheep, the effects of IFNT on the endometrium include the following: (1) inhibition of estrogen receptor alpha and oxytocin receptor gene transcription to abrogate oxytocin receptor expression and thus production of luteolytic pulses of PGF2α; (2) induction of a large number of classical ISGs; and (3) stimulation of a number of

progesterone-induced genes that can be termed elongation- and implantation-related genes [74]. The genes induced by progesterone in the LE and GE between Days 10 and 12 post-mating are hypothesized to be essential for conceptus survival and growth [105]. They encode a number of secreted factors (CST3, CST6, CTSL1, GRP, LGALS15, IGFBP1, SERPINA14, SPP1, STC1), enzymes (HSD11B1, PTGS2) and transporters (SLC2A1, SLC2A5, SLC5A1, SLC7A2). The net outcome of the progesterone-induced changes that occur on Day 12 and after is modification of the uterine luminal milieu, including an increase in select amino acids, glucose, and proteins that stimulate blastocyst growth into an ovoid and then filamentous conceptus [103, 315]. Although IFNT levels were much lower in the uterine lumen of IFNT MAO infused ewes in Study Two, the expression of all studied progesterone induced and elongation- and implantation-related genes (*CTSL1, GRP, IGFBP1, LGALS15, SLC2A1, SLC2A5, SLC5A1, SLC7A2*) were not different than in control ewes. Thus, the lack of induction or stimulation of those genes is likely not the cause of conceptus defects associated with the loss of IFNT. Of note, one of the studied genes (*SLC2A5*) was higher in the endometria of ewes infused with IFNT MAO. Similar to the other studied genes, *SLC2A5* is stimulated by infusion of IFNT as well as PGs into the lumen of the ovine uterus [57]. Given that PGs and IFNT were lower in the endometria from the IFNT MAO-infused ewes, increased expression of *SLC2A5* in the endometrium of those ewes suggests it is sensitive to abnormally developing conceptuses. Indeed, the endometrium of cattle can sense the difference between a conceptus derived from nuclear transfer or *in vitro* fertilization on Days 18 or 20 of pregnancy [316, 317].

A number of transcriptional profiling experiments conducted with human cells, ovine endometrium, bovine endometrium, and bovine peripheral blood lymphocytes have elucidated classical Type I ISGs induced by IFNT during early pregnancy [72, 103, 314, 318, 319]. Numerous classical ISG are induced or stimulated in the endometrium during conceptus elongation in both cattle and sheep [74, 103]. For instance, *ISG15* mRNA can be detected in the LE of the ovine uterus on Days 10 or 11 of the estrous cycle and pregnancy, but is undetectable in LE by Days 12 to 13 of pregnancy [320]. In response to IFNT from the elongating conceptus, *ISG15* expression is strongly induced in the stratum compactum stroma and GE by Days 13 to 14, and expression extends to the stratum spongiosum stroma, deep GE, and myometrium as well as resident immune cells of the ovine uterus by Days 15 to 16 of pregnancy [320, 321]. Further, PGs from the elongating conceptus can also moderately stimulate expression of classical ISGs [322]. As expected, reduced IFNT and PG levels in the uterine lumen were accompanied by substantial lack of induction of classical ISGs in the endometrium of ewes infused with IFNT MAO (Figure 4). Accordingly, the lack of classical ISGs in the uterus may be responsible for the defect in conceptus elongation and trophectoderm survival observed in ewes infused with IFNT MAO. One challenge is to determine which of the large number of classical ISGs mediate the embryotrophic actions of IFNT [74, 323-325]. In fact, only a few classical ISGs have been studied with respect to potential effects on the elongating conceptus. One classical ISG with reported biological effects on trophectoderm function during ovine conceptus elongation is CXCL10 (chemokine (C-X-C motif) ligand 10; alias

IP-10) [326]. Another classical ISG (ISG15) is secreted into the uterine lumen during early pregnancy in sheep and cattle where it may function as a cytokine [327].

The effects of all Type I IFNs, including IFNT, are mediated through a cell surface receptor, which is composed of two subunits IFNAR1 and IFNAR2 [328]. IFNAR2 is considered to be the ligand binding subunit of the receptors because of its ability to bind Type I IFNs with relatively high affinity [328]. The current model for assembly of the IFN signaling complex is that a Type I IFN initially binds IFNAR2 with the subsequent recruitment of IFNAR1 to initiate signaling [329]. Engagement of this IFNAR2-IFN-IFNAR1 complex activates the canonical JAK-STAT-IRF signaling pathway resulting in transcriptional activation or repression of ISGs that encode the effectors of the IFN response, such as antiviral proteins, regulators of cell proliferation and differentiation, and immunoregulatory proteins [98]. Initially, the peri-implantation ovine conceptus was presumed to be unresponsive to the IFNT it produced, as *IFNAR* mRNAs could not be detected in the elongating ovine conceptus [293]. However, other studies found evidence for IFNAR1 protein in Day 14 and 16 conceptuses [294] as well as *IFNAR1* mRNA in Day 15 and 20 conceptuses [295]. Recent RNA sequencing data from our laboratory (GEO accession GSE58967) found *IFNAR1* mRNA (2 Reads per kilobase transcript per million reads or RPKM) in Day 14 ovine conceptuses and essentially no *IFNAR2* mRNA (RPKM=0.0125) as compared with *IFNT* (20,347 RPKM) and *PTGS2* (1,093 RPKM). In Study Two, elongated, morphologically normal, and filamentous type conceptuses were present in the uterus of IFNAR1/2

MAO infused ewes on Day 14 post-mating. Expression of classical ISGs and progesterone-induced elongation- and implantation-related genes was not different in those ewes compared to control ewes, as was total PG levels in the uterine lumen. However, IFNT levels were approximately two-fold lower in the uterine lumen of ewes infused with IFNAR1/2 MAO as compared to the Control MO, but not as low as observed in ewes infused with IFNT MAO. The results can be interpreted to indicate that the autocrine effects of IFNT via IFNAR1 are certainly not required for conceptus elongation, but they may influence *IFNT* gene expression. Further studies are needed to determine if ovine conceptuses will implant and establish pregnancy in the absence of IFNAR function in the trophectoderm.

Given that IFNAR2 is not expressed in the Day 14 ovine conceptus, it is likely that the effects of IFNT are mediated by IFNAR1, which has the ability to induce a unique set of ISGs in response to IFNB independent of IFNAR2 [330]. In that study, IFNB did not activate STAT1 or induce classical ISGs in *Ifnar2* null mouse cells, but it did activate the PI3-AKT1 signaling pathway and a unique set of genes in *Ifnar2* null cells, including *Il1B*, *Il6*, *Cxcl2*, *Serpine1*, *Pges*, and *Arg2*. The idea that IFNT signals through a non-canonical signaling pathway in the LE of the ovine uterus during early pregnancy is supported by a number of different studies [100, 110, 111, 331-333]. Although IFNT can induce classical ISGs in ovine trophectoderm cells *in vitro* (*BST2, ISG15, OAS1*) [295] and in many ovine and bovine endometrial cell types *in vitro* [334, 335], those genes are not expressed in the Day 14 ovine conceptus based on RNA-Seq data (GEO accession GSE58967)

as well as *in vivo* studies [332, 335-337]. Thus, the observation that IFNT can induce classical ISGs in culture ovine trophectoderm cells is likely an artifact of *in vitro* culture.

In conclusion, results of the present are the first, to our knowledge, to provide *in vivo* evidence that IFNT is embryotrophic and an essential regulator of conceptus elongation. Paracrine effects of IFNT on the endometrium predominantly mediate its embryotrophic actions, although autocrine effects on the trophectoderm via IFNAR1 may also be important. Further studies are needed to completely define the non-canonical IFNT-IFNAR1 signaling pathway in the trophectoderm and endometrium and understand the biological effects of classical ISGs on conceptus elongation and thus the establishment and maintenance of pregnancy.

ACKNOWLEDGMENTS

The authors deeply appreciate members of the Spencer laboratory who assisted with animal care and surgeries (Greg Burns, Piotr Dorniak, Justyna Filant, Brenda Jesernig, Andrew Kelleher, Carolyn Spencer, Wang Peng).

SECTION III:

Peroxisome proliferator activator receptor gamma (PPARG) regulates conceptus elongation in sheep

Kelsey Brooks, Gregory Burns, and Thomas E. Spencer

This work has been published in:

Biol Reprod. 2015 Feb;92(2):42. doi: 10.1095/biolreprod.114.123877. Epub 2014 Dec 17.

ABSTRACT

The ovine blastocyst hatches from the zona pellucida by day 8 and develops into an ovoid or tubular conceptus (embryo and associated extraembryonic membranes) that grows and elongates into a filamentous form between days 12 and 16. The trophectoderm of the elongating conceptus synthesizes and secretes interferon tau (IFNT) as well as prostaglandins (PGs) via prostaglandin synthase two (PTGS2). Intrauterine infusion of a PTGS2 inhibitor prevents conceptus elongation in sheep. Although many PGs are secreted, PGI2 and PGJ2 can activate nuclear peroxisome proliferator activator receptors (PPARs) that heterodimerize with retinoic X receptors (RXRs) to regulate gene expression and cellular function. Expression of *PPARD, PPARG*, *RXRA*, *RXRB* and *RXRG* is detected in the elongating ovine conceptus, and nuclear PPARD and PPARG are present in the trophectoderm. Consequently, PPARD and PPARG are hypothesized to have essential roles in conceptus elongation in ruminants*. In utero* loss-of-function studies of PPARD and PPARG in the ovine conceptus trophectoderm were conducted using morpholino antisense oligonucleotides (MAO) that inhibit mRNA translation. Elongating, filamentous type conceptuses were recovered from ewes infused with a control morpholino or PPARD MAO. In contrast, PPARG MAO resulted in severely growth-retarded conceptuses or conceptus fragments with apoptotic trophectoderm. In order to identify PPARG regulated genes, PPARG ChIP-Seq and RNA-Seq were conducted using Day 14 ovine conceptuses. These analyses revealed candidate PPARG-regulated genes involved in biological pathways including lipid and glucose uptake, transport, and

metabolism. Collectively, results support the hypothesis that PTGS2-derived PGs and PPARG are essential regulators of conceptus elongation with specific roles in trophectoderm survival and proliferation.

INTRODUCTION

In sheep, the morula stage embryo enters the uterus between Days 4 and 5 of pregnancy [15]. The embryo forms a blastocyst by Day 6, which then hatches from the zona pellucida by Day 8. The blastocyst develops into a tubular form by Day 12 and is now termed a conceptus (embryo/fetus and associated extraembryonic membranes), which rapidly grows into an elongated, filamentous form by Day 14 [15, 35]. Hatched blastocysts do not elongate *in vitro*, as substances secreted from the endometrial epithelia, luminal (LE) and glandular (GE), are essential for their development from a spherical into a filamentous form [19, 21]. Conceptus elongation involves exponential increases in length and weight of the trophectoderm [18] and onset of extraembryonic membrane differentiation that is vital for embryonic survival and formation of a functional placenta [15, 338]. The cellular processes involved in conceptus elongation include trophectoderm proliferation, migration, apposition and transient attachment to the endometrial LE [339]. Successively, the elongated conceptus begins the process of central implantation and placentation and establishment of pregnancy [28]. The trophectoderm of the elongating ruminant conceptus synthesizes and secretes prostaglandins (PGs) as well as interferon tau (IFNT), which is the maternal recognition of pregnancy signal that acts on the endometrium to inhibit production of luteolytic pulses of PGF2α [19, 20], thereby ensuring continued progesterone

production by the corpus luteum [71]. Progesterone from the ovary induces a number of genes in the endometrial LE and GE that are hypothesized to regulate conceptus elongation; further, IFNT acts on the endometrium to stimulate transcription of a number of the progesterone-induced elongation and implantation related genes in the LE and GE as well as classical Type I IFN-stimulated genes (ISGs) in the stroma [72-74].

In both sheep and cattle, the conceptus and endometrium synthesize and secrete substantial amounts of PGs during early pregnancy, including PGE2, PGF2α, PGI2 and PGD2, that can be measured in the uterine lumen [132, 134]. Prostaglandin G/H synthase and cyclooxygenase 2 (PTGS2) is the dominant cyclooxygenase expressed in the conceptus trophectoderm and LE of the endometrium of ruminants. Of note, the elongating conceptus synthesizes and secretes more PGs than the underlying endometrium, resulting in higher PG levels in the uterine lumen of Days 12 to 16 pregnant compared to cyclic sheep [132-134]. Prostaglandins are important for conceptus elongation in sheep, because intrauterine infusion of meloxicam, a selective PTGS2 inhibitor, into the uterine lumen from Days 8 to 14 post-mating completely inhibited conceptus elongation [57]. Receptors for PGs are present in all cell types of the endometrium and conceptus during early pregnancy in sheep [57, 137]. Thus, PGs may have paracrine as well as autocrine and intracrine effects on endometrial function and conceptus development [74]. Available evidence supports the idea that conceptus-derived PGs act in a paracrine manner to modulate expression of progesterone-

induced elongation- and implantation-related genes in the endometrium that, in turn, promote conceptus elongation via effects on the trophectoderm [192, 340].

In addition to extracellular effects, PGs can elicit intracellular effects by activating the peroxisome proliferator activator receptor delta (PPARD) and gamma (PPARG) nuclear hormone receptors [138]. Specifically, PGI2 is a ligand for PPARD, and PGD2 spontaneously forms 15-deoxy-Δ12,14-PGJ2 within cells that is a ligand for PPARG [139-142]. The trophectoderm cells of the elongating ovine conceptus as well as the endometrial epithelia express PPARD and PPARG as well as their dimerization partners, the retinoic X receptors (RXRs) [137]. In other cell types and organs, ligand-dependent activation of PPARs regulates the transcription of genes involved in control of energy and glucose homeostasis, lipid metabolism and affect cell proliferation and differentiation [143, 152, 181]. Genetic studies in mice found both PPARG and PPARD to be essential for placental development and differentiation, because null mice display severe defects in placentation resulting in embryonic lethality [141]. In mink, PPARG is implicated in trophoblast differentiation and invasion during early pregnancy [341]. *In vitro* studies using human trophoblast cells found that PPARG regulates fatty acid uptake and activation of PPARG induces accumulation of lipids as well as trophoblast differentiation [152]. Connections between the placenta and maternal decidua are lost in *Ppard* null mice due to abnormal giant cell differentiation and results in embryonic lethality [342, 343]. In the skin, PPARD potentiates cell polarization and migration [185]. Thus, the cellular effects of PPARD and PPARG in other cell types and placentae support the idea that conceptus elongation and

trophoblast cell proliferation and differentiation in ruminants may be regulated by PPARD and PPARG. Indeed, lipid uptake and metabolism is likely a key feature of conceptus elongation given the rapid growth of the trophectoderm as well as production of lipid-derived PGs via PTGS2.

In order to test the hypothesis that PPARD and PPARG have essential biological roles in conceptus elongation, an *in vivo* morpholino loss of function study was conducted to specifically inhibit *PPARD* or *PPARG* mRNA translation in the trophectoderm of the developing ovine conceptus. Further, PPARG gene targets were determined in the Day 14 conceptus using a combination of ChIP-Seq and RNA-Seq analyses.

MATERIALS AND METHODS

Morpholino Design and Validation

Design. Morpholino oligonucleotides were designed and synthesized by Gene Tools (Philomath, OR). The PPARG morpholino antisense oligonucleotide (MAO) (AAAACGGCATCTCTGTGTCAACCAT) targeted the first 25 bp of the ovine *PPARG* mRNA, whereas the PPARD MAO (AGGCCCGGTCATAGCTCTGGCATCA) targeted the 5' UTR of the ovine *PPARD* mRNA. A random oligo 25-N morpholino was used as a control, as it is synthesized with a random base at every position and does not target any known mRNAs (Gene Tools).

Validation. Oligos analogous to the MAO targeting portion of the ovine *PPARD* and *PPARG* mRNA coding sequences (CDS) were synthesized by

Integrated DNA Technologies (Supplementary Table 1). Oligos were designed to include a 5' *NheI* overhang, portion of the mRNA to be bound by the MAO, and a 3' *NheI* overhang. The psiCHECK2 dual luciferase (LUC) reporter plasmid (Promega, Madison, WI) was digested with the restriction enzyme *NheI*, and subsequently treated with antarctic phosphatase (New England Biolaboratory). Coding sequence oligos were annealed and ligated into psiCHECK2, upstream and in-frame with LUC, using T4 DNA ligase (Life Technologies, Carlsbad, CA). The resulting vectors were sequenced (Washington State University Molecular Biology and Genomics Core) for verification. Human 293T cells were transfected with psiCHECK2:PPARD CDS LUC or psiCHECK2:PPARG CDS LUC vectors using Lipofectamine 2000 (Life Technologies). After 6 h, cells were incubated with Endo-Porter delivery reagent (GeneTools) (6 µl per 1 ml) and 2, 4 or 8 µM of PPARD MAO, PPARG MAO, or Control MO. After 48 h, cell lysates were analyzed for luciferase activity using dual luciferase reporter assay system (Promega).

Animal Experiments

All experimental and surgical procedures were approved by the Institutional Animal Care and Use Committee of Washington State University. Mature Columbia Rambouillet crossbred ewes (*Ovis aries*) were observed for onset of estrus (designated Day 0) and mated to an intact ram of proven fertility. On Day 7 post-mating, ewes were subjected to a mid-ventral laparotomy. Using methods described previously [244, 296], the base of the uterine horn ipsilateral to the CL was double ligated using non-absorbable umbilical tape to prevent migration and growth of the conceptus through the uterine body into the contralateral uterine

horn; this surgical procedure does not affect conceptus implantation or development [296]. A vinyl catheter (Item no. 0007760; Durect Corporation, Cupertino, CA), connected to a preloaded and equilibrated Alzet 2ML1 Osmotic Pump (Durect Corporation), was then inserted 1 cm distal to the tubo-uterine junction into the lumen of the uterine horn ipsilateral to the ovary containing a corpus luteum. The pump was then affixed to the mesosalpinx supporting the oviduct using cyanoacrylate glue (SUPER GLUE, Bentonville, AR) and secured by suturing the mesosalpinx to the perimetrium of the uterine horn using 0 Coated Vicryl suture (Ethicon, Somerville, NJ). The Alzet 2ML1 Osmotic Pump is calibrated to constantly deliver 10 µl per h (240 µl/day) for 7 days.

Ewes (n≥5 per treatment) were implanted on Day 7 post-mating with an osmotic pump containing either: (1) Control MO; (2) PPARD MAO; or (3) PPARG MAO. Each pump was equilibrated in sterile PBS at 37ºC for 24 h and contained 100 nmol of the morpholino along with 50 µl of Gene Tools Aqueous Endo Porter delivery reagent diluted to a final volume of 2 ml of sterile PBS. All ewes were euthanized on Day 14 post-mating and tissues were immediately collected. The catheterized uterine horn was flushed with 10 ml of PBS (pH 7.2), and the state of conceptus development was assessed under bright field illumination using a SMZ1000 photomicroscope fitted with a DS-Fi1 digital camera (Nikon Instruments Inc., Lewisville, TX). The volume of the recovered uterine flushing was measured and recorded, and the flushing clarified by centrifugation (3000 x g at 4°C for 15 min). The supernatant was carefully removed with a pipet, mixed, aliquoted, frozen in liquid nitrogen, and stored at -80°C. Several sections (~0.5 cm) from the mid-

portion of each uterine horn as well as portions of the conceptus were fixed in fresh 4% paraformaldehyde in PBS (pH 7.2). After 24 h, fixed tissues were changed to 70% ethanol for 24 h and then dehydrated and embedded in Paraplast-Plus (Oxford Labware, St. Louis, MO). The remaining endometrium was physically dissected from the myometrium using curved scissors, flash frozen in liquid nitrogen, and stored at -80°C for subsequent RNA extraction.

Quantification of IFNT in Uterine Flush

The amount of IFNT in the uterine flush was determined by Western dot blot analysis as previously described [105]. A sample of the uterine flush (100 µl) from each ewe was diluted to 200 µl final volume with 10 mM Tris buffered saline (TBS). A nitrocellulose membrane (GE Healthcare-Life Sciences, Pittsburgh, PA), presoaked with TBS, was loaded into a BioRad dot blot apparatus (Hercules, CA) backed by Whatman filter paper. Wells were subsequently washed with 200 µl TBS prior to addition of the diluted uterine flush sample, and then rinsed with 200 µl TBS. The membrane was allowed to air dry and then blocked in 5% (wt/vol) milk/TBS with 0.1% Tween 20 (TBST) for 1 h at room temperature. The membrane was then incubated in primary rabbit anti-ovine IFNT serum [344] at 1:1000 dilution in 5% milk/TBST overnight at 4°C. The blot was then washed for 30 min in TBST followed by incubation with goat anti-rabbit IgG horseradish peroxidase conjugate (Thermo Scientific, Waltham, MA) at 1:5,000 diluted in 5% milk/TBST for 1 h at room temperature. The blot was washed again for 30 min in TBST. Immunoreactive IFNT was detected using SuperSignal West Pico Chemiluminescent Substrate (Thermo Scientific) and quantified with a ChemiDoc

MP system and Image Lab 4.1 software (BioRad). The data are expressed as total relative amount of IFNT in the uterine flush determined by adjusting for the recovered volume of uterine flushing.

Quantification of PGs in the Uterine Flush

Prostaglandins in the uterine flush were measured by sensitive enzyme immunoassay (EIA) from Cayman Chemical (catalog no. 514012; Ann Arbor, MI). The antiserum used in this assay exhibits high cross reactivity for most PGs, which allows quantification of all the PGs in a given sample with a single assay. Total PGs in the uterine flush were measured according to the manufacturer's recommendations in a single assay with a sensitivity of 15.6 pg/ml. The data are expressed as total amounts of PGs, determined by adjusting for the recovered volume of uterine flush.

Total RNA Isolation and Real-Time PCR Analysis

Total RNA was isolated from endometrial samples using Isol-RNA lysis reagent (5 Prime, Gaithersburg, MD). To eliminate genomic DNA contamination, extracted RNA was treated with DNase I and purified using RNeasy MinElute cleanup kit (Qiagen, Valencia, CA). The quantity and quality of total RNA were determined by spectrometry. Total RNA (1 µg) from each sample was reverse transcribed in a total reaction volume of 20 µl using iScript RT supermix (BioRad, Hercules, CA). Reverse transcription was performed as follows: 5 min at 25°C; 30 min at 42°C; and 5 min at 85°C. Control reactions in the absence of reverse

transcriptase were prepared for each sample to test for genomic DNA contamination. The resulting cDNA was stored at -20°C for further analysis.

Real-time PCR was performed using a CFX384 Touch Real Time System with SsoAdvanced Universal SYBR Green Supermix (BioRad, Hercules, CA). Previously published primers for *CXCL10, CTSL1, GAPDH, IGFBP1, ISG15, RSAD2, SLC2A1, SLC5A1* and *SLC7A2* were used [57], and primers for ovine *GRP* and *LGALS15* were designed and synthesized by Integrated DNA technologies (Coralville, IA) (Supplementary Table 1). Each sample was analyzed in duplicate with the following conditions for 40 cycles: 95°C for 30 sec; 95°C for 5 sec; and 60°C for 30 sec. A dissociation curve was generated at the end of amplification to ensure that a single product was amplified. PCR reactions without template and template substituted with total RNA were used as a negative control to verify experimental results. The threshold line was set in the linear region of the amplification plot above the baseline noise, and quantification cycle (Cq) values were determined as the cycle number in which the threshold line intersected the amplification curve. Ovine *GAPDH* was used as the reference gene.

Immunohistochemistry

Fixed conceptuses were embedded in paraffin wax and sectioned (6 µm). Sections were mounted on slides, deparaffinized in xylene substitute, and rehydrated in a graded alcohol series. Sections were then submitted to hematoxylin and eosin (H & E) staining (Scytek, Logan, UT), immunohistochemistry, or TUNEL apoptosis assay. For immunohistochemistry,

antigen retrieval was performed by incubating sections affixed to slides for 10 min in boiling 10 mM citrate buffer (pH 6.0). After cooling to room temperature, sections were incubated with 10% normal goat serum in PBS (pH 7.5) for 10 min at room temperature and then overnight at 4°C with rabbit anti-Ki67 IgG (cat. no. ab66155; Abcam, Cambridge, MA, USA) at 1.2 µg/ml in 1% BSA in PBS (pH 7.5). Sections were washed in PBS and incubated with biotinylated secondary antibody at 5 µg/ml (cat. no. PK-4001; Vector Laboratories, Burlingame, CA, USA) for 1 h at 37°C. Immunoreactive Ki67 protein was visualized using Vectastain ABC kit (Vector Laboratories) using diamino-benzidine tetrahydrochloride as the chromagen. Sections were counterstained with hematoxylin, and coverslips were affixed to slides with Permount mounting medium (Fisher Scientific, Fairlawn, NJ, USA). Images of representative fields were recorded using a Nikon Eclipse 90i model photomicroscope fitted with a DS-Ri1 digital camera.

TUNEL apoptosis assay

Terminal deoxynucleotidyl transferase (TdT)-mediated dUTP nick-end labeling (TUNEL) assay (Catalog No. G3250; Promega) was performed according to the manufacturer's instructions for paraffin-embedded tissue with slight modification. Briefly, the sections were rehydrated and fixed in 4% methanol free paraformaldehyde (PFA) in PBS for 15 min at room temperature. The tissue was permeabilized with Proteinase K for 8 min, washed with PBS, and fixed in PFA. Slides were then covered with equilibration buffer for 5-10 minutes at room temperature followed by incubation with TdT incubation buffer (containing TdT and nucleotide mix) for 1 h at 37°C in a humidified chamber. The reaction was

terminated by submersion of slides in 2X SSC for 15 minutes at room temperature. The sections were washed with PBS and coverslips applied using Vectashield mounting media with DAPI (Vector Laboratories). Images of representative fields were recorded using a Nikon Eclipse 90i model photomicroscope fitted with a DS-Ri1 digital camera. Brightfield and epifluorescent (DAPI and FITC) images were collected using NIS Elements BR 3.2 software (Nikon). Background fluorescence was corrected based on FITC intensity of positive control slides produced by DNase I (Qiagen) treatment according to TUNEL assay instructions (Promega).

Chromatin Immunoprecipitation Sequencing (ChIP-Seq)

Genpathway FactorPath ChIP analysis was conducted by ActiveMotif (Carlsbad, CA, USA) using flash frozen day 14 ovine conceptuses (n=4). Conceptus tissue samples (~100 mg) were submersed in 1% formaldehyde in PBS, cut into small pieces, and incubated at room temperature for 15 min. Fixation was stopped by the addition of 0.125 M glycine. Tissue pieces were then treated with a TissueTearor (BioSpecProducts, Bartlesville, OK, USA) and finally spun down and washed twice in PBS. Chromatin was isolated by disrupting the cells with a Dounce homogenizer. Lysates were sonicated using a Misonix Sonicator 3000 (Misonix, Vernon Hills, IL, USA) equipped with a microtip in order to shear the DNA to an average length of 300 to 500 bp. Lysates were cleared by centrifugation and stored at -80°C. Genomic DNA (input) was prepared by treating aliquots of chromatin with RNase, proteinase K, and heat for decrosslinking, followed by phenol/chloroform extraction and ethanol precipitation. Purified DNA was quantified on a NanoDrop spectrophotometer (Thermo Fisher Scientific Inc.).

Extrapolation to the original chromatin volume allowed determination of the total chromatin yield. For each ChIP reaction, 30 µg of chromatin was precleared with protein A agarose beads (Life Technologies). Immunoprecipitation was performed using 4 µg of rabbit anti PPARG polyclonal IgG (Cat. No. sc-7196; Santa Cruz Biotechnology, Santa Cruz, CA, USA). Following overnight incubation at 4°C, Protein A agarose was added, and incubation at 4°C continued for another 3 h. Immune complexes were washed 2 times each with a series of buffers consisting of the deoxycholate sonication buffer, high-salt buffer, LiCl buffer, and TE buffer. Immune complexes were eluted from the beads with SDS buffer and subjected to RNase treatment and proteinase K treatment. Crosslinks were reversed by incubation overnight at 65°C, and ChIP DNA purified by phenol-chloroform extraction and ethanol precipitation.

Input and ChIP DNA were amplified using an Illumina ChIP-Seq DNA Sample Prep Kit (Illumina, San Diego, CA, USA). Briefly, DNA ends were polished and 5'-phosphorylated using T4 DNA polymerase, Klenow polymerase, and T4 polynucleotide kinase. After addition of 3'-adenine to blunt ends using Klenow (3'-5' exo minus), Illumina genomic adapters were ligated, and the sample was size-fractionated to 200-250 bp on a 2% agarose gel. After a PCR amplification (30 sec at 98°C; 10 sec at 98°C, 30 sec at 65°C, and 30 sec at 72°C for 18 cycles; and then 5 min at 72°C) with Phusion High-Fidelity DNA Polymerase (NEB), the resulting DNA libraries were tested by reverse transcription quantitative PCR (RT-qPCR) at the same specific genomic regions as the original ChIP DNA to assess quality of the amplification reactions. The DNA libraries were sent to Illumina

Sequencing Services and sequenced using an Illumina HiSeq 2000. Sequences (50 base, single end) were aligned to the *Ovis aries* genome (NCBI Build 37, August 2012, Oar_v3.1) using the BWA algorithm. Alignments were extended *in silico* at their 3'-ends to a length of 150 bp and assigned to 32-nt bins along the genome. The resulting histograms were stored in binary analysis results (BAR) files. Peak locations were determined by applying a threshold of 18 (5 consecutive bins containing 18 aligns) and storing the resulting intervals in browser extensible data (BED) files. Interval locations in BED format are deposited in the NCBI Gene Expression Omnibus (GSE59011). The BED files were analyzed using GenPathway software (Active Motif) that provides information on genomic annotation, peak metrics, and sample comparisons for all intervals. The model based analysis of ChIP-Seq (MACS) peak-finding algorithm was used to normalize ChIP against the input control ($P<10^{7}$; mfold 8,30, bandwidth 150) [345]. Motif analysis was conducted through TOMTOM analysis of the JASPAR CORE 2014 vertebrate MEME database [346]. Gene list functional enrichment analysis was conducted using ToppFun (https://toppgene.cchmc.org/) using default settings [347].

RNA Sequencing (RNA-Seq)

Flash frozen Day 14 ovine conceptuses (n=4) were homogenized in RLT plus buffer and RNA isolated using RNeasy Plus kit (Qiagen). Samples of total RNA (5 µg) were depleted of ribosomal RNA using Ribominus Eukaryote System v2 (Ambion, Austin, TX). Ion Total RNA-seq Kit v2 (Life Technologies) was used to construct strand specific sequencing libraries from ribosomal depleted samples

(20 ng) with several deviations from the protocol. Enzymatic RNA fragmentation was carried out at 37°C for 90 sec. Fragmented RNA was purified using 1.0X AMPure XP beads (Beckman-Coulter Genomics, Danvers, MA). The cDNA and final libraries were purified with 0.8X AMPure XP beads. Emulsion PCR was performed on an Ion One Touch 2 instrument, using the Ion P1 Template OT2 200 v3 reagents. Sequencing beads were quantified and evaluated by flow cytometry using a Guava Easy Cyte (Millipore, Billerica, MA) with Sybr Gold (Molecular Bioprobes, Eugene, OR) before loading on an Ion P1 semiconductor sequencing chip. Libraries (n=4) were sequenced on an Ion Proton using Ion P1 200 v3 sequencing reagents and 440 flows (Life Technologies) at the Washington State University Molecular Biology and Genomics Core. The barcoded libraries were pooled three per P1 chip for sequencing. Base calling and primary analysis was performed using Torrent Suite 4.0.2. Reads, at least 16 million per sample, were quality trimmed (error probability 0.01) and mapped to Ensembl genes (*Ovis aries* Oar_v3.1.75) with a CLC Genomics Server 6.0 (CLC bio, Aarhus, Denmark) using default settings. Associated gene names and descriptions were downloaded from the Ensembl Genes 75 database using BioMart and used to annotate the RNA-seq experiment table. Expression values were calculated as reads per kilobase of transcript per million mapped reads (RPKM). Expression values were square root transformed and visualized with box plots to verify similar sample distribution. Processed and raw BAM files were deposited in the NCBI Gene Expression Omnibus (GSE58967). A list of expressed genes was extracted by filtering the results table at RPKM ≥ 1 for all samples.

Statistical Analysis

All quantitative data were subjected to least-squares analyses of variance (ANOVA) using the General Linear Models (GLM) procedures of the Statistical Analysis System (SAS Institute Inc., Cary, NC). For analyses of real-time PCR data, *in vivo* treatment was used as the independent variable in the statistical model with *GAPDH* values used as a covariate. Error terms used in test of significance were identified according to the expectation of the mean squares for error. Significance ($P<0.05$) was determined by probability differences of least-squares means (LSM).

RESULTS

PPARG MAO inhibits ovine conceptus elongation

Morpholinos are short chains of morpholino subunits comprised of a nucleic acid base, a morpholine ring, and a non-ionic phosphorodiamidate intersubunit linkage [348]. Morpholino antisense oligonucleotides (MAOs) were designed to inhibit translation of either ovine *PPARD* or *PPARG* mRNAs, and they act through RNase H-independent steric interference to block translation of target genes [297]. Effectiveness of MAO to inhibit translation of target mRNA was assessed using an *in vitro* assay. Cells were transfected with a CDS-LUC vector and then treated with morpholinos. As illustrated in Figure 1, LUC reporter activity was lower ($P<0.05$) in cells treated with PPARD MAO or PPARG MAO compared to the Control morpholino. The reduction in luciferase reporter activity in the MAO-treated cells is

due to the MAO binding to the *PPARD* or *PPARG* CDS and repressing translation of *LUC* mRNA due to steric hindrance.

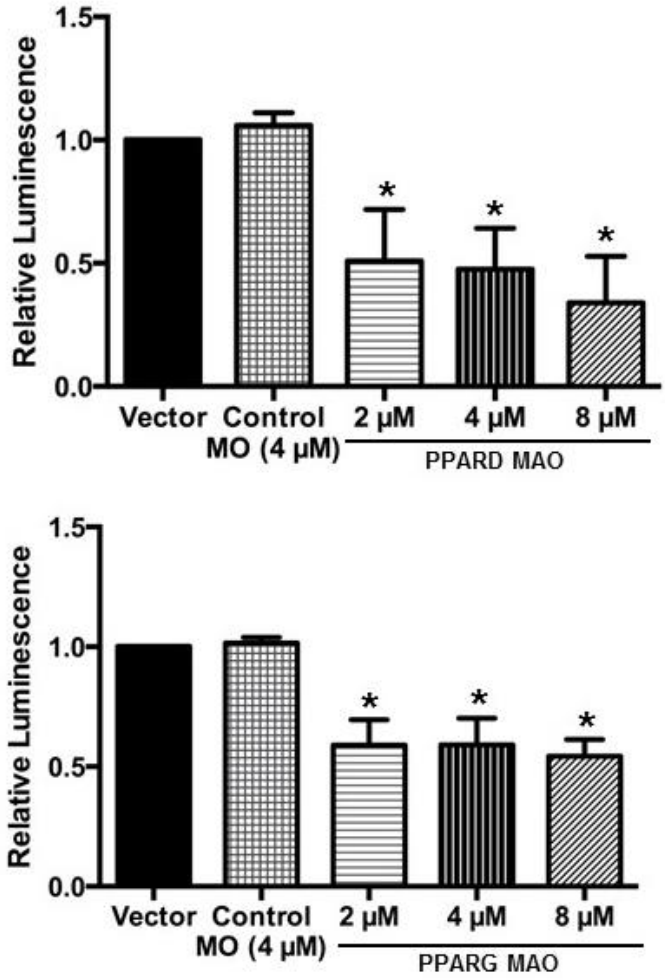

FIGURE 1. In vitro validation of PPARD and PPARG morpholino activity. (A) Morpholino antisense oligonucleotides (MAOs) were designed to inhibit translation of ovine *PPARD* or *PPARG* mRNAs. HEK 293T cells were transfected with psiCHECK2, a luciferase reporter vector, containing a portion of the coding sequence (CDS) for either ovine *PPARD* or *PPARG* upstream and in frame with the luciferase (LUC) gene. After 6 h, cells were treated with nothing (Vector only), a Control morpholino (MO; 4 µM) or specific MAO (2, 4 or 8 µM) along with the Endo-porter delivery reagent. After 48 h, LUC was assayed in lysed cells. Data for the morpholinos is presented as relative to the vector only. Differences ($P<0.05$; MAO vs Control MO) are denoted with an asterisk (*).

In vivo loss of function studies were then conducted to determine the effect of PPARD and PPARG MAO on conceptus elongation in sheep. This approach is based on previous studies demonstrating that labeled morpholinos are effectively delivered to the mononuclear trophectoderm cells of the conceptus after *in utero* administration [244, 298]. Pregnancy rates were not different (P>0.10) and averaged 80% in morpholino infused ewes. As summarized in Table 1, conceptuses recovered from ewes receiving intrauterine infusions of Control MO and PPARD MAO were elongated and filamentous, consistent with normal conceptus morphology in Day 14 pregnant ewes [18, 35]. However, conceptuses from PPARG MAO infused ewes were visibly growth retarded and malformed. Histological examination found that conceptuses recovered from ewes infused with Control MO or PPARD MAO contained many mononuclear trophectoderm cells lined with endoderm (Figure 2). In contrast, those receiving PPARG MAO were noticeably smaller with almost no distinct mononuclear trophectoderm cells or endoderm.

Elongation of the conceptus in ruminants is primarily driven by proliferation of the mononuclear trophectoderm cells [15]. Analysis of cell proliferation was conducted by immunostaining conceptuses for Ki67, a nuclear protein that is a marker of cell proliferation [299]. Abundant Ki67 protein was observed in the nuclei of most mononuclear trophectoderm cells in the elongated, filamentous conceptuses from ewes infused with Control MO and PPARD MAO (Figure 3). The growth retarded, malformed conceptuses from PPARG MAO infused ewes also contained Ki67-positive cells. Next, apoptosis in the conceptuses was assessed

using a fluorometric TUNEL assay [300, 301]. Apoptotic trophectoderm cells were particularly prevalent in the malformed conceptuses recovered from PPARG MAO infused ewes, but very low in elongating, filamentous conceptuses from Control MO and PPARD MAO infused ewes (Figure 2).

PPARG MAO reduces IFNT and PG in the uterine lumen and modifies expression of genes in the endometrium related to conceptus elongation and implantation

Given that the trophectoderm cells of the elongating conceptus synthesize and secrete PGs and IFNT, the abundance of those factors in the uterine lumen can be used as an indirect measure of conceptus development and viability as well as trophectoderm cell number [57, 90, 132, 285]. Consistent with retarded conceptus growth, IFNT and PGs were substantially lower ($P<0.01$) in the uterine lumen of ewes infused with PPARG MAO as compared to those infused with the Control MO (Table 1). In contrast, the amount of IFNT and PGs in the uterine lumen of PPARD MAO-infused ewes was not different ($P>0.10$) than Control MO ewes, which is consistent with conceptus morphology. The amount of total protein in the uterine luminal fluid was not different ($P>0.10$) in the morpholino-infused ewes (data not shown).

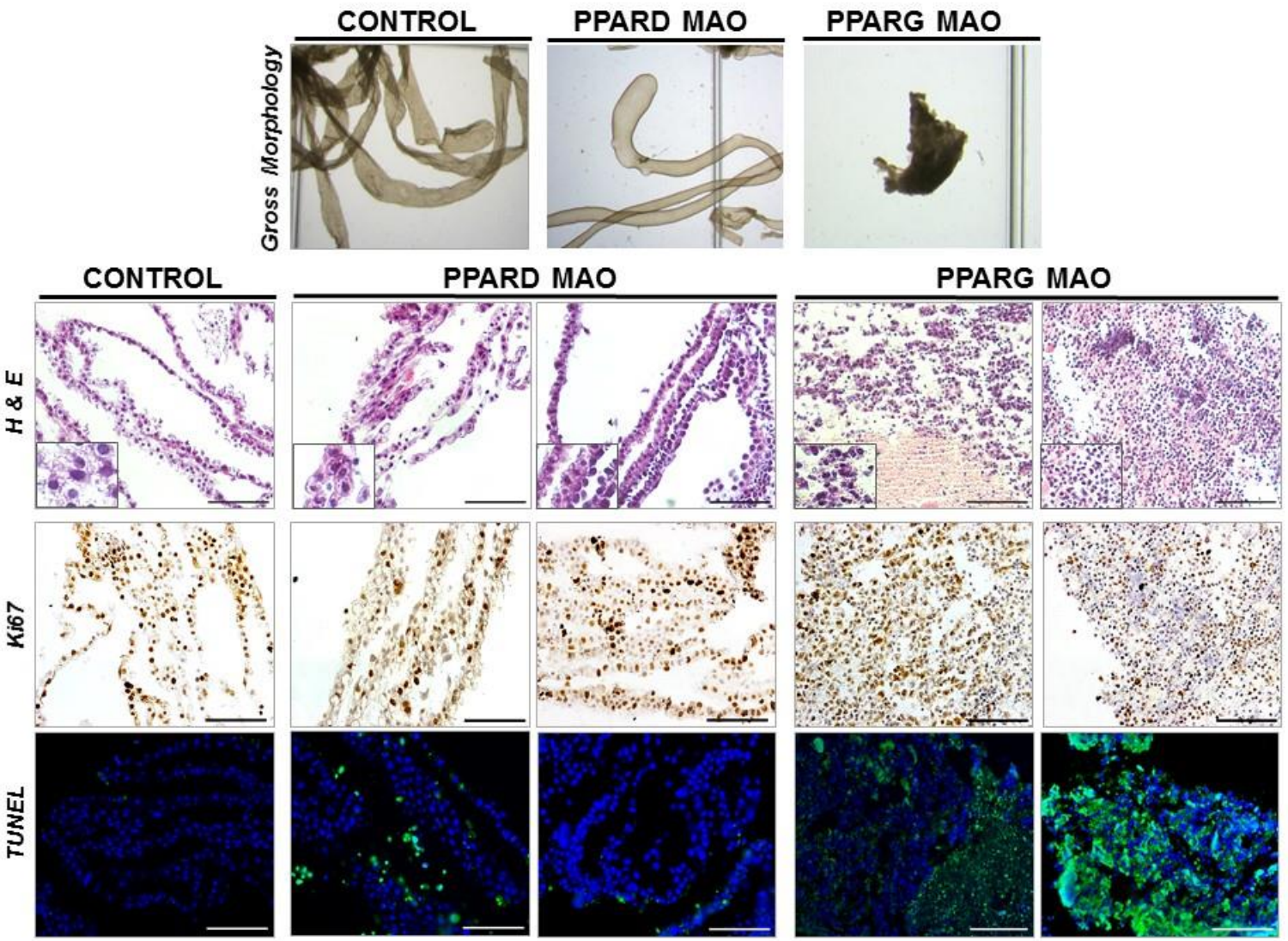
CONTROL
PPARD MAO
PPARG MAO
Gross Morphology
CONTROL
PPARD MAO
PPARG MAO
H & E
Ki67
TUNEL

FIGURE 2. Effect of morpholino treatment on conceptus morphology, proliferation and apoptosis. Control MO, PPARD MAO or PPARG MAO was infused into the uterine lumen of sheep beginning on Day 7 post-mating, and conceptuses were recovered on Day 14 (n≥5 per morpholino type). Conceptus morphology was examined using an inverted microscope. Portions of the conceptuses were fixed in paraformaldehyde, embedded in paraffin, sectioned and stained with hematoxylin and eosin (H&E). The inset in the left lower portion is a higher magnification (40X) photomicrograph of the conceptus. Cell proliferation was assessed by immunostaining for Ki67 protein; sections were lightly counterstained with hematoxylin. A fluorometric TUNEL assay was performed to detect apoptotic cells in the conceptus sections. Data are representative of conceptuses from all ewes. Scale bars represent 100 µm.

TABLE 1. Effect of morpholino treatment on Day 14 ovine conceptus morphology and total amounts of interferon tau (IFNT) and prostaglandins (PGs) in the uterine lumen

	Conceptus		Uterine Lumen	
Morpholino Type	**Number**	**Morphology**	**Total IFNT** (RU x 10^3 ± SE)	**Total PGs** (ng ± SE)
Control MO	13	Elongated & Filamentous	125.5 ± 21	1934.3 ± 679
PPARD MAO	7	Elongated & Filamentous	90.4 ± 27	2821.1 ± 976
PPARG MAO	7	Small & Malformed	19.5 ± 22*****	307.9 ± 682*****

* MAO vs. Control MO (P< 0.01)

A number of elongation- and implantation-related genes are induced by progesterone in the LE and GE of the endometrium between Days 10 and 12 post-estrus/mating and further stimulated by IFNT and/or PGs from the conceptus between Days 12 and 14 in early pregnant sheep (see [74] for review). In addition, a large number of classical Type I IFN-stimulated genes (ISGs) are induced by IFNT predominantly in the uterine stroma and GE. As illustrated in Figure 3, the abundance of classical Type I ISG mRNA (*CXCL10, ISG15, RSAD2*) was substantially lower ($P<0.001$; 23-, 26-, and 10-fold, respectively) in the endometrium of ewes infused with PPARG MAO as compared to those receiving Control MO. In contrast, *ISG* expression was not different ($P>0.10$) in the endometria of ewes infused with Control MO as compared to PPARD MAO. The majority of elongation- and implantation-related genes (*GRP, IGFBP1, LGALS15, SLC2A1, SLC5A1, SLC7A2*) were not different ($P>0.10$) in the endometria of PPARG MAO and PPARD MAO as compared to Control MO ewes (data not shown). However, *CTSL1* and *SLC2A5* mRNA levels were higher ($P<0.05$ and $P<0.001$, respectively) in the endometrium of ewes receiving PPARG MAO as compared to Control MO. In contrast, expression of those genes was not different ($P>0.10$) in the endometrium of ewes infused with PPARD MAO as compared to Control MO.

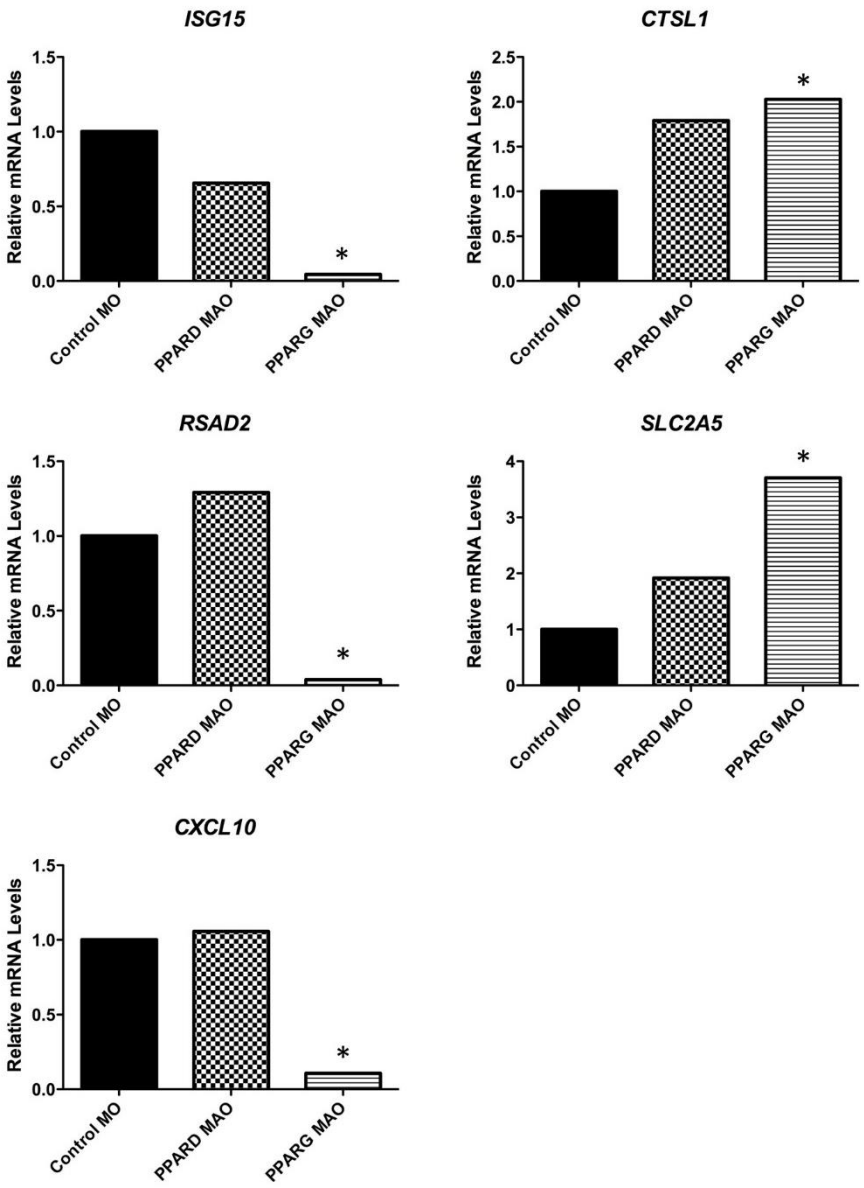

FIGURE 3. Expression of classical IFN-stimulated genes (ISGs) and elongation- and implantation-related genes in the endometrium. Control MO, PPARD MAO or PPARG MAO was infused into the uterine lumen of sheep beginning on Day 7 post-mating, and conceptuses were recovered on Day 14 (n≥5 per morpholino type). Relative abundance of mRNA in the endometrium was determined by qPCR using only samples from ewes whose uterine flush contained a conceptus. Data are expressed as fold change relative to Control MO infused sheep. Differences (P<0.05; MAO vs Control MO) are denoted with an asterisk (*).

Identification and distribution of PPARG binding sites in Day 14 ovine conceptus

Results of the loss-of-function study support the idea that PPARG, but not PPARD, in the trophectoderm regulates conceptus elongation. Given that PPARG regulated genes have not been defined in the ruminant conceptus and that PPARG regulates conceptus elongation, ChIP-Seq analysis was conducted to determine PPARG binding sites in the Day 14 ovine conceptus (Figure 4 and Supplementary Table 2). Of the 2,288 PPARG bound intervals identified by ChIP-Seq, 1,518 were within 10,000 bp of genes, 723 were within promoter regions (identified as being -7500/+2500 bp of transcription start sites), and 344 were within 500 bp of transcriptional start sites based on the current NCBI *Ovis aries* annotation. An increased frequency of PPARG binding near transcriptional start sites was noted (Figure 4B). NCBI genes with CpGs and PPARG binding intervals within promoter regions totaled 778 with 568 PPARG binding sites within 200 bp of CpG islands (Figure 4C). PPARG binding interval distribution was analyzed relative to genomic boundaries, which revealed 1,833 NCBI genes within 10,000 bp of PPARG binding intervals. As illustrated in Figure 4D, PPARG binding sequences (60 bp surrounding summits) were analyzed by MEME and TOMTOM and returned a motif identical to the conserved PPARG binding motif (name MA0065.2, PPARG:RXRA) [349, 350].

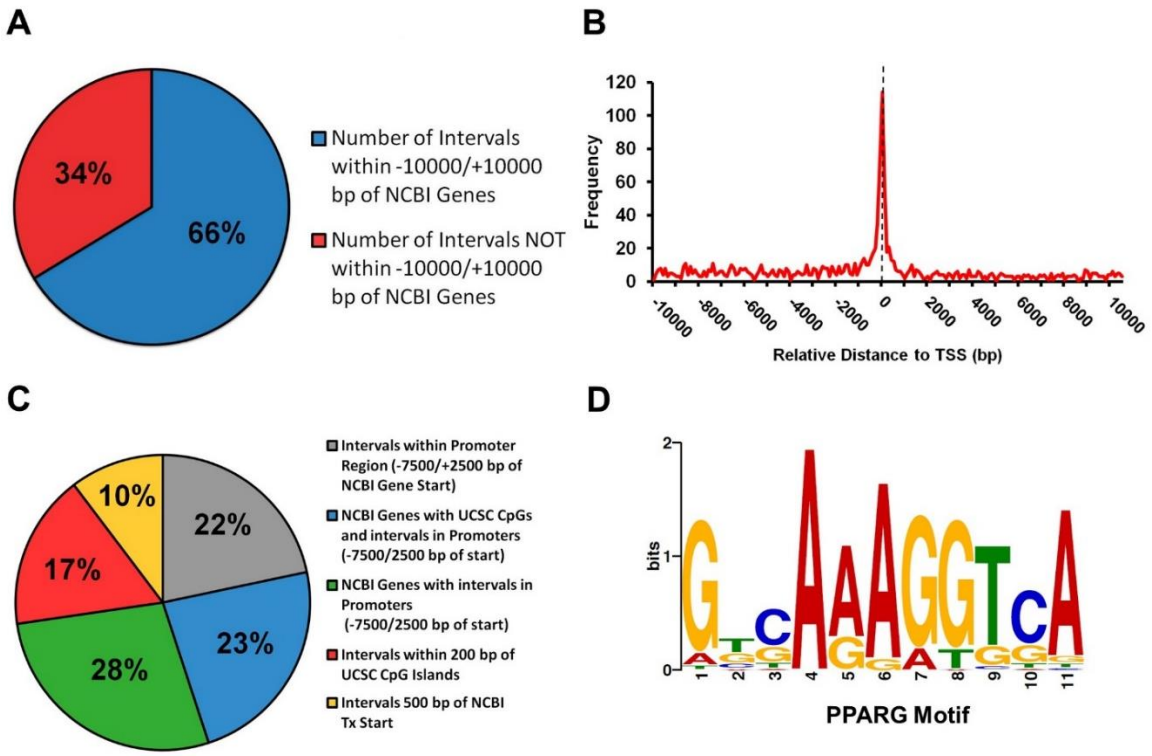

FIGURE 4. PPARG binding locations in the Day 14 conceptus. Location of PPARG binding in the Day 14 ovine conceptus was determined by ChIP-Seq analysis. A total of 2,288 binding intervals were identified. (A) Distribution of PPARG binding intervals within 10,000 bp of NCBI genes. (B) Distribution of PPARG binding intervals relative to the transcriptional start site (TSS) or genes. PPARG binding sites were present within 10,000 bp of 1,833 predicted genes. (C) Distribution of genome-wide PPARG binding locations relative to NCBI genes. (D) PPARG consensus binding motif identified in PPARG-bound intervals using TOMTOM motif comparison tool.

Gene expression in the Day 14 ovine conceptus

In order to determine genes potentially activated or repressed by PPARG in the elongating ovine conceptus, RNA sequencing (RNA-Seq) of Day 14 conceptuses was performed to identify expressed genes (see Supplementary Table 3). Using a RPKM>1 criterion, 8,775 genes were expressed in the Day 14 ovine conceptus. As summarized in Table 2, RNA-Seq identified multiple genes known to be abundantly and uniquely expressed in the mononuclear trophectoderm cells of the elongating ovine conceptus including *IFNT* (20,347 RPKM) and *pregnancy specific antigen* (also known as *pregnancy-associated glycoprotein* or *PAG*; 2,526 RPKM) [351]. Other genes of note include: *PTGS2* (1,093 RPKM), *PPARD* (23 RPKM), and *PPARG* (22 RPKM) as well as *RXRA* and *RXRB* (2 and 4 RPKM, respectively). Cell cycle regulation, DNA replication, RNA processing as well as protein transport and localization were functionally enriched in genes expressed in the Day 14 ovine conceptus based on ToppFun functional enrichment analysis (Table 3 and Supplementary Table 4).

TABLE 2. Selected mRNAs in the Day 14 conceptus determined by RNA-Seq analysis

Gene Name	Description	Mean RPKM[1]
IFNT	Ovis aries trophoblast protein-1 (TP-1)	20,347
PINLYP	phospholipase A2 inhibitor and LY6/PLAUR domain containing	14,292
KRT8	keratin 8	6,211
PAG	pregnancy-specific antigen	2,526
FADS2	fatty acid desaturase 2	2,132
PTGS2	prostaglandin G/H synthase and cyclooxygenase	1,093
ELOVL5	ELOVL fatty acid elongase 5	958
SLC25A5	solute carrier family 25, member 5	520
PTGES3	prostaglandin E synthase 3 (cytosolic)	319
HSD17B1	hydroxysteroid (17-beta) dehydrogenase 1	295
SLC2A1	solute carrier family 2, facilitated glucose transporter member 1	99
PTGIS	prostaglandin I2 (prostacyclin) synthase	76
IGF2BP1	insulin-like growth factor 2 mRNA binding protein 1	64
FASN	fatty acid synthase	41
PPARD	peroxisome proliferator-activated receptor delta	23
PPARG	peroxisome proliferator-activated receptor gamma	22
RXRB	retinoid X receptor, beta	4
RXRA	retinoid X receptor, alpha	2

[1]Relative abundance of transcripts is provided as reads per kilobase per million (RPKM)

TABLE 3. Functional annotation analysis of genes expressed in the Day 14 ovine conceptus

ID	Biological Process	Genes	P-value
GO:0000278	mitotic cell cycle	640	5.31E-84
GO:0022402	cell cycle process	798	2.58E-78
GO:0006396	RNA processing	526	1.65E-76
GO:0033554	cellular response to stress	870	1.45E-63
GO:0006974	cellular response to DNA damage stimulus	485	6.69E-55
GO:0016071	mRNA metabolic process	450	6.92E-52
GO:0044265	cellular macromolecule catabolic process	535	1.03E-49
GO:0046907	intracellular transport	845	4.74E-45
GO:0006259	DNA metabolic process	603	4.02E-44
GO:0006397	mRNA processing	316	1.62E-43
GO:0006281	DNA repair	314	2.47E-43
GO:0009057	macromolecule catabolic process	621	1.76E-42
GO:0044772	mitotic cell cycle phase transition	322	4.78E-42
GO:0051301	cell division	411	5.29E-42
GO:0008380	RNA splicing	263	1.29E-41
GO:0044770	cell cycle phase transition	324	6.13E-41
GO:0070727	cellular macromolecule localization	669	7.61E-40
GO:0034613	cellular protein localization	664	6.05E-39
GO:0051726	regulation of cell cycle	492	1.16E-38

Identification of potential PPARG target genes in the Day 14 ovine conceptus

Next, the PPARG ChIP-Seq and RNA-Seq datasets were integrated to identify potential genes regulated by PPARG in the Day 14 ovine conceptus (Table 4 and Supplementary Table 5). Of the 8,775 genes expressed in the Day 14 ovine conceptus, only 1,066 of them were bound by PPARG (Figure 5). Genes with the greatest number of PPARG binding intervals and expressed in the conceptus include *iron-responsive element binding protein 2* (*IREB2*), *heterogeneous nuclear ribonucleoprotein H3* (*HNRNPH3*), and *aspartyl-tRNA synthetase* (*DARS*). Genes bound by PPARG and expressed included *keratin 8* (6,211 RPKM), *pregnancy specific antigen* (2,526 RPKM), and *FADS2* and *FADS1* (2,132 and 1,804 RPKM). Candidate PPARG-regulated genes were enriched in biological processes related to lipid biosynthesis and lipid metabolism based on ToppFun analysis (Table 5 and Supplementary Table 6).

Genes bound by PPARG but not expressed in the Day 14 conceptus included, *ribosomal protein L13a* (*RPL13a*), *wingless-type MMTV integration site family, member 10B* (*WNT10B*), and *keratin 80* (*KRT80*). Genes bound by PPARG but not expressed were not enriched for any specific biological process based on ToppFun analysis.

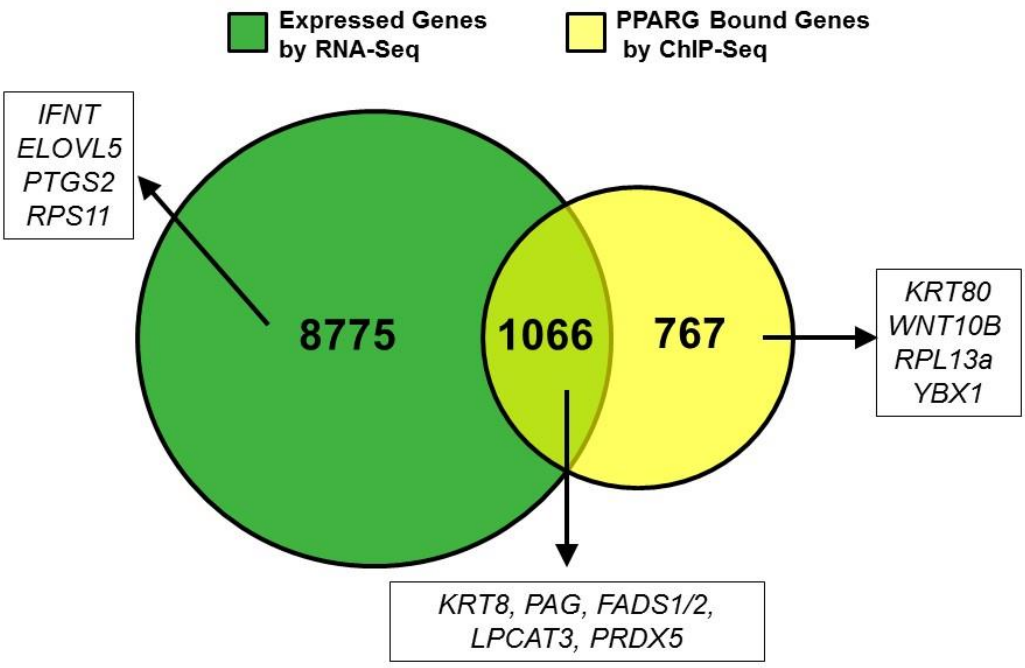

FIGURE 5. Venn diagram illustrating genes expressed in the Day 14 ovine conceptus and bound by PPARG. Gene expression in the Day 14 conceptus was determined by RNA-Seq analysis. Genes with a PPARG binding location within 10 kb of their transcriptional start site (TSS) are shown based on ChIP-Seq analysis. Examples of genes previously implicated in conceptus development or lipid metabolism pathways are provided.

TABLE 4. Selected genes bound by PPARG and expressed in the Day 14 conceptus and genes bound by PPARG but not expressed in the Day 14 ovine conceptus

Gene Name	Avg. Interval Value[1]	Gene Description
PPARG Bound and Expressed[2]		
HNRNPH3	109	heterogeneous nuclear ribonucleoprotein H3 (2H9)
DARS	97	aspartyl-tRNA synthetase
DENR	95	density-regulated protein
RBM39	94	RNA binding motif protein 39
QARS	93	glutaminyl-tRNA synthetase
QRICH1	93	glutamine-rich 1
RPS16	93	ribosomal protein S16
TMEM18	90	transmembrane protein 18
IREB2	89	iron-responsive element binding protein 2
PSMD5	89	proteasome (prosome, macropain) 26S subunit, non-ATPase, 5
TMCO1	88	transmembrane and coiled-coil domains 1
PFN1	87	profilin 1
RNF167	87	ring finger protein 167
SLC25A11	87	solute carrier family 25 (mitochondrial carrier; oxoglutarate carrier), member 11
CIAPIN1	86	cytokine induced apoptosis inhibitor 1
PPARG Bound and Not Expressed[2]		
LOC780525	112	fms-related tyrosine kinase 3 ligand
RPL13A	112	ribosomal protein L13a
WNT10B	104	wingless-type MMTV integration site family, member 10B
KRT80	94	keratin 80
ITGAE	92	integrin, alpha E (antigen CD103, human mucosal lymphocyte antigen 1; alpha polypeptide)
MSMB	90	microseminoprotein, beta-
NCOA4	90	nuclear receptor coactivator 4
LOC101116026	89	protein CutA homolog
GP1BA	87	glycoprotein Ib (platelet), alpha polypeptide
CAGE1	86	cancer antigen 1
BRSK1	83	BR serine/threonine kinase 1
MDH	81	malate dehdrogenase
LOC101115115	80	platelet glycoprotein 4-like

LOC101112913	76	uncharacterized LOC101112913
CRYGN	74	crystallin, gamma N

[1]Avg. interval value refers to the average fragment densities of all bins within the PPARG binding interval

[2]Expression was based on RNA-Seq analysis.

TABLE 5. Functional annotation analysis of PPARG bound and expressed genes in the Day 14 ovine conceptus

ID	Biological Process	# Genes	P-value
GO:0008654	phospholipid biosynthetic process	32	3.85E-10
GO:0008610	lipid biosynthetic process	58	9.76E-10
GO:0044255	cellular lipid metabolic process	73	2.69E-08
GO:0006644	phospholipid metabolic process	35	3.69E-08
GO:0019752	carboxylic acid metabolic process	72	2.87E-07
GO:0006629	lipid metabolic process	88	3.22E-07
GO:0044265	cellular macromolecule catabolic process	60	6.89E-06
GO:0046907	intracellular transport	93	8.91E-06
GO:0019432	triglyceride biosynthetic process	10	6.55E-05
GO:0046460	neutral lipid biosynthetic process	10	8.98E-05
GO:0006631	fatty acid metabolic process	28	3.12E-04
GO:0006638	neutral lipid metabolic process	14	3.16E-04
GO:0005975	carbohydrate metabolic process	56	3.80E-04
GO:0006641	triglyceride metabolic process	13	4.86E-04
GO:0030258	lipid modification	17	5.49E-04
GO:0006520	cellular amino acid metabolic process	35	9.53E-04

DISCUSSION

In the present study, an *in utero* loss-of-function approach found that PPARG is an essential regulator of conceptus elongation. The approach of combining PPARG ChIP-Seq and RNA-Seq transcriptome analyses of the ovine conceptus allowed for identification of potential genes and biological pathways regulated by PPARG in the trophectoderm. To our knowledge, this is the first report of PPARG ChIP-Seq and RNA-Seq analysis of the ovine conceptus. Information contained in those analyses is a valuable resource for future studies to understand the cellular and molecular mechanisms governing conceptus growth and trophectoderm function in ruminants. The present and other studies strongly support the idea that PTGS2-derived PGJ2 actions via PPARG have important biological roles in the transport, cellular uptake, storage, and metabolism of lipids, glucose, fatty acids and PGs in the trophectoderm of the elongating conceptus [137, 352]. In the present study, loss of PPARG but not PPARD in the trophectoderm compromised conceptus elongation. The visibly growth retarded and malformed conceptuses from PPARG MAO infused ewes had essentially no morphologically normal trophectoderm cells. Results of the present study support the idea that the growth retardation and malformation of the conceptuses from PPARG MAO infused ewes was due to primarily to apoptosis in the trophectoderm. The substantially reduced IFNT and PGs in the uterine lumen is consistent with the lack of mononuclear trophectoderm cells in the growth-retarded conceptuses. As expected, reduced IFNT levels in the uterine lumen were accompanied by substantial lack of induction of classical Type I ISGs in the endometrium [73, 103,

108, 290]. Of note, two genes, the CTSL1 protease and SLC2A5 facilitative glucose/fructose transporter, were higher in the endometria of ewes with malformed conceptuses. During a normal pregnancy, expression of these progesterone-induced endometrial epithelial genes is increased by IFNT as well as PGs from the elongating conceptus [57]. Given that PGs and IFNT were lower in the endometria from the PPARG MAO-infused ewes, increased expression of *CTSL1* and *SLC2A5* in the endometrium of ewes receiving PPARG MAO treatment suggests they are sensitive to abnormally developing conceptuses. Indeed, the endometrium of cattle can sense the difference between a conceptus derived from nuclear transfer and *in vitro* fertilization on Days 18 or 20 of pregnancy [316, 317]. Future studies should determine if other genes are altered in the endometrium of early pregnant sheep gestating unhealthy conceptuses.

Proliferation of the trophectoderm is a key process involved in conceptus elongation and is thought to rely on glucose, amino acids, lipids and proteins provided by the endometrium, particularly since in vitro-derived blastocysts will not form a conceptus that elongates in culture [353-356]. Treatment of cultured ovine trophoblast cells with glucose stimulates their proliferation and migration [357]. In the ovine ULF, total glucose increases 6-fold between Days 10 and 15 of pregnancy [66]. Candidate gene profiling experiments found that multiple facilitative (SLC2A1, SLC2A3, SLC2A4) and sodium-dependent (SLC5A1, SLC5A11) glucose transporters are expressed in the trophectoderm of the conceptus [358]. The present study found that many other members of the SLC glucose transporter family were expressed in the Day 14 ovine conceptus including

SLC2A3 and SLC5A1. The fate and activities of glucose within the trophectoderm of the elongating ovine conceptus has not been reported. In adipocytes, the transcription factor SREBP1/ADD1 promotes glycolytic conversion of glucose to acetyl-CoA, and subsequently the synthesis of fatty acids from acetyl-CoA [359, 360]. In adipose tissue, SREBP1/ADD1 also stimulates the expression of PPARG, which influences the storage of glucose-derived fatty acids as well promotes differentiation of pre-adipocytes into fat cells [361, 362]. In extravillous cytotrophoblasts of human placentae, PPARG is thought to regulate the accumulation of neutral lipids in the syncytiotrophoblasts and uptake of free fatty acids (FFA) [172]. Of note, *Pparg* null murine embryos lack lipid droplets that are normally present in wild type placentas [166, 363]. In the elongating ovine conceptus, lipid droplets are observed in the cytoplasm of trophectoderm cells [364]. Little information is available on lipids in the uterine lumen during early pregnancy or their role in conceptus elongation; however, an increase in trophectoderm cell number during conceptus elongation likely depends upon provision of lipids from the uterus, particularly given the large amounts of PGs synthesized and released by the developing ovine conceptus [57, 132, 133]. As illustrated in Figure 6, prostaglandins can be transported into the cell or can be derived enzymatically from cell membrane phospholipids through an arachidonic acid intermediate created from diacylglycerol via phospholipase A2 (PLA2) or fatty acids. The PLA2-derived arachidonate is then brought to either the cyclooxygenase pathway or the lipoxygenase pathway [172, 361, 362]. The cyclooxygenase pathway produces PGH2, which can be metabolized into to active

prostaglandins including PGD2, PGE2, PGF2α and prostacyclin or PGI2 via cell-specific prostaglandin isomerases and synthases [166, 363, 365]. Prostaglandins synthesized and secreted by the elongating conceptus acts in a paracrine manner to stimulate expression of elongation- and implantation-related genes in the endometrium of early pregnant sheep [78]. Those PGs are important, because inhibition of PTGS2 activity by infusion of a selective PTGS2-specific inhibitor into the uterus from Days 8 to 14 post-mating inhibited the ovoid conceptus from elongating [57].

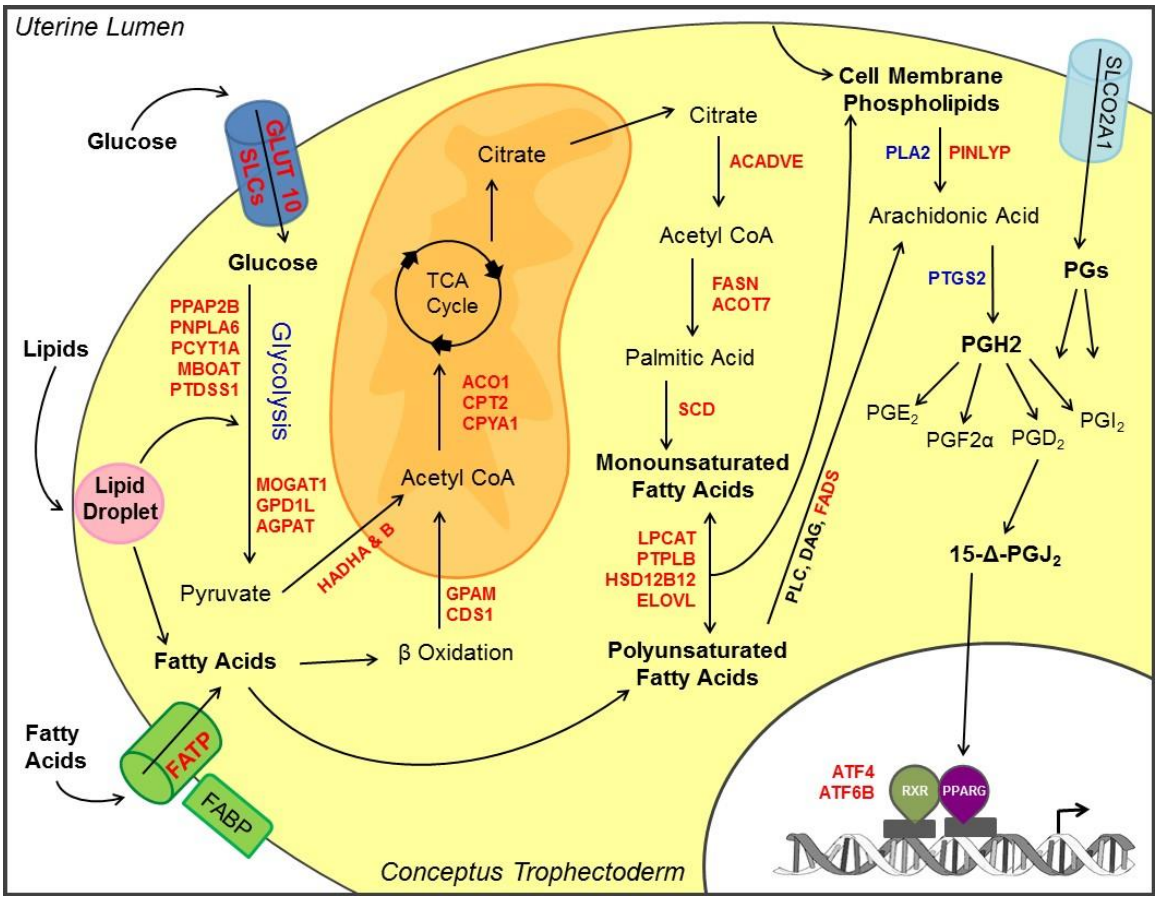

FIGURE 6. Summary of potential PPARG regulated genes and pathways **involved** in glucose, lipid and fatty acid uptake and metabolism in the conceptus trophectoderm. Genes bound by PPARG and expressed in the conceptus trophectoderm are represented in red. See text in Discussion for an explanation.

Glucose, lipids, fatty acids and PGs likely have important biological roles in trophectoderm metabolism, growth and survival during conceptus elongation (Figure 5). The ChIP-Seq analysis in the present study supports a biological role for PPARG in fatty acid uptake and metabolism in the conceptus trophectoderm. Similarly, a recent ChIP-Seq analysis of PPARG in primary adipocyte cells found regulation of fatty acid binding proteins (FABP), fatty acid transport proteins (FATP), and fatty acid desaturases (FADS1 and FADS2), which catalyze the desaturation of unsaturated fatty acids to generate arachidonic acid (AA) and other eicosanoid precursors [366]. Polyunsaturated fatty acids (PUFA) are essential constituents of membrane phospholipids with important roles in regulation of cell membrane fluidity and are used an energy source during embryo maturation and the extended periods of cell proliferation preceding implantation in a number of species [367]. Cell surface proteins, such as fatty acid transporter (FAT/CD36), FATP and FABP, are present in human trophoblast membranes and are involved in translocation and fatty acid uptake into cells [170]. Other candidate PPARG regulated and expressed genes in the Day 14 ovine conceptus identified in the present study and others include: phospholipase A2 inhibitor and Ly6/PLAUR domain-containing protein-like (PINLYP), which may be involved in regulation of lipid synthesis from membrane phospholipids to promote stability in the elongating trophectoderm [368, 369]; lysophosphatidylcholine acyltransferase 3 (LPCAT3) an enzyme involved in fatty acid remodeling of phospholipids and metabolism of bioactive lipids [370]; and monoacylglycerol O-acyltransferase 1 (MOGAT1) which catalyzes the synthesis of diacylglycerols, the precursor of physiologically

important lipids such as triacylglycerol and phospholipids [371]. Collectively, available results support the idea that PTGS2-derived PGJ2 acts via PPARG to regulate expression of genes in involved in the uptake of glucose, lipids and fatty acids and their metabolism in the mononuclear trophectoderm cells of the elongating ovine conceptus. Although not addressed in the present study, PPARG and perhaps PPARD may also be involved in differentiation of trophoblast giant binucleate cells from the mononuclear trophectoderm cells in the ruminant conceptus [341, 372].

Investigation of genes and pathways regulated by PPARG could help determine key pathways that are essential for conceptus elongation and, more specifically, trophectoderm survival and proliferation. Increased knowledge of those pathways is important, as the majority of pregnancy loss in ruminants occurs early in gestation and is due to either failure during blastocyst formation or post blastocyst embryonic failure during the critical time of conceptus elongation [373]. *In vivo* loss of function studies are necessary to further our understanding of the complex molecular and cellular events surrounding conceptus development and early pregnancy events and may be made more feasible with the recent emergence of genomic editing tools involving meganucleases [374, 375].

ACKNOWLEDGMENTS

The authors thank Dr. Paul Labhart (Active Motif, Carlsbad, CA, USA) for performing the ChIP-seq analysis and Mark Wildung (Molecular Biology and Genomics Core, Washington State University, Pullman, WA, USA) for performing the RNA-Seq analyses.

SUPPLEMENTAL TABLES

SUPPLEMENTAL TABLE 1. Primer information for cloning and qPCR analysis

SUPPLEMENTAL TABLE 2. Complete information on PPARG ChIP-Seq analysis of the day 14 ovine conceptus

SUPPLEMENTAL TABLE 3. Complete information on RNA-Seq analysis of the day 14 ovine conceptus including expression data annotated with sheep and cattle databases as well as boxplots and cluster analysis

SUPPLEMENTAL TABLE 4. Functional enrichment analysis of genes expressed in the day 14 ovine conceptus using ToppFun bioinformatic analysis

SUPPLEMENTAL TABLE 5. Complete information on genes bound by PPARG and expressed in the day 14 ovine conceptus

SUPPLEMENTAL TABLE 6. Functional enrichment analysis of genes bound by PPARG and expressed in the day 14 ovine conceptus using ToppFun bioinformatic analysis

Available online at
http://www.biolreprod.org/content/early/2014/12/15/biolreprod.114.123877

SECTION IV:

Biological Roles of Hydroxysteroid (11-Beta) Dehydrogenase 1 (HSD11B1), HSD11B2, and Glucocorticoid Receptor (NR3C1) in Sheep Conceptus Elongation

Kelsey Brooks, Gregory Burns, and Thomas E. Spencer

This work has been published in:

Biol Reprod. 2015 Aug;93(2):38. doi: 10.1095/biolreprod.115.130757. Epub 2015 Jun 17.

ABSTRACT

In sheep, the elongating conceptus synthesizes and secretes interferon tau (IFNT), as well as prostaglandins (PGs) and cortisol. The enzymes, hydroxysteroid (11-beta) dehydrogenase 1 (HSD11B1) and HSD11B2, interconvert cortisone and cortisol. In sheep, *HSD11B1* is expressed and active in the conceptus trophectoderm as well as in the endometrial luminal epithelia; in contrast, *HSD11B2* expression is most abundant in conceptus trophectoderm. Cortisol is a biologically active glucocorticoid and ligand for the glucocorticoid receptor (NR3C1 or GR) and mineralocorticoid receptor (NR3C2 or MR). Expression of MR is not detectable in either the ovine endometrium or conceptus during early pregnancy. In tissues that do not express MR, HSD11B2 protects cells from the growth-inhibiting and/or pro-apoptotic effects of cortisol, particularly during embryonic development. In Study One, an *in utero* loss-of-function analysis of HSD11B1 and HSD11B2 was conducted in the conceptus trophectoderm using morpholino antisense oligonucleotides (MAO) that inhibit mRNA translation. Elongating, filamentous conceptuses were recovered on Day 14 from ewes infused with control morpholino or HSD11B2 MAO. In contrast, HSD11B1 MAO resulted in severely growth-retarded conceptuses or conceptus fragments with apoptotic trophectoderm. In Study Two, clustered regulatory interspaced short repeat (CRISPR)/Cas9 genome editing was used to determine the role of GR in conceptus elongation and development. Elongating, filamentous type conceptuses (12-14 cm in length) were recovered from ewes gestating control embryos (n=7/7) and gestating GR-edited embryos (n=6/7). These results support the idea that the

effects of HSD11B1-derived cortisol on conceptus elongation are indirectly mediated by the endometrium and are not directly mediated through GR in the trophectoderm.

INTRODUCTION

In sheep, the morula stage embryo enters into the uterus on Day 6 (Day 0 is the day of estrus and mating), hatches from the zona pellucida on Day 8, and by Day 12 has developed to an ovoid or tubular form. The ovoid conceptus continues to grow and elongate into a filamentous form, reaching 12-14 cm in length by Day 14 [22, 376]. The elongating conceptus is primarily composed of mononuclear trophectoderm cells lined with endoderm [19, 29, 339]. Blastocyst survival and growth into an elongated conceptus requires secretions of the endometrial luminal (LE) and glandular epithelia (GE) [40, 72]. [19, 21]. Changes in endometrial epithelial gene expression during early pregnancy are regulated primarily by progesterone from the corpus luteum and also influenced by interferon tau (IFNT), prostaglandins (PGs), and cortisol from the trophectoderm of the elongating conceptus [40, 41, 103, 315]. IFNT acts on the endometrium to inhibit production of luteolytic pulses of PGF2α, therefore maintaining the corpus luteum and progesterone production [47]. Both the developing conceptus and endometrium synthesize and secrete substantial amount of PGs during early pregnancy. Prostaglandins are important for conceptus elongation in sheep because intrauterine infusion of meloxicam, a selective PTGS2 inhibitor, into the

uterine lumen from Days 8 to 14 after mating completely inhibited conceptus elongation [57].

Hydroxysteroid (11-beta) dehydrogenase 1 (HSD11B1) and cortisol are implicated in regulation of conceptus growth and development in early pregnant sheep [74]. Two isoforms of 11-beta-hydroxysteroid dehydrogenase, HSD11B1 and HSD11B2, act to modulate the actions of glucocorticoids [377]. HSD11B1 is a low affinity NADP(H)-dependent bidirectional dehydrogenase/reductase for glucocorticoids. The direction of HSD11B1 activity is determined by the relative abundance of NADP+ and NADPH cofactors. In the presence of a high NADPH to NADP+ ratio, which can be generated by hexose-6-phosphate dehydrogenase (H6PD), HSD11B1 acts predominately as a keto-reductase to generate active cortisol from inactive cortisone [197]. In contrast, HSD11B2 is a high-affinity NADPH-dependent unidirectional dehydrogenase that metabolizes cortisol to cortisone. First identified as a candidate progesterone-regulated gene by endometrial microarray analysis, *HSD11B1* is expressed specifically in the endometrial LE of the ovine uterus and induced by progesterone and stimulated by IFNT [192, 378]. Although *HSD11B2* mRNA was detectable at very low levels in all endometrial cell types during estrous cycle and pregnancy, it was particularly abundant in conceptus trophectoderm [192]. Thus, two isoforms of HSD11B enzymes regulate cortisol regeneration or inactivation in the ovine endometrium and/or conceptus during the peri-implantation stage of pregnancy. HSD11B1 activity was detected in the conceptus and trophectoderm cells can generate bioactive cortisol from cortisone [58]. Importantly, intrauterine administration of a

specific HSD11B1 inhibitor, PF 915275, prevented conceptus elongation [59]. Cortisol can elicit actions on cells via the glucocorticoid receptor (nuclear receptor subfamily 3, group C, member 1 or NR3C1 or GR) and the mineralocorticoid receptor (nuclear receptor subfamily 3, group C, member 2 or NR3C2 or MR). Immunoreactive GR protein is present in all endometrial cells of ovine uterus during the estrous cycle and pregnancy as well as in the conceptus trophectoderm [57, 192, 378]; however, expression of MR was not detected in the ovine uterus or conceptus of cyclic or early pregnant sheep.

Available evidence supports the working hypothesis that cortisol, generated by HSD11B1 in the endometrial epithelia and/or trophectoderm, acts via GR in the trophectoderm to regulate conceptus elongation. To test this hypothesis, an *in vivo* morpholino (MO) loss of function study was conducted to specifically inhibit *HSD11B1* or *HSD11B2* mRNA translation in the trophectoderm of the developing conceptus. Further, the role of GR in conceptus development and elongation was determined using CRISPR/Cas9 based genome editing [273, 379].

MATERIALS AND METHODS

Morpholino Design

Design. Morpholino oligonucleotides were designed and synthesized by Gene Tools (Philomath, OR). The HSD11B1 morpholino antisense oligonucleotide (MAO) (TCATAAAAGCCATCAGACAGGGATC) was designed to target 25 bp surrounding the initial portion of the ovine *HSD11B1* mRNA (GenBank accession no. NM_001009395.1). The *HSD11B2* MAO (CCGACGGCCAGGGCCAGCTTTCCAT) was designed to target the first 25 bp of

the ovine *HSD11B2* mRNA (GenBank accession no. NM_001009460.1). A random oligo 25-N morpholino was used as a control, which is synthesized with a random base at every position and does not target any known mRNAs or genes (Gene Tools).

Validation. Oligos analogous to the MAO-targeting portion of the ovine *HSD11B1* and *HSD11B2* mRNA coding sequences (CDS) were synthesized by IDT (Supplemental Table 1). Oligos were designed to include a 5' *NheI* overhang, a portion of the mRNA to be bound by the MAO, and a 3' *NheI* overhang. The psiCHECK2 dual luciferase (LUC) reporter plasmid (Promega) was digested with the restriction enzyme *NheI* and subsequently treated with antarctic phosphatase (New England Biolabs). Coding sequence oligos were annealed and ligated into psiCHECK2, upstream and in-frame with LUC, using T4 DNA ligase (Life Technologies). The resulting vectors were sequenced (Washington State University Molecular Biology and Genomics Core, Pullman, WA) for verification. Human 293T cells were transfected with psiCHECK2:HSD11B1 CDS LUC or psiCHECK2:HSD11B2 CDS LUC vectors using Lipofectamine 2000 (Life Technologies). After 6 h, cells were incubated with 2, 4, or 8 µM HSD11B1 MAO, HSD11B2 MAO, or control MO complexed to the Endo-Porter delivery reagent (6 µl per 1 ml; Gene Tools). After 48 h, cell lysates were analyzed for LUC activity using a dual LUC reporter assay system (Promega).

Design and Construction of CRISPR/Cas9 gRNAs

Guide RNAs (gRNAs) were designed to regions within Exon 2 of ovine *GR* that encodes the GR DNA binding domain using the Cas9 Online Designer (http://cas9.wicp.net). Four gRNAs with the fewest predicted off targets were selected. Specificity of the designed gRNAs was confirmed by searching for similar ovine sequences containing a PAM domain in GenBank. The selected gRNAs were synthesized as ssDNA oligos containing *BsmBI* restriction enzyme overhangs by Integrated DNA Technologies (IDT) (Supplemental Table 1) and annealed and ligated into pT7-gRNA vector (Addgene #46759) using T4 DNA ligase (Invitrogen). The resulting vectors were sequenced for verification purposes, and used as templates for RNA synthesis using the MEGAshortscript kit (Ambion, Austin, TX). Wildtype *Cas9* mRNA was synthesized from pX330-T7 Wt (Addgene: # 42230) using mMESSAGE mMACHINE Ultra kit (Ambion) after plasmid digestion with *EcoRI*. Synthesized RNA was quantified using the Qubit RNA BR assay kit (Life Technologies) and stored at -80°C until use. Prior to zygote injection, the 4 gRNAs were combined to a final concentration of 200 ng/µl and then diluted 1:2 with 200 ng/µl *Cas9* mRNA for a final concentration of 100 ng/µl gRNAs and *Cas9* mRNA.

Animal Experiments

All experimental and surgical procedures were approved by the Institutional Animal Care and Use Committee of Washington State University. For both studies, mature Columbia Rambouillet crossbred ewes (*Ovis aries*) were observed for onset of estrus (designated Day 0). Ewes were mated to an intact ram of proven fertility on Days 0 and 1.

Study One. On Day 8 post-mating, ewes (n≥5 per treatment) were subjected to a mid-ventral laparotomy, and a uterine horn ipsilateral to the ovary containing a corpus luteum was ligated and fitted with an osmotic pump containing either: (1) random oligo 25-N control MO; (2) HSD11B1 MAO; or (3) HSD11B2 MAO. Each pump contained a total of 100 nmol of the indicated morpholino complexed with 50 µl of Gene Tools Endo-Porter Aqueous delivery reagent in 2 ml sterile PBS (Hyclone, Logan, UT). All ewes were necropsied on Day 14 post-mating. The female reproductive tract was recovered, and the ligated uterine horn gently flushed with 10 ml of sterile PBS (pH 7.2). If present, the state of conceptus development was assessed using a Nikon SMZ1000 stereomicroscope (Nikon Instruments Inc., Lewisville, TX) fitted with a Nikon DS-Fi1 digital camera. The volume of the uterine flush was measured, and the flush clarified by centrifugation (3000 x g at 4°C for 15 min). The supernatant was carefully removed with a pipet, mixed, aliquoted, frozen in liquid nitrogen, and stored at -80°C. Portions of the conceptus were fixed in fresh 4% paraformaldehyde in PBS (pH 7.2). After 24 h, fixed tissues were changed to 70% ethanol for 24 h and then dehydrated and embedded in Paraplast-Plus (Oxford Labware, St. Louis, MO). The endometrium was physically dissected from the remainder uterine horn using curved scissors. Endometrial samples as well as any remaining conceptus tissue were frozen in liquid nitrogen, and stored at -80°C for subsequent RNA extraction.

Study Two. Ewes were synchronized to estrus using an Eazi-Breed Controlled Internal Drug Releasing (CIDR) device for 12 days. Superovulation of donor ewes was achieved through twice daily injections of follicle stimulating

hormone (FSH) (Bioniche, Belleville, Ontario, Canada) over a four-day period from Days 9 to 12 after CIDR insertion. Dosage decreased daily (50, 40, 35 and 30 mg, respectively). On Day 11, the CIDR was removed, and ewes were administered 15 mg prostaglandin F2 alpha (Lutalyse), and mated to fertile rams at estrus. Embryos were collected from donor females approximately 36 h post estrus. Oviducts were flushed from the uterotubal junction through the fimbriated end with 20 ml embryo flush media (Bioniche). One cell zygotes were identified and isolated with the aid of a dissecting microscope. Recovered embryos were injected with either: (1) 100 ng/µl *Cas9* mRNA; or (2) 100 ng/µl *Cas9* mRNA along with 20 ng/µl of each gRNA for a total of 100 ng/µl gRNA. Following microinjection, embryos were cultured to the blastocyst stage and then transferred (3–4 per recipient) into the uterus of synchronized recipient ewes. Recipient ewes were synchronized to estrus using procedures similar to those employed for embryo donors except FSH was not administered to induce superovulation. All recipient ewes were euthanized on Day 14 post-mating and tissues were immediately collected. The uterus was flushed with 20 ml of PBS (pH 7.2), and the number of conceptuses and state of conceptus development was assessed under bright field illumination using a SMZ1000 photomicroscope fitted with a DS-Fi1 digital camera (Nikon). The volume of the recovered uterine flushing was measured and recorded, and the flushing clarified by centrifugation (3000 x g at 4°C for 15 min). The supernatant was carefully removed with a pipet, mixed, aliquoted, frozen in liquid nitrogen, and stored at -80°C. Several sections (~0.5 cm) from the mid-portion of each uterine horn as well as portions of the conceptus were fixed in fresh 4% paraformaldehyde

in PBS (pH 7.2). After 24 h, fixed tissues were changed to 70% ethanol for 24 h and then dehydrated and embedded in Paraplast-Plus (Oxford Labware, St. Louis, MO). The remaining endometrium was physically dissected from the myometrium using curved scissors, flash frozen in liquid nitrogen, and stored at -80°C for subsequent RNA extraction. The remaining conceptus tissue was flash frozen in liquid nitrogen, and stored at -80°C for subsequent extraction using the AllPrep RNA/DNA/Protein extraction kit (Qiagen).

Assessment of GR editing and off target effects

A region of GR Exon 2, surrounding the targeted region for gene editing, was amplified from conceptus genomic DNA using TaKaRa Ex Taq proofreading DNA polymerase (Clontech, Mountain View, CA) and long range PCR primers (Supplemental Table 1). Additional regions of the ovine genome were selected to screen for off target effects based on their complementarily to the gRNAs, genomic location, expression in the Day 14 conceptus, and possession of a similar protospacer adjacent motif (PAM) sequence. All PCR amplified regions were separated on an agarose gel and extracted using the QIAquick Gel Extraction Kit (Qiagen). Single, isolated products were used as a template for Sanger sequencing.

Microinjection, culture, and transfer of ovine zygotes

In vitro synthesized mRNA coding for Cas9 (100 ng/µl) and 4 GR targeting gRNAs (100 ng/µl) were injected into the cytoplasm of zygotes recovered 36 hr post estrus using a FemtoJet microinjector (Eppendorf; Hamburg, Germany). *In*

vitro synthesized *Cas9* mRNA only (100 ng/µl) was injected into some zygotes as a control. Microinjection was performed in M199 holding media (M199 Hanks (10.6 mg/ml, Sigma), HEPES (0.6 mg/ml, Gibco), $NaHCO_3$ (0.35 mg/ml, Fisher), FBS (10%, Hyclone), Gentamicin (0.05 mg/ml, Sigma)) on the heated stage of a Nikon Eclipse Ti inverted microscope (Nikon). Injected zygotes were then transferred to EVOLVE media (KSOMaa EVOLVE (Zenith Biotech, Guilford, CT) with Probumin BSA (4 mg/ml) and Gentamicin (0.05 mg/ml, Invitrogen)) under mineral oil (Irvine Scientific, Santa Ana, CA) for culture at 38.5°C in an atmosphere of 5% CO2/5% O2/90% N2 until transfer. Blastocysts were surgically transferred into the uterus of recipient ewes on Day 9 post-estrus.

Quantification of IFNT in Uterine Flush

The amount of IFNT in the uterine flush was determined by Western dot blot analysis as previously described using an antibody that is specific for IFNT [105]. A sample of the uterine flush (100 µl) from each ewe was diluted to 200 µl final volume with 50 mM Tris and 150 mM NaCl (TBS). A nitrocellulose membrane (GE Healthcare-Life Sciences, Pittsburgh, PA), presoaked with TBS, was loaded into a BioRad dot blot apparatus (Hercules, CA) backed by Whatman filter paper. Wells were subsequently washed with 200 µl TBS prior to addition of the diluted uterine flush sample, and then rinsed with 200 µl TBS. The membrane was allowed to air dry and then blocked in 5% (wt/vol) milk/TBS with 0.1% Tween 20 (TBST) for 1 h at room temperature. The membrane was then incubated in primary rabbit anti-ovine IFNT serum [344] at 1:1000 dilution in 5% milk/TBST overnight at 4°C The blot was then washed for 30 min in TBST followed by incubation with goat anti-

rabbit IgG horseradish peroxidase conjugate (Thermo Scientific, Waltham, MA) at 1:5,000 diluted in 5% milk/TBST for 1 h at room temperature. The blot was washed again for 30 min in TBST. Immunoreactive IFNT was detected using SuperSignal West Pico Chemiluminescent Substrate (Thermo Scientific) and quantified with a ChemiDoc MP system and Image Lab 4.1 software (BioRad). The data are expressed as total relative amount of IFNT in the uterine flush determined by adjusting for the recovered volume of uterine flushing.

Quantification of PGs in the Uterine Flush

Prostaglandins in the uterine flush were measured by sensitive enzyme immunoassay (EIA) from Cayman Chemical (catalog no. 514012; Ann Arbor, MI) as described previously [58, 380, 381]. The antiserum used in this assay exhibits high cross reactivity for most PGs, which allows quantification of all the PGs in a given sample with a single assay (Cayman Chemicals). Total PGs in the uterine flush were measured according to the manufacturer's recommendations in a single assay with a sensitivity of 15.63 pg/ml. The data are expressed as total amounts of PGs, determined by adjusting for the recovered volume of uterine flush.

Quantification of Cortisol in the Uterine Flush

Quantification of cortisol in the uterine flush was assessed by sensitive enzyme immunoassay (EIA) from Cayman Chemical (catalog no. 500360) as described previously [58, 59]. Total cortisol in the uterine flush was measured according to the manufacturer's recommendations in a single assay with a

sensitivity of 6.55 pg/ml. The data are expressed as total amounts of cortisol, as determined by adjusting for the recovered volume of uterine flush.

Endometrial Total RNA Isolation and Real-Time PCR Analysis

Total RNA was isolated from frozen endometrial samples using Isol-RNA lysis reagent (5 Prime, Gaithersburg, MD). To eliminate genomic DNA contamination, extracted RNA was treated with DNase I and purified using RNeasy MinElute cleanup kit (Qiagen, Valencia, CA). The quantity and purity of total RNA were determined by spectrometry. Total RNA (1 µg) from each sample was reverse transcribed in a total reaction volume of 20 µl using iScript RT supermix (Bio-Rad, Hercules, CA). Reverse transcription was performed as follows: 5 min at 25°C; 30 min at 42°C; and 5 min at 85°C. Control reactions in the absence of reverse transcriptase were prepared for each sample to test for genomic DNA contamination. The resulting cDNA was stored at -20°C for further analysis.

Real-time PCR was performed using a CFX384 Touch Real Time System with SsoAdvanced Universal SYBR Green Supermix (Bio-Rad, Hercules, CA). Previously published primers for *CXCL10, CTSL1, GAPDH, GRP, IGFBP1, ISG15, LGALS15, RSAD2, SLC2A1, SLC5A1* and *SLC7A2* were used [57], and primers for ovine *ACTB* and *RPL19* were designed and synthesized by Integrated DNA technologies (Coralville, IA) (Supplementary Table 1). Each sample was analyzed in duplicate with the following conditions for 40 cycles: 95°C for 30 sec; 95°C for 5 sec; and 60°C for 30 sec. A dissociation curve was generated at the end of amplification to ensure that a single product was amplified. PCR reactions without

template and template substituted with total RNA were used as a negative control to verify experimental results. The threshold line was set in the linear region of the amplification plot above the baseline noise, and quantification cycle (Cq) values were determined as the cycle number in which the threshold line intersected the amplification curve. Ovine *GAPDH, ACTB,* and *RPL19* were used as reference genes.

Immunohistochemistry

Fixed conceptuses were embedded in paraffin wax and sectioned with a microtome (8 µm). Sections were mounted on slides, deparaffinized in xylene substitute, and rehydrated in a graded alcohol series. Sections were then submitted to hematoxylin and eosin (H & E) staining (Scytek, Logan, UT), immunohistochemistry, or TUNEL apoptosis assay. For immunohistochemistry, antigen retrieval was performed by incubating sections affixed to slides for 10 min in boiling 10 mM citrate buffer (pH 6.0). After cooling to room temperature, sections were incubated with 10% normal goat serum in PBS (pH 7.5) for 10 min at room temperature and then overnight at 4°C with rabbit anti-Ki67 IgG (cat. no. ab66155; Abcam, Cambridge, MA, USA) at 1.2 µg/ml in 1% BSA in PBS (pH 7.5). Sections were washed in PBS and incubated with biotinylated secondary antibody at 5 µg/ml (cat. no. PK-4001; Vector Laboratories, Burlingame, CA, USA) for 1 h at 37°C. Immunoreactive Ki67 protein was visualized using Vectastain ABC kit (Vector Laboratories) using diamino-benzidine tetrahydrochloride as the chromagen. Sections were counterstained with hematoxylin, and coverslips were affixed to slides with Permount mounting medium (Fisher Scientific, Fairlawn, NJ, USA).

Images of representative fields were recorded using a Nikon Eclipse 90i model photomicroscope fitted with a DS-Ri1 digital camera.

TUNEL apoptosis assay

Apoptosis was assessed using a terminal deoxynucleotidyl transferase (TdT)-mediated dUTP nick-end labeling (TUNEL) assay (Catalog No. G3250; Promega) according to the manufacturer's instructions for paraffin-embedded tissue with slight modification. Briefly, sections were rehydrated and fixed in 4% methanol free paraformaldehyde (PFA) in PBS for 15 min at room temperature. The tissue was permeabilized with Proteinase K for 8 min, washed with PBS, and fixed in PFA. Slides were then covered with equilibration buffer for 5-10 minutes at room temperature followed by incubation with TdT incubation buffer (containing TdT and nucleotide mix) for 1 h at 37°C in a humidified chamber. The reaction was terminated by submersion of slides in 2X SSC for 15 minutes at room temperature. The sections were washed with PBS and coverslips applied using Vectashield mounting media with DAPI (Vector Laboratories). Images of representative fields were recorded using a Nikon Eclipse 90i model photomicroscope fitted with a DS-Ri1 digital camera. Brightfield and epifluorescent (DAPI and FITC) images were collected using NIS Elements BR 3.2 software (Nikon). Background fluorescence was corrected based on FITC intensity of positive control slides produced by DNase I (Qiagen) treatment according to TUNEL assay instructions (Promega).

GR Activation ELISA

The preparation of cellular nuclear extracts and measurement of the GR DNA-binding activity were performed with a nuclear extraction kit (Affymetrix-Panomics, Santa Clara, CA, USA) and an GR ELISA kit (Affymetrix-Panomics), respectively, according to the manufacturer's protocols.

The DNA binding activity of GR in Cas9 and GR edited conceptuses was measured using a GR ELISA kit (Part # EK1060; Affymetrix-Panomics, Cleveland, OH) according to manufacturer's instructions. Briefly, total cellular protein was isolated from conceptuses in RLT buffer (Qiagen) by acetone precipitation. The extracted protein (10 ug) was incubated with the provided GR specific probe for 30 min, allowing activated GR molecules to bind the GR consensus binding site on the biotinylated oligonucleotide (GR probe). Oligonucleotides were then immobilized on a streptavidin coated 96-well plate. GR bound oligonucleotide were detected by GR primary antibody, and detection was quantified using a horseradish peroxidase (HRP)-conjugated secondary antibody which reacts with the tetramethylbenzidine substrate to provide a sensitive colorimetric readout which was quantified by spectrophotometry at 450 nm.

Statistical Analysis

All quantitative data were subjected to least-squares analyses of variance (ANOVA) using the General Linear Models (GLM) procedures of the Statistical Analysis System (SAS Institute Inc., Cary, NC). For analyses of real-time PCR data, *GAPDH*, *ACTB* and *RPL19* values were used as covariates. Data are expressed as fold change relative to endometria from Control MO infused sheep.

Error terms used in test of significance were identified according to the expectation of the mean squares for error. Significance ($P<0.05$) was determined by probability differences of least-squares means (LSM).

RESULTS

Study 1: Effect of HSD11B1 and HSD11B1 Inhibition by MAO

Morpholino antisense oligonucleotides (MAOs) were designed to inhibit translation of either ovine *HSD11B1* or *HSD11B2* mRNAs. The effectiveness of each MAO to inhibit translation of the target mRNA was assessed *in vitro* using HEK 293T cells transiently transfected with a LUC reporter construct possessing the targeted MAO binding sequence upstream of renilla luciferase (HSD11B1 CDS-LUC or HSD11B2 CDS-LUC). As illustrated in Figure 1, treatment of cells with HSD11B1 MAO or HSD11B2 MAO inhibited ($P<0.01$) LUC reporter activity, whereas the Control MO had no effect ($P> 0.10$) on activity.

HSD11B1, but not HSD11B2 MAO inhibits ovine conceptus elongation

Following *in vitro* validation, *in vivo* loss of function studies were conducted to determine the effect of HSD11B1 and HSD11B2 MAO on conceptus elongation in sheep. This approach is based on previous studies demonstrating that labeled morpholinos are effectively delivered to the mononuclear trophectoderm cells of the conceptus after *in utero* administration [244, 298]. This approach has been used to understand the biological roles of multiple proteins (enJSRVs envelope, SLC7A1, IFNT and IFNAR1/2, PPARG and PPARD) in conceptus elongation and trophectoderm development in sheep [244, 380, 381]. In this study, morpholinos

were constantly infused into the uterine lumen beginning on Day 7 post-mating using implanted osmotic pumps, which is preferred over bolus administration based on our recent study [380].

As summarized in Table 1 and shown in Figure 2, conceptuses (n=13) recovered from ewes receiving intrauterine infusions of Control MO were elongated and filamentous (12-14 cm in length), consistent with normal gross morphology of conceptuses from Day 14 pregnant ewes [18, 35]. Similarly, conceptuses (n=6) recovered from HSD11B2 MAO-infused ewes were elongated and filamentous. In contrast, no conceptus (n=3), conceptus fragments (n=2), or a growth-retarded conceptus (n=1) was recovered from the uterus of ewes (n=6) infused with HSD11B1 MAO. Histological examination found that conceptuses recovered from ewes infused with Control MO contained mononuclear trophectoderm cells lined with endoderm (Figure 2). In contrast, those conceptuses receiving HSD11B1 MAO lacked distinct mononuclear trophectoderm cells or endoderm. Conceptuses recovered from ewes receiving HSD11B2 MAO possessed distinct trophectoderm cells with some of those cells containing large vacuoles.

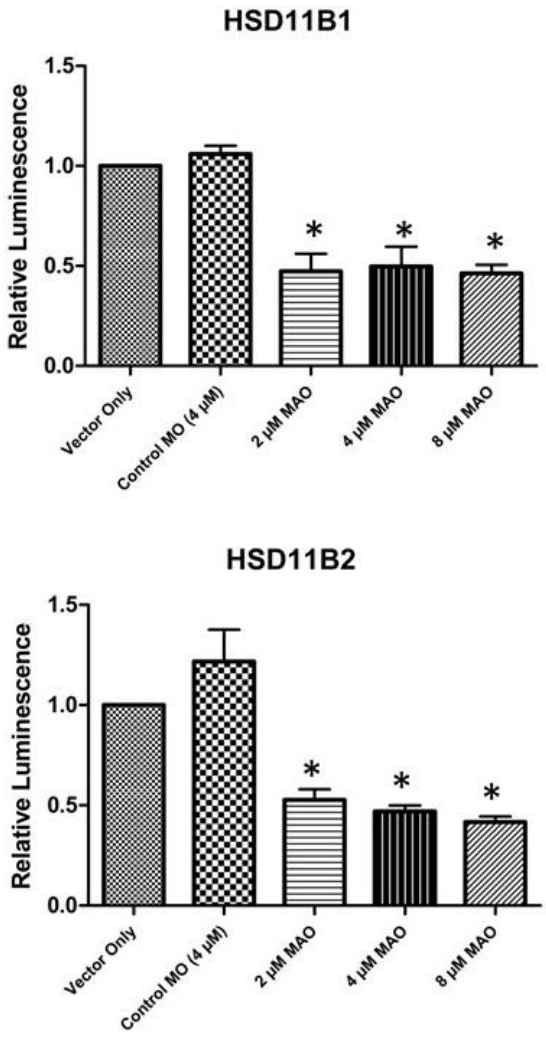

FIGURE 1. In vitro validation of HSD11B1 and HSD11B2 mopholino activity. Morpholino antisense oligonucleotides were designed to inhibit translation of ovine *HSD11B1* or *HSD11B2* mRNAs. HEK 293T cells were transfected with psiCHECK2, a LUC reporter vector, containing a portion of the CDS for either ovine *HSD11B1* or *HSD11B2* mRNA upstream and in frame with the *LUC* gene. After 6 h, cells were treated with nothing (Vector only), control MO (MO; 4 µM), or a specific MAO (2, 4, or 8 µM) along with the Endo- Porter delivery reagent. After 48 h, LUC was assayed in lysed cells. Data for the morpholinos are presented as relative to the vector only. Differences ($P<0.05$; MAO vs. Control MO) are denoted with an asterisk (*).

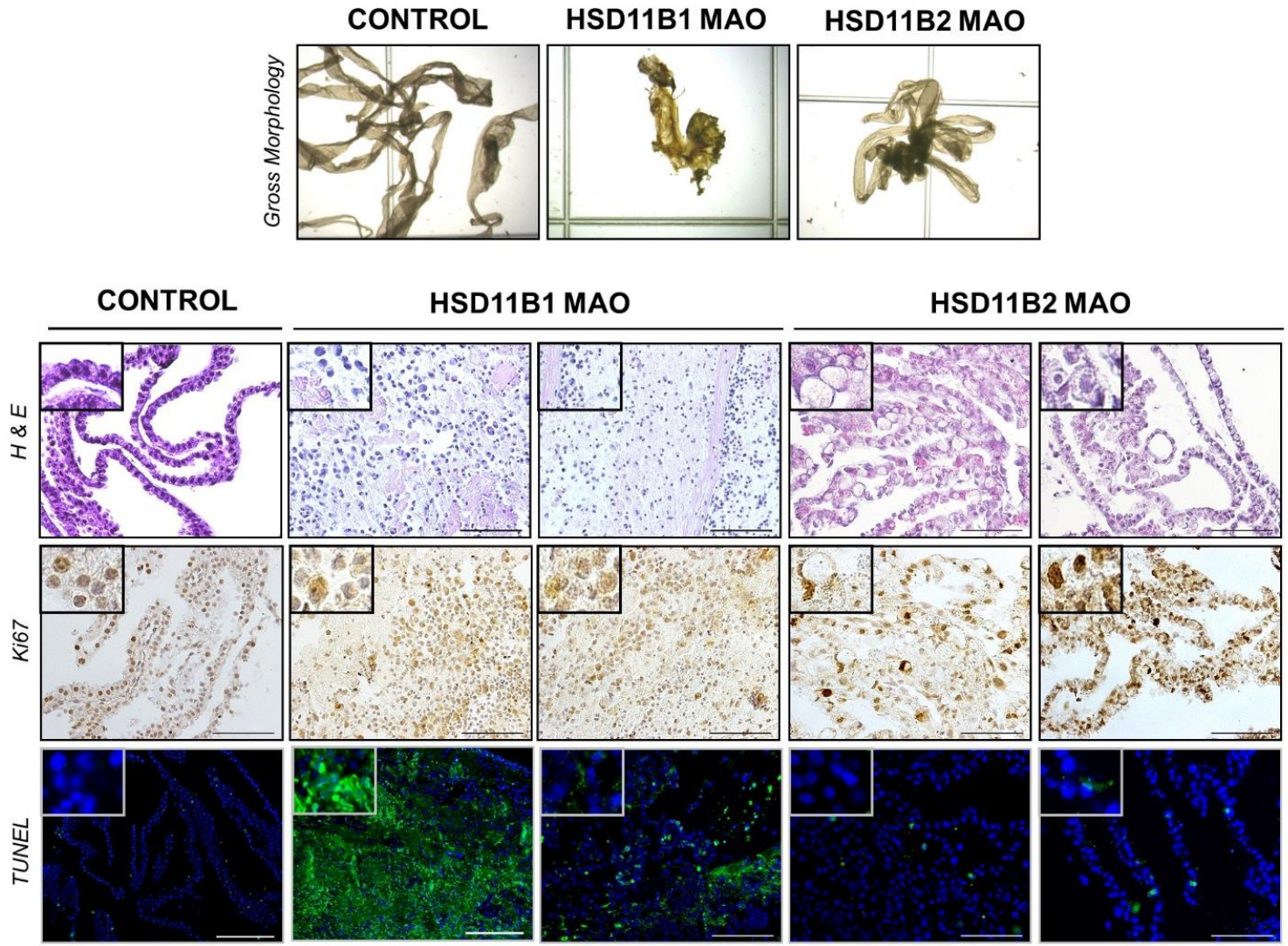
CONTROL
HSD11B1 MAO
HSD11B2 MAO
Gross Morphology
CONTROL
HSD11B1 MAO
HSD11B2 MAO
H & E
Ki67
TUNEL

FIGURE 2. Effect of morpholino treatment on conceptus morphology, histology, proliferation and apoptosis. Control MO, HSD11B1 MAO or HSD11B2 MAO was infused into the uterine lumen of ewes with a ligated uterine horn beginning on Day 7 post-mating (n≥7 per morpholino type) using an osmotic pump. Conceptuses were recovered on Day 14. Grids within morphology images are 1.4 cm^2. Conceptus morphology was examined using a stereomicroscope. Portions of the conceptuses were then fixed in paraformaldehyde, embedded in paraffin, sectioned and stained with hematoxylin and eosin (H&E). The inset in the upper left corner is a higher magnification (40x) photomicrograph of the conceptus. Cell proliferation was assessed by immunostaining for Ki67 protein, and sections were lightly counterstained with hematoxylin. A fluorometric TUNEL assay was performed to detect apoptotic cells in sections of the conceptus. Data are representative of conceptuses from all ewes. Scale bars represent 100 µm.

TABLE 1: Effect of morpholino treatment on conceptus development assessed on Day 14

	Conceptus		**Uterine Lumen**		
Treatment Type	**#**	**Morphology**	**Total IFNT** (RU x 10^3 ± SE)	**Total PGs** (ng ± SE)	**Total Cortisol** (ng ± SE)
Control MO	13	Elongated & Filamentous	126 ± 21	1934 ± 679	6 ± 4
HSD11B1 MAO	5	Growth Retarded or Fragmented	46 ± 26*	766 ± 858	6 ± 3
HSD11B2 MAO	6	Elongated & Filamentous	41 ± 21*	553 ± 670	8 ± 2

* MAO vs. Control MO (P< 0.05)

Proliferation of the mononuclear trophectoderm cells is a primary driver of conceptus elongation in ruminants [15]. Analysis of cell proliferation in the conceptuses was conducted by immunostaining for Ki67, a nuclear protein and marker of cell proliferation [299]. Abundant Ki67 protein was observed in the nuclei of most mononuclear trophectoderm cells in the elongated, filamentous conceptuses from ewes infused with Control MO and HSD11B2 MAO (Figure 2). The growth retarded, malformed conceptuses from HSD11B1 MAO infused ewes also contained cells positive for Ki67. Apoptosis in the conceptuses was assessed using a fluorometric TUNEL assay [300, 301]. Apoptotic trophectoderm cells were very low in elongated, filamentous conceptuses from Control MO and HSD11B2 MAO infused ewes, but were particularly prevalent in the malformed conceptuses recovered from HSD11B1 MAO infused ewes (Figure 2).

Inhibition of HSD11B1 and HSD11B2 reduces IFNT in the uterine lumen and decreases expression of genes in the endometrium related to conceptus elongation and implantation

The trophectoderm cells of the elongating conceptus synthesize and secrete PGs and IFNT, therefore the abundance of these factors in the uterine lumen can be used as an indirect measure of conceptus development and viability as well as trophectoderm cell number [57, 90, 132, 285]. Consistent with retarded conceptus growth and/or abnormal trophectoderm morphology, IFNT was substantially lower ($P<0.05$) in the uterine lumen of ewes infused with HSD11B1 MAO as well as HSD11B2 MAO as compared to those infused with the Control MO (Table 1). The amount of PGs and cortisol present in the uterine lumen of

HSD11B1 MAO and HSD11B2 MAO-infused ewes was not different (P>0.10) compared to ewes infused with Control MO.

Between Days 10 and 12 post-estrus/mating a number of elongation- and implantation-related genes are induced by progesterone in the LE and GE of the endometrium [56, 63, 103, 105]. Those genes encode proteins that are secreted or transport specific nutrients (amino acids, glucose) into the uterine lumen and are hypothesized to regulate trophectoderm functions important for conceptus elongation. These genes are further stimulated by IFNT and/or PGs from the ovine conceptus between Days 12 and 14 of early pregnancy (see [74] for review). In addition, a large number of classical Type I IFN-stimulated genes (ISGs) are induced by IFNT predominantly in the uterine stroma and GE [100, 335, 382, 383]. As illustrated in Figure 3, the abundance of classical Type I *ISG* mRNA (*CXCL10, ISG15, RSAD2*) was substantially lower (P<0.01) in the endometrium of ewes infused with HSD11B1 MAO or HSD11B2 MAO as compared to those receiving Control MO. Other elongation- and implantation-related genes (*GRP, IGFBP1, LGALS15)* were differentially decreased (P< 0.05) in the endometria of HSD11B1 MAO and HSD11B2 MAO as compared to Control MO ewes. However, *SLC2A1, SLC2A5,* and *SLC2A7* mRNA levels were not different (P>0.10) in the endometrium of ewes receiving HSD11B1 MAO or HSD11B2 MAO as compared to Control MO (data not shown).

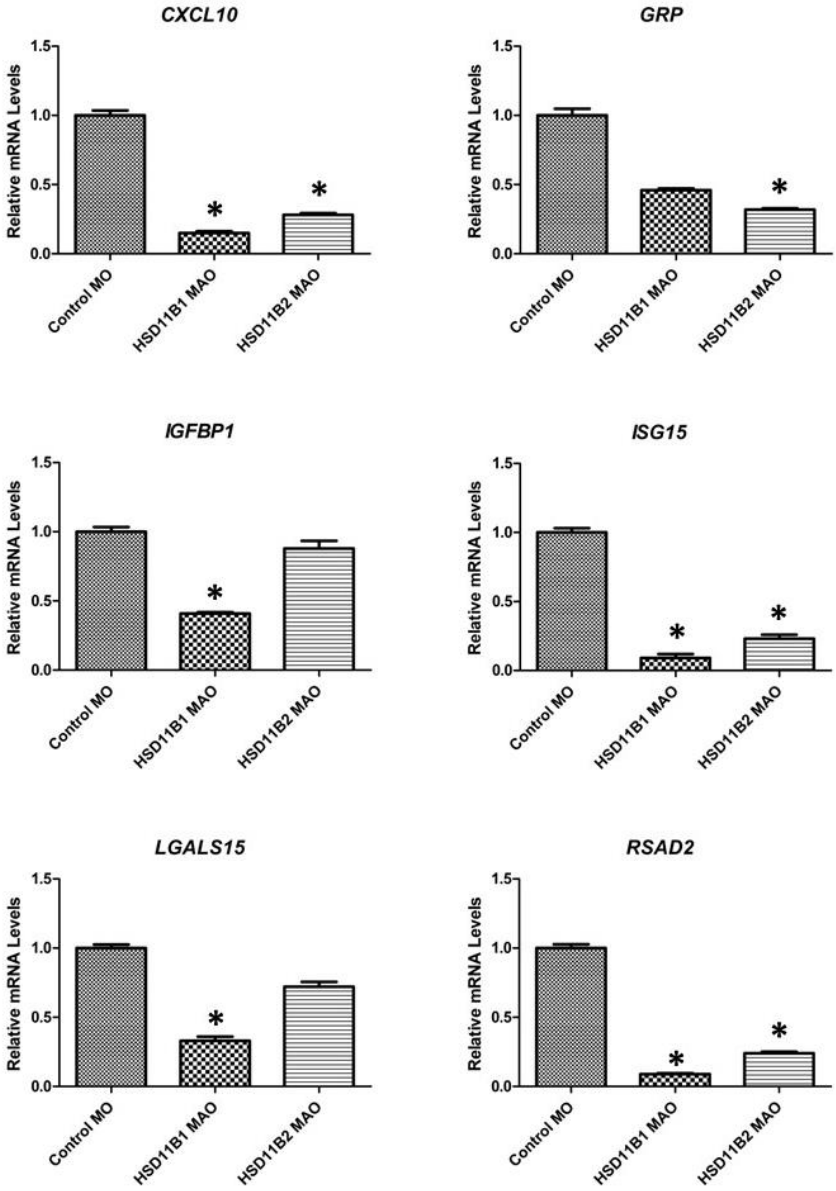

FIGURE 3. Expression of classical IFN-stimulated genes (ISGs) and elongation- and implantation-related genes in the endometrium from morpholino-treated ewes. Control MO, HSD11B1 MAO or HSD11B2 MAO was infused into the uterine lumen of ewes with a ligated uterine horn beginning on Day 7 post-mating (n≥7 per morpholino type) using an osmotic pump. Conceptuses were recovered on Day 14, and endometrium frozen for RNA extraction. The relative abundance of mRNA was determined by quantitative real time PCR (qPCR) using only samples of endometrium from ewes whose uterine flush contained a conceptus. Data are expressed as fold change relative to endometria from Control MO infused sheep. The asterisk (*) denotes differences ($P<0.05$) in mRNA abundance of Control MO vs MAO ewes based on LSM analysis.

Study 2: CRISPR/Cas9 mediated genome editing in the ovine conceptus

Recent advances in the bacterial clustered regularly interspaced short palindromic repeat (CRISPR)/Cas9 system has enabled precise editing of mammalian genomes [379]. Originally adapted from prokaryotes where it is used as a defense mechanism [384], the CRISPR/Cas9 system requires 3 components: (1) a RNA containing a region complementary to the target sequence (crRNA); (2) a RNA containing a region complementary to the crRNA (tracrRNA); and (3) Cas9 nuclease, the enzymatic protein which will cleave the DNA [385]. Commonly, a single guide RNA (gRNA), designed adjacent to an essential PAM sequence is constructed to serve the roles of both crRNA and tracrRNA. The gRNA/Cas9 complex scans the genome and catalyzes a double strand break (DSB) at regions that are complementary to the gRNA. Increased specificity in DSB induction comes from the necessity of the PAM sequence. Genome editing through the use of wild type Cas9 can either cause random mutations, or through the use of multiple gRNAs, can cause deletions by non-homologous end joining (NHEJ) following DSB repair.

Targeting of Glucocorticoid receptor (GR)

Results of the HSD11B1 and HSD11B2 loss-of-function studies in Study One, as well as another recent study [59], support the idea that the inter-conversion of cortisol and cortisone by HSD11B1 and HSD11B2 in the trophectoderm plays a role in conceptus development. Since the developing ovine conceptus does not express the MR, the actions of cortisol are hypothesized to act

through the GR [232]. Four different gRNAs targeting the DNA binding region of ovine GR, encoded by Exon 2 of the *GR* gene, were designed to direct Cas9 induced DNA editing and repair resulting in nucleotide deletion through homologous recombination and/or frame shift mutations (Figure 4A). The targeted region was selected based on read mapping of *GR* mRNA of the Day 14 conceptus (GSE58967) to Ensembl genomic sequence (Oar_v 3.1.75) (Figure 4A). The potential for alternative exon usage made targeting Exon 2 a more desirable choice for inducing editing that would be retained in the final protein product. Conceptuses were recovered from recipient ewes receiving either *Cas9* mRNA only or GR targeting gRNAs along with *Cas9* mRNA. DNA was isolated from recovered conceptuses, and the targeted region of *GR* was amplified and Sanger sequenced. Amplification of the targeted region produced 2 distinct PCR products in the GR edited conceptuses (n=5). For these conceptuses, both PCR products were sequenced and biallelic deletions were detected. In the remaining (n=2) conceptuses, differences in sequence mutations were not distinguishable between the two alleles. Representative sequencing results from the edited conceptuses are shown in Figure 4B. All 7 control conceptuses (Cas9 only) and one GR targeted conceptus had no sequence alterations. However, the other 6 GR targeted conceptuses were edited (Figure 4B). As shown in Figure 4C, the inferred amino acid sequence based on sequencing analysis of genomic DNA from the edited conceptuses predicted that the GR editing caused either a frame shift mutation resulting in a premature stop (mutant 2 and 4), deletion of the essential zinc finger portion of the DNA binding domain (mutant 1 and 5), or frame shift mutation

(mutant 3 and 6). Potential off target modifications (Supplemental Table 2), screened for each gRNA, were not detectable in the recovered conceptuses (data not shown).

All conceptuses recovered from ewes receiving blastocysts derived from zygotes injected with Cas9 only were elongated and filamentous (n=7), consistent with the morphology of day 14 conceptuses recovered from normal pregnant ewes (n=9) (Table 2 and Figure 5). Further, conceptuses recovered from ewes receiving blastocysts derived from zygotes injected with gRNAs and Cas9 to edit Exon 2 of the *GR* gene, were also elongated and filamentous (n=6). Histological analysis found no detectable differences in the trophectoderm cells and underlying endoderm of GR edited conceptuses compared to Cas9 control or normal conceptuses (Figure 5). Analysis of cell proliferation in the conceptuses was conducted by immunostaining for Ki67. Ki67 protein was abundant in the nuclei of most mononuclear trophectoderm cells in the elongated, filamentous conceptuses from ewes receiving either Cas9 control or GR edited embryos (Figure 5). Apoptosis in the conceptuses was assessed using a fluorometric TUNEL assay. As expected, apoptotic trophectoderm cells were sparse in the modified conceptuses and comparable to that seen in the normal conceptuses (Figure 5). A sensitive GR ELISA kit was used to quantify activation of GR in wildtype and GR edited conceptuses (Figure 6). The GR edited conceptuses contained very low to no GR activity as compared to the Cas9 control conceptuses.

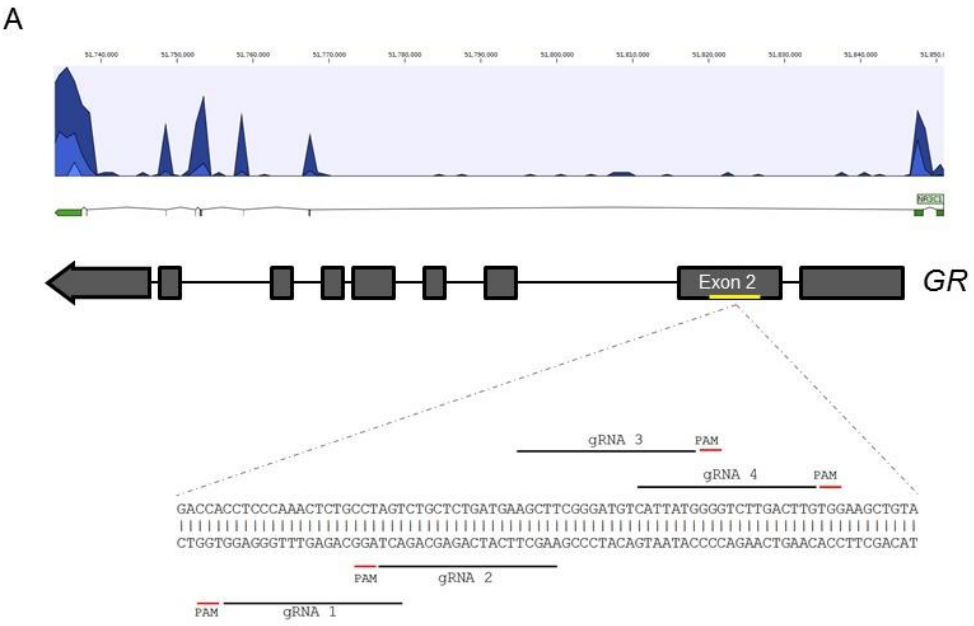

B

Nucleotide Sequence:

WT	GACCACCTCCCAAACTCTGCCTAGTCTGCTCTGATGAAGCTTCGGGATGTCATTATGGGGTCTTGACTTGTGGAAGCTGTA
GR Mut 1	GACCACCT----------GATGAAGCTTCGGGATGTCATTATGGGGTCTTGACTTGTGGAAGCTGTA
GR Mut 2	GACCACCTCCCAA----------TCTGATGAAGCTTCGGGATGTCATTATGGGGTCTTGACTTGTGGAAGCTGTA
GR Mut 3	GACCACCT----------TATGGGGTCTTGACTTGTGGAAGCTGTA
GR Mut 4	GACCACCTCCCAA----------GCTCTGATGAAGCTTCGGGATGTCATTATGGGGTCTTGACTTGTGGAAGCTGTA
GR Mut 5	GACCACCT----------TGCTCTGATGAAGCTTCAGGATGTCATTATGGGGTCTTGACTTGTGGAAGCTGTA
GR Mut 6	GACCACCT----------TATGGGGTCTTGACTTGTGGAAGCTGTA

C

Amino Acid Sequence:

WT	AATGPPPKLCLVCSDEASGCHYGVLTCGSCKVFFKRAVEGQHNYLCAGRNDCIIDKIRRKN
GR Mut 1	AATGPP--------DEASGCHYGVLTCGSCKVFFKRAVEGQHNYLCAGRNDCIIDKIRRKN
GR Mut 2	AATGPPPNLMKLRDVIMGS*
GR Mut 3	AATGPPYGVLTCGSCKVFFKRAVEGQHNYLCAGRNDCIIDKIRRKNCPACRYRKCLQAGMN
GR Mut 4	AATGPPPKL*
GR Mut 5	AATGPP---------DEASGCHYGVLTCGSCKVFFKRAVEGQHNYLCAGRNDCIIDKIRRKN
GR Mut 6	AATGPPYGVLTCGSCKVFFKRAVEGQHNYLCAGRNDCIIDKIRRKNCPACRYRKCLQAGMN

FIGURE 4. Design and effect of CRISPR gRNAs targeting the ovine GR for genomic editing. (A) Read mapping of *GR* mRNA from the Day 14 conceptus is presented relative to the ovine *GR* gene. The region of Exon 2 encoding the GR DNA binding was selected for editing (depicted in red in B and C). Superovulated ewes were bred at estrus (n=5), and one-cell zygotes were recovered 36 hours post-mating. Zygotes were injected with either: (1) wildtype *Cas9* RNA alone; or (2) wildtype *Cas9* RNA along with 4 guide RNAs targeting the ovine *GR*. Injected zygotes were developed to the blastocyst stage in culture and then transferred to Day 8 recipient ewes. Conceptuses were recovered on Day 14. (B) DNA was isolated from recovered from all conceptuses, and the targeted region of *GR* was amplified and Sanger sequenced. All but one of the GR targeted conceptuses had alterations in the *GR* gene. (C) Sequence analysis for that 6 of the GR targeted conceptuses were edited, causing either a premature stop (mutant 2 and 4), deletion of the essential zinc finger portion of the DNA binding domain (mutant 1 and 5), or frame shift mutation (mutant 3 and 6).

TABLE 2: Effect of GR gene editing on conceptus development assessed on Day 14

	Conceptus		Uterine Lumen		
Type	**#**	**Morphology**	**Total IFNT** (RU x 10^3 ± SE)	**Total PGs** (ng ± SE)	**Total Cortisol** (ng ± SE)
Normal	9	Elongated & Filamentous	634 ± 259	2320 ± 755	6± 3
Cas9 Control	7	Elongated & Filamentous	876 ± 367	1075 ± 1067	7± 3
GR Edited	7	Elongated & Filamentous	233 ± 300	1695 ± 871	7± 3

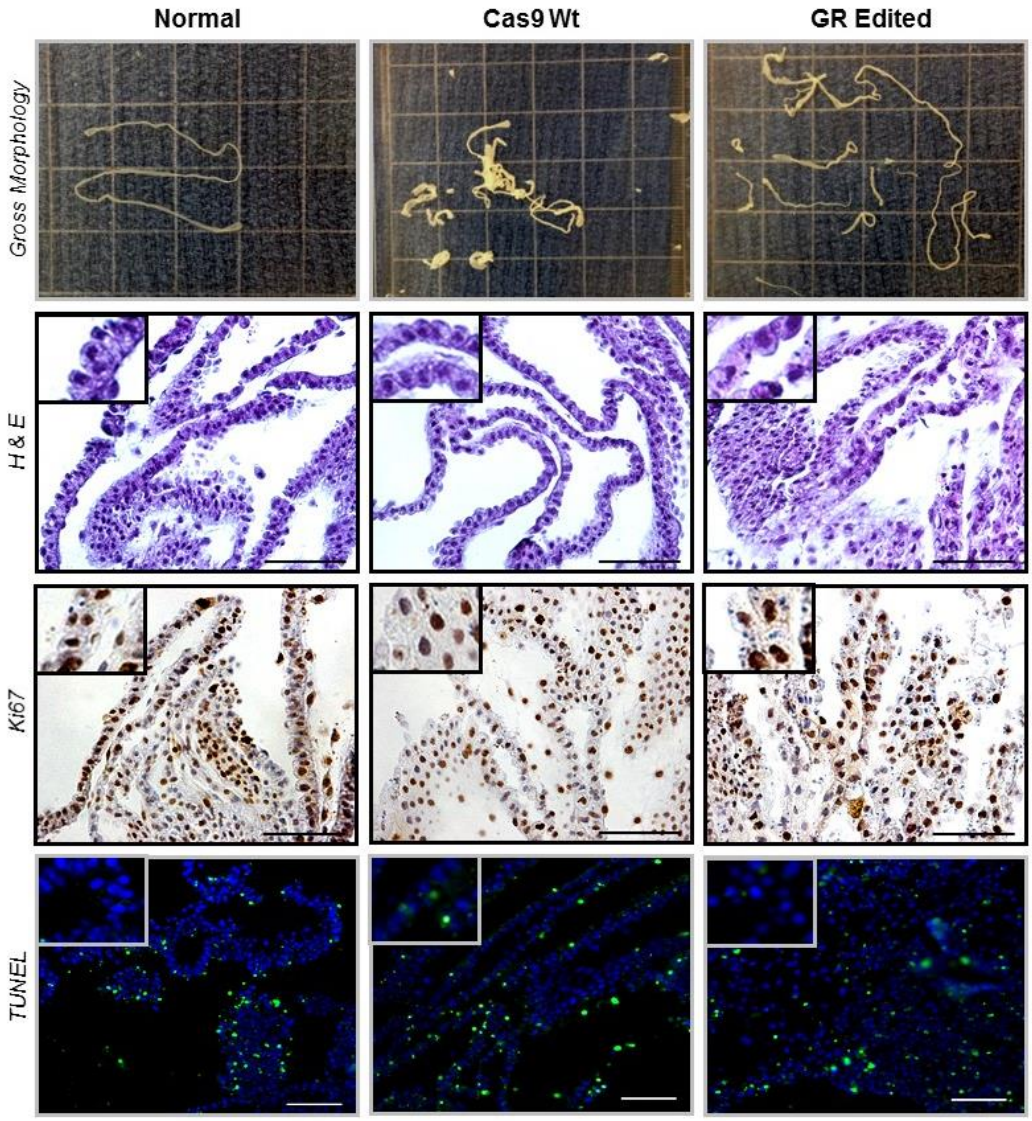

FIGURE 5. Effect of CRISPR/Cas9 treatment on conceptus morphology, histology, proliferation and apoptosis. Superovulated ewes were bred at estrus (n=5), and one-cell zygotes were recovered 36 hours post-mating. Zygotes were injected with either: (1) wildtype Cas9 RNA alone; or (2) wildtype Cas9 RNA along with 4 guide RNAs targeting the ovine GR gene. Injected zygotes were developed to the blastocyst stage in culture and then transferred to Day 8 recipient ewes. Conceptuses were recovered on Day 14. Portions of the conceptuses were then fixed in paraformaldehyde, embedded in paraffin, sectioned and stained with hematoxylin and eosin (H&E). The inset in the upper left corner is a higher magnification (40x) photomicrograph of the conceptus. Cell proliferation was assessed by immunostaining for Ki67 protein, and sections were lightly counterstained with hematoxylin. A fluorometric TUNEL assay was performed to detect apoptotic cells in sections of the conceptus. Data are representative of conceptuses from all ewes. Scale bars represent 100 µm. Grids within the morphology images are 1.4 cm^2.

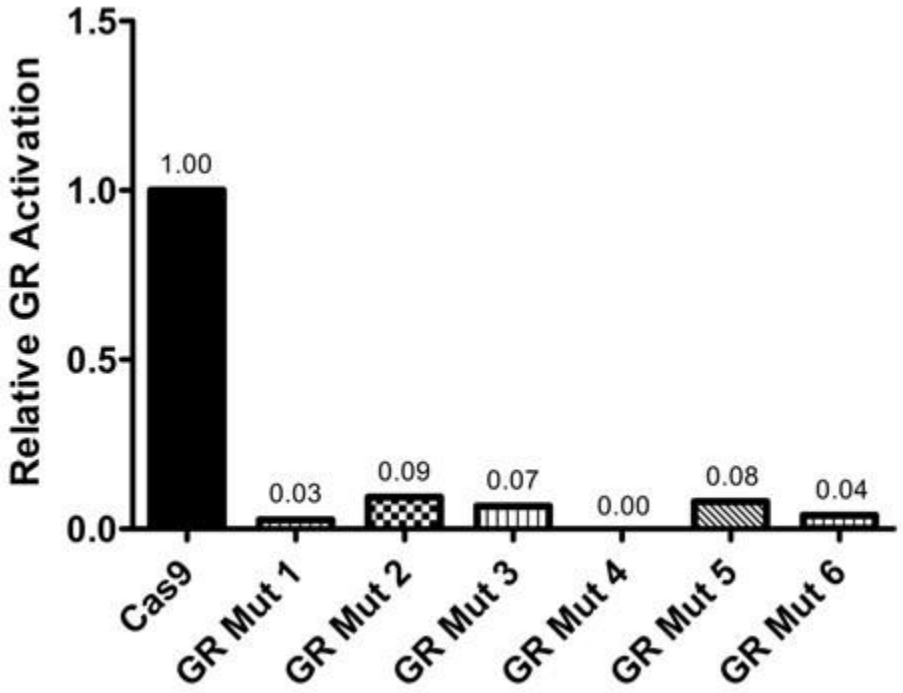

FIGURE 6. Effect of GR CRISPR editing on GR DNA binding. Exon 2 containing the DNA binding domain for GR was selected for editing based on read mapping of *GR* mRNA of the Day 14 conceptus. Superovulated ewes were bred at estrus (n=5), and one-cell zygotes were recovered 36 hours post-mating. Zygotes were injected with either: (1) wildtype *Cas9* RNA alone; or (2) wildtype *Cas9* RNA along with 4 guide RNAs targeting the ovine *GR*. Injected zygotes were developed to the blastocyst stage in culture and then transferred to Day 8 recipient ewes. Conceptuses were recovered on Day 14. Total protein from Cas9 and GR gRNA injected conceptuses was isolated and analyzed using a transcription factor activation ELISA. DNA binding efficiency of GR edited conceptuses are represented relative to Cas9 treated conceptuses.

Consistent with conceptus development and morphology, no differences in total amounts of IFNT, PGs or cortisol was observed in the uterine flush (Table 2). Further, the levels of *CXCL10, CTSL, GRP, IGFBP1, ISG15, LGALS15, RSAD2, SLC2A1, SLC2A5* and *SLC2A7* mRNA were not different (P>0.10) in the endometrium of ewes with elongated GR edited conceptuses compared to those with elongated Cas9 control or normal conceptuses (data not shown).

DISCUSSION

In the present study, *in utero* MAO and CRISPR/Cas9 genome editing loss-of-function studies found that HSD11B1, but not HSD11B2 or GR, is an essential regulator of conceptus elongation and trophectoderm survival. These results support the hypothesis that factors from the endometrium (PGs and cortisol) as well as from the conceptus (IFNT and PGs) coordinately regulate conceptus elongation during early pregnancy in sheep [74, 103]. We previously reported that infusion of PF 915275, a selective pharmaceutical inhibitor of HSD11B1, into the uterus from Days 10 to 14 of pregnancy inhibited conceptus elongation [59]. However, that study could not discern the specific role of HSD11B1 in the conceptus trophectoderm, as HSD11B1 is expressed and active in the endometrial LE and conceptus trophectoderm [58, 192]. Thus, Study One utilized MAO to conduct a loss-of-function study in the trophectoderm, as the infused MAO are primarily delivered to the conceptus and have effects on mRNA translation *in utero* [244]. Morpholino oligos are short chains of morpholino subunits designed specifically to block translation of target RNAs through RNase H-independent steric interference [297]. They are comprised of a nucleic acid base, a morpholine

ring, and a non-ionic phosphorodiamidate intersubunit linkage [348]. The results of Study One support the idea that HSD11B1 is required for trophectoderm survival and conceptus elongation. Conceptuses recovered from ewes receiving HSD11B1 MAO were severely growth retarded and malformed, likely due to the increased levels of apoptosis observed in the trophectoderm. The substantially reduced amount of IFNT in the uterine lumen is consistent with conceptus morphology and reduced number and viability of trophectoderm cells [73, 323]. As expected, reduced IFNT levels in the uterine lumen were accompanied by decreased expression of classical type I ISGs and elongation- and implantation-related genes in the endometrium [103, 108, 290]. Levels of cortisol and PGs within the uterine lumen were not different between treatment groups, but those factors are also synthesized and secreted by the endometrial LE in both uterine horns [59, 78, 192].

Glucocorticoids are essential for the maintenance of cellular homeostasis in many tissues and enable physiological responses to manage physical and emotional stress [386]; regulate carbohydrate and protein metabolism as well as exert complex effects on lipid deposition and degradation [236]; regulate immune and inflammatory processes as well as host defense [237, 238]; and have complex effects on target tissues, exerting a spectrum of outcomes including both positive and negative effects on cell growth. Glucocorticoids binding and activation of GR elicits modulation of gene transcription within the nucleus [387, 388]. Given that GR is expressed in the both the conceptus trophectoderm and endometrium, the prevailing hypothesis is that cortisol from the conceptus trophectoderm acts via GR to regulate genes important for conceptus elongation [192]. In fetal membranes

GR stimulates a number of genes implicated in regulation of cell growth, differentiation and apoptosis as well cellular metabolism, signal transduction, and membrane transport [389-392]. In the ovine uterus, intrauterine infusion of cortisol stimulated the expression of a number of elongation- and implantation-related genes in the endometrium that are implicated in regulation of conceptus elongation via effects on the trophectoderm [59].

Study Two was conducted to determine the biological role of GR in conceptus survival and elongation. The structure of the 5' end of the ovine *GR* mRNA prohibits MAO loss-of-function studies. Thus, we utilized the novel CRISPR/Cas9 system that enables precision genomic editing (for review see [273]). The ease of CRISPR/Cas9 design over zinc finger nucleases and transcription activator-like effector nucleases has made it a preferred editing method [393]. The injection of 4 gRNAs was effective in stimulating Cas9 editing of the ovine *GR* gene in zygotes, resulting in conceptuses with a GR loss-of-function mutation based on DNA sequencing and analysis of GR activity. Collectively, results from that study do not support the hypothesis that GR in the conceptus regulates conceptus elongation, since GR-edited conceptuses were developmentally, morphologically and biochemically normal as compared to control Cas9 conceptuses. Thus, HSD11B1-generated cortisol from the trophectoderm and endometrium does not regulate trophectoderm survival and conceptus elongation via GR in the conceptus trophectoderm itself. Rather, these studies support the idea that cortisol from the conceptus trophectoderm and endometrial LE acts in a paracrine and autocrine manner, respectively, on the

endometrial LE to regulate expression of elongation- and implantation-related genes that, in turn, regulate trophectoderm survival and proliferation for conceptus elongation. Indeed, intrauterine infusion of cortisol at early pregnancy levels was found to stimulate expression of elongation- and implantation-related genes that are important regulators of trophectoderm cell growth and differentiation [394, 395].

Unlike HSD11B1, which has both dehydrogenase and reductase activity depending on the abundance of NADPH, HSD11B2 unidirectionally converts cortisol to cortisone [396-398]. In tissues expressing the MR, HSD11B2 is thought to protect the MR from cortisol binding, allowing aldosterone to bind the non-selective receptor. Although the conceptus does not express MR (T.E. Spencer, unpublished results and GEO GSE58967), HSD11B2 is expressed in the trophectoderm of the elongating ovine conceptus [192]. In the placenta, HSD11B2 serves as a barrier to limit exposure of the fetus to maternal glucocorticoids [399, 400] and implicated as a regulator of trophoblast invasion during early pregnancy in humans [401]. In Study One, conceptus elongation and development appeared unaffected in HSD11B2 MAO infused ewes based on gross morphology. However, histological analysis of the conceptus and biochemical analysis of the uterine luminal fluid indicated that HSD11B2 loss did affect the conceptus. The conceptuses were elongated, but IFNT production by those conceptuses was lower, as evidenced by less IFNT protein in the uterine lumen. Likewise, the endometrium had lower levels of IFN-stimulated gene expression in those ewes. Further, many of the trophectoderm cells from the HSD11B2-MAO infused ewes

appeared to be vacuolated in the histological analyses. Of note, pituitary tumors from Cushing's disease patients often reveals extensive cellular vacuolization, presumably an indicator of high cellular cortisol levels in those tissues [402]. *In vitro* studies have shown a correlation between cellular stress and the size and number of cytoplasmic lipid vacuoles in cells under normal or pathological conditions [403]. Accordingly, the vacuoles observed in the HSD11B2-MAO conceptuses may be the result in increased intracellular cortisol levels due the lack of HSD11B2 to convert cortisol to cortisone.

Studies in humans and mice have implicated HSD11B2 in regulation of placental and fetal growth. Decreased HSD11B2 activity in the human placenta has been associated with intrauterine growth restriction [400, 404]. Similarly, *Hsd11b2* null mice give birth to lower weight pups compared to wildtype littermates [405]. A study of extremely small birth weight infants (born weighing under 1 kg) also found a correlation between placental HSD11B2 activity and birth weight [406]. Additional studies reported an association between elevated cortisol concentrations in maternal urine and decreased birth weight, consistent with decreased placental cortisol metabolism [407]. These results imply that exposure of the fetal tissues to cortisol by metabolism at the maternal-fetal interface after placentation may have a more pronounced effect on fetal development than during the peri-implantation period of conceptus attachment and trophoblast invasion.

In summary, these studies support the ideas that: HSD11B1 in the ovine trophectoderm is important for conceptus elongation; GR in the conceptus trophectoderm does not mediate effects of cortisol; and HSD11B1 in the

trophectoderm and endometrial epithelia generates cortisol that acts via GR in the endometrium to regulate expression of genes important for trophectoderm survival and proliferation during conceptus elongation.

ACKNOWLEDGMENTS

The authors greatly appreciate members of the Spencer laboratory who assisted with animal care and surgeries (Brenda Jesernig, Andrew Kelleher, Joao Moraes, Wang Peng).

SECTION V:

Lentiviral targeting of PTGS2 in the ovine conceptus trophectoderm

Kelsey Brooks, Gregory W Burns, Grant Trobridge, Thomas E Spencer

ABSTRACT

The trophectoderm of the elongating ruminant conceptus, as well as the endometrium synthesizes and secretes prostaglandins (PG) via prostaglandin synthase two (PTGS2). The elongating conceptus synthesizes and secretes more PG than the underlying endometrium. Thus, PG levels are much greater in the uterine lumen of pregnant as compared to cyclic animals. Previous studies have found that inhibition of *PTGS2 in utero* prevents conceptus elongation in sheep. Additionally, infusion of PGs upregulates expression of a number of elongation and implantation related genes in the endometrium. This study sought to determine the role of conceptus-derived PGs in conceptus implantation. An RNAi based approach was employed to target *PTGS2* in the conceptus trophectoderm. siRNAs targeting ovine *PTGS2* were designed and knockdown efficiency assessed *in vitro* using a luciferase based approach. Of the five siRNAs tested, two significantly reduced LUC:PTGS2 expression *in vitro*. Those siRNA sequences were used to construct shRNA hairpins, and cloned into the lentiviral vectors pLVTHM, pGIPZ and pLL3.7. Each lentiviral vector was selected based on the promoter driving expression of the hairpin and GFP expression. Lentivirus expressing shRNAs reduced LUC:PTGS2 abundance *in vitro*. To assess the effect of PTGS2 knockdown *in vivo*, ovine blastocysts were collected on day 8 and transduced with shRNA expressing lentivirus for 6 hr prior to transfer into a recipient ewe. Conceptuses were collected on day 14, and assessed for GFP, siRNA and PTGS2 expression. Although siRNA and GFP expression was robust from all three vectors in the trophectoderm, no reduction in PTGS2 expression was identified.

INTRODUCTION

In sheep, the morula-stage embryo enters the uterus on days 4 to 6 post-mating and forms a blastocyst that contains an inner cell mass surrounded by a monolayer of trophectoderm [15]. After hatching from the zona pellucida (days 8 to 10), the blastocyst grows from an ovoid to tubular form and is then termed a conceptus (embryo-fetus and associated extraembryonic membranes) [15, 35]. The ovoid conceptus is roughly 1 mm in length on day 11 begins to elongate on day 12 and forms a filamentous conceptus of 15 to 19 cm or more in length by day 15 that occupies the entire length of the uterine horn ipsilateral to the corpus luteum (CL). Conceptus elongation involves exponential increases in length and weight of the trophectoderm [18] and onset of extraembryonic membrane differentiation that is vital for embryonic survival and formation of a functional placenta [15, 338]. Hatched blastocysts do not elongate *in vitro*, as substances secreted from the endometrial epithelia, particularly the glandular epithelium, are essential for their development [19, 21].

The trophectoderm of the elongating ruminant conceptus synthesizes and secretes prostaglandins (PGs) as well as interferon tau (IFNT), which is the maternal recognition of pregnancy signal that acts on the endometrium to inhibit production of luteolytic pulses of PGF2α [19, 20], thereby ensuring continued progesterone production by the corpus luteum [71]. Ovarian progesterone induces a number of genes in the endometrial LE and GE that are hypothesized to regulate conceptus elongation. Factors produced by the developing conceptus then act on the endometrium to further stimulate transcription of a number of the progesterone-

induced elongation and implantation related genes [72-74]. During early pregnancy in both sheep and cattle, the conceptus and endometrium synthesize and secrete substantial amounts of PGs including PGE2, PGF2α, PGI2 and PGD2 [132, 134]. Prostaglandin G/H synthase and cyclooxygenase 2 (PTGS2) is the dominant cyclooxygenase expressed in the conceptus trophectoderm and LE of the endometrium. The elongating conceptus synthesizes and secretes more PGs than the underlying endometrium, resulting in higher PG levels in the uterine lumen of pregnant compared to cyclic sheep [132-134]. Prostaglandins are important for conceptus elongation in sheep, because intrauterine infusion of meloxicam, a selective PTGS2 inhibitor, into the uterine lumen from Days 8 to 14 post-mating completely inhibited conceptus elongation [57]. Cell surface receptors and nuclear receptors for PGs are present in all cell types of the endometrium and conceptus during early pregnancy in sheep [57, 137]. Thus, PGs may have paracrine as well as autocrine and intracrine effects on endometrial function and conceptus development [74]. Available evidence supports the idea that conceptus-derived PGs act in a paracrine manner to modulate expression of progesterone-induced elongation- and implantation-related genes in the endometrium that, in turn, promote conceptus elongation via effects on the trophectoderm [192, 340].

RNA interference (RNAi) is an evolutionarily conserved mechanism by which double-stranded RNA (dsRNA) activates sequence-specific gene silencing through mRNA degradation [408, 409]. Introduction of synthetic small interfering RNAs (siRNAs), or vectors that express a short-hairpin RNA (shRNA) are often used to activate the RNAi pathways and induce target specific gene silencing. In

cells where delivery of siRNAs or vectors containing shRNAs is problematic, lentiviral transduction can be used for genomic integration and stable shRNA expression [256, 410, 411]. Specifically, lentiviral treatment of blastocyst stage embryos produces transgene expression exclusively in the trophectoderm allowing for gene targeting of placental tissue without influencing the inner cell mass (ICM). Lentiviral mediated transfer of shRNAs has been demonstrated as an effective strategy for modifying gene expression in trophoblast cell lineages in both rats and sheep [260, 412].

In order to test the hypothesis that PTGS2 derived PGs from the conceptus trophectoderm have essential biological roles in conceptus elongation, an *in vivo* loss of function study was conducted using lentiviral delivery of PTGS2 targeting shRNAs.

MATERIALS AND METHODS

siRNA design and validation

Design: siRNA sequences were designed against ovine PTGS2 (GenBank accession no. NM_001009432.1) using the online design program from MIT (http://sirna.wi.mit.edu/) [413]. Targeting location and sequences are provided in Table 1. Control siRNA was designed by scrambling the siRNA sequence for siRNA #5. Targeting specificity was determined by BLAST analysis against the ovine genome.

siRNA validation by protein expression: The complete CDS for ovine *PTGS2* (GenBank accession no. NM_001009432.1) was synthesized and

incorporated into pCMV6-Entry (pCMV:PTGS2) by Origene (Rockville, MD). Cos7 cells were transfected with 50 ng pCMV:PTGS2 and siRNAs (6.25, 12.5 and 25 nM) using Lipofectamine 2000 (Invitrogen) in a 24 well plate. After 48 h, media was removed, and cells were washed in PBS before lysis in mammalian protein extraction reagent (M-PER) (Pierce, Rockford, IL). Equal amounts of protein were mixed with Laemmli sample buffer (31.5 mM Tris-HCl (pH 6.8), 10% glycerol, 5% β-mercaptoethanol, 1% SDS, 0.01% bromophenol blue), denatured at 95°C for 5 min, and separated by SDS-PAGE at a constant voltage of 150 V for approximately 90 minutes in 1X running buffer (25 mM Tris, 192 mM glycine, 0.1% SDS). Proteins were transferred to 0.45 µm Protran BA 85 nitrocellulose membrane (GE Healthcare, Buckinghamshire, UK) in Towbin transfer buffer (25 mM Tris, 192 mM glycine, 20% methanol) at 100 V for 60 minutes. Membranes were placed in blocking buffer (TBS, 5% non-fat milk, 0.1% Tween 20) for 1 hour at room temperature and then incubated in primary rabbit anti-mouse PTGS2 antibody (Cayman, Ann Arbor, MI, #160106) at 1:500 dilution in blocking buffer overnight at 4°C. Membranes were then washed with TBS containing 0.1% Tween 20 (TBST) before incubation with goat anti-rabbit HRP conjugated secondary antibody (Thermo Scientific) at 1:10,000 dilution for 1 hour at room temperature. Membranes were washed with excess TBST and incubated with SuperSignal West Pico Chemiluminescent Substrate (Thermo Scientific) for 3 minutes prior to imaging.

siRNA validation by luciferase: The complete CDS for ovine PTGS2 was PCR amplified from pCMV6-Entry:PTGS2 using high fidelity polymerase and

primers containing *XhoI* and *NotI* restriction enzyme (RE) overhangs for subsequent cloning into psiCHECK2. The psiCHECK2 dual luciferase (LUC) reporter plasmid (Promega) was digested with *XhoI* and *NotI* followed by antarctic phosphatase treatment (New England Biolabs). The PCR product containing the CDS for PTGS2 was then ligated into psiCHECK2, downstream and in-frame with LUC, using T4 DNA ligase (Life Technologies). The resulting vector (psiCHECK2:PTGS2) was sequenced (Washington State University Molecular Biology and Genomics Core) for verification. Cos7 cells were transfected with 0.25 ng psiCHECK2:PTGS2 and siRNAs (6.25, 12.5 and 25 nM) using Lipofectamine 2000 (Invitrogen) in a 24 well plate. After 48 h, cell lysates were analyzed for LUC activity using a dual LUC reporter assay system (Promega).

shRNA design and cloning into pLVTHM, pGIPZ, and pLL3.7 lentivectors

Validated siRNA sequences were used to construct long double stranded shRNA oligos. Sense and antisense oligos were synthesized by IDT to contain: 5' RE overhang, siRNA sequence, loop structure, complementary siRNA sequence, polyT, 3' RE overhang (Figure 1). Each lentiviral vector was RE digested, and treated with antarctic phosphatase (New England Biolabs). The RE *ClaI* and *MluI* were used to digest pLVTHM, pGIPZ was digested with *XhoI* and *MluI*, and pLL3.7 was digested using *HpaI* and *XhoI* RE. Following annealing of the shRNA oligos to form double stranded shRNA cassettes, the inserts were treated with poly nucleotide kinase (PNK), and ligated into each vector. Resulting lentiviral vectors were then sequenced for verification. Lentiviral vectors (250ng) were transfected along with psiCHECK2:PTGS2 (250 ng) into Cos7 cells using Lipofectamine 2000

(Invitrogen) in a 24 well plate. Cell lysates were analyzed for LUC activity using a dual LUC reporter assay system (Promega) 48 hrs post transfection.

Figure 1. shRNA insert design.

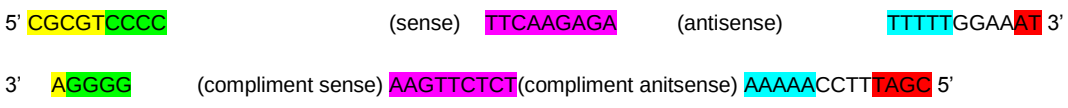

Lentivirus production

Lentiviral vectors were produced as described previously [414]. Lentiviral vectors were self-inactivating pRRL vector backbones and were pseudotyped with VSV-G envelope and produced by transient transfection of 293T cells and concentrated 100-fold as previously described [414]. Lentiviral vectors were titered by transducing HT1080 cells and counting the positive cells with a fluorescent activated cell sorter and exceeded a concentration of 10^{10} TU/ml for each vector.

Lentiviral transduction of Cos7 and OTR cells

Cos7 cells were transduced with lentivirus (10^5, 10^6, 10^7 TU/ml) in the presence of 8ng/ul of polybrene when 40% confluent in a 24 well plate. Lentivirus containing media was changed 24 hr post transduction. At 48 hr post transduction, cells were transfected with 50 ng psiCHECK2:PTGS2 using Lipofectamine 2000 (Invitrogen). Cell lysates were analyzed for LUC activity using a dual LUC reporter assay system (Promega) 48 hr post transfection.

Ovine primary trophectoderm cells (OTR) were isolated and maintained as previously described [55]. Cells were cultured in DMEM/F-12 supplemented with 10% FBS, insulin (700 nM), pyruvate (1.0 mM), nonessential amino acids (0.1 mM), and antibiotics (50 U penicillin, 50 µg streptomycin) in 5% CO_2 at 37ºC. OTR cells were transduced with lentivirus (10^5, 10^6, 10^7 TU/ml) in the presence of 8ng/ul of polybrene. Lentivirus containing media was changed 24 hr post transduction. GFP expression was assessed 48 h post transduction, fluorescent images were collected using NIS Elements BR 3.2 software on a Nikon Eclipse Ti microscope (Nikon Instruments Inc., Melville, NY).

Animal breeding and collections

All experimental and surgical procedures were approved by the Institutional Animal Care and Use Committee of Washington State University. Columbia Rambouillet crossbred ewes (Ovis aries) were synchronized to estrus using an Eazi-Breed Controlled Internal Drug Releasing (CIDR) device for 12 days. Superovulation of donor ewes was achieved through twice daily injections of follicle stimulating hormone (FSH) (Bioniche, Belleville, Ontario, Canada) over a four-day period from Days 9 to 12 after CIDR insertion. Dosage decreased daily (50, 40, 35 and 30 mg, respectively). On Day 11, the CIDR was removed, and ewes were administered 15 mg prostaglandin F2 alpha (Lutalyse), and mated to fertile rams at estrus. Embryos were collected from donor females approximately on day 8 post estrus. Uteri were flushed towards the uterotubal junction 20 ml embryo flush media (Bioniche). Blastocysts were identified and isolated with the aid of a dissecting microscope. Recovered blastocysts were cultured in EVOLVE media

(KSOMaa EVOLVE (Zenith Biotech, Guilford, CT) with Probumin BSA (4 mg/ml) and Gentamicin (0.05 mg/ml, Invitrogen)) containing lentivirus under mineral oil (Irvine Scientific, Santa Ana, CA) at 38.5°C in an atmosphere of 5% CO2/5% O2/90% N2 for 6 hrs. Immediately following 6 hrs of lentiviral exposure, embryos were washed and transferred (3–4 per recipient) into the uterus of synchronized recipient ewes. Recipient ewes were synchronized to estrus using procedures similar to those employed for embryo donors except FSH was not administered to induce superovulation. All recipient ewes were euthanized on Day 14 post-mating and tissues were immediately collected. The uterus was flushed with 20 ml of PBS (pH 7.2), and the number of conceptuses and state of conceptus development was assessed under bright field illumination using a SMZ1000 photomicroscope fitted with a DS-Fi1 digital camera (Nikon). Fluorescence was determined using a Leica MZ10 F stereo microscope. Conceptus tissue was flash frozen in liquid nitrogen, and stored at -80°C for subsequent RNA extraction.

Conceptus DNA/RNA extraction and qPCR

DNA and RNA was isolated from frozen conceptus samples using Isol-RNA lysis reagent (5 Prime, Gaithersburg, MD). To eliminate genomic DNA contamination, extracted RNA was treated with DNase I and purified using RNeasy MinElute cleanup kit (Qiagen, Valencia, CA). The quantity and purity of total RNA were determined by spectrometry. Total RNA (500 ng) from each sample was reverse transcribed in a total reaction volume of 20 µl using iScript RT supermix (Bio-Rad, Hercules, CA). Reverse transcription was performed as follows: 5 min at 25°C; 30 min at 42°C; and 5 min at 85°C. To quantify siRNA expression, total

RNA from conceptuses reverse transcribed with a miScript II RT kit using the miScript HiFlex Buffer (Qiagen) according to the manufacturer's instructions. Control reactions in the absence of reverse transcriptase were prepared for each sample to test for genomic DNA contamination. The resulting cDNA was stored at -20°C for further analysis.

Real-time PCR was performed using a CFX384 Touch Real Time System with SsoAdvanced Universal SYBR Green Supermix (Bio-Rad). Previously published primers for *GAPDH* and *PTGS2* were used [57], and primers for GFP and each siRNA were designed and synthesized by IDT (Table 2). Each sample was analyzed in triplicate with the following conditions for 40 cycles: 95°C for 30 sec; 95°C for 5 sec; and 60°C for 30 sec. A dissociation curve was generated at the end of amplification to ensure that a single product was amplified. PCR reactions without template and template substituted with total RNA were used as a negative control to verify experimental results. The threshold line was set in the linear region of the amplification plot above the baseline noise, and quantification cycle (Cq) values were determined as the cycle number in which the threshold line intersected the amplification curve. Ovine *GAPDH* was used as reference gene for *PTGS2* and GFP.

Statistical Analysis

All quantitative data were subjected to least-squares analyses of variance (ANOVA) using the General Linear Models (GLM) procedures of the Statistical Analysis System (SAS Institute Inc., Cary, NC). Data are expressed as fold change

relative to control untreated, vector only, GFP lentivirus treated, or scramble lentivirus treated as denoted in each experiment. Error terms used in test of significance were identified according to the expectation of the mean squares for error. Significance ($P<0.05$) was determined by probability differences of least-squares means (LSM).

RESULTS

siRNA knockdown In vitro

siRNAs were designed against the CDS for *PTGS2* and tested using psiCHECK2, a reporter vector which expresses Renilla luciferase as a fusion protein with PTGS2. This design allows for quantitation of siRNA knockdown based on changes in Renilla abundance, and its subsequent luminescence compared to control firefly luciferase abundance. A total of 5 siRNAs were designed to target ovine *PTGS2* (Table 1) and, when transfected *in vitro* with psiCHECK2:PTGS2, displayed effective reduction in Renilla luciferase expression (Figure 2A). Robust knockdown was achieved using siRNA #2, which decreased the LUC:PTGS2 by an average of 80% across all siRNA treatment concentrations. Additionally, siRNA #3 was very effective with 77% knockdown at all treatment concentrations. The effectiveness of the designed siRNAs to knockdown *PTGS2* expression was also assessed by Western blot (Figure 2B). Transfection of an expression vector containing the CDS for *PTGS2*, pCMV:PTGS2 with the siRNAs again found siRNA #2 and #3 to be most effective in targeting of *PTGS2*.

TABLE 1: PTGS2 siRNA design

PTGS2 siRNAs	Targeting Region (bps)	siRNA sequence (5'-3')
#1	256-278	AACATTGTCAATAAGATCTCCTT
#2	496-518	AAAGTACTTCTAAGAAGAAAGTT
#3	888-910	CAGAGTGTGTGATGTGCTTAAAC
#4	1189-1211	AACTCTGTCTTACTGGAACATGG
#5	1628-1650	AAATCATCAACACTGCCTCAATT
Scramble	Scramble	GTTAATAGAACTGATAAGACTAA

Table 2: qPCR Primers + miRNA qPCR primers

Primer Name	Direction	Sequence (5'-3')
GFP	Forward	CACATGAAGCAGCACGACTTCT
GFP	Reverse	AACTCCAGCAGGACCATGTGAT
Turbo GFP	Forward	GACGGTGAGCTGGTGATATG
Turbo GFP	Reverse	CCGGAAATCGTCGTGGTATT
siRNA 3	Forward	GCCGAACTTTCTTCTTAGAAGTACTTTAA
siRNA 4	Forward	GTTTAAGCACATCACACACTCTG
Scramble	Forward	CCGGAAATCGTCGTGGTATT

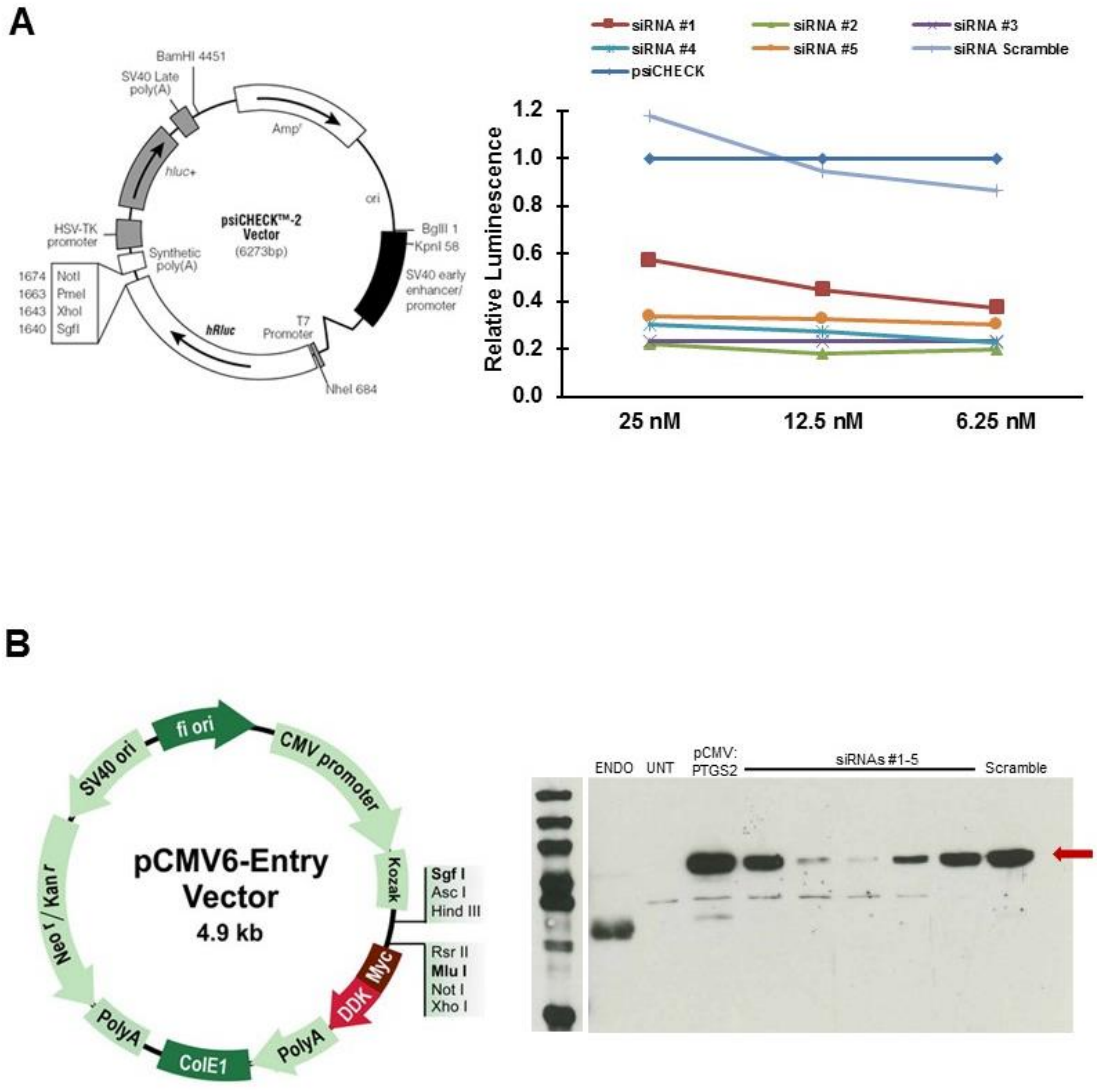

FIGURE 2. siRNA efficiency analysis. Multiple siRNAs were designed targeting ovine *PTGS2*. Cos7 cells were transfected with either psiCHECK2, a vector containing the target gene fused to Renilla luciferase, or pCMV:PTGS2 an expression vector containing the CDS for PTGS2 driven by the CMV promoter. Following plasmid transfection, cells were treated with siRNAs and their knockdown efficiency was assessed either by luminescence or Western blot. **(A)** Diagram of the psiCHECK2 vector backbone and results of luminescence assay for siRNAs at multiple concentrations. **(B)** Diagram of the pCMV:PTGS2 vector backbone and western blot of siRNA knockdown from cells transfected with each siRNA. Targeting sequence of the siRNAs producing the greatest knockdown (siRNA 2 and siRNA 3) were used to produce shRNA cassettes for lentiviral production.

shRNA knockdown In Vitro

The siRNAs most effective at reducing *PTGS2* expression were synthesized as shRNAs cassettes and subcloned into the lentivectors, pLVTHM, pGIPZ and pLL3.7. The efficiency of the shRNAs in reducing PTGS2 expression was again assessed using the psiCHECK2:PTGS2 luciferase reporter assay (Figure 3). The lentivector pLVTHM contains the H1 promoter driving expression of the shRNA cassette, and EF1α promoter driving GFP expression. Both shRNA #2 and shRNA #3 were effective in reducing LUC:PTGS2 expression as shRNAs resulting in 74% and 72% ($P<0.05$) reduction, respectively, in expression compared to the control. The lentivector pGIPZ contains the CMV promoter driving expression of turbo GFP as well as the shRNA, and contains an IRES sequence between GFP and the shRNA hairpin. Use of this vector resulted in decreased abundance of LUC:PTGS2 of 75% and 72% ($P<0.05$). Finally, use of the lentivector pLL3.7, which contains the mouse U6 promoter driving shRNA expression and CMV driving GFP, was assessed. This vector resulted in the greatest reduction in LUC:PTGS2 abundance with 84% and 87% reduction ($P<0.05$) compared to control.

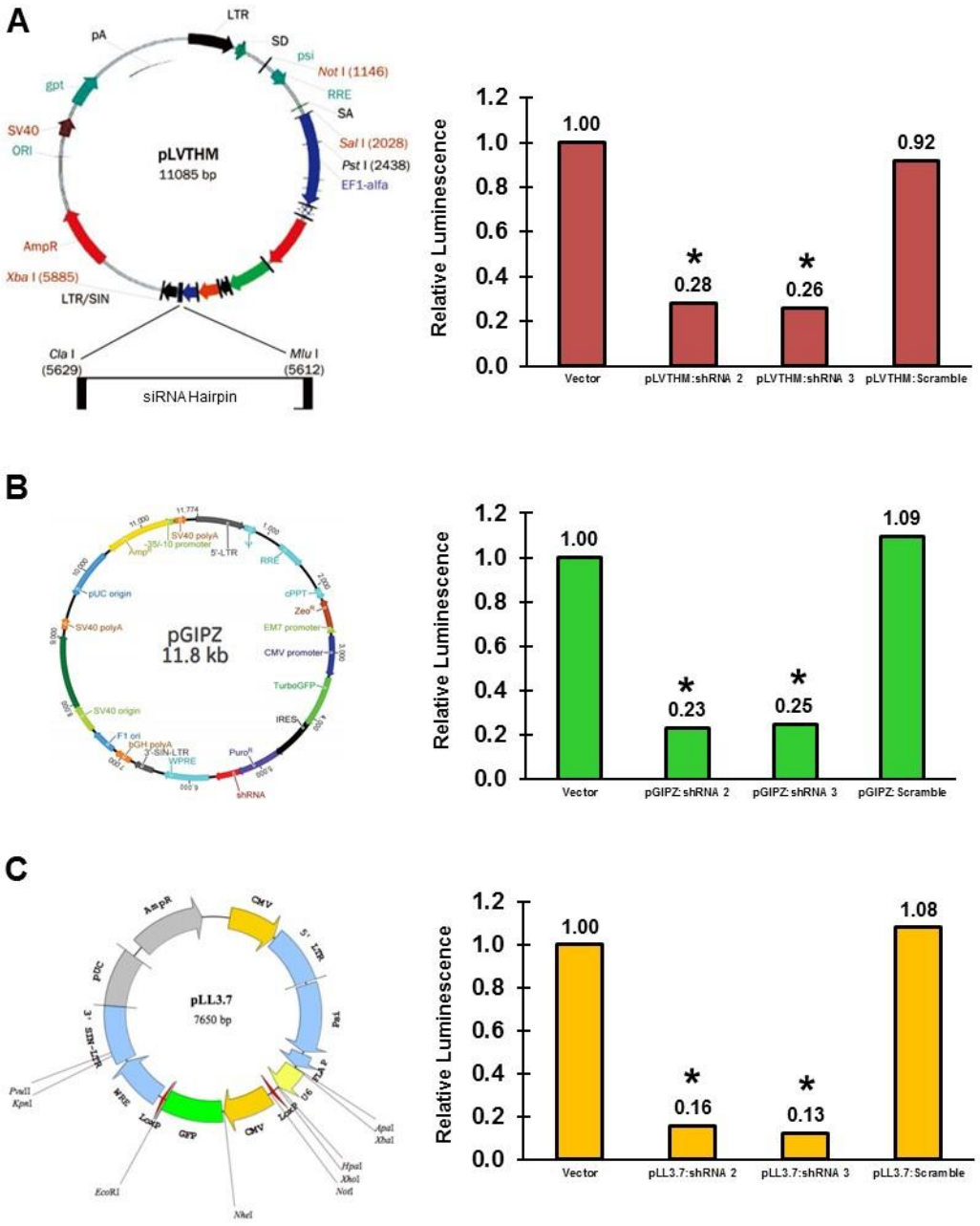

FIGURE 3. shRNA efficiency analysis. The targeting sequence of siRNA 2 and 3 were used to design shRNA cassettes for incorporation into the lentiviral targeting vectors pLVTHM, pGIPZ and pLL3.7. Effectiveness of the shRNAs to target ovine *PTGS2* was assessed via luciferase 48 hours post transfection of psiCHECK2:PTGS2 and lentiviral vectors. Relative luminescence compared to psiCHECK:PTGS2 only treated cells is presented as bar graphs for shRNAs in **(A)** pLVTHM, **(B)** pGIPZ and **(C)** pLL3.7. Differences ($P<0.05$) compared to luminescence from psiCHECK2:PTGS2 only are denoted with an asterisk (*).

Lentiviral delivery of shRNAs In vitro

Since siRNA #2 and siRNA #3 were effective at targeting PTGS2 as both siRNAs and shRNAs, lentiviruses were constructed using each of the tested lentivectors. The effectiveness of shRNAs delivered by lentivirus was then assessed using the psiCHECK2:PTGS2 luciferase reporter vector (Figure 4). Transduction of Cos7 cells with pLVTHM lentivirus at concentrations of 10^5, 10^6, and 10^7 TU/ml resulted in decreased LUC:PTGS2 expression of 5%, 16% and 29% ($P<0.05$ for 10^7 TU/ml). Additionally, use of pGIPZ lentivirus did not result in decreased abundance of LUC:PTGS2 at any concentration. Transduction of pLL3.7 lentivirus reduced LUC:PTGS2 expression by 4%, 13% and 54% ($P<0.05$ for 10^7 TU/ml). Lentiviral knockdown of PTGS2 via pGIPZ was also assessed via western blot following transfection of Cos7 cells with pCMV:PTGS2 (Figure 5). Treatment of cells with control and targeting lentivirus at 10^5, 10^6 and 10^7 TU/ml did not notably reduce PTGS2 expression.

To assess the ability of the lentivirus to transduce the trophectoderm of the developing embryo, a primary ovine trophectoderm (OTR) cell line was used. Cells were transduced with 10^7 TU/ml lentivirus, and GFP expression was assessed by using fluorescent microscopy (Figure 6A) followed by qPCR. GFP expression was assessed 48 hrs post transduction showing increased ($P<0.05$) GFP expression in cells treated with pLVTHM, pGIPZ and pLL3.7 lentivirus compared to untreated cells (Figure 6B).

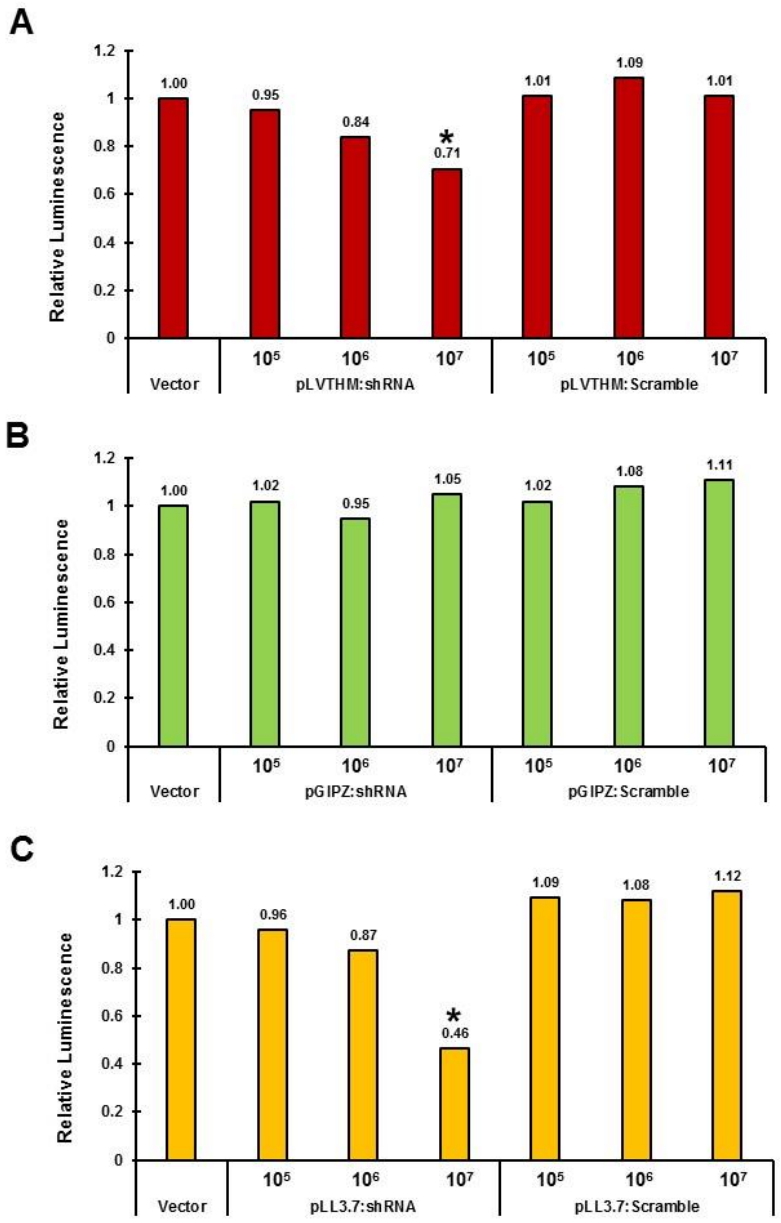

FIGURE 4. Efficiency analysis of lentiviral delivery of shRNA. Cos7 cells were transduced with lentivirus expressing *PTGS2* targeting shRNA 3, or control scramble lentivirus prior to transfection with psiCHECK2:PTGS2. Relative luminescence at lentiviral concentrations of 10^5, 10^6 and 10^7 TU/ml was assessed 48 hr post transfection. **(A)** pLVTHM lentivirus. **(B)** pGIPZ lentivirus. **(C)** pLL3.7 lentivirus. Differences ($P<0.05$) compared to luminescence from psiCHECK2:PTGS2 only are denoted with an asterisk (*).

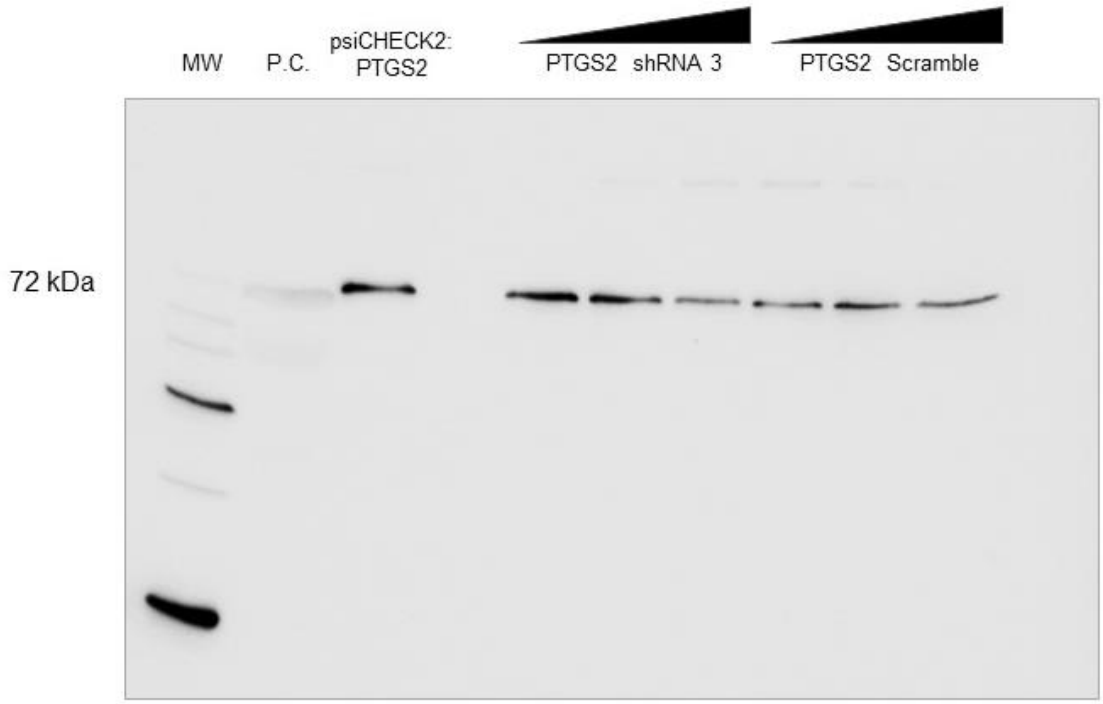

FIGURE 5. Western blot analysis of lentiviral delivery of shRNA. Cos7 cells were transduced with *PTGS2* targeting pGIPZ shRNA 3 lentivirus and control scramble lentivirus at concentrations of 10^5, 10^6 and 10^7 TU/ml. Transduced cells were then ptransfected with pCMV:PTGS2. PTGS2 Protein abundance was assessed 48 hr post transfection via Western blot.

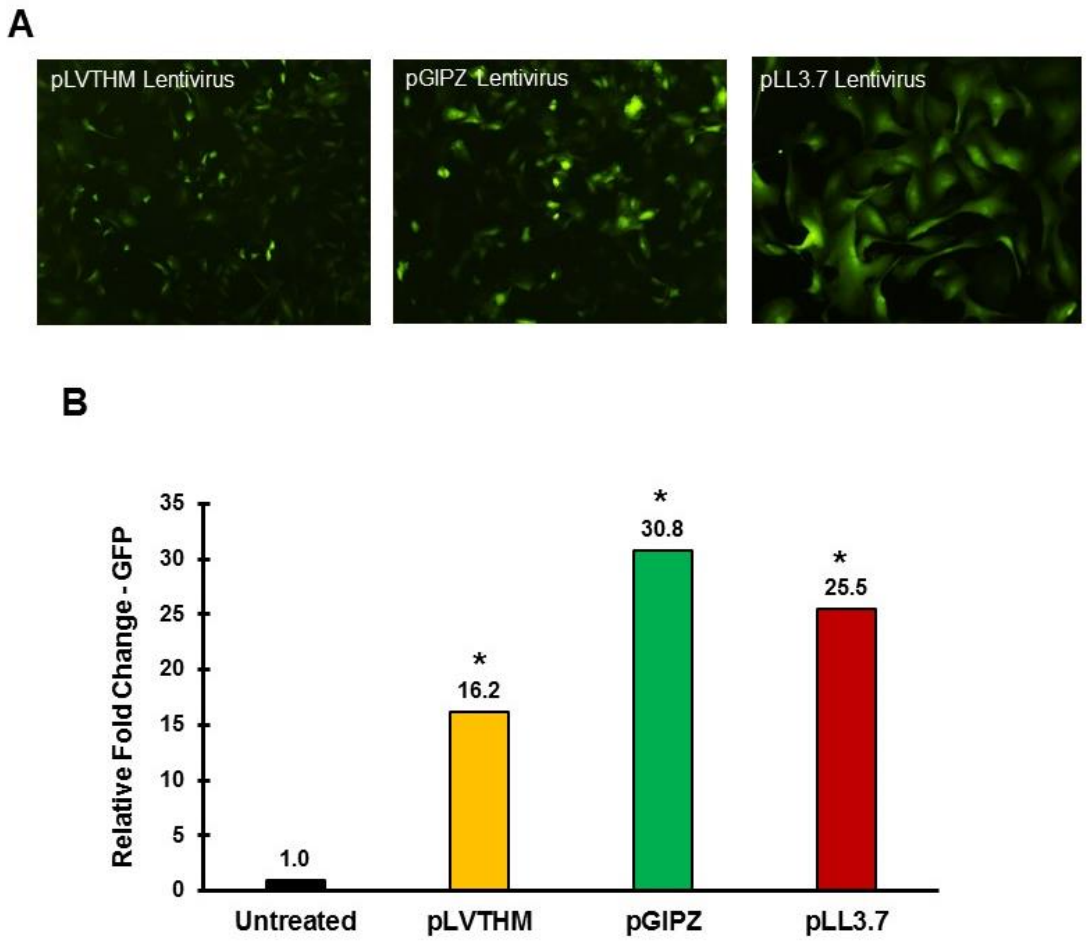

FIGURE 6. Lentiviral transduction of trophoblast cells in vitro. Primary ovine trophoblast cells (OTR), isolated from day 14 conceptuses were transduced with pLVTHM, pGIPZ and pLL3.7 shRNA 3 lentivirus at a concentration of 10^7 TU/ml. Expression of GFP was assessed 48 hrs post-transduction by epifluorescence **(A)** as well as qPCR **(B)**. Relative GFP expression for each shRNA expressing lentivirus was compared to control untreated OTR cells. Differences ($P<0.05$) compared in relative GFP expression are denoted with an asterisk (*).

Lentiviral delivery of shRNAs in vivo

Ovine blastocysts were collected from superovulated donor ewes and transduced with 10^{10} TU/ml of each lentiviral vector for 6 hr prior to transfer into a recipient ewe. Conceptuses recovered on day 14 from ewes receiving pLVTHM,

pGIPZ and pLL3.7 lentiviral treated embryos were fully elongated, and GFP expression was visually detectable via epifluorescence (Figure 7). Conceptuses from the pGIPZ treated group had notably brighter GFP expression than either pLL3.7 or pLVTHM, most likely a result of utilization of turbo GFP in the pGIPZ vector.

qPCR assessment of conceptus lentiviral transduction

Conceptuses from each lentiviral treatment group were collected on day 14, and were analyzed for expression of *PTGS2*, siRNA and GFP (Figure 8). Additionally, conceptus DNA was assessed by qPCR for GFP to determine the number of viral integrations for each treatment. Compared to control day 14 conceptuses, *PTGS2* expression was unchanged in conceptuses treated with pLVTHM, pGIPZ and pLL3.7 lentivirus (Figure 8A). In conceptuses treated with pLVTHM lentivirus, targeting siRNA expression was 156 fold higher than in control conceptuses ($P<0.05$) (Figure 8B). In conceptuses treated with pGIPZ lentivirus, siRNA expression was 13 fold higher than control, and in pLL3.7 treated conceptuses siRNA expression was increased 100 fold ($P<0.05$). Quantification of GFP showed increased expression of 2-, 8- and 6- fold for pLVTHM, pGIPZ and pLL3.7 over control conceptuses respectively ($P>0.05$) (Figure 7C). To determine the number of lentiviral integrations, qPCR for GFP was conducted using genomic DNA from the lentiviral treated conceptuses (Figure 8D). Conceptuses treated with a control GFP lentivirus were used for comparison and qPCR showed no difference in genomic viral copy numbers between conceptuses treated with control GFP, pLVTHM, pGIPZ and pLL3.7 lentivirus.

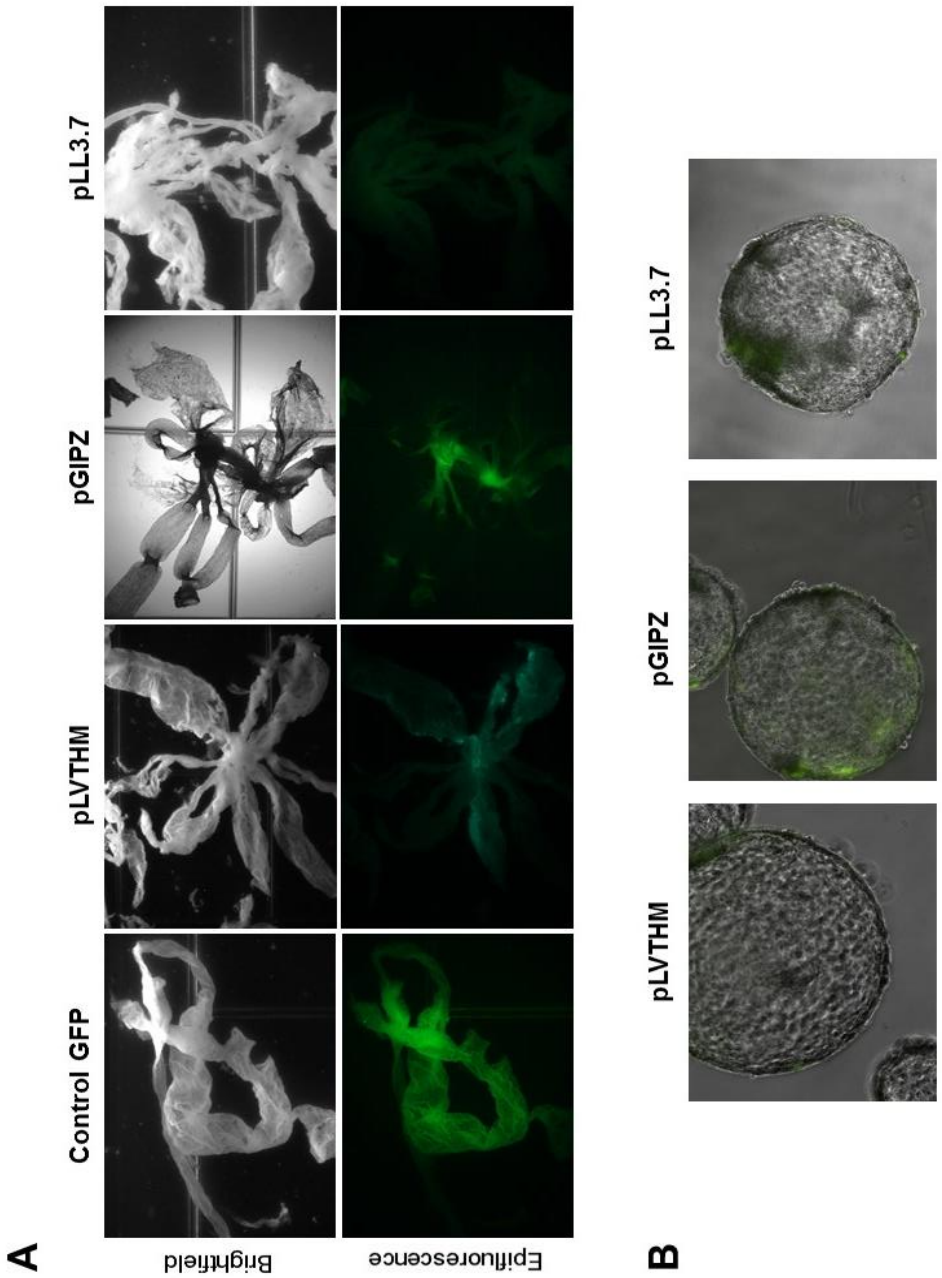

FIGURE 7. Lentivirus transduction of ovine conceptuses. (A) Blastocyst stage embryos were recovered from superovulated donor ewes on day 8 of pregnancy. Blastocysts were cultured in the presence of lentivirus at a concentration of 10^{10} TU/ml for 6 hrs prior to transfer to a recipient ewe. Lentiviral transduced conceptuses were recovered on day 14, and GFP expression visualized via epifluorescence. **(B)** Additionally, zygotes were recovered from super ovulated ewes and treated via continuous injection of concentrated (10^{10} TU/ml) shRNA 3 expressing lentivirus into the perivitelline space.

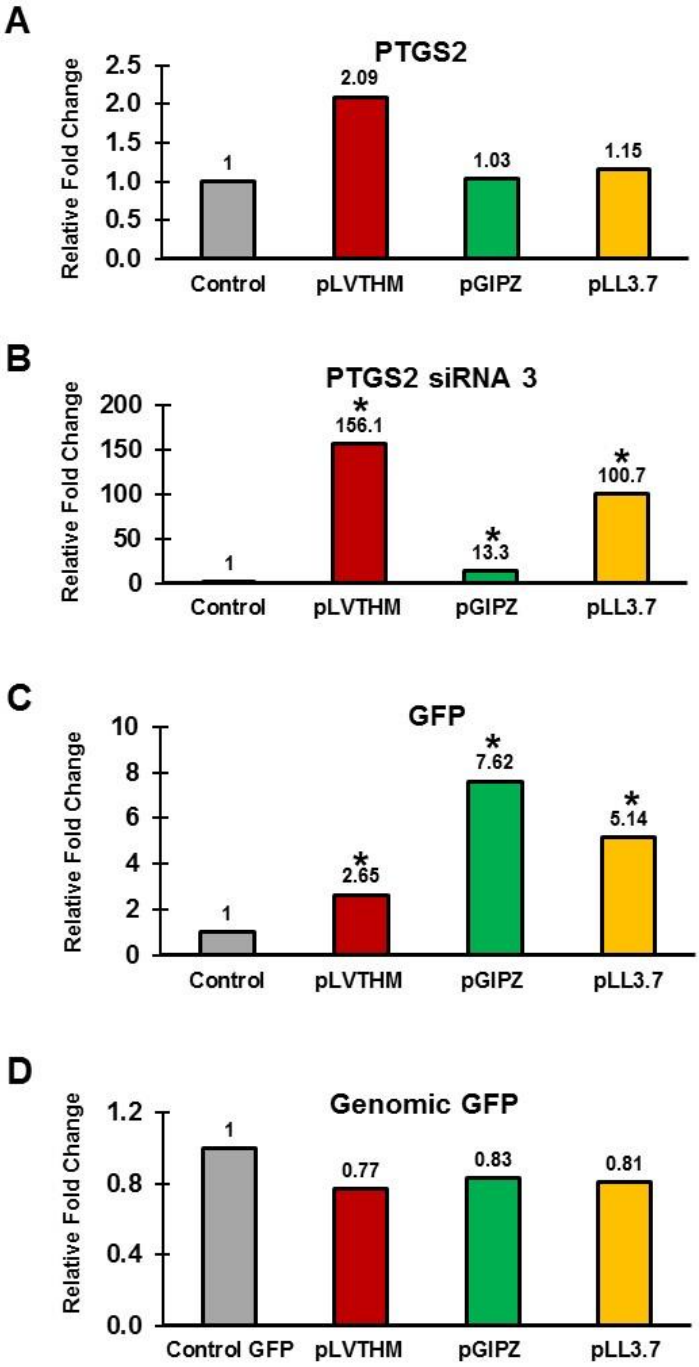

FIGURE 8. qPCR analysis of lentivirus treated conceptuses. Conceptuses from blastocysts treated with lentivirus expressing shRNA 3 from pLVTHM, pGIPZ and pLL3.7 were analyzed for expression of **(A)** *PTGS2*, **(B)** shRNA 3, and **(C)** GFP mRNA. Additionally, the incorporation of lentiviral DNA into the genome was assessed via qPCR for GFP from isolated conceptus DNA. Differences ($P<0.05$) compared to control conceptuses are denoted with an asterisk (*).

DISCUSSION

The trophectoderm of the blastocyst is the first epithelial layer to be established during embryo development in mammals. In ruminants, the conceptus trophectoderm undergoes significant proliferation and elongation prior to implantation. Conceptus elongation is necessary for the production of IFNT, the maternal recognition of pregnancy signal, and maintenance of pregnancy. Following elongation and implantation the conceptus trophectoderm gives rise to extraembryonic tissues of the placenta which is essential for embryo growth and development. The trophectoderm is permissive to lentiviral infections, and provides a non-permeable physical barrier to the viral particles, thereby shielding the cells of the inner cell mass from infection. This feature of the trophectoderm has allows for trophectoderm specific lentiviral infection, and modification of gene expression in the trophectoderm and trophectoderm derived cells only in laboratory animals such as the rat and mouse [256, 260], as well as domestic species such as sheep and pigs [258, 415].

Recent studies have demonstrated that lentiviral infection of blastocyst-stage embryos can be an effective approach to study trophoblast gene function [256, 260, 411, 416, 417]. Lentiviral gene delivery for both gene knock-in, as well as shRNA expression for gene targeting have been well characterized in laboratory animals [260]. Additionally, successful gene targeting through lentiviral delivery of shRNAs to the ovine trophectoderm has also been reported [412, 416]. The present study, siRNAs designed to ovine PTGS2 were successful in decreasing expression of the luciferase reporter (LUC:PTGS2). The designed siRNAs were

also successful in decreasing target gene expression went transcribed from the shRNA lentivectors pLVTHM, pGIPZ and pLL3.7. However, delivery of the shRNA expressing vector via lentiviral transgenesis did not result in knockdown of the target mRNA *in vivo*. The inability of lentiviral delivered shRNA expressing vectors to consistently reduce *PTGS2* expression *in vivo* may be due to multiple factors including genetic mosaicism during integration, epigenetic transgene silencing, or inefficient lentivector promoter usage.

Studies using mice and rats have indicated that genetic mosaicism occurs when using viral constructs, even when transducing zygotes at the single cell stage [257, 418, 419]. Two potential scenarios are thought to lead to genetic mosaicism; incomplete viral integration before the initial cell division, and prolonged persistence of the lentiviral preintegration complex. Following lentiviral exposure, the lentivector must undergo a series of complicated steps prior to genomic integration. It must: 1) bind to its receptor; 2) become internalized; *3*) uncoated; *4*) be reverse transcribed; and *5*) the preintegration complex must be translocated into the nucleus; and *6*) integrated into the genome. Although wild-type lentiviruses take 1–2 hr to integrate [420], VSV-G-pseudotyped lentiviral vectors have been shown to require at least 12 hr for initial signs of integration, and most of the integration can take up to 48 hr or longer [421]. Although blastocysts in this study were transduced with lentivirus for 6 hr prior to transfer into recipient as previously reported [260, 416], this may not have been enough time for complete viral integration in all cells. Incomplete integration followed by subsequent rounds of cellular division characteristic of trophectoderm growth during this time may have

reduced the efficacy of shRNA expression and/or GFP production. Additional treatment time may be necessary and would require optimization to allow for maximum integration without compromising blastocyst quality. Another cause of genetic mosaicism could be due to the relatively long half-life of the lentiviral vector, which has been shown in other studies to range from 8–9 h *in vitro* [422]. It is possible that lentiviral preintegration complexes could persist for several rounds or more of cell division before integration, resulting in genetic mosaicism and expression difference in individual cells. In experiments such as this, where genes hypothesized to be essential for conceptus elongation are targeted by shRNAs, cells which are more readily transduced may fall at a disadvantage and be replaced by those wildtype cells which are unaffected.

Gene expression mosaicism between cell types, and within distinct regions of specific organs has been reported following lentiviral transgenesis in mice [423-425]. In those studies epigenetic silencing was implicated as the cause of mosaic gene expression. Lentiviral studies using the CMV promoter to drive transgene expression of *GM-CSF* in mice found variable protein secretion that was independent of copy number and implicated to be the result of position effects of the integration, leading to the activation of promoter silencing mechanisms [424]. It was once through that lentiviral vector-mediated expression is more resistant to epigenetic silencing, such as methylation [426, 427] or histone deacetylation [428, 429] compared with previous viral delivery methods. That theory has since been disproven [430]. In the present study, the lack of GFP and PTGS2 targeting shRNA expressed by transduced conceptuses could result from gene silencing through

epigenetic modification, especially in conceptuses treated with pGIPZ lentivirus which uses the CMV promoter driving both GFP and shRNA expression.

Selections of an internal promoter can be an important factor in the context of successful lentiviral transgenesis. Many studies have focused on optimization of cellular promoters to maintain persistent transgene expression for extended periods of time. To assist in proper selection, promoter selection assays can be purchased to allow for assessment of promoters activity within the cells of interest prior to lentiviral construction. Use of the viral CMV promoter for lentiviral transduction of spermatogonial stem cells [431] or chicken eggs [432] was shown to have negative effects on gene silencing. However, use of the cellular PGK promoter for production of transgenic chickens [433] and cattle [415] was found to have ubiquitous expression in all tissues analyzed [433] with a constant level of GFP fluorescence [415]. The H1 promoter in the pLVTHM lentivector used to drive RNA pol III transcription of the shRNA has not previously been shown to be effective in cells of the ovine trophectoderm, but it is one of the most commonly used promoters in lentiviral vectors. In this study, the pLVTHM lentivirus had robust siRNA expression, although did not decrease PTGS2 expression in the conceptus trophectoderm. As an alternative choice, the pGIPZ lentivector containing the CMV promoter was selected as a strong candidate to increase shRNA and GFP expression in the transduced conceptuses. Although GFP expression increased with use of the pGIPZ lentivector, siRNA expression was not increased over levels seen from the pLVTHM vector. It is possible that due to the design of the pGIPZ vector, where CMV is driving expression of GFP followed by the shRNA, that

siRNA expression was not as robust as in the other vectors which utilized two separate promoters for GFP and the shRNAs. The pLL3.7 lentivector utilizes the mouse U6 promoter to drive shRNA expression and is a popular promoter choice for mammalian cell lines. In this study, *in vitro* transduction with pLL3.7 produced the most significant decrease in LUC:PTGS2 expression. Although shRNA expression was abundant in the conceptus following lentiviral transduction with pLL3.7, *PTGS2* expression was not affected. Therefore, additional studies in the cells of the conceptus trophectoderm are necessary to determine optimal promoter usage. Of note, lentiviral transduction of the conceptus trophectoderm using a vector containing the human U6 promoter driving shRNA expression has been affective in achieving target knockdown. In addition to optimal promoter selection, it is possible that the location of the proviral integration may have had additional effects on promoter regions. This possibility further complicates optimization of lentiviral vectors for transgenesis.

With recent widespread utilization of the CRISPR/Cas9 system for gene editing, the demand for use of lentiviral delivery of shRNAs to assess gene function through knockout is lessening. However, lentiviral delivery of shRNA to the trophectoderm should be an effective and specialized tool for studying gene function in trophoblast and placenta when properly optimized. To circumvent the need to optimize lentiviral protocols, transfection of blastocysts with CRISPR/Cas9 plasmids could be used for trophoblast specific targeting [434]. In ruminants, the ICM is not necessary for conceptus elongation, and exploitation of this phenomenon could allow for the study of factors effecting conceptus elongation

without complication from gene knockout in the ICM. Tetraploid blastomeres, generated by fusing together two-cell embryos, form trophoblast and extra-embryonic endoderm, but not fetal tissue. This technique (tetraploid complementation) could be utilized for trophoblast and placental based studies using the CRISPR/Cas9 system to genetically modify zygotes prior to fusion at the two-cell, allowing for knockout studies of genes present in the trophoblast without complication by knockout effects on the embryo.

SECTION VI:

Analysis of the Uterine Epithelial Transcriptome and Luminal Fluid Proteome During the Peri-implantation Period of Pregnancy in Sheep

Kelsey Brooks, Gregory W. Burns, Joao G. N. Moraes and Thomas E. Spencer

This work has been submitted for publication in *Biology of Reproduction*

ABSTRACT

Available studies support the idea that the uterine epithelia and their secretions have important biological roles in conceptus survival, elongation and implantation in sheep. The present study evaluated the transcriptome of the uterine luminal epithelium (LE), glandular epithelium (GE) and conceptus and proteome of the uterine luminal fluid (ULF) during the peri-implantation period of pregnancy. Transcriptome (RNA-sequencing) analysis was conducted on LE and GE isolated from uteri of day 10, 12, 14, 16, and 20 pregnant sheep isolated by laser capture microdissection. In the LE, the total number of expressed genes increased between days 10 and 20, whereas expressed genes in the GE increased from days 10 to 14 and then decreased to day 20. The majority of expressed genes in LE and GE from days 10 to 14 were associated with cell survival and growth, while genes associated with cell organization and protein synthesis were most abundant on days 16 and 20. Total expressed genes in the conceptus was greatest on day 12, decreased to day 16, and then increased to day 20. Genes abundantly expressed in the elongating conceptus included *IFNT*, *PTGS2*, *MGST1*, *FADS1* and *FADS2*, whereas *SERPINA1, CSH1* and *PLET1* were most abundant in the day 20 conceptus. Total proteins in the ULF, identified by mass spectrometry, increased from days 10 to 16, many of which have known biological roles in cellular reorganization or as proteases or chaperone proteins. These results support the idea that conceptus elongation and implantation involves extrinsic and intrinsic factors. Further, this study provides critical information that serves as a foundation for future studies aimed a discovering new regulatory pathways governing uterine

receptivity, conceptus elongation, trophectoderm differentiation, conceptus-endometrial interactions and pregnancy establishment in ruminants.

INTRODUCTION

In sheep, the morula stage embryo enters the uterus between days 4 and 5 of pregnancy and then forms a blastocyst that contains an inner cell mass and a blastocoele or central cavity surrounded by a monolayer of trophectoderm [15, 35]. After hatching from the zona pellucida (days 8 to 10), the hatched blastocyst slowly grows into a tubular or ovoid form and is then termed a conceptus (embryo/fetus and associated extraembryonic membranes) [15, 338]. The ovoid conceptus of about 0.5 to 1 cm on day 11 begins to elongate on day 12 and forms a filamentous conceptus of 10 to 15 cm or more in length by day 14 that occupies the entire length of the uterine horn ipsilateral to the corpus luteum. Next, the elongated conceptus completes the process of implantation involving firm attachment and adhesion to the luminal epithelium (LE). Conceptus elongation involves exponential increases in length and weight of the trophectoderm and onset of extraembryonic membrane differentiation, including gastrulation of the embryo and formation of the yolk sac and allantois that are vital for embryonic survival and formation of a functional placenta [435]. Trophoblast giant binucleate cells (BNC) first appear in the sheep conceptus beginning on day 14 and are thought to arise from mononuclear trophectoderm cells which have undergone nuclear division without cytokinesis [33, 37]. By day 20, BNCs make up 15-20% of the trophectoderm. Migration of BNCs towards the LE, followed by fusion with individual LE cells produces trinucleate fetomaternal hybrid cells [37]. Continued

BNC migration and fusion, together with displacement and/or apoptosis of the remaining LE, gives rise to multinucleated syncytial plaques that cover the caruncles by day 24 and are important for placental formation in ruminants [33, 37, 38].

Hatched blastocysts and trophoblastic vesicles do not elongate *in vitro*, but do so when transferred to the uterus of either sheep or cows [19, 20]. The uterine gland knockout (UGKO) sheep model, which lacks glandular epithelium (GE) and has much reduced LE, exhibits a failure in conceptus elongation resulting in recurrent pregnancy loss [81]. Thus, the uterine epithelia and its secretions are essential for conceptus survival, growth and establishment of pregnancy in ruminants. The uterine luminal fluid (ULF) or histotroph is a complex mixture of proteins, lipids, amino acids, sugars, ions and extracellular vesicles (exosomes/microvesicles) that is derived primarily from the transport and/or synthesis and secretion of substances by the endometrial epithelia [3, 7, 436-438]. Ovarian progesterone drives spatial and temporal changes in uterine epithelial gene expression, including induction of conceptus elongation- and implantation-related genes after day 10, that modify the ULF to stimulate conceptus elongation via effects on trophectoderm proliferation, migration and attachment [439]. Microarray analysis of endometrium during the peri-implantation period, as well as candidate gene studies, identified many genes whose expression changes with day and pregnancy status and, based on their biological functions, are implicated in conceptus elongation and development [79, 289, 378]. However, comprehensive knowledge of the endometrial epithelial and conceptus

transcriptome as well as ULF proteome during the establishment of pregnancy has not been reported for sheep, but is important to understand conceptus elongation and pregnancy establishment [22, 318].

Therefore, the objective here was to profile gene expression in the uterine epithelia (LE and GE) and conceptus and proteins in the ULF during the peri-implantation period of pregnancy in sheep. The results provide critical information that serves as a foundation for future studies aimed a discovering new regulatory pathways governing uterine receptivity, conceptus elongation, trophectoderm differentiation, conceptus-endometrial interactions and pregnancy establishment in ruminants.

MATERIALS AND METHODS

Animal Experiments

All experimental and necropsy procedures were approved by the Institutional Animal Care and Use Committee at Washington State University. Mature Columbia Rambouillet crossbred ewes (*Ovis aries*) were observed for onset of estrus (designated day 0). Ewes were mated to an intact ram of proven fertility on days 0 and 1. On days 10, 12, 14, 16, and 20 post-mating, ewes ($n \geq 5$ per day) were necropsied, and reproductive tracts recovered. Both uterine horns were gently flushed with 20 ml of sterile phosphate buffered saline (PBS) (137 mM NaCl; 2.7 mM KCl; 4.3 mM Na2HPO4; 1.47 mM KH2PO4, pH 7.2) on days 10, 12, 14 and 16 to collect ULF and the conceptus. The uterine lumen was gently flushed with 20 ml of sterile PBS (pH 7.2) to collect ULF and the conceptus. The state of conceptus development was assessed for all time points using a Nikon SMZ1000

stereomicroscope (Nikon Instruments Inc., Melville, NY). Uterine flush was clarified by centrifugation (3000 x g at 4°C for 15 min). The supernatant was carefully removed with a pipet, mixed, aliquoted, frozen in liquid nitrogen, and stored at -80°C. On days 12, 14 and 16 the entire conceptus was frozen, the embryonic disk was not removed. On day 20, the embryo with allantois was removed before freezing the remainder of the conceptus. Several sections (~0.5 cm) from the mid-portion of each uterine horn ipsilateral to the ovary were placed in Optimum Cutting Temperature Compound (OCT; Sakura Finetek USA, Inc., Torrance, CA), frozen in liquid nitrogen vapor, and stored at -80°C. Conceptus tissue was placed in a 1.5 ml tube, frozen in liquid nitrogen, and stored at -80°C for subsequent RNA extraction.

Laser Capture Microdissection (LCM)

Uteri frozen in OCT were cryosectioned (10 µm) using a Leica CM1950 cryostat (Leica Microsystems, Wetzlar, Germany). Three tissue sections were mounted per slide to RNase-free polyethylene naphthalate-coated slides (Carl Zeiss, Munich, Germany) and immediately placed on dry ice. Slides were fixed and stained immediately following sectioning using previously described methods [440]. Briefly, slides were transferred from dry ice into ice-cold 95% ethanol for 30 sec, then washed in 75% ethanol for 30 sec. Tissue sections were stained in freshly filtered 1% cresyl violet solution in 75% ethanol for 1 min. Tissue sections were then dehydrated through 75% ethanol (30 sec) and 95% ethanol (30 sec), followed by two 30 sec and one 5 min incubation in anhydrous 100% ethanol. Slides were dried for 10 min at room temperature and stored in sealed containers

at -80ºC until use. The LE and GE were visually identified and separately captured from a single slide of three uterine sections for each animal. Slides were discarded after 60 min of use on the laser capture microdissection (LCM) LMD7 microscope (Leica Microsystems).

RNA Extraction and Sequencing of Isolated Endometrial LE and GE

Total RNA was extracted from cells collected from the LE and GE (n= 5 animals per day per tissue) using the RNeasy MinElute kit (Qiagen, Valencia, CA). The integrity and concentration of RNA was determined using a RNA 6000 Pico Kit and Bioanalyzer 2100 (Agilent Technologies, Santa Clara, CA). A total of 10-24 ng of RNA was collected from each tissue, for each animal. Prior to sequencing, 5 ng of total RNA was amplified using the Ovation RNA-Seq System V2 (cat. # 7102; Nugen, San Carlos, CA). The resulting single primer isothermal amplified (SPIA) cDNA was cleaned using the QIAquick PCR Purification Kit (Qiagen). The Ion Plus Fragment library kit (Life Technologies, Waltham, MA) was used to construct Ion Proton sequencing libraries from SPIA LCM cDNA (200 ng). Sonication (Bioruptor, Diagenode Inc., Denville, NJ) was used to fragment the cDNA. End repaired cDNA was purified using 1.0X v/v AMPure XP beads (Beckman-Coulter Genomics, Danvers, MA). Following barcode adapter ligation and 7 cycles of amplification, the final libraries were size selected by capturing the fragments bound between 0.7X and 1.0X v/v AMPure XP beads. Emulsion PCR was performed on an Ion Chef instrument using the Ion P1 Hi-Q reagents. Sequencing beads were quantified and evaluated by flow cytometry using a Guava Easy Cyte (Millipore, Billerica, MA) with Sybr Gold (Molecular Bioprobes, Eugene,

OR) before loading on an Ion P1 v3 semiconductor sequencing chip. Libraries were sequenced on an Ion Proton using Ion P1 Hi-Q sequencing reagents and 520 flow cells (Life Technologies) by the Washington State University Molecular Biology and Genomics Core. Three barcoded libraries were pooled per P1 chip for sequencing. Base calling and primary analysis was performed using Torrent Suite 4.6.

RNA Sequencing of Conceptuses

Day 12. Total RNA was extracted from day 12 conceptuses (n = 5) using the RNeasy plus kit with on column DNase digestion (Qiagen). Total RNA quality and quantity was determined using a RNA 6000 Pico Kit and Bioanalyzer 2100 (Agilent Technologies, Santa Clara, CA). A total of 374-512 ng of RNA was collected from each conceptus, for each animal. Prior to sequencing, 50 ng of total RNA was amplified using the Ovation RNA-Seq System V2 (Nugen). Following amplification, libraries were constructed and sequenced at the University of Missouri DNA Core following the manufacturer's protocol with reagents supplied in Illumina's TruSeq DNA PCR-Free sample preparation kit (cat. # FC-121-3001). Briefly, cDNA (0.5 µg) was sheared using standard Covaris methods (Covaris, Inc., Woburn, MA) to generate average fragmented sizes of 350 bp. The resulting 3' and 5' overhangs were converted to blunt ends by an end repair reaction which uses a 3' to 5' exonuclease activity and polymerase activity. A single adenosine nucleotide was added to the 3' end of the blunt fragments followed by the ligation of Illumina indexed paired-end adapters. The adaptor ligated library was purified twice with sample purification beads and quantified using the KAPA library

quantification kit (cat. # KK4824; Kapa Biosystems, Inc., Wilmington, MA) and library fragment size confirmed on the Fragment Analyzer (cat. # DNF-472; Advanced Analytical Technologies, Inc., Ankeny, IA). Libraries were diluted and sequenced as 100 bp paired-end sequences on the Illumina HiSeq 2500 platform.

Days 14, 16 and 20. Total RNA was extracted from conceptuses (n = 5 per day) and quality checked as described for day 12 conceptuses. RNA samples were enriched for mRNA by selective depletion of ribosomal RNA using RiboMinus Eukaryote Kit for RNA-Seq (cat. # A1083708, Thermo Fisher Scientific Inc., Wilmington, DE). Libraries were prepared and sequenced by Global Biologics LLC (Columbia, MO, USA). Ribosome-depleted RNA was used as input for the Illumina TruSeq Stranded mRNA HT library construction procedure (San Diego, CA, USA). Prior to sequencing, RNA was fragmented and RT primers were hybridized for cDNA synthesis. The resulting cDNA was prepared for sequencing by 3' adenylation, adapter ligation, and PCR amplification (98ºC for 30 sec; 14 cycles of 98ºC for 10 sec, 60ºC for 30 sec, 72ºC for 30 sec; 72ºC for 5 minutes). Library validation was performed using a Fragment Analyzer (Advanced Analytical) with HiSens NGS reagents followed by quantitation using the Qubit HS DNA assay (cat. # Q32851; Thermo Fisher Scientific, Inc.) and qPCR library kit for Illumina platforms (Kappa Biosystems, Inc.). Libraries were pooled and sequenced as 100 bp paired-end sequences on the Illumina HiSeq 2500 platform.

RNA Sequencing Data Analysis

Analysis of RNA-seq data was completed using a CLC Genomics Server 6.0 and CLC Genomics Workbench 7.0.4 (CLC bio, Aarhus, Denmark). Ion reads

were quality trimmed (error probability 0.02) with default parameters. Illumina reads were quality trimmed (error probability 0.001) with default parameters and 13 bp were removed from the 5' end of each read. All sequences were mapped to the *Ovis aries* genome (Oar_v3.1) with Ensembl version 75 annotations requiring paired mapping and using reads per kilobase of transcript per million (RPKM) for expression values. Quality control was assessed with a boxplot of square root transformed expression values verifying that all samples displayed similar distributions. Differential expression of genes was determined using the empirical analysis of Digital Gene Expression method in CLC Genomics Workbench incorporated from the edgeR Bioconductor package. A list of all expressed genes was extracted by filtering the results table at RPKM ≥ 5 for at least one sample group. Genes were filtered (FDR $P < 0.05$ and fold change ≥ ± 2), expression was $\log_2$ transformed, and sample clustering was confirmed by principal component analysis. Raw FASTQ files were deposited in the NCBI Gene Expression Omnibus (submission in progress).

The list of differentially expressed genes (DEG) from all days and tissues were used for K-means clustering. Transformed expression values ($\log_2$, RPKM) were clustered by Euclidian distance using the hierarchical clustering of features tool in CLC Genomics Workbench. The heat maps were used for preliminary assessments of the number of gene clusters. The K-means clustering tool in CLC Genomics Workbench was run using the same input with partitions set to the number of clusters visualized. Transformed group means were used for clustering by Euclidian distances.

Endogenous retroviral elements from the Jaagsiekte sheep retrovirus (enJSRV) and syncytin envelope (Env) protein (SYN_RUM1) are not currently annotated by RefSeq or Ensembl. Thus, expression was calculated for those endogenous retroviral elements using the following strategies. The *Ovis aries SYN-RUM1* envelope coding sequence (JX412969.1) from NCBI was used as input for a BLAT search against the Oar_v3.1.84 genome at Ensembl [441]. The top three matches by E-value were selected as potential endogenous *SYN-RUM1 env* genes. All reads mapped to the genome for RNA-sequencing were exported from CLC Genomics Workbench (8.5.1) as BAM files. Due to the number of endogenous Jaagsiekte Sheep Retrovirus (enJSRV) genomic integrations, the exogenous JSRV (NC_001494.1) genome was downloaded and unmapped reads from conceptus RNA-sequencing samples were mapped to the exogenous genome with CLC Genomics Workbench. Mapped reads were exported in BAM format. BAM files were sorted and indexed with samtools (1.3) [442]. BEDtools2 multicov (2.19.0) [443] was used to extract read counts per sample with BED files listing gene intervals. Read counts were then normalized and reported as counts per million mapped reads (CPM).

Heat maps were generated in R (3.2.3) using the pheatmap package (1.0.8). Expression values, RPKM or CPM, were $\log_2$ transformed and manually sorted for input. The matrices were supplied to pheatmap with options for row and column clustering set to false and exported as PDF files.

Ingenuity Pathway Analysis (IPA)

Identification of enriched pathways in the LE, GE and conceptus was conducted through the use of Ingenuity Pathway Analysis software (IPA, Qiagen). For each day, a list of genes which were differentially expressed compared to the previous collected time point (> 2-fold change, $P < 0.05$) were uploaded to the IPA tool. Genes were overlaid onto the IPA global molecular network to create gene networks from information contained in the Ingenuity Knowledge Base. The IPA functional analysis tools identified the biological functions and/or pathways that were most significant to the data set ($P < 0.05$) according to a right-tailed Fisher's exact test.

Liquid Chromatography (LC) Mass Spectrometry (MS) Analysis

Proteins were precipitated from the ULF samples using the ProteoExtract Protein Precipitation Kit (Calbiochem). The protein pellet was then solubilized in 100 µL of 6M urea. Dithiothreitol (DTT; 200 mM) was added to a final concentration of 5 mM, and samples were incubated for 30 min at 37°C. Next, 20 mM iodoacetamide (IAA) was added to a final concentration of 15 mM and incubated for 30 min at room temp, followed by the addition of 20 µL DTT to quench the IAA. Trypsin/Lys-C (Promega) was added to the sample and incubated for 4 hours at 37°C. Samples were then diluted to at least 1M urea by the addition of 50 mM AMBIC and digested overnight at 37°C. The following day, samples were desalted using Macro Spin Column (Nest Group).

Digested peptides were analyzed by LC-MS/MS on a Thermo Scientific Q Exactive Orbitrap Mass spectrometer in conjunction Proxeon Easy-nLC II HPLC (Thermo Scientific) and Proxeon nanospray source. The digested peptides were

loaded a 100 µm x 25 mm Magic C18 100Å 5U reverse phase trap where they were desalted online before being separated using a 75 µm x 150 mm Magic C18 200Å 3U reverse phase column. Peptides were eluted using a 90 min gradient with a flow rate of 300 nl per min. A MS survey scan was obtained for the m/z range 300-1600, MS/MS spectra were acquired using a top 15 method, where the top 15 ions in the MS spectra were subjected to HCD (High Energy Collisional Dissociation). An isolation mass window of 2.0 m/z was for the precursor ion selection, and normalized collision energy of 27% was used for fragmentation. A five second duration was used for the dynamic exclusion.

Tandem mass spectra were extracted and charge state deconvoluted by Proteome Discoverer (Thermo Scientific). All MS/MS samples were analyzed using X! Tandem (The GPM, thegpm.org; version TORNADO (2013.02.01.1)). X! Tandem was set up to search *Ovis aries* Proteome database, the cRAP database of common laboratory contaminants (www.thegpm.org/crap; 114 entries) plus an equal number of reverse protein sequences assuming the digestion enzyme trypsin. X! Tandem was searched with a fragment ion mass tolerance of 20 parts per million (ppm) and a parent ion tolerance of 20 ppm. The IAA derivative of cysteine was specified in X! Tandem as a fixed modification. Deamidation of asparagine and glutamine, oxidation of methionine and tryptophan, sulphone of methionine, tryptophan oxidation to formylkynurenin of tryptophan and acetylation of the n-terminus were specified in X! Tandem as variable modifications.

Scaffold (version Scaffold 4.0.6.1, Proteome Software Inc., Portland, OR) was used to validate MS/MS based peptide and protein identifications. Peptide

identifications were accepted if they exceeded specific database search engine thresholds. X! Tandem identifications required at least -Log (Expect Scores) scores of greater than 1.2 with a mass accuracy of 5 ppm. Protein identifications were accepted if they contained at least 2 identified peptides. Using the parameters above, the Decoy False Discovery Rate (FDR) was calculated to be 1.1% on the protein level and 0.0% on the spectrum level [444]. The minimum number of unique peptides was set at 2 in order for a protein to be identified. Peptide threshold was set at 95% peptide probability, with +2 accepted charge, and parent mass tolerance of 10 parts per million. Further analysis was conducted on peptides identified as exclusive and unique to each protein following the removal of protein clusters. Additional filtering of proteins with 4 or more total spectral counts in at least 4 of the 5 samples was applied to compile final lists. Total spectrum counts for proteins were used for comparisons and statistical analysis. The FDR was adjusted using the Benjamini-Hochberg procedure to identify significance based on Fisher's exact test results. To determine the potential origin of proteins in the ULF, the proteomic data were cross-referenced with transcriptome data from the LE, GE and conceptus. A list of proteins identified in the ULF (> 10 average spectral counts) and their expression in either the LE, GE or conceptus (RPKM > 5) were used for further analysis.

RESULTS

Gene Expression in the Uterine Epithelia and Conceptus

Transcriptional profiling of LCM-isolated uterine LE and GE as well as intact conceptuses was conducted using RNA sequencing. Sequencing of the libraries

yielded more than 18.3, 18.1 and 43.5 million quality reads for the LE, GE and conceptus samples, respectively. Based on average RPKM values of less than five, 77%, 74% and 62% of genes were not expressed in the LE, GE and conceptus. Genes were filtered at a total normalized count cutoff of 5 before to fitting the data into a negative binomial distribution, estimating dispersions and using the exact test implemented in edgeR.

Luminal Epithelium (LE). Between days 10 and 20, the total number of expressed genes (RPKM $\geq$ 5) in the LE increased from 3,108 to 4,172 (Figures 1 and 2, Table 1 and Supplemental Table 1). Between days 10 and 12, expression of 9 genes decreased and 12 genes increased ($P \leq 0.05$, $\geq$ 2-fold). From days 12 to 14, 522 genes increased and 171 genes decreased. Similarly, expression of 138 genes increased, while 202 decreased from days 14 to 16. From days 16 to 20, only 1 gene increased, while the expression of 2 genes decreased. The top 10 most abundantly expressed genes in the LE, excluding ribosomal proteins, included *IFI6, RBP4, UBA52, PFN1, CST6, S100A2, TXN, COX6B1, OST4* and *NUPR1*.

Glandular Epithelium (GE). As shown in Figures 1 and 2 and summarized in Table 2, the total number of genes expressed (RPKM $\geq$ 5) in the GE increased from 4,409 to 5,194 from days 10 to 14 and then decreased from days 14 to 20 (4,326) (Supplemental Table 2). Few genes changed ($P \leq 0.05$, $\geq$ 2-fold) between days 10 and 12 (18 increased, 43 decreased), but abundant differences between days 12 and 14 were observed with 833 genes increased and 231 decreased. From days 14 to 16, 246 genes increased and 643 decreased in the GE. However,

expression of only a few genes changed in the GE from days 16 to 20 (11 increased, 4 decreased). In the GE, the top 10 most abundant expressed genes were *S100G, GRP, IFI6, B2M, SERPINA14, ND2, RHOBTB3, RPL31, MT-ND5, NUPR1* and *PABPC1*.

Conceptus. The total number of genes expressed (RPKM $\geq$ 5) in the in the conceptus increased from 2,053 on day 12 to 3,367 on day 14 (Figures 1 and 2, Table 3, and Supplementary Table 3). On day 16, 767 genes were expressed, and 1,098 on day 20. Between days 12 and 14, 2,604 genes increased in the conceptus and 1,866 decreased in abundance. Comparison of gene expression changes between days 14 and 16 identified 1,369 genes of which 715 increased and 654 decreased. Between days 16 and 20, expression of 1,242 genes changed with 863 increased and 379 decreased. The abundance of numerous genes increased between days 12 and 14 including pregnancy specific antigen (*PSA*) (3,073-fold), *IFNT* (125-fold), *TKDP* (473-fold) and *PPARG* (107-fold). From days 14 to 16, genes increased from days 14 to 16, such as *FABP5* (33-fold) and *AFP* (42-fold), and decreased including *PTGS2* (36-fold) and *FADS2* (14-fold). Between days 16 and 20, expression of *ESM1* increased (897-fold) as did *IL2RB* (435-fold), while *SLC34A2* decreased 90-fold and *IFNT* decreased 15-fold. Several genes known to be expressed in trophoblast giant BNCs increased from days 14 to 20 including *PAG6* and placental lactogen (*CSH1*).

Individual heat maps were created for genes expressed in the conceptus incorporating known genes, genes implicated in BNC formation and placentation, genes of interest, and genes from endogenous retroviruses (Fig. 2). The envelope

(env) sequence of the endogenous Jaagsiekte sheep retrovirus (*enJSRVs env*) was most abundant on day 12 (3,037 CPM) and decreased on day 14 (246 CPM), day 16 (96 CPM) and day 20 (29 CPM) (Fig. 2D). Expression of *Syn-Rum1* at two genomic locations were identified in the day 16 and day 20 ovine conceptus. Expression of the retroviral envelope protein syncytin (*SYN-RUM1*) increased from days 12 (2 CPM) to 20 (37 CPM).

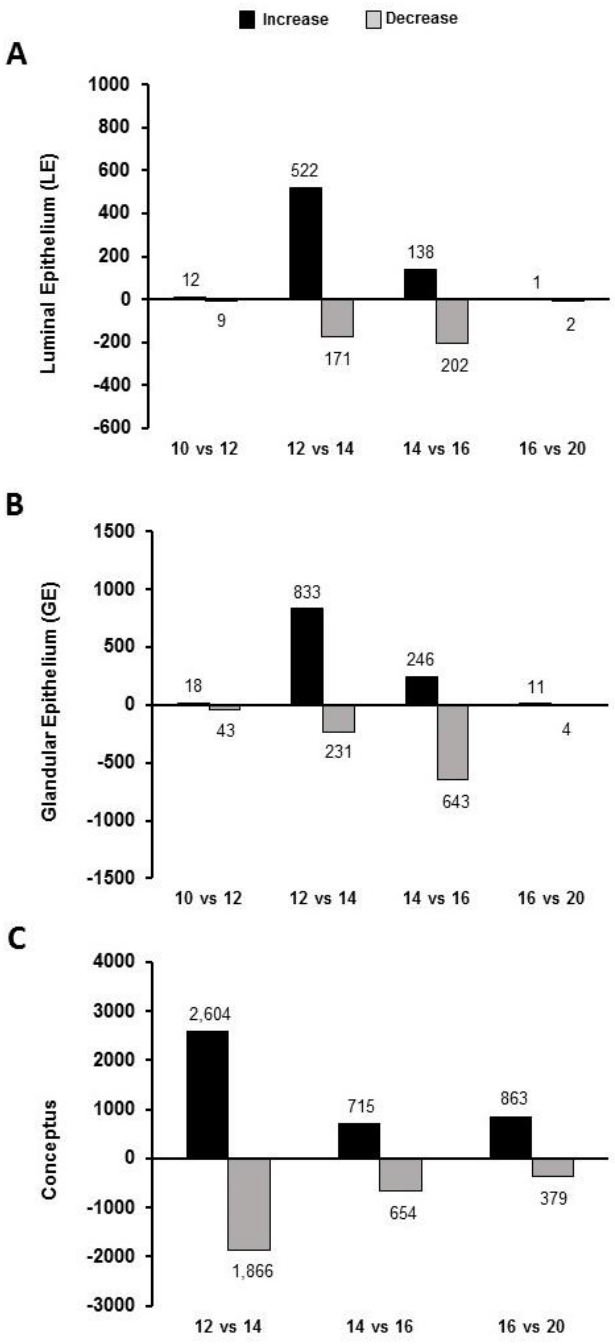

Figure 1. Gene expression changes in the LE, GE and conceptus. Genes expressed in the isolated LE and GE or conceptus from pregnant ewes as determined by RNA-seq (RPKM cutoff of 5). Bar graphs represent the number of genes whose expression increased or decreased (RPKM $\geq$ 5, FDR $P \leq 0.05$, > 2-fold change) from the previous day. Representative list of genes with expression changes between days is included in Table 1 and full gene list is in Supplemental Tables 1, 2 and 3.

TABLE 1. Select list of genes expressed in the uterine luminal epithelium (LE)

	Gene Symbol	Fold Change	FDR *P*-value	RPKM Day 1 vs 2		Description
10 vs 12	*AGR2*	185	0.0028	0	98	anterior gradient 2
	SLC5A1	69	0.0325	0	49	solute carrier family 5, member 1
	HSD11B1	57	0.0011	1	89	corticosteroid 11-beta-dehydrogenase isozyme 1
	RBP4	38	0.0158	7	321	retinol binding protein 4
	CST6	14	0.0003	13	225	cystatin E/M
	CST3	9	0.0400	22	264	cystatin C
12 vs 14	*GRP*	125	0.0042	1	109	gastrin-releasing peptide
	PFN1	21	<0.0001	85	1294	profilin 1
	S100A2	18	0.0004	81	1067	S100 calcium binding protein A2
	FURIN	18	0.0005	2	29	furin
	PAPPA	15	0.0040	1	16	pregnancy-associated plasma protein A
	NUPR1	12	<0.0001	54	531	nuclear protein, transcriptional regulator, 1
	RSAD2	9	0.0019	3	26	radical S-adenosyl methionine domain containing 2
	OST4	7	0.0000	77	449	oligosaccharyltransferase 4
	CST6	7	0.0029	225	1159	cystatin E/M

	SLC2A1	5	0.0027	66	258	solute carrier family 2, member 1
	UBA52	4	0.0067	454	1307	ubiqitin RPL40 fusion protein
	TXN	4	0.0008	352	1065	thioredoxin
14 vs 16	*LY6G6C*	421	0.0006	0	88	lymphocyte antigen 6 complex
	PIP	96	0.0100	0	14	prolactin-induced protein
	MUC20	72	0.00183	0	13	mucin 20, cell surface associated
	SLC36A2	14	0.0300	5	101	solute carrier family 36, member 2
	RSAD2	-5	0.0500	26	7	radical S-adenosyl methionine domain containing 2
	OST4	-7	0.0002	449	93	oligosaccharyltransferase 4 homolog
	IFI6	-7	0.0228	2539	542	interferon, alpha-inducible protein 6
16 vs 20	*CYP26A1*	95	0.0400	0	46	cytochrome P450, family 26, subfamily A, polypeptide 1
	KIAA1551	-5	0.0400	202	43	KIAA1551
	SLC13A5	-23	0.0100	16	1	solute carrier family 13, member 5

TABLE 2. Select list of genes expressed in the uterine glandular epithelium (GE)

	Gene Symbol	Fold Change	FDR *P*-value	RPKM Day 1 vs 2		Description
10 vs 12	*SCGN*	24	0.0099	1	25	secretagogin, EF-hand calcium binding protein
	IFI6	11	0.0044	30	440	interferon, alpha-inducible protein 6
	KLF11	8	0.0043	1	14	Kruppel-like factor 11
	MEP1B	7	<0.0001	13	100	meprin A, beta
	ODC1	-6	0.0005	22	4	ornithine decarboxylase 1
	S100G	-10	<0.0001	7248	755	S100 calcium binding protein G
12 vs 14	*ISG17*	111	<0.0001	2	180	interferon stimulated gene 17
	RSAD2	91	<0.0001	2	132	radical S-adenosyl methionine domain containing 2
	CLEC4F	56	0.0008	0	11	C-type lectin domain family 4, member F
	OAS2	13	<0.0001	8	89	2'-5'-oligoadenylate synthetase 2
	NUPR1	9	<0.0001	103	808	nuclear protein, transcriptional regulator, 1
	LGALS3BP	9	<0.0001	5	40	lectin, galactoside-binding, soluble, 3 binding protein
	CTGF	6	0.0001	91	450	connective tissue growth factor

	STAT1	4	0.0056	7	25	signal transducer and activator of transcription 1
	RPL31	3	0.0007	411	1072	ribosomal protein L31
	B2M	2	0.0093	526	1072	beta-2-microglobulin
14 vs 16	*S100G*	7	0.0002	318	2308	S100 calcium binding protein G
	RHOBTB3	-2	0.0200	1154	544	rho-related BTB domain containing 3
	PABPC1	-2	0.0038	670	319	cytoplasmic 1 polyA binding protein
	MT-ND5	-3	0.0200	747	242	NADH-ubiquinone oxidoreductase chain 5
	KLF11	-4	0.0100	25	8	kruppel-like factor 11
	IGFBP7	-7	0.0011	101	15	insulin-like growth factor binding protein 7
	PPARD	-15	0.0044	24	2	peroxisome proliferator-activated receptor delta
	FGF10	-20	0.0400	14	1	fibroblast growth factor 10
16 vs 20	*SPP1*	87	<0.0001	6	413	osteopontin
	GRP	74	0.0009	75	4989	gastrin-releasing peptide
	SERPINA1 4	65	0.0001	41	2326	serpin peptidase inhibitor, clade A , member 14
	STC1	60	<0.0001	1	60	stanniocalcin 1
	SEC11C	40	<0.0001	5	190	SEC11 homolog C
	INHBA	16	0.0006	4	61	inhibin, beta A
	HIF1A	3	0.0400	68	192	hypoxia inducible factor 1, alpha

TABLE 3. Select list of genes expressed in the conceptus

	Gene Symbol	Fold Change	FDR *P*-value	RPKM Day 1 vs 2		Description
12 vs 14	*PSA*	3074	<0.0001	1	4107	pregnancy-specific antigen
	CLEC16A	1252	<0.0001	1	4225	C-type lectin domain family 16, member A
	IFNT	125	<0.0001	54	1513 0	interferon tau-1
	PPARG	108	<0.0001	0	26	peroxisome proliferator-activated receptor gamma
	TKDP	62	<0.0001	6	803	trophoblast kunitz domain protein
	FADS2	39	<0.0001	26	2274	fatty acid desaturase 2
	FADS1	21	<0.0001	35	1706	fatty acid desaturase 1
	MGST1	13	<0.0001	83	2459	microsomal glutathione S-transferase 1
	PTGS2	10	<0.0001	115	2508	prostaglandin-endoperoxide synthase 2
	CDX2	8	<0.0001	1	13	caudal type homeobox 2
	ATF4	2	0.0011	68	264	activating transcription factor 4
	COX1	-4	<0.0001	15420	8412	cytochrome c oxidase subunit 1
14 vs 16	*AFP*	41	<0.0001	5	268	alpha-fetoprotein
	FABP5	33	<0.0001	23	1032	fatty acid-binding protein
	RAN	3	<0.0001	83	465	ras-related nuclear protein
	DDX54	3	0.0015	4	22	DEAD (Asp-Glu-Ala-Asp) box polypeptide 54

	DDX5	2	0.0001	157	317	DEAD (Asp-Glu-Ala-Asp) box helicase 5
	KRT8	-2	0.0001	2750	1764	keratin 8, type II
	DDX17	-3	<0.0001	118	78	DEAD (Asp-Glu-Ala-Asp) box helicase 17
	ATF6	-3	<0.0001	52	23	activating transcription factor 6
	SLC34A2	-14	<0.0001	882	84	solute carrier family 34, member 2
	SLC27A6	-64	<0.0001	214	4	solute carrier family 27, member 6
16 vs 20	*ESM1*	896	<0.0001	0	151	endothelial cell-specific molecule 1
	IL2RB	435	<0.0001	0	263	interleukin 2 receptor, beta
	PAG11	110	<0.0001	0	49	pregnancy-associated glycoprotein 11
	CSH1	70	<0.0001	0	23	chorionic somatomammotropin hormone
	PLET1	40	<0.0001	76	2949	placenta expressed transcript 1
	PAG6	33	0.0018	0	5	pregnancy-associated glycoprotein 6
	SERPINA1	30	<0.0001	48	1435	serpin peptidase inhibitor, clade A, member 1
	GCM1	25	<0.0001	0	12	glial cells missing homolog 1
	PAG4	7	<0.0001	6	40	pregnancy-associated glycoprotein 4
	PGF	3	0.0015	23	79	placental growth factor

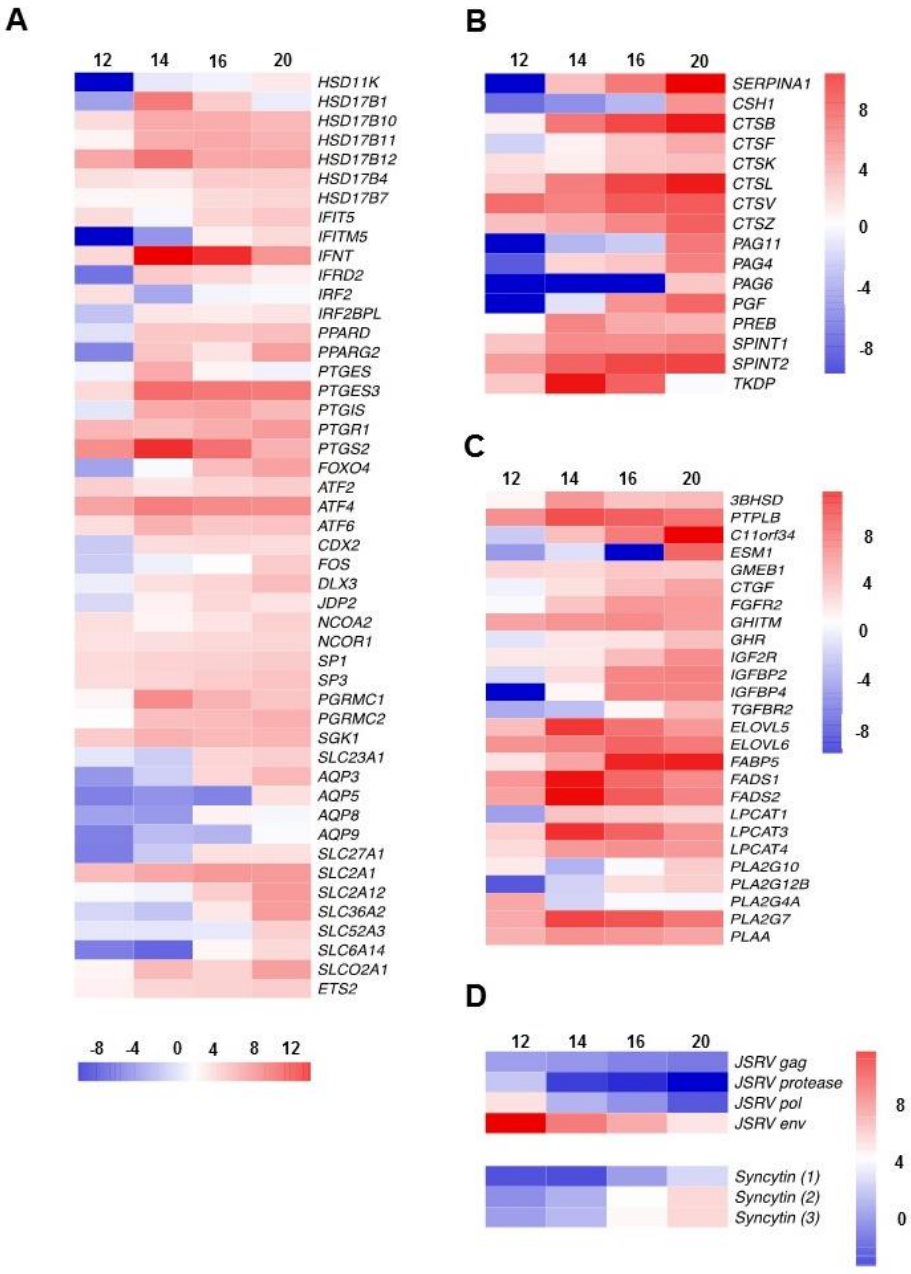

Figure 2. Heat maps of select genes expressed in the conceptus. Gene expression changes in the conceptus as determined by RNA-seq. Each column represents a single time point. Blue colored squares indicate low expression, white squares indicate moderate expression, and red squares represent high expression. (A) Select genes already investigated in the ovine conceptus. (B) Genes expressed in binucleate cells. (C) Genes of particular interest and not previously investigated in the sheep conceptus. (D) Endogenous JSRVs (Jaagiekte Sheep Retroviruses) and syncytin (Syn-Rum1) expression. Data presented as $\log_2$ transformed mean RPKM values (A-C) and as $\log_2$ transformed mean CPM values for endogenous JSRVs and Syncytin (D).

Pathway Analysis

Ingenuity Pathway Analysis (IPA) was used to identify enriched cellular processes in the uterine epithelia and conceptus across days based on differentially expressed genes (Table 4 and Supplemental Table 4). In the LE from days 10 to 12, DEGs were associated with organismal development, inflammatory response, and molecular transport processes. From days 12 to 14, DEGs were associated with lipid metabolism, cellular movement, cell death and survival, as well as cellular development. From days 14 to 16, DEGs were associated with cell signaling, cellular assembly and organization, post-translational modifications, and protein synthesis. The DEGs in the LE from days 16 to 20 were associated with lipid metabolism, small molecule biochemistry and molecular transport.

In the GE from days 10 to 12, IPA analysis found that pathways for cell death and survival, cell morphology, cell-to-cell signaling and interactions, and cellular function and maintenance were enriched in the DEgs. From days 12 to 14, DEGs were associated with cellular movement, cell death and survival, cellular growth and proliferation, and protein synthesis. From days 14 to 16, DEGs were associated with molecular transport, protein synthesis, cell function and maintenance, post transcriptional modifications and RNA trafficking. From days 16 to 20, DEGs were associated with cellular growth and proliferation, tissue development and molecular transport.

In the conceptus, enriched pathways between days 12 and 14 included cell death and survival, cellular assembly and organization, gene expression and

proteins synthesis. From days 14 to 16, the pathway for cell death and survival was again enriched as well cellular growth and proliferation, protein synthesis and cell cycle. In the conceptus from days 16 and 20, additional pathways such as cellular morphology, cellular development, and molecular transport were identified.

TABLE 4. Cellular processes enriched in the uterine luminal epithelia (LE), glandular epithelia (GE) and conceptus from IPA analysis

Day	Tissue	Category	*P*-value	# Molecules
10 vs 12	**LE**	Inflammatory Response	3.56E-04	7
		Organismal Development	6.27E-05	6
		Small Molecule Biochemistry	7.48E-05	6
12 vs 14	**LE**	Cell Death and Survival	2.82E-06	129
		Cellular Movement	7.38E-07	94
		Lipid Metabolism	3.27E-07	60
14 vs 16	**LE**	Cellular Assembly and Organization	3.31E-03	8
		Cell Signaling	3.31E-03	6
		Protein Synthesis	3.31E-03	6
16 vs 20	**LE**	Lipid Metabolism	1.87E-03	2
		Small Molecule Biochemistry	1.87E-03	2
		Molecular Transport	1.73E-03	2
10 vs 12	**GE**	Cell Death and Survival	6.34E-04	3

		Cell-To-Cell Signaling and Interaction	6.34E-04	3
		Cell Morphology	6.34E-04	2
12 vs 14	**GE**	Cellular Growth and Proliferation	4.27E-15	257
		Protein Synthesis	2.12E-11	135
		Cellular Movement	2.66E-11	171
14 vs 16	**GE**	Cellular Function and Maintenance	2.61E-03	21
		RNA Post-Transcriptional Modification	1.04E-03	14
		Molecular Transport	5.03E-05	13
16 vs 20	**GE**	Cellular Growth and Proliferation	2.09E-06	5
		Tissue Development	2.75E-05	5
		Molecular Transport	3.23E-05	6
12 vs 14	**Conceptus**	Cell Death and Survival	6.71E-21	548
		Cellular Assembly and Organization, Function and Maintenance	1.21E-12	266
		Gene Expression	2.10E-12	261
14 vs 16	**Conceptus**	Cellular Growth and Proliferation	8.50E-22	868
		Cell Cycle	6.54E-17	288
		Protein Synthesis	6.21E-12	243
16 vs 20	**Conceptus**	Cellular Development	3.86E-06	203
		Cell Morphology	6.87E-07	183
		Molecular Transport	4.6E-11	175

Gene Expression Clusters in the LE, GE and Conceptus

K-means cluster analysis was used to group genes with similar expression profiles across time points in the LE and GE (12 clusters) and conceptus (15 clusters) (Figure 3 and Supplemental Table 5). In the LE, cluster 5 was composed of genes whose expression peaked on day 14 including *B9D1, DFNA5,* and *NPTX2*. Cluster 8 included genes whose expression was lowest on day 14, but then increased substantially by day 16. Those genes included *MUC20, CCNB3*, and *PIP*. Cluster 11 included genes with high expression prior to and following day 14, including *ELOVL5, UBE2A* and *RBKS*. Finally, cluster 12 identified genes whose expression continually increased across early pregnancy in the LE and included *HSD11B1, CST6*, and *GRP*.

Similar expression patterns were seen in the GE (Figure 3B). Genes whose expression patterns peaked at day 14, but remained elevated on day 16 and 20 (Cluster 1) included *FGF10, ING1* and *PAOX*. In cluster 3, grouped genes whose expression remained elevated on days 10 to 14 until decreasing on day 16 to 20, included *SOX17, NUDT18,* and *APOE*. Genes whose expression increased across all days were grouped in cluster 7, including *OAS1* and *OAS2*, *ISG17* and *IRF7*. In cluster 10, genes whose expression remained low until day 14 and then increased included *GRP, OST,* and *SERPINA14*.

In the conceptus, genes whose expression was lowest on day 14 but then increased by day 16 were identified in cluster 4 and included *CLDN8, SOD3* and *ZCCHC16* (Figure 3C). Cluster 9 included genes whose expression continuously

increased between day 12 and 20, including *PEG10, HGF* and *PGF*. Gene expression changes which increased from days 10 to 14 and remained elevated were identified in cluster 12, including *PRSS46, PARVG* and *PSCA*. Additionally, genes whose expression peaked at day 14 and then decreased on day 16 and 20 included *LPCAT3*, *FADS2, IFNT* and *TEX11* in cluster 14.

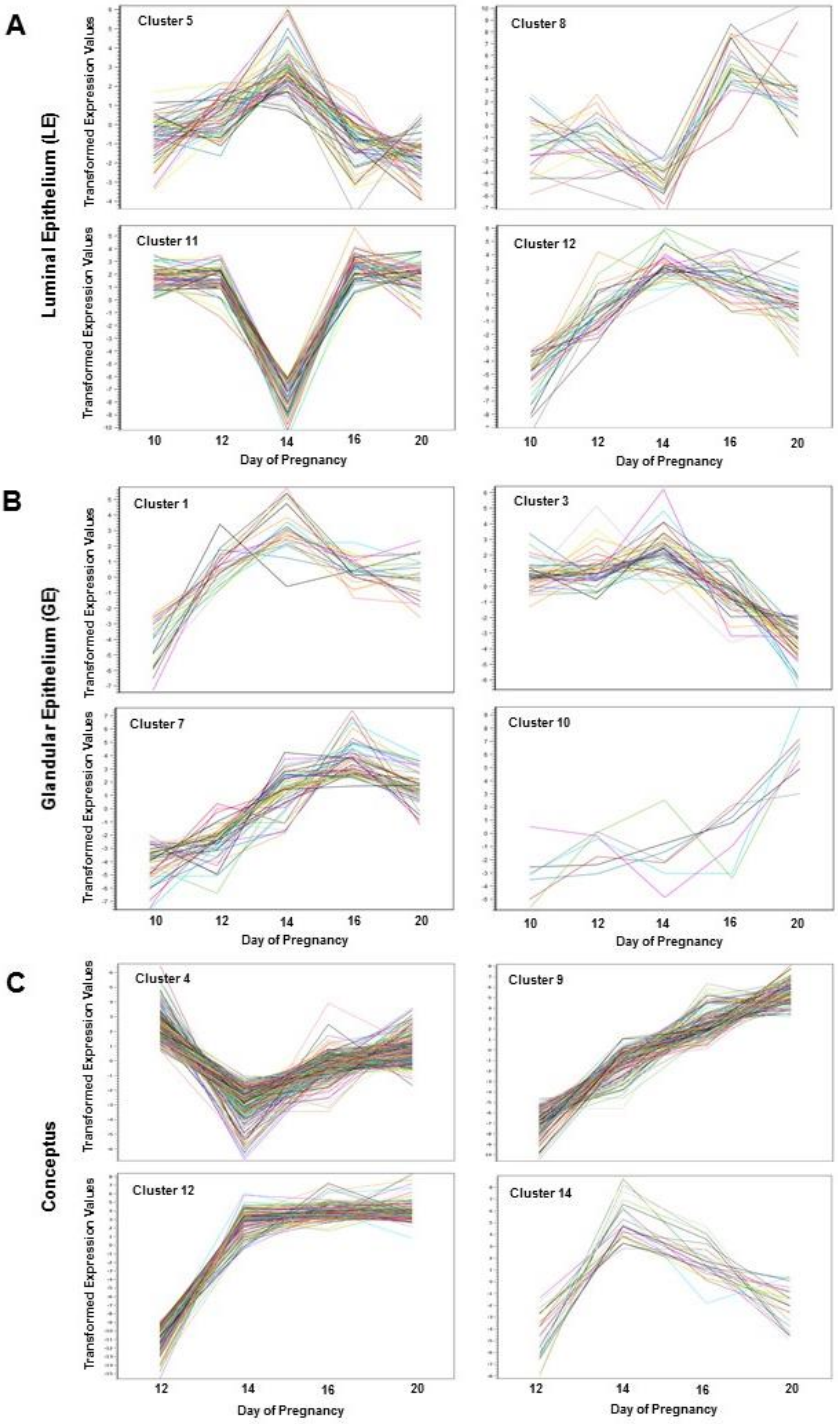

Figure 3. Gene expression profiles in the LE, GE and conceptus assessed by K-means clustering. Gene clusters were identified using K-means clustering of RNA-Seq data into 12 partitions for LE and GE and 15 partitions for conceptus. Four representative clusters are presented for each cell or tissue type. Genes present in each cluster are provided in Supplemental Table 5.

ULF Proteome

Proteins in the ULF were identified and quantified using mass spectrometry. This approach detected (>10 spectral counts) over 1,400 proteins in the ULF. As expected, the most predominant protein in all samples was serum albumin (ALB). On day 10, the ULF contained 79 unique proteins which increased on day 12 to 102 proteins, 167 proteins on day 14, and 201 on day 16 (Fig. 4A, Table 5 and Supplemental Table 6).

Analyses found 14 proteins whose abundance changed ($\geq$ 2-fold, $P < 0.05$) in the ULF between days 10 and 12 (see Figs. 4B and 4C, Table 5 and Supplemental Table 6). Between days 12 and 14, the abundance of 53 proteins changed in the ULF with 58 proteins changed between days 14 and 16 (Fig. 4B). Proteins which were newly present or absent on each day (light bars of Fig. 4C) were distinguished from those previously present but whose abundance changed (dark bars of Fig. 4C). Comparison of day 10 to 12 identified 30 proteins that increased and 7 proteins that decreased in abundance; of the 30 proteins that increased, 21 were previously undetectable (< 10 average spectral counts) in day 10 ULF, but present by day 12 (> 10 average spectral counts) including MET, HEXB, LRP2 and PSAP. From days 12 to 14, a total of 83 proteins increased while 17 proteins decreased in abundance in the ULF. Fifty-nine of the proteins that increased were previously absent from the day 12 ULF including HSPA8, SOD3, and TIMP2. Comparison of day 14 to 16 ULF identified 64 proteins whose abundance was greater on day 16, and 38 whose abundance decreased between days 14 and 16. Of the 64 proteins which increased, 46 where not previously

present in the day 14 ULF including RPS21, EPRS, PSPH and AZGP1. Additional proteins present in the day 14 but not in the day 16 ULF included ENO1, IL1R2, GC, HSPA8, PGK1 and CST3.

TABLE 5. Select proteins in the uterine luminal fluid (ULF)

	Symbol	Description	Average Spectral Counts
Day 10	ALB	serum albumin	644
	CP	ceruloplasmin	131
	WFDC2	WAP four-disulfide core domain protein 2	101
	LRP2	low-density lipoprotein receptor-related protein 2	82
	C3	complement C3-like	33
	CST6	Cystatin E/M	30
Day 12	LRP2	low density lipoprotein-related protein 2	58
	HEXB	beta-hexosaminidase subunit beta	50
	CST3	cystatin C	28
	IGFBP1	insulin-like growth factor-binding protein-1	23
	PSAP	proactivator polypeptide isoform 3	23
	IGFBP3	insulin-like growth factor-binding protein-3	22
	CTSL1	cathepsin L1 isoform 1	21
	MET	met proto-oncogene precursor	17
Day 14	SOD3	extracellular superoxide dismutase 3	91
	HSPA8	Heat Shock 70kDa Protein 8	59
	CST3	cystatin C	38
	GC	vitamin D-binding protein	26
	PGK1	phosphoglycerate kinase 1	23
	LGALS3BP	galectin-3-binding protein	23
	IL1R2	interleukin-1 receptor type 2	21
	NPC2	epididymal secretory protein E1	20
	H3	histone H3	17

	RBP4	retinol-binding protein 4	16
	ENO1	alpha-enolase isoform 1	14
	TIMP2	metallopeptidase inhibitor 2	11
Day 16	PSPH	Phosphoserine Phosphatase	77
	AZGP1	nucleophosmin-like	76
	CYTB	Cystatin-B	40
	LAP3	cytosol aminopeptidase	40
	MYH9	myosin-9-like	26
	EZR	ezrin	25
	EPRS	bifunctional glutamate/proline tRNA ligase	8

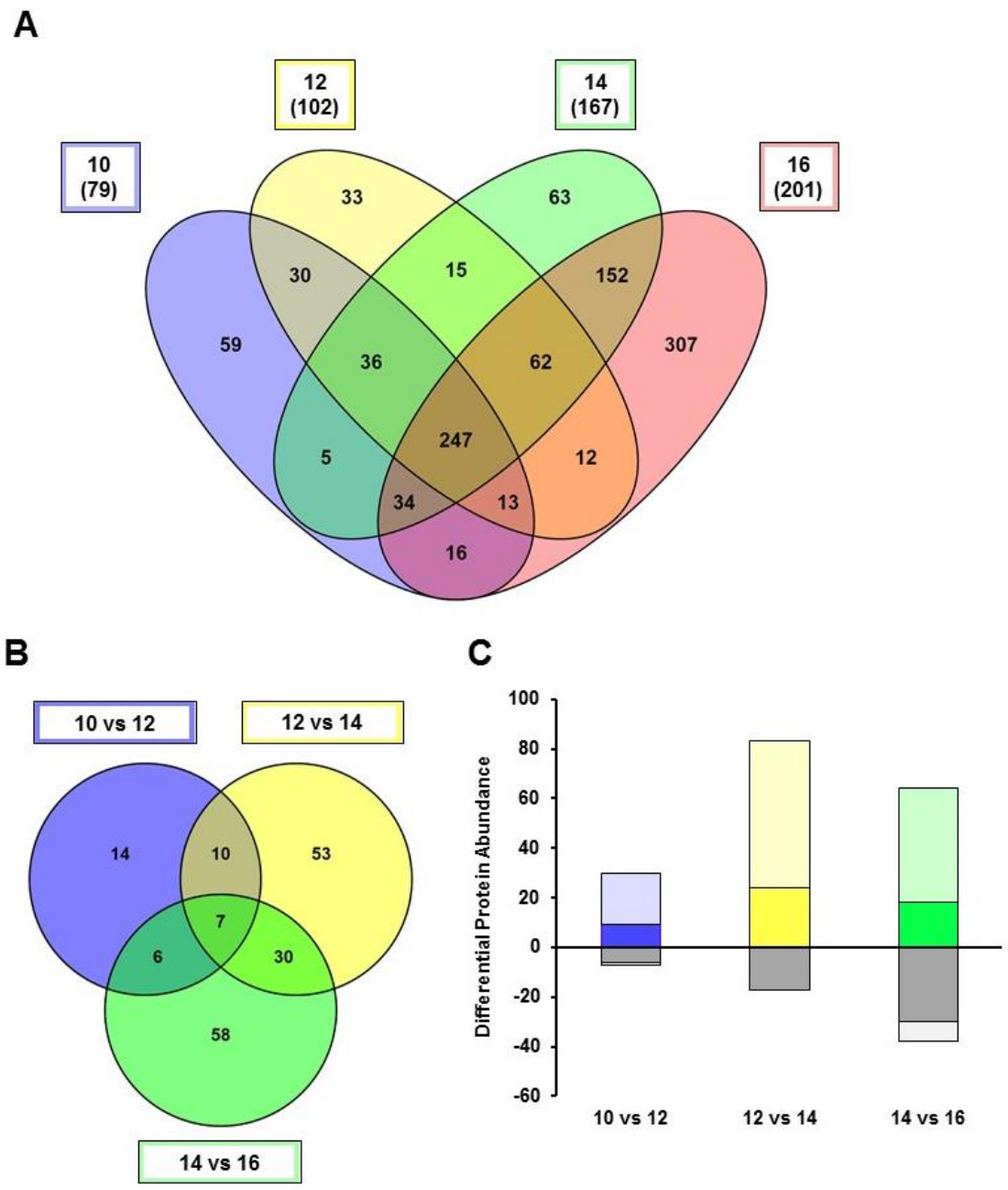

Figure 4. Diagrams illustrating differences in protein abundance in the ULF between days of early pregnancy. (A) Venn diagram of proteins identified (> 10 spectral counts in 2 samples) in the ULF of day 10, 12, 14 and 16 pregnant ewes. (B) Venn diagram of protein changes in the ULF between days (> 10 spectral counts in 2 samples, $P > 0.01$, > 0.5 fold change). (C) Graphical representation of the number of proteins whose abundance increased or decreased from the previous day (dark bar) and proteins which are newly present or absent on each day (light bar).

To determine the potential origin of proteins in the ULF, proteomic data was integrated with transcriptome data. A selection of proteins identified in the ULF (> 10 average spectral counts) and expression of their encoded genes in the LE, GE or conceptus (RPKM > 5) are presented in Figure 5. In day 10 ULF, *ACTG1* and *TMSB4Y* are expressed more abundantly by the GE, while *EFEMP1*, *GAPDH* and *HEXB* are more predominantly expressed by the LE. In day 12 ULF, *ANXA1*, *B2M* and *BCL2L15* are expressed in the LE, while *MEP1B* and *CLU1* are more abundant in the GE. The day 12 conceptus had abundant *GAPDH*, *KRT8* and *HSPA8* expression and the encoded proteins were also present in the ULF. On day 14, *BCL2L15* was expressed in the LE, as was *CST6, CTSL1* and *RBP4*. As expected, IFNT was present in the day 14 ULF and was *IFNT* was expressed exclusively in the conceptus. Additional genes expressed by the conceptus and identified in the ULF included *KRT8* and an inhibitor of *PLA2* (*iPLA2*). ALPL, CP and MEP1B in day 14 ULF were likely of GE origin based on expression. On day 16 of pregnancy, IFNT continued to be abundant in the ULF, as did KRT8 and iPLA2 from the conceptus. Gene expression levels of *CST3*, *CST6* and *CTSL1* continued to increase in the LE on day 16 and the encoded proteins were present in the ULF.

Figure 5. Integration of transcriptomic and proteomic data. Proteins in the ULF were cross referenced to genes expressed in the LE, GE and conceptuses. Average RPKM values are presented for each gene corresponding to protein in the ULF (> 10 average spectral counts)

To determine if transcriptomic changes in the LE, GE and conceptus contributed to changes in the abundance of proteins in the ULF, protein abundance across days of pregnancy was compared to the transcriptome data for select genes (Figure 6). The dynamics of proteins and gene expression across days of pregnancy are presented using two y-axes, one for RPKM of gene expression and other for spectral counts of protein data. In the ULF, the abundance of CST3 increases from 28 to 146 total spectral counts between days 12 and 14, then decreases to 50 spectral counts on day 16. The expression of *CST3* in the LE follows a similar pattern, increases from day 12 to 14 and then decreases on day 16 and 20. The expression of *CP* by both the LE and GE on day 10 and 12 is reflected in CP abundance in the ULF. As *CP* expression decreases in the LE between day 12 and 14, protein abundance in the ULF also decreases from day 12 to 16. Peak IGFBP1 abundance in the ULF occurs on day 14 (38 total sepctral counts), concurrent with the expression of *IGFBP1* in the LE. The abundance of HEXB in the ULF is also greatest on day 14 (147 total spectral counts), although the expression of *HEXB* is higher on day 12 (403 RPKM), and day 16 (497 RPKM) compared to day 14 (258 RPKM). *PSAP3* is expressed by the LE, GE and conceptus during early pregnancy with peak protein abundance in the ULF on day 14 (59 total spectral counts). Expression of *PSAP3* is most abundanct in the GE (123 RPKM) and conceptus (114 RPKM) on day 14, and expression by the

conceptus continues to increase from day 14 to 20 (217 RPKM). The abundance of WFDC2 in the ULF is highest on day 10 (101 total spectral counts), and decreases to 22 total spectral counts on day 16. Expression of *WFDC2* by the LE and GE follows a similar pattern, decreasing from day 10 (LE 94 RPKM) to 16 (LE 22 RPKM). Although expression in the conceptus increases from day 14 (31 RPKM) to 16 (124 RPKM) with no increase seen in protein abundance.

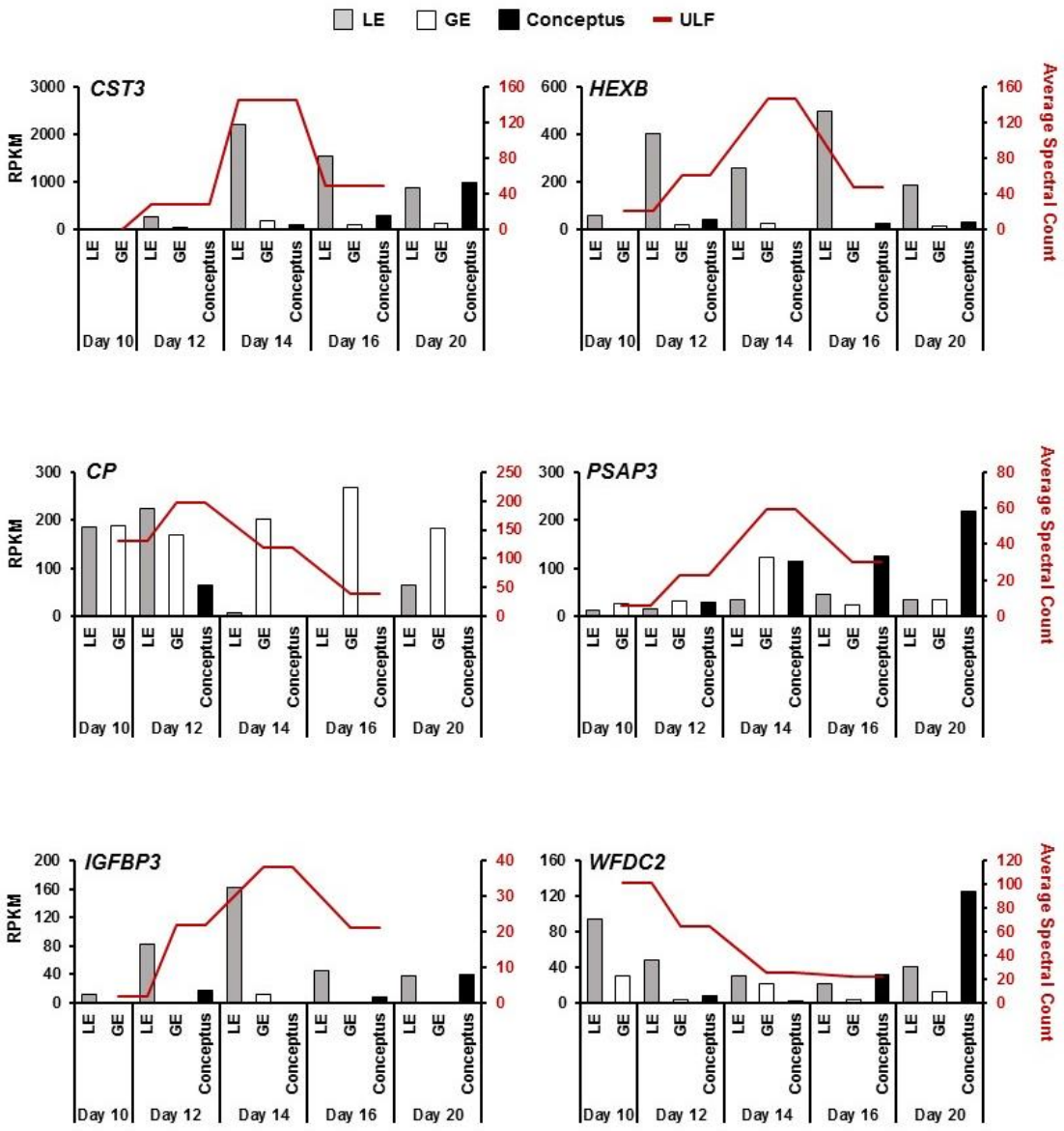

Figure 6. Integration of transcriptomic and proteomic data across day of pregnancy for select proteins in the ULF. Proteins identified in the ULF during early pregnancy were cross referenced to genes expressed in the LE and GE on day 10, the LE, GE and conceptus on day 12, 14 and 16. Average RPKM values are presented for each gene in each tissue by day of pregnancy (bar graph). While protein abundance in the ULF for each day of pregnancy is represented by day (line graph).

DISCUSSION

Dynamic changes in the uterine epithelial and conceptus transcriptome were observed in the present study in association with the onset of rapid trophectoderm growth needed for conceptus elongation. This result was not unexpected based on candidate gene and microarray studies of endometria and conceptuses from sheep during the peri-implantation period of pregnancy [103, 315, 445, 446]. Available evidence strongly supports the ideas that uterine epithelial gene expression during establishment of pregnancy in ruminants is principally regulated by progesterone from the ovary and factors from the developing conceptus. After ovulation, the ovarian corpus luteum forms and progesterone induces a number of genes in the uterine LE and GE implicated in conceptus elongation and implantation. Many of the protein products produced in response to downregulation of the progesterone receptor have been characterized in luminal fluid of sheep previously [447-449]. In addition to stimulation P4, factors from the mononucleate trophectoderm cells (PGs, IFNT, cortisol) and trophoblast giant BNC (placental lactogen or CSH1 and placenta growth hormone or GH) of the conceptus also act on the uterine epithelia to modify gene expression. Factors from the conceptus act on the uterus to stimulate some of the progesterone induced elongation- and implantation-related genes in the uterine LE and GE as well as induce or upregulate additional progesterone-independent genes such as ISGs. The outcome of dynamic changes in the uterine epithelial transcriptome is modification of the ULF and subsequent effects on conceptus survival, elongation and implantation. An important outcome of this study is provision of critical

information that serves as a foundation for future studies aimed a discovering new regulatory pathways governing uterine receptivity, conceptus elongation, trophectoderm differentiation, conceptus-endometrial interactions and pregnancy establishment in ruminants.

The design of this study, incorporating LCM to isolate the LE and GE from the ovine uterus, provides important cell-specific information that can be obscured in transcriptome analysis of the whole endometrium, because it contains many different cell types including a preponderance of stroma and endothelium. One caveat of the approach is that LCM yields low abundance of RNA, which necessitated use of an amplification step prior to library construction and sequencing. The chosen whole genome amplification system is rapid and sensitive and eliminates the need for poly(A) selection or rRNA depletion. Similarly, the day 12 conceptuses yielded low amounts of RNA and necessitated use of whole genome amplification prior to library construction. As with any amplification procedure, some bias is unavoidable and low abundance transcripts may not be amplified in a robust manner. The approach to study the ULF proteome using nano-LC-MS/MS is comprehensive, but the preponderance of albumin and other serum-derived proteins decreases the ability to identify low abundance proteins. Additionally, analysis of transcriptomic and proteomic data is dependent on the quality of genome and proteome annotation. Nevertheless, RNA-sequencing data generated by this approach here confirmed previously reported studies utilizing a number of different quantification methods including RNA blots, real-time PCR and *in situ* hybridization [103, 315, 445, 446].

The LE performs a number of different functions important for establishment of pregnancy. First, it regulates attachment of the mononuclear trophectoderm cells to the uterus [450]. Transient attachment of the trophectoderm to the LE is likely a key component of trophoblast outgrowth and migration needed for growth and elongation of the conceptus. Second, changes in LE gene expression between days 10 and 12 presumably drive initial growth of the hatched blastocyst into an ovoid conceptus prior to rapid trophoblast elongation that begins on day 13 [315, 445, 451]. Progesterone changes the LE transcriptome and induces expression of many genes between days 10 and 12 or 14. Those elongation- and implantation-related genes encode enzymes (HSD11B1, PTGS2) that produce bioactive factors, secreted growth factors (GRP, LGALS15), proteases and protease inhibitors (CST3, CST6, CTSL1), binding proteins (IGFBP1), and transport proteins for glucose (SLC2A1, SLC5A1, SLC5A11) and amino acids (SLC7A2) [103] [451]. The present study confirmed the known temporal alterations in expression of many of those genes (Supplemental Table 1). Further, an increased amount of the encoded proteins was found in the ULF for many of the upregulated LE genes. For example, CST3 and IGFBP1 protein increased in the ULF between days 10 and 12, and CST3, IGFBP1 and CST6 protein increased in the ULF between days 12 and 14 (Supplemental Table 6).

A number of novel LE-derived factors can be acquired from the present study that may play a role in epithelial cell function and conceptus elongation based on their known or purported biological functions to regulate cell proliferation, migration, attachment and/or differentiation. For instance, *AGR2* was upregulated

in the LE between days 10 and 12; it is a proto-oncogene that encodes a secreted protein with biological roles in cell survival, migration, differentiation, and growth, and is also implicated in epithelial barrier function and integrity [378]. *FURIN* was upregulated between days 12 and 14 and encodes a type 1 membrane bound protease that processes protein and peptide precursors trafficking through the secretory pathway. Some of its substrates include proparathyroid hormone, transforming growth factor beta 1 precursor, proalbumin, pro-beta-secretase, membrane type-1 matrix metalloproteinase, beta subunit of pro-nerve growth factor and von Willebrand factor [452]. *PAPPA* was upregulated between days 12 and 14; it encodes a secreted metalloproteinase which cleaves insulin-like growth factor binding proteins (IGFBPs) and is thought to promote cell proliferation [453]. Between days 14 and 16, a number of interesting genes were upregulated including *PIP* (prolactin-induced protein) and *MUC20* (mucin 20). PIP has the ability to bind immunoglobulin G (IgG), IgG-Fc, and CD4-T cell receptor suggesting a wide range of immunological functions [454, 455]; it also exerts aspartyl proteinase activity and is able to cleave fibronectin, a glycoprotein of the extracellular matrix which bind to integrins [456, 457]. *MUC20* encodes a member of the mucin protein family implicated in inhibiting trophoblast invasion during implantation in domestic animals, mice and humans [9, 24, 458]. A smaller number of genes were upregulated in the LE between days 16 and 20 including *C11orf34* (*PLET1*). PLET1 (placenta expressed transcript 1) is only expressed in the LE of the bovine uterus [459] and is an epigenetically regulated cell surface protein that provides essential cues to direct trophoblast stem cell differentiation [460].

The endometrial glands of the uterus are unequivocally required for pregnancy in sheep [21]. Adult UGKO sheep are infertile and exhibit recurrent pregnancy loss, thereby revealing an essential role for uterine glands and their secretions in survival and development of the conceptus [81, 435]. Morphologically normal blastocysts were present in the uterus of UGKO sheep after mating on day 9, but conceptuses were absent or severely growth-retarded when assessed on day 14 post-mating [21]. The lack of conceptus survival and elongation in UGKO ewes was hypothesized to result from the absence of specific secretions normally produced by the uterine glands. Consequently, secretions of the GE have a primary influence on survival and growth of the hatched blastocyst after day 9. Similar to the LE, available studies support the idea that progesterone induces and conceptus factors, such as CSH1 and PAGs, stimulate a number of genes in the GE of the ovine uterus [40, 461]. Given that the surface area of the GE substantially exceeds that of the LE, the GE is likely to be the major epithelial cell type impacting conceptus growth and development. Further, the LE disappears from much of the endometrium by day 20 [28].

Although the uterine glands are of paramount importance for conceptus survival and elongation, our knowledge of the GE transcriptome and ULF histotroph remains incomplete [35]. Over the past decade or so, studies found that the uterine glands express genes that encode for secreted factors (CTGF, GRP, WNT11), amino acid transporters (SLC1A1, SLC1A4, SLC1A5, SLC7A1, SLC7A2, SLC7A5, SLC7A8, SLC43A2), glucose transporters (SLC2A1, SLC2A5, SLC2A12, SLC5A1, SLC5A11), secreted migration and attachment factors

(SPP1), a regulator of calcium/phosphate homeostasis (stanniocalcin one or STC1), secreted peptidases (CTSH, CTSL, CTSS, CTSZ), secreted protease inhibitors (CST3, CST6), and an immunomodulatory factor (SERPINA14 also known as uterine milk protein or uterine serpin). The present study confirmed the temporal alterations in expression of many of those GE genes. Further, the expression of classical IFNT-stimulated genes (ISGs) was observed in the GE, but not LE, after day 12 [462, 463]. IFN regulatory factor 2 (IRF2), a potent transcriptional repressor of ISG expression, is specifically expressed in the LE and restricts IFNT induction ISGs to the GE, stroma and myometrium during early pregnancy in sheep [100, 464]. Many of the known GE-expressed genes encode proteins hypothesized to alter the ULF by increasing select amino acids, glucose, cytokines and growth factors (Supplemental Table 6). The net result of the dynamic changes in uterine epithelial gene expression during early pregnancy is the production of secreted factors in the ULF that support blastocyst survival and growth into an ovoid conceptus and elongation.

The present study identified many new genes in the GE that likely have a role in epithelial cell function and conceptus elongation based on their known or proposed biological functions (Supplemental Table 2). For instance between days 10 and 12, a number of genes were induced or increased in the GE including *MEP1B* and *SCGN*. MEP1B is a secreted zinc metalloendopeptidase that is abundantly expressed in epithelial cells, particularly in the intestine and kidney [465]. MEP1B protein increased substantially in the ovine ULF between days 10 and 12 (Supplemental Table 6). In the bovine uterus, MEP1B is expressed only in

the GE and upregulated by progesterone by day 13 [466]. Cleavage of MEP1B substrates can lead to their degradation or activation. Substrates for enzymatic cleavage by MEP1B include SPP1 and GRP, which are known to components of ULF in sheep. *SCGN* encodes a secreted calcium-binding protein related to calbindin D-28K and calretinin and involved in calcium flux and cell proliferation [467]. Between days 12 and 14, a large number of genes are upregulated in the GE including CLEC4F, CTGF, and LGALS3BP (Supplemental Table 2). *CLEC4F* encodes a member of the C-type lectin/C-type lectin-like domain (CTL/CTLD) superfamily that have diverse functions, such as cell adhesion, cell-cell signaling, glycoprotein turnover, and roles in inflammation and immune response [468]. CTGF mediates heparin- and divalent cation-dependent cell adhesion in many cell types and enhances fibroblast growth factor-induced cell proliferation. In the pig uterus, *CTGF* is expressed in the LE and GE, and CTGF is a component of ULF [469]. LGALS3BP is part of a family of beta-galactoside-binding proteins implicated in modulating cell-cell and cell-matrix interactions. It appears to be implicated in immune response associated with natural killer and lymphokine-activated killer cell cytotoxicity. Of note, LGALS3BP protein increased in ULF between days 12 and 14 (Supplemental Table 6).

A number of genes were also increased between days 14 and 16 in the GE including *S100G* (Supplemental Table 2). *S100G* encodes calbindin D9K, a vitamin D-dependent calcium-binding protein that increases Ca^{2+} absorption and transport in the intestine [470]. A smaller number of genes increased in the GE between days 16 and 20, including *INHBA* and *SEC11C* (Supplemental Table 2).

SEC11C is a component of the microsomal signal peptidase complex which removes signal peptides from nascent proteins as they are translocated into the lumen of the endoplasmic reticulum. *INHBA* encodes a beta subunit that combines with an alpha subunit to form a pituitary FSH secretion inhibitor [471]. The beta A subunit can also form a homodimer, activin A, and also joins with a beta B subunit to form a heterodimer, activin AB, both of which stimulate FSH secretion. Of note, *INHBA* was recently found to be upregulated during early pregnancy in the endometrium and expressed only the GE of the day 18 pregnant sheep uterus [472]. An increased understanding of GE-expressed genes should discover important pathways regulating conceptus elongation and trophectoderm differentiation for implantation.

Conceptus growth and differentiation during the peri-implantation period of pregnancy is undoubtedly regulated by both extrinsic and intrinsic factors involved in cell growth and migration, changes in cell morphology, and cellular differentiation. Extrinsic influences on conceptus elongation and implantation include factors emanating from the endometrium that are primarily regulated by progesterone and paracrine effects of conceptus-derived factors such as PGs, IFNT, cortisol, CSH1 and GH. Intrinsic factors are not well defined, but likely include transcription factors and autocrine acting factors. This study provides the first comprehensive analysis of the conceptus transcriptome in sheep. The present study confirmed previous findings that *IFNT* and *PTGS2* gene expression increased substantially in the conceptus between days 12 and 14 and then declined by day 20 [57, 78, 94]. IFNT is the maternal recognition of pregnancy

signal in ruminants, and its effect on gene expression in the endometrium has been well defined in sheep [87, 103]. Prostaglandins produced by *PTGS2* in the conceptus trophectoderm and endometrial LE play important roles in modulation of uterine epithelia and conceptus trophectoderm during the peri-implantation window [57, 78]. Both IFNT and PTGS2 are essential for conceptus elongation *in utero* [57, 380]. A large number of genes are induced or increased in the conceptus after day 12 that include *CLEC16A, EPN1, FABP5, FADS1, FADS2*, and *KRT8*. CLEC16A regulates mitophagy, a selective form of autophagy necessary for mitochondrial quality control and health [473]. EPN1 encodes a protein that binds clathrin and is involved in the endocytosis of clathrin-coated vesicles. KRT8 plays a role in maintaining cellular structural integrity in epithelial cells and also functions in signal transduction and cellular differentiation [474]. *FABP5* encodes a cytoplasmic fatty acid binding protein that bind long-chain fatty acids and other hydrophobic ligands. FABPs may play roles in fatty acid uptake, transport, and metabolism. *FADS1* and *FADS2* are members of the fatty acid desaturase (FADS) gene family that regulate unsaturation of fatty acids and may be important for production of PGs [475]. Prostaglandins produced by the elongating conceptus regulate a subset of endometrial epithelial elongation and implantation related genes in sheep [78]. Lipid transport and metabolism is likely very important for conceptus elongation due to high levels of PG production and rapid hyperplasia and hypertrophy of the trophectoderm between days 12 to 20.

An increased understanding of transcription factors and RNA binding proteins expressed in the developing conceptus is expected to reveal novel

intrinsic regulators of conceptus growth for trophoblast elongation and differentiation. One of the most abundant factors in the day 14 conceptus was *RAN*, a small GTP binding protein from the RAS superfamily that is essential for the translocation of RNA and proteins through the nuclear pore and also involved in control of DNA synthesis and cell cycle progression [476]. Four members of the DEAD-box RNA helicase family (*DDX1, DDX5, DDX17, DDX54*) were expressed in the conceptus; those proteins are implicated in a number of cellular processes including translation initiation and RNA splicing [477] and involved in embryogenesis and cellular growth in mice [478]. Expression of several transcription factors (*ATF4*, *ATF6, CDX2*) increased in the elongating conceptus. In human pregnancies, *ATF4* regulates the expression of placental growth factor (PGF) which is homologous to vascular endothelial growth factor [479]. In mice, *CDX2* controls cell differentiation in the trophectoderm [480]. Interactions between CDX2, ETS2 and JUN regulate expression of *IFNT* in the ovine trophectoderm [481].

Between days 14 and 16, BNCs begin to differentiate from the mononuclear trophoblast cells within the conceptus [37]. BNCs are important for placentation in sheep, as they migrate and fuse with the LE and each other to form multinucleated syncytia that form the foundation of the placental cotyledons that interdigitate with endometrial caruncles to form placentomes for hematotrophic nutrition of the conceptus. They also express a number of unique genes that encode secreted factors such as CSH1 (placental lactogen), pregnancy associated glycoproteins (PAGs) and progesterone. Those secreted BNC-derived factors act on the

endometrial GE as well as other endometrial cell types and maternal tissues to regulate maternal adaptations to pregnancy. In the present study, expression of *CSH1* increased (70-fold) between day 16 and 20, and CSH1 was shown to act synergistically with progesterone and IFNT to promote GE hypertrophy and secretory function [79]. The function of PAGs is not known, but they are released into the maternal blood circulation after day 20 and can be used as a pregnancy test [33]. *PAG4*, *PAG6* and *PAG11* expression increased substantially from day 16 to 20. *GCM1* expression increased 25-fold between days 16 and 20; it encodes a DNA-binding protein that is necessary for placental development in mice. *GCM1* is expressed in the labyrinth in differentiated syncytiotrophoblast cells and is involved in chorioallantoic branching morphogenesis and syncytiotrophoblast differentiation [482]. The conceptus transcriptome determined in the present study can be used to identify new intrinsic factors regulating placental growth and differentiation during early pregnancy.

Expression of endogenous retroviral elements in the placenta occurs in multiple species [483]. An endogenous retroviral envelope protein, termed syncytin, is expressed in the placentae of humans and mice as well as number of other species. In mice and humans, syncytin is involved in fusion of the cytotrophoblast cells to form the syncytial layer of the placenta [484-488]. In sheep, syncytin is termed *Syn-Rum1*. In the present study, expression of *Syn-Rum1* was identified from two genomic locations in the day 16 and day 20 ovine conceptus, which is consistent with the hypothesis that syncytin plays a role in trophoblast cell fusion to from BNC and multinucleated syncytia in ruminants [488]. Prior to

identification of syncytins in ruminants, it was proposed that endogenous retroviruses have an important role in placental evolution [244, 489, 490]. Endogenous Jaagsiekte sheep retroviruses (*enJSRVs*) are expressed in both the conceptus trophectoderm and uterine epithelia during early pregnancy in sheep [491]. Several of the enJSRVs have a complete intact open reading frame for all genes including envelope (env), gag, pol and protease [492]. The *enJSRVs env* mRNA and Env protein are expressed in mononuclear trophectoderm cells and are particularly abundant in the BNC and syncytial plaques of placentomes [491]. In the present study, expression of enJSRVs *gag, protease, pol* and *env* genes was determined in the conceptus. Abundant expression of *pol* (31 CPM) and *env* (3,038 CPM) was observed in the day 12 and 14 conceptus. The *enJSRVs env* regulate mononuclear trophectoderm cell proliferation and perhaps trophoblast BNC differentiation [493, 494]. Transcriptomic data from the present study can be used to search for novel retroviral elements and retroviral-influenced genes that potentially regulate conceptus elongation, implantation and placentation.

In summary, this study comprehensively determined genes in the uterine epithelia and conceptus and proteins in the ULF during the peri-implantation phase of pregnancy. The data serve as a foundation to discover novel regulatory pathways governing conceptus-endometrial interactions, conceptus elongation, trophectoderm differentiation, and establishment of pregnancy in ruminants. These studies are important, as the majority of pregnancy loss in ruminants occurs during the peri-implantation period and is likely due to endometrial dysfunction or miscommunication between the developing embryo and the uterine environment

[373, 495]. Further, the transcriptome data from this study can be used to facilitate functional studies of genes in the conceptus using the CRISPR/Cas9 system for genome engineering [279]. Such *in vivo* loss of function studies are required to further our understanding of the complex molecular and cellular events involved in conceptus elongation and placental differentiation.

ACKNOWLEDGMENTS

The authors greatly appreciate members of the Spencer laboratory who assisted with animal care and surgeries (Brenda Jesernig, Andrew Kelleher, Wang Peng and Monique McMahon-Hide). As well as the DNA Core staff at Washington State University, especially Mark Wildung, and the University of Missouri.

SUPPLEMENTAL TABLES

Supplemental Table 1. Differentially expressed genes in the uterine luminal epithelium (LE)

Supplemental Table 2. Differentially expressed genes in the uterine glandular epithelium (GE)

Supplemental Table 3. Differentially expressed genes in the conceptus

Supplemental Table 4. Ingenuity pathway analysis of differentially expressed genes in the uterine epithelia and conceptus

Supplemental Table 5. Expression clusters of differentially expressed genes in the uterine epithelia and conceptus

Supplemental Table 6. Proteins in the uterine luminal fluid determined by mass spectrometry

Supplemental Table 7. Tissue and RNA collection information for conceptus RNA seq

Available after publication at http://www.biolreprod.org/

SUMMARY AND CONCLUSIONS

Collectively, these studies support the central hypothesis that factors from the ovary (progesterone), the conceptus (interferon tau, prostaglandins, and cortisol) and endometrium (prostaglandins and cortisol) regulate endometrial function and conceptus survival and development in sheep. Factors produced by the elongating conceptus have autocrine or intracrine effects to regulate gene expression in the conceptus trophectoderm important for development. Further, paracrine effects on endometrial gene expression alter the production, transport and secretion of substances (glucose, amino acids, proteins, hormones, etc.) into the uterine lumen that support conceptus development via effects on trophectoderm proliferation, migration, attachment and adhesion for implantation and pregnancy establishment.

Interferon tau (IFNT) is the maternal recognition of pregnancy signal and acts on the endometrium to inhibit transcription of *ESR1* and *OXTR* thereby preventing luteolytic pulses of PGF2α that would otherwise cause CL regression (see [39, 315, 463, 496] for review). In addition to antiluteolytic effects, IFNT stimulates expression of a number of progesterone-induced genes (*CST3, CST6, CTSL, GRP, HSD11B1, IGFBP1, LGALS15, SLC2A1, SLC2A5, SLC5A11, SLC7A2*) specifically in the endometrial LE/sGE and/or GE (see [72, 103, 288, 497]) for review). Results of the present study support the idea that IFNT from the developing conceptus is essential for elongation, and signals through IFN receptors 1 and 2 (IFNAR1/2) present on the uterine epithelia but not the

trophectoderm itself. Uterine infusion of a morpholino targeting IFNT from day 7 to 14 of pregnancy decreased conceptus growth. However, infusion of morpholinos targeting IFNAR1/2 did not affect conceptus elongation. These results support a role for IFNT in conceptus elongation beyond maternal recognition of pregnancy, but do not implicate autocrine signaling through the IFNAR1/2 complex in the trophectoderm to be essential for conceptus elongation. Although much is known about the actions of IFNT on the uterus, identification of the factors regulating induction of conceptus elongation and IFNT production remains to be determined. Studies profiling transcription factors association with interferon regulatory elements in cultured ovine and bovine trophoblast cell lines have identified numerous potential regulators including ETS2, AP-1, CDX2 and DLX3 [481, 498-501]. Studies in the mouse placenta implicate TEAD4 as the master regulator of trophoblast differentiation during blastocyst formation, and as a regulator of CDX2 and Eomes, which are important for trophoblast differentiation in mice [480, 502, 503]. Investigation into the control of trophoblast changes for elongation in ruminants, and by association the production of IFNT, through TEAD4 would be an interesting topic for future study. Inhibition of TEAD4 through morpholino targeting similar to the studies presented here would determine if TEAD4 it has a similar role in trophoblast differentiation during elongation in ruminants as it does in trophoblast differentiation during early embryo development in other species. Identification of genes upstream of IFNT could provide potential therapeutic targets for increasing trophoblast growth during conceptus elongation to rescue

pregnancies which would normally be lost due to low levels of IFNT from small conceptuses.

The conceptus and endometrium synthesize a variety of prostaglandins (PG) during early pregnancy in both sheep and cattle [135, 285, 504]. The dominant cyclooxygenase expressed in both the endometrium and trophectoderm of the elongating conceptus is PTGS2 [135, 285, 504]. Although IFNT prevents the release of luteolytic PGF2α pulses, it does not inhibit PTGS2 expression or non-pulsatile PG production by the endometrium during early pregnancy [112, 505]. Day 14 sheep conceptuses *in vitro* release mainly cyclooxygenase metabolites including PGF2α, 6-keto-PGF1α, a stable metabolite of PGI2, and PGE2 [76], and Day 16 conceptuses produce substantially more of those prostaglandins than Day 14 conceptuses [75]. Prostaglandins are essential for conceptus elongation, as intrauterine infusions of meloxicam, a selective PTGS2 antagonist, prevents conceptus elongation in early pregnant sheep [57, 192]. Membrane and nuclear receptors for PGs are present in all cell types of the ovine endometrium and conceptus during early pregnancy, therefore PTGS2-derived PGs from the conceptus are thought to have paracrine, autocrine, and perhaps intracrine effects on endometrial function and conceptus development during early pregnancy [57, 506]. Results of the present studies provide strong evidence that prostaglandins regulate trophectoderm gene expression important for conceptus elongation in sheep through activation of nuclear peroxisome proliferator-activating receptor gamma (PPARG).

In the studies presented here, inhibition of nuclear prostaglandin signaling through infusion of a morpholino targeting PPARG resulted in inhibition of conceptus elongation. However, inhibition of PPARD from day 7 to 14 did not affect conceptus elongation. Investigation of PPARG regulated genes in the day 14 conceptus revealed many gene targets involved in cell growth and metabolism as well as fatty acid utilization. PPARs play an important role in the transport, cellular uptake, storage, and use of lipids and their derivatives in many tissues [143]. In adipocytes, PPARG is association with both cellular differentiation and the storage of lipids. Unlike adipocytes, the regulation of lipid release as well as uptake and storage is important for maintaining homeostasis in the placenta [507]. Lipids and fatty acids are hypothesized to act as precursors for both PG synthesis, as well as contribute phospholipids to the growing cell membrane during conceptus elongation. Fatty acids can also provide energy to support tissue proliferation, as the use of fatty acids as an energy source produces twice the caloric value per unit compared to use of carbohydrates and proteins [508]. Metabolic profiling of the ULF in cows has demonstrated the availability of a variety of lipids and fatty acids for utilization by the elongating conceptus during early pregnancy, and has identified changes in the metabolic profile that may be associated with important biological events occurring during elongation [509, 510]. Modification to the lipid content of ruminant diets could provide a potential avenue for increasing important fatty acids in the endometrium, and therefore ULF, of pregnant animals to support conceptus development [511, 512].

Evidence from the studies present here have shown PPARG to be important for conceptus elongation, though the importance of PPAR regulated genes for PG production or phospholipid uptake was not determined. In the presented PPARG ChIP-seq data, PPARG is shown to regulate FADS and FATP in the day 14 conceptus trophectoderm. A morpholino based approach to inhibit conversion of polyunsaturated fatty acids to the PG precursor, arachidonic acid, by FADS would provide information on lipid utilization in the conceptus. Additional gene knockout techniques to inhibit PTGS2 would also provide information on the importance of PG production by the conceptus during early pregnancy. To test the hypothesis that fatty acid uptake for membrane growth is important for conceptus elongation gene knockdown studies utilizing morpholinos targeting FATP could be used. Further investigation into fatty acid utilization by the conceptus would provide information on key pathways in the placenta regulating lipid storage and mobilization. As reduced lipid utilization could impair conceptus elongation, as well as PG synthesis important for modulation of uterine genes important for conceptus development and implantation during early pregnancy in ruminants.

Previous studies have shown that P4 induces and conceptus IFNT stimulates *HSD11B1* expression in the endometrium of sheep [192, 446]. *HSD11B1* is expressed both in endometrial LE/sGE as well as conceptus trophectoderm, while *HSD11B2* is expressed only in the conceptus trophectoderm [58, 192]. HSD11B1 acts as a keto-reductase to generate biologically active cortisol from inactive cortisone, but can also act bi-directionally and inactivate cortisol as well [58, 197]. HSD11B2 acts only to metabolize cortisol into inactive

cortisone. Cortisol regulates gene expression via the nuclear receptor subfamily 3, group C, member 1 (NR3C1 or glucocorticoid receptor (GR)), a transcriptional regulator that modulates expression of primary target genes that either directly affect cellular physiology or alter the expression of other secondary target genes, which then confer hormonal responses [513, 514]. GR is expressed in all endometrial cells of the ovine uterus during pregnancy as well as in the conceptus trophectoderm [58, 192]. The present studies found that HSD11B1, but not HSD11B2, is essential for conceptus elongation, but cortisol does not act through the GR in the conceptus to regulate this elongation. Uterine infusion of morpholino inhibiting HSD11B1 from day 7 to 14 of pregnancy prevented conceptus elongation. However, inhibition of HSD11B2 with morpholino during the same treatment window did not influence conceptus elongation, but did result in severely vacuolated, histologically abnormal conceptuses. Results from gene editing experiments conducted in these studies targeting GR in zygotes using the CRISPR/Cas9 system, found that GR is not essential for conceptus elongation and development up to day 14. Although GR was found not to play a role in regulation of trophoblast elongation, based on expression values from the RNA-seq experiments, *GR* increases in the conceptus between day 16 and 20 when conceptus elongation is complete, and attachment for placentation has begun. Using the same method presented here to create GR knockout conceptus, the role of GR during placentation and early pregnancy could be investigated *in vivo*. In studies investigating the effects of synthetic glucocorticoids such as dexamethasone and betamethasone on the placenta prior to parturition, it was

found that the BNC population decreased in treated ewes [235]. This observation implicates cortisol signaling in maintenance of BNCs, and its actions through GR as additional studies have shown BNCs to contain nuclear GR early in pregnancy [515]. The role of GR in BNC function, and cortisol regeneration in the placenta during early pregnancy could provide information on downstream signaling pathways regulated by GR. This information could assist in identification of alternative targets to promote lung development in underdeveloped neonatal infants, without effecting placental tissues.

In humans, glucocorticoid treatment can have positive as well as negative effects during pregnancy (see [232] for review). Administration of synthetic glucocorticoids during pregnancy can alter normal development of the fetus and compromise pregnancy success by inhibiting cytokine-PG signaling, restricting trophoblast invasion, and inducing apoptosis in placenta [225, 227-232]. While endogenous glucocorticoids are hypothesized to have positive effects during early pregnancy (see [232] for review), including stimulation of chorionic gonadotropin secretion by the trophoblast, promotion of trophoblast growth/invasion, and stimulation of placental transport of glucose, lactate and amino acids [221-226]. Thus, further investigation into the mechanistic aspects of cortisol signaling, and the role of GR activation early pregnancy should remain the focus of future studies.

Ruminant blastocysts and trophoblastic vesicles do not elongate *in vitro*, but do so when transferred to the uterus of recipient animals [19, 20]. The uterine gland knockout (UGKO) sheep model, which lacks glandular epithelium (GE) and has reduced luminal epithelium (LE), exhibits a failure in conceptus elongation resulting

in recurrent pregnancy loss [81]. Thus, the uterine epithelia and its secretions are essential for conceptus survival, growth and establishment of pregnancy. Microarray analysis of the endometrium during the peri-implantation period, as well as candidate gene studies have identified many genes whose expression changes with day and pregnancy status and, based on their biological functions, are implicated as regulators of conceptus elongation and development [79, 289, 378]. However, comprehensive knowledge of the endometrial and conceptus transcriptome and ULF proteome during the establishment of pregnancy has not been reported for sheep, but is important to understand pregnancy establishment [22, 318]. Therefore, the transcriptome of the uterine LE, GE and conceptus as well as the proteome of the uterine luminal fluid (ULF) during the peri-implantation period of pregnancy was analyzed. Significant changes in gene expression were seen in all three tissues, as well as differences in proteins present in the ULF across days. This study provides comprehensive transcriptomic and proteomic data that can serve as a foundation for future studies aimed a discovering new regulatory pathways governing uterine receptivity, conceptus elongation, trophectoderm differentiation, conceptus-endometrial interactions and pregnancy establishment in ruminants. Identification of gene expression changes essential for elongation could be identified through knockout/knockdown strategies similar to those presented here. Potential targets included genes which undergo substantial expression changes in the conceptus trophectoderm concurrent with elongation, such as pregnancy specific antigen and germ cell nuclear factor (GCNF). Pregnancy specific antigen is a conceptus-derived antigen present in the

maternal serum that is secreted by trophoblast and placental tissue during early pregnancy. It belongs to the aspartic proteinase family and has greater than 50% amino acid sequence identity to pepsin, cathepsin D, and cathepsin E [351]. Although highly expressed by the day 14 conceptus, its role in early pregnancy has not be investigated. Germ cell nuclear factor (GCNF, or NR6A1) is also upregulated between day 12 and 14 in the ovine conceptus. In adult mice, GCNF transcripts are predominantly expressed in spermatogenic cells and growing oocytes of the gonads, but are found in unfertilized oocytes and preimplantation embryos [516]. It is therefore thought that GCNF in early embryos is a maternal protein that could be involved in the regulation of zygotic gene expression and preimplantation embryonic development. Its role in embryo development in domestic species remains to be determined. Further investigation of important gene expression changes promoting conceptus elongation will further our understanding of the early stages of embryonic development in ruminants and allow for design of strategies to reduce embryonic mortality.

In summary, results of the presented studies suggest that factors from the developing conceptus play a vital role in regulation of gene expression in both the trophectoderm and endometrium necessary for successful establishment of pregnancy in ruminants. Opportunities for future research include: (a) mining of the transcriptomic and proteomic data to identify novel factors influencing conceptus development; (b) identification of signaling pathways regulating the induction of conceptus elongation; (c) increased understanding of PPARG regulated lipid uptake and utilization for growth and development in the conceptus trophectoderm;

(d) determination of cortisol signaling pathways and the role of GR following conceptus elongation. Utilization of the CRISPR/Cas9 system for genome editing is an indispensable tool for studying pathways of interest in the conceptus trophectoderm as well as the endometrium. Knowledge gained from studies on conceptus-endometrial interactions during early pregnancy in ruminants is necessary to understand the multifactorial phenomenon of recurrent pregnancy loss and provide a basis for new strategies to improve pregnancy outcomes and reproductive efficiency.

REFERENCES

1. Bartol FF, Wiley AA, Spencer TE, Vallet JL, Christenson RK. Early uterine development in pigs. J Reprod Fertil Suppl 1993; 48:99-116.

2. Cunha GR. Alterations in the developmental properties of stroma during the development of the urogenital ridge into ductus deferens and uterus in embryonic and neonatal mice. J Exp Zool 1976; 197:375-388.

3. Gray CA, Bartol FF, Tarleton BJ, Wiley AA, Johnson GA, Bazer FW, Spencer TE. Developmental biology of uterine glands. Biol Reprod 2001; 65:1311-1323.

4. Atkinson BA, King GJ, Amoroso EC. Development of the caruncular and intercaruncular regions in the bovine endometrium. Biol Reprod 1984; 30:763-774.

5. Wimsatt WA. Hew Histological Observations on the Placenta of the Sheep. Am J Anat 1950; 87:391-436.

6. Amoroso EC. The interaction of the trophoblast and endometrium at the time of implantation in the sheep. J Anat 1951; 85:428-429.

7. Bazer FW. Uterine protein secretions: Relationship to development of the conceptus. J Anim Sci 1975; 41:1376-1382.

8. Bazer FW, First NL. Pregnancy and parturition. J Anim Sci 1983; 57 Suppl 2:425-460.

9. Carson DD, Bagchi I, Dey SK, Enders AC, Fazleabas AT, Lessey BA, Yoshinaga K. Embryo implantation. Dev Biol 2000; 223:217-237.

10. Kane MT, Morgan PM, Coonan C. Peptide growth factors and preimplantation development. Hum Reprod Update 1997; 3:137-157.

11. Roberts RM, Bazer FW. The functions of uterine secretions. J Reprod Fertil 1988; 82:875-892.

12. Simmen RC, Simmen FA. Regulation of uterine and conceptus secretory activity in the pig. J Reprod Fertil Suppl 1990; 40:279-292.

13. Yamanaka Y, Ralston A, Stephenson RO, Rossant J. Cell and molecular regulation of the mouse blastocyst. Dev Dyn 2006; 235:2301-2314.

14. Johnson MH, McConnell JM. Lineage allocation and cell polarity during mouse embryogenesis. Semin Cell Dev Biol 2004; 15:583-597.

15. Guillomot M. Cellular interactions during implantation in domestic ruminants. J Reprod Fertil Suppl 1995; 49:39-51.

16. Geisert RD, Brookbank JW, Roberts RM, Bazer FW. Establishment of pregnancy in the pig: II. Cellular remodeling of the porcine blastocyst during elongation on day 12 of pregnancy. Biol Reprod 1982; 27:941-955.

17. Bazer FW, Spencer TE, Johnson GA, Burghardt RC, Wu G. Comparative aspects of implantation. Reproduction 2009; 138:195-209.

18. Wales RG, Cuneo CL. Morphology and chemical analysis of the sheep conceptus from the 13th to the 19th day of pregnancy. Reprod Fertil Dev 1989; 1:31-39.

19. Flechon JE, Guillomot M, Charlier M, Flechon B, Martal J. Experimental studies on the elongation of the ewe blastocyst. Reprod Nutr Dev 1986; 26:1017-1024.

20. Heyman Y, Camous S, Fevre J, Meziou W, Martal J. Maintenance of the corpus luteum after uterine transfer of trophoblastic vesicles to cyclic cows and ewes. J Reprod Fertil 1984; 70:533-540.

21. Gray CA, Burghardt RC, Johnson GA, Bazer FW, Spencer TE. Evidence that absence of endometrial gland secretions in uterine gland knockout ewes compromises conceptus survival and elongation. Reproduction 2002; 124:289-300.

22. Spencer TE, Burghardt RC, Johnson GA, Bazer FW. Conceptus signals for establishment and maintenance of pregnancy. Anim Reprod Sci 2004; 82-83:537-550.

23. Wintenberger-Torres S, Flechon JE. Ultrastructural evolution of the trophoblast cells of the pre-implantation sheep blastocyst from day 8 to day 18. J Anat 1974; 118:143-153.

24. Burghardt RC, Johnson GA, Jaeger LA, Ka H, Garlow JE, Spencer TE, Bazer FW. Integrins and extracellular matrix proteins at the maternal-fetal interface in domestic animals. Cells Tissues Organs 2002; 172:202-217.

25. Singh H, Aplin JD. Adhesion molecules in endometrial epithelium: tissue integrity and embryo implantation. J Anat 2009; 215:3-13.

26. Burghardt RC, Burghardt JR, Taylor JD, 2nd, Reeder AT, Nguen BT, Spencer TE, Bayless KJ, Johnson GA. Enhanced focal adhesion assembly reflects increased mechanosensation and mechanotransduction at maternal-conceptus interface and uterine wall during ovine pregnancy. Reproduction 2009; 137:567-582.

27. Rowson LE, Moor RM. Development of the sheep conceptus during the first fourteen days. J Anat 1966; 100:777-785.

28. Guillomot M, Flechon JE, Wintenberger-Torres S. Conceptus attachment in the ewe: an ultrastructural study. Placenta 1981; 2:169-182.

29. Guillomot M, Flechon JE, Leroy F. Blastocyst development and implantation. In: Thibault C, Levasseur MC, Hunter RHF (eds.), Reproduction in Mammals and Man. Paris: Ellipses; 1993: 387-411.

30. Guillomot M, Guay P. Ultrastructural features of the cell surfaces of uterine and trophoblastic epithelia during embryo attachment in the cow. Anat Rec 1982; 204:315-322.

31. Wooding FB, Staples LD, Peacock MA. Structure of trophoblast papillae on the sheep conceptus at implantation. J Anat 1982; 134 (Pt 3):507-516.

32. Boshier DP. A histological and histochemical examination of implantation and early placentome formation in sheep. J Reprod Fertil 1969; 19:51-61.

33. Wooding FB. Current topic: the synepitheliochorial placenta of ruminants: binucleate cell fusions and hormone production. Placenta 1992; 13:101-113.

34. Hoffman LH, Wooding FB. Giant and binucleate trophoblast cells of mammals. J Exp Zool 1993; 266:559-577.

35. Spencer TE, Johnson GA, Bazer FW, Burghardt RC. Implantation mechanisms: insights from the sheep. Reproduction 2004; 128:657-668.

36. Wimsatt WA. Observations of the morphogenesis, cytochemistry and significance of the binucleate giant cells of the placenta of ruminants. J Anat 1951; 89:233-282.

37. Wooding FB. Role of binucleate cells in fetomaternal cell fusion at implantation in the sheep. Am J Anat 1984; 170:233-250.

38. Wooding FB. The role of the binucleate cell in ruminant placental structure. J Reprod Fertil Suppl 1982; 31:31-39.

39. Spencer TE, Johnson GA, Bazer FW, Burghardt RC, Palmarini M. Pregnancy recognition and conceptus implantation in domestic ruminants: roles of progesterone, interferons and endogenous retroviruses. Reprod Fertil Dev 2007; 19:65-78.

40. Spencer TE, Johnson GA, Burghardt RC, Bazer FW. Progesterone and placental hormone actions on the uterus: insights from domestic animals. Biol Reprod 2004; 71:2-10.

41. Bazer FW, Roberts RM, Thatcher WW. Actions of hormones on the uterus and effect on conceptus development. J Anim Sci 1979; 49:35-45.

42. Kelly PA, Robertson HA, Friesen HG. Temporal pattern of placental lactogen and progesterone secretion in sheep. Nature 1974; 248:435-437.

43. Goding JR. The demonstration that PGF2alpha is the uterine luteolysin in the ewe. J Reprod Fertil 1974; 38:261-271.

44. McCracken J. Prostaglandin F-2 alpha and corpus luteum regression. Ann N Y Acad Sci 1971; 180:456-472.

45. Guiochon-Mantel A, Bailly A, Loosfelt H, Perrot-Applanat M, Lescop P, Vu Hai M, Misrahi M, Atger M, Milgrom E. Progesterone receptor: structure, function, and immunolocalization. In: Dumont JE, Nunez J, King RJ (eds.), Hormones and Cell Regulation, vol. 210: John Libbey Eurotext, Ltd.; 1990: 49-57.

46. Abayasekara DR, Sheldrick EL, Flick-Smith HC, Flint AP. Role of protein kinase C in the inhibitory action of trophoblast interferons on expression of the oxytocin receptor in sheep endometrium. Endocrine 1995; 3:151-158.

47. Spencer TE, Bazer FW. Temporal and spatial alterations in uterine estrogen receptor and progesterone receptor gene expression during the estrous cycle and early pregnancy in the ewe. Biol Reprod 1995; 53:1527-1543.

48. Wilmut I, Sales DI. Effect of an asynchronous environment on embryonic development in sheep. J Reprod Fertil 1981; 61:179-184.

49. Lawson RA, Parr RA, Cahill LP. Evidence for maternal control of blastocyst growth after asynchronous transfer of embryos to the uterus of the ewe. J Reprod Fertil 1983; 67:477-483.

50. Lawson RA, Cahill LP. Modification of the embryo-maternal relationship in ewes by progesterone treatment early in the oestrous cycle. J Reprod Fertil 1983; 67:473-475.

51. Mann GE. Pregnancy rates during experimentation in dairy cows. Vet J 2001; 161:301-305.

52. Garrett JE, Geisert RD, Zavy MT, Morgan GL. Evidence for maternal regulation of early conceptus growth and development in beef cattle. J Reprod Fertil 1988; 84:437-446.

53. Nephew KP, McClure KE, Ott TL, Dubois DH, Bazer FW, Pope WF. Relationship between variation in conceptus development and differences in estrous cycle duration in ewes. Biol Reprod 1991; 44:536-539.

54. Gray CA, Abbey CA, Beremand PD, Choi Y, Farmer JL, Adelson DL, Thomas TL, Bazer FW, Spencer TE. Identification of endometrial genes regulated by early pregnancy, progesterone, and interferon tau in the ovine uterus. Biol Reprod 2006; 74:383-394.

55. Farmer JL, Burghardt RC, Jousan FD, Hansen PJ, Bazer FW, Spencer TE. Galectin 15 (LGALS15) functions in trophectoderm migration and attachment. FASEB J 2008; 22:548-560.

56. Satterfield MC, Hayashi K, Song G, Black SG, Bazer FW, Spencer TE. Progesterone regulates FGF10, MET, IGFBP1, and IGFBP3 in the endometrium of the ovine uterus. Biol Reprod 2008; 79:1226-1236.

57. Dorniak P, Bazer FW, Spencer TE. Prostaglandins regulate conceptus elongation and mediate effects of interferon tau on the ovine uterine endometrium. Biol Reprod 2011; 84:1119-1127.

58. Dorniak P, Welsh TH, Jr., Bazer FW, Spencer TE. Endometrial HSD11B1 and cortisol regeneration in the ovine uterus: effects of pregnancy, interferon tau, and prostaglandins. Biol Reprod 2012; 86:124.

59. Dorniak P, Welsh TH, Jr., Bazer FW, Spencer TE. Cortisol and interferon tau regulation of endometrial function and conceptus development in female sheep. Endocrinology 2013; 154:931-941.

60. Song G, Spencer TE, Bazer FW. Cathepsins in the ovine uterus: regulation by pregnancy, progesterone, and interferon tau. Endocrinology 2005; 146:4825-4833.

61. Song G, Spencer TE, Bazer FW. Progesterone and interferon-tau regulate cystatin C in the endometrium. Endocrinology 2006; 147:3478-3483.

62. Whitley JC, Shulkes A, Salamonsen LA, Vogiagis D, Familari M, Giraud AS. Temporal expression and cellular localization of a gastrin-releasing peptide-related gene in ovine uterus during the oestrous cycle and pregnancy. J Endocrinol 1998; 157:139-148.

63. Song G, Satterfield MC, Kim J, Bazer FW, Spencer TE. Gastrin-releasing peptide (GRP) in the ovine uterus: regulation by interferon tau and progesterone. Biol Reprod 2008; 79:376-386.

64. Satterfield MC, Gao H, Li X, Wu G, Johnson GA, Spencer TE, Bazer FW. Select nutrients and their associated transporters are increased in the ovine uterus following early progesterone administration. Biol Reprod 2010; 82:224-231.

65. Gao H, Wu G, Spencer TE, Johnson GA, Li X, Bazer FW. Select nutrients in the ovine uterine lumen. I. Amino acids, glucose, and ions in uterine lumenal flushings of cyclic and pregnant ewes. Biol Reprod 2009; 80:86-93.

66. Gao H, Wu G, Spencer TE, Johnson GA, Bazer FW. Select Nutrients in the Ovine Uterine Lumen. III. Cationic Amino Acid Transporters in the Ovine Uterus and Periimplantation Conceptuses. Biol Reprod 2008.

67. Johnson GA, Spencer TE, Burghardt RC, Bazer FW. Ovine osteopontin: I. Cloning and expression of messenger ribonucleic acid in the uterus during the periimplantation period. Biol Reprod 1999; 61:884-891.

68. Song G, Bazer FW, Wagner GF, Spencer TE. Stanniocalcin (STC) in the endometrial glands of the ovine uterus: regulation by progesterone and placental hormones. Biol Reprod 2006; 74:913-922.

69. Leslie MV, Hansen PJ. Progesterone-regulated secretion of the serpin-like proteins of the ovine and bovine uterus. Steroids 1991; 56:589-597.

70. Stewart MD, Johnson GA, Gray CA, Burghardt RC, Schuler LA, Joyce MM, Bazer FW, Spencer TE. Prolactin receptor and uterine milk protein expression in the ovine endometrium during the estrous cycle and pregnancy. Biol Reprod 2000; 62:1779-1789.

71. Wathes DC, Lamming GE. The oxytocin receptor, luteolysis and the maintenance of pregnancy. J Reprod Fertil Suppl 1995; 49:53-67.

72. Spencer TE, Johnson GA, Bazer FW, Burghardt RC. Fetal-maternal interactions during the establishment of pregnancy in ruminants. Soc Reprod Fertil Suppl 2007; 64:379-396.

73. Hansen TR, Henkes LK, Ashley RL, Bott RC, Antoniazzi AQ, Han H. Endocrine actions of interferon-tau in ruminants. Soc Reprod Fertil Suppl 2010; 67:325-340.

74. Dorniak P, Bazer FW, Spencer TE. Physiology and Endocrinology Symposium: biological role of interferon tau in endometrial function and conceptus elongation. J Anim Sci 2013; 91:1627-1638.

75. Lewis GS, Waterman RA. Metabolism of arachidonic acid in vitro by ovine conceptuses recovered during early pregnancy. Prostaglandins 1985; 30:263-283.

76. Charpigny G, Reinaud P, Tamby JP, Creminon C, Guillomot M. Cyclooxygenase-2 unlike cyclooxygenase-1 is highly expressed in ovine embryos during the implantation period. Biol Reprod 1997; 57:1032-1040.

77. Hwang DH, Pool SH, Rorie RW, Boudreau M, Godke RA. Transitional changes in arachidonic acid metabolism by bovine embryos at different developmental stages. Prostaglandins 1988; 35:387-402.

78. Dorniak P, Bazer FW, Wu G, Spencer TE. Conceptus-derived prostaglandins regulate endometrial function in sheep. Biol Reprod 2012; 87:9, 1-7.

79. Spencer TE, Bazer FW. Uterine and placental factors regulating conceptus growth in domestic animals. In: Journal of Animal Science, vol. 82; 2004: E4-13.

80. Spencer TE, Gray CA. Sheep uterine gland knockout (UGKO) model. Methods Mol Med 2006; 121:85-94.

81. Gray CA, Taylor KM, Ramsey WS, Hill JR, Bazer FW, Bartol FF, Spencer TE. Endometrial glands are required for preimplantation conceptus elongation and survival. Biol Reprod 2001; 64:1608-1613.

82. Pontzer CH, Torres BA, Vallet JL, Bazer FW, Johnson HM. Antiviral activity of the pregnancy recognition hormone ovine trophoblast protein-1. Biochem Biophys Res Commun 1988; 152:801-807.

83. Fillion C, Chaouat G, Reinaud P, Charpigny JC, Martal J. Immunoregulatory effects of ovine trophoblastin protein (oTP): all five isoforms suppress PHA-induced lymphocyte proliferation. J Reprod Immunol 1991; 19:237-249.

84. Roberts RM. A novel group of interferons associated with the early ovine and bovine embryo. J Interferon Res 1989; 9:373-378.

85. Pontzer CH, Russell SW. Interferons exhibit temporally distinct regulation of two bovine macrophage Fc receptors. J Leukoc Biol 1990; 47:258-264.

86. Roberts RM. Conceptus interferons and maternal recognition of pregnancy. Biol Reprod 1989; 40:449-452.

87. Bazer FW, Spencer TE, Ott TL. Interferon tau: a novel pregnancy recognition signal. Am J Reprod Immunol 1997; 37:412-420.

88. Bazer FW, Burghardt RC, Johnson GA, Spencer TE, Wu G. Interferons and progesterone for establishment and maintenance of pregnancy: interactions among novel cell signaling pathways. Reprod Biol 2008; 8:179-211.

89. Imakawa K, Anthony RV, Kazemi M, Marotti KR, Polites HG, Roberts RM. Interferon-like sequence of ovine trophoblast protein secreted by embryonic trophectoderm. Nature 1987; 330:377-379.

90. Roberts RM, Cross JC, Leaman DW. Interferons as hormones of pregnancy. Endocr Rev 1992; 13:432-452.

91. Roberts RM, Leaman DW, Cross JC. Role of interferons in maternal recognition of pregnancy in ruminants. Proc Soc Exp Biol Med 1992; 200:7-18.

92. Stewart HJ, McCann SH, Barker PJ, Lee KE, Lamming GE, Flint AP. Interferon sequence homology and receptor binding activity of ovine trophoblast antiluteolytic protein. J Endocrinol 1987; 115:R13-15.

93. Roberts RM, Liu L, Alexenko A. New and atypical families of type I interferons in mammals: comparative functions, structures, and evolutionary relationships. Prog Nucleic Acid Res Mol Biol 1997; 56:287-325.

94. Farin CE, Imakawa K, Hansen TR, McDonnell JJ, Murphy CN, Farin PW, Roberts RM. Expression of trophoblastic interferon genes in sheep and cattle. Biol Reprod 1990; 43:210-218.

95. Ashworth CJ, Bazer FW. Changes in ovine conceptus and endometrial function following asynchronous embryo transfer or administration of progesterone. Biol Reprod 1989; 40:425-433.

96. McCracken JA, Custer EE, Lamsa JC. Luteolysis: a neuroendocrine-mediated event. Physiol Rev 1999; 79:263-323.

97. Lamming GE, Wathes DC, Flint AP, Payne JH, Stevenson KR, Vallet JL. Local action of trophoblast interferons in suppression of the development of oxytocin and oestradiol receptors in ovine endometrium. J Reprod Fertil 1995; 105:165-175.

98. Stark GR, Kerr IM, Williams BR, Silverman RH, Schreiber RD. How cells respond to interferons. Annu Rev Biochem 1998; 67:227-264.

99. Rosenfeld CS, Han CS, Alexenko AP, Spencer TE, Roberts RM. Expression of interferon receptor subunits, IFNAR1 and IFNAR2, in the ovine uterus. Biol Reprod 2002; 67:847-853.

100. Choi Y, Johnson GA, Burghardt RC, Berghman LR, Joyce MM, Taylor KM, Stewart MD, Bazer FW, Spencer TE. Interferon regulatory factor-two restricts expression of interferon-stimulated genes to the endometrial stroma and glandular epithelium of the ovine uterus. Biol Reprod 2001; 65:1038-1049.

101. Stewart MD, Choi Y, Johnson GA, Yu-Lee LY, Bazer FW, Spencer TE. Roles of Stat1, Stat2, and interferon regulatory factor-9 (IRF-9) in interferon tau regulation of IRF-1. Biol Reprod 2002; 66:393-400.

102. Stewart MD, Johnson GA, Bazer FW, Spencer TE. Interferon-tau (IFNtau) regulation of IFN-stimulated gene expression in cell lines lacking specific IFN-signaling components. Endocrinology 2001; 142:1786-1794.

103. Spencer TE, Sandra O, Wolf E. Genes involved in conceptus-endometrial interactions in ruminants: insights from reductionism and thoughts on holistic approaches. Reproduction 2008; 135:165-179.

104. Guillomot M, Betteridge KJ, Harvey D, Goff AK. Endocytotic activity in the endometrium during conceptus attachment in the cow. J Reprod Fertil 1986; 78:27-36.

105. Satterfield MC, Bazer FW, Spencer TE. Progesterone regulation of preimplantation conceptus growth and galectin 15 (LGALS15) in the ovine uterus. Biol Reprod 2006; 75:289-296.

106. Satterfield MC, Song G, Hayashi K, Bazer FW, Spencer TE. Progesterone regulation of the endometrial WNT system in the ovine uterus. Reprod Fertil Dev 2008; 20:935-946.

107. Bazer FW, Wu G, Spencer TE, Johnson GA, Burghardt RC, Bayless K. Novel Pathways for Implantation and Establishment and Maintenance of Pregnancy in Mammals. Mol Hum Reprod 2009.

108. Bazer FW, Spencer TE, Johnson GA. Interferons and uterine receptivity. Seminars in reproductive medicine 2009; 27:90-102.

109. Platanias LC. Mechanisms of type-I- and type-II-interferon-mediated signalling. Nature Reviews Immunology 2005; 5:375-386.

110. Banu SK, Lee J, Stephen SD, Nithy TK, Arosh JA. Interferon tau regulates PGF2alpha release from the ovine endometrial epithelial cells via activation of novel JAK/EGFR/ERK/EGR-1 pathways. Molecular Endocrinology 2010; 24:2315-2330.

111. Lee J, Banu SK, Nithy TK, Stanley JA, Arosh JA. Early pregnancy induced expression of prostaglandin E2 receptors EP2 and EP4 in the ovine endometrium and regulated by interferon tau through multiple cell signaling pathways. Mol Cell Endocrinol 2012; 348:211-223.

112. Charpigny G, Reinaud P, Tamby JP, Creminon C, Martal J, Maclouf J, Guillomot M. Expression of cyclooxygenase-1 and -2 in ovine endometrium during the estrous cycle and early pregnancy. Endocrinology 1997; 138:2163-2171.

113. Smith WL, Garavito RM, DeWitt DL. Prostaglandin endoperoxide H synthases (cyclooxygenases)-1 and -2. J Biol Chem 1996; 271:33157-33160.

114. Smith WL, Dewitt DL. Prostaglandin endoperoxide H synthases-1 and -2. Adv Immunol 1996; 62:167-215.

115. Marnett LJ, Rowlinson SW, Goodwin DC, Kalgutkar AS, Lanzo CA. Arachidonic acid oxygenation by COX-1 and COX-2. Mechanisms of catalysis and inhibition. J Biol Chem 1999; 274:22903-22906.

116. Hla T, Bishop-Bailey D, Liu CH, Schaefers HJ, Trifan OC. Cyclooxygenase-1 and -2 isoenzymes. Int J Biochem Cell Biol 1999; 31:551-557.

117. Shinohara H, Balboa MA, Johnson CA, Balsinde J, Dennis EA. Regulation of delayed prostaglandin production in activated P388D1 macrophages by group IV cytosolic and group V secretory phospholipase A2s. J Biol Chem 1999; 274:12263-12268.

118. Smith WL, DeWitt DL, Garavito RM. Cyclooxygenases: structural, cellular, and molecular biology. Annu Rev Biochem 2000; 69:145-182.

119. Hara S, Miyata A, Yokoyama C, Inoue H, Brugger R, Lottspeich F, Ullrich V, Tanabe T. Isolation and molecular cloning of prostacyclin synthase from bovine endothelial cells. J Biol Chem 1994; 269:19897-19903.

120. Kuwamoto S, Inoue H, Tone Y, Izumi Y, Tanabe T. Inverse gene expression of prostacyclin and thromboxane synthases in resident and activated peritoneal macrophages. FEBS Lett 1997; 409:242-246.

121. Suzuki T, Watanabe K, Kanaoka Y, Sato T, Hayaishi O. Induction of hematopoietic prostaglandin D synthase in human megakaryocytic cells by phorbol ester. Biochem Biophys Res Commun 1997; 241:288-293.

122. Tanabe T, Tohnai N. Cyclooxygenase isozymes and their gene structures and expression. Prostaglandins Other Lipid Mediat 2002; 68-69:95-114.

123. Tanabe T, Miyata A, Nanayama T, Tone Y, Ihara H, Toh H, Takahashi E, Ullrich V. Human genes for prostaglandin endoperoxide synthase-2, thromboxane synthase and prostacyclin synthase. Adv Prostaglandin Thromboxane Leukot Res 1995; 23:133-135.

124. Tazawa R, Xu XM, Wu KK, Wang LH. Characterization of the genomic structure, chromosomal location and promoter of human prostaglandin H synthase-2 gene. Biochem Biophys Res Commun 1994; 203:190-199.

125. Appleby SB, Ristimaki A, Neilson K, Narko K, Hla T. Structure of the human cyclo-oxygenase-2 gene. Biochem J 1994; 302 (Pt 3):723-727.

126. Otto JC, DeWitt DL, Smith WL. N-glycosylation of prostaglandin endoperoxide synthases-1 and -2 and their orientations in the endoplasmic reticulum. J Biol Chem 1993; 268:18234-18242.

127. Otto JC, Smith WL. Photolabeling of prostaglandin endoperoxide H synthase-1 with 3-trifluoro-3-(m-[125I]iodophenyl)diazirine as a probe of membrane association and the cyclooxygenase active site. J Biol Chem 1996; 271:9906-9910.

128. Spencer AG, Thuresson E, Otto JC, Song I, Smith T, DeWitt DL, Garavito RM, Smith WL. The membrane binding domains of prostaglandin endoperoxide H synthases 1 and 2. Peptide mapping and mutational analysis. J Biol Chem 1999; 274:32936-32942.

129. Luong C, Miller A, Barnett J, Chow J, Ramesha C, Browner MF. Flexibility of the NSAID binding site in the structure of human cyclooxygenase-2. Nat Struct Biol 1996; 3:927-933.

130. Swinney DC, Mak AY, Barnett J, Ramesha CS. Differential allosteric regulation of prostaglandin H synthase 1 and 2 by arachidonic acid. J Biol Chem 1997; 272:12393-12398.

131. Shitashige M, Morita I, Murota S. Different substrate utilization between prostaglandin endoperoxide H synthase-1 and -2 in NIH3T3 fibroblasts. Biochim Biophys Acta 1998; 1389:57-66.

132. Lewis GS. Prostaglandin secretion by the blastocyst. J Reprod Fertil Suppl 1989; 37:261-267.

133. Lewis GS, Thatcher WW, Bazer FW, Curl JS. Metabolism of arachidonic acid in vitro by bovine blastocysts and endometrium. Biol Reprod 1982; 27:431-439.

134. Lewis GS, Waterman RA. Effects of endometrium on metabolism of arachidonic acid by bovine blastocysts in vitro. Prostaglandins 1983; 25:881-889.

135. Ulbrich SE, Schulke K, Groebner AE, Reichenbach HD, Angioni C, Geisslinger G, Meyer HH. Quantitative characterization of prostaglandins in the uterus of early pregnant cattle. Reproduction 2009; 138:371-382.

136. Pettipher R, Hansel TT. Antagonists of the prostaglandin D2 receptor CRTH2. Drug News Perspect 2008; 21:317-322.

137. Cammas L, Reinaud P, Bordas N, Dubois O, Germain G, Charpigny G. Developmental regulation of prostacyclin synthase and prostacyclin receptors in the ovine uterus and conceptus during the peri-implantation period. Reproduction 2006; 131:917-927.

138. Goetzl EJ, An S, Smith WL. Specificity of expression and effects of eicosanoid mediators in normal physiology and human diseases. FASEB J 1995; 9:1051-1058.

139. Forman BM, Tontonoz P, Chen J, Brun RP, Spiegelman BM, Evans RM. 15-Deoxy-delta 12, 14-prostaglandin J2 is a ligand for the adipocyte determination factor PPAR gamma. Cell 1995; 83:803-812.

140. Kliewer SA, Lenhard JM, Willson TM, Patel I, Morris DC, Lehmann JM. A prostaglandin J2 metabolite binds peroxisome proliferator-activated receptor gamma and promotes adipocyte differentiation. Cell 1995; 83:813-819.

141. Lim H, Dey SK. PPAR delta functions as a prostacyclin receptor in blastocyst implantation. Trends Endocrinol Metab 2000; 11:137-142.

142. Lim H, Gupta RA, Ma WG, Paria BC, Moller DE, Morrow JD, DuBois RN, Trzaskos JM, Dey SK. Cyclo-oxygenase-2-derived prostacyclin mediates embryo implantation in the mouse via PPARdelta. Genes Dev 1999; 13:1561-1574.

143. Desvergne B, Wahli W. Peroxisome Proliferator-Activated Receptors: Nuclear Control of Metabolism. Endocr Rev 1999; 20:649-688.

144. Tan NS, Michalik L, Desvergne B, Wahli W. Multiple expression control mechanisms of peroxisome proliferator-activated receptors and their target genes. J Steroid Biochem Mol Biol 2005; 93:99-105.

145. Laudet V, Hanni C, Coll J, Catzeflis F, Stehelin D. Evolution of the nuclear receptor gene superfamily. EMBO J 1992; 11:1003-1013.

146. Nolte RT, Wisely GB, Westin S, Cobb JE, Lambert MH, Kurokawa R, Rosenfeld MG, Willson TM, Glass CK, Milburn MV. Ligand binding and co-activator assembly of the peroxisome proliferator-activated receptor-gamma. Nature 1998; 395:137-143.

147. Xu HE, Lambert MH, Montana VG, Parks DJ, Blanchard SG, Brown PJ, Sternbach DD, Lehmann JM, Wisely GB, Willson TM, Kliewer SA, Milburn MV. Molecular recognition of fatty acids by peroxisome proliferator-activated receptors. Mol Cell 1999; 3:397-403.

148. Nolte RT, Wisely GB, Westin S, Cobb JE, Lambert MH, Kurokawa R, Rosenfeld MG, Willson TM, Glass CK, Milburn MV. Ligand binding and co-activator assembly of the peroxisome proliferator- activated receptor-gamma. Nature 1998; 395:137-143.

149. Werman A, Hollenberg A, Solanes G, Bjorbaek C, Vidal-Puig AJ, Flier JS. Ligand-independent activation domain in the N terminus of peroxisome proliferator-activated receptor gamma (PPARgamma). Differential activity of PPARgamma1 and -2 isoforms and influence of insulin. J Biol Chem 1997; 272:20230-20235.

150. Miyata KS, McCaw SE, Marcus SL, Rachubinski RA, Capone JP. The peroxisome proliferator-activated receptor interacts with the retinoid X receptor in vivo. Gene 1994; 148:327-330.

151. Mangelsdorf DJ, Borgmeyer U, Heyman RA, Zhou JY, Ong ES, Oro AE, Kakizuka A, Evans RM. Characterization of three RXR genes that mediate the action of 9-cis retinoic acid. Genes Dev 1992; 6:329-344.

152. Wahli W, Braissant O, Desvergne B. Peroxisome proliferator activated receptors: transcriptional regulators of adipogenesis, lipid metabolism and more. Chem Biol 1995; 2:261-266.

153. Xu L, Glass CK, Rosenfeld MG. Coactivator and corepressor complexes in nuclear receptor function. Curr Opin Genet Dev 1999; 9:140-147.

154. Heery DM, Kalkhoven E, Hoare S, Parker MG. A signature motif in transcriptional co-activators mediates binding to nuclear receptors. Nature 1997; 387:733-736.

155. Torchia J, Rose DW, Inostroza J, Kamei Y, Westin S, Glass CK, Rosenfeld MG. The transcriptional co-activator p/CIP binds CBP and mediates nuclear-receptor function. Nature 1997; 387:677-684.

156. Zhu Y, Qi C, Calandra C, Rao MS, Reddy JK. Cloning and identification of mouse steroid receptor coactivator-1 (mSRC-1), as a coactivator of peroxisome proliferator-activated receptor gamma. Gene Expr 1996; 6:185-195.

157. Zhu Y, Qi C, Jain S, Rao MS, Reddy JK. Isolation and characterization of PBP, a protein that interacts with peroxisome proliferator-activated receptor. J Biol Chem 1997; 272:25500-25506.

158. Puigserver P, Wu Z, Park CW, Graves R, Wright M, Spiegelman BM. A cold-inducible coactivator of nuclear receptors linked to adaptive thermogenesis. Cell 1998; 92:829-839.

159. Miyata KS, McCaw SE, Meertens LM, Patel HV, Rachubinski RA, Capone JP. Receptor-interacting protein 140 interacts with and inhibits transactivation by, peroxisome proliferator-activated receptor alpha and liver-X-receptor alpha. Mol Cell Endocrinol 1998; 146:69-76.

160. Heinlein CA, Ting HJ, Yeh S, Chang C. Identification of ARA70 as a ligand-enhanced coactivator for the peroxisome proliferator-activated receptor gamma. J Biol Chem 1999; 274:16147-16152.

161. Oberfield JL, Collins JL, Holmes CP, Goreham DM, Cooper JP, Cobb JE, Lenhard JM, Hull-Ryde EA, Mohr CP, Blanchard SG, Parks DJ, Moore LB, et al. A peroxisome proliferator-activated receptor gamma ligand inhibits adipocyte differentiation. Proc Natl Acad Sci U S A 1999; 96:6102-6106.

162. Berger J, Moller DE. The mechanisms of action of PPARs. Annu Rev Med 2002; 53:409-435.

163. Davies SS, Pontsler AV, Marathe GK, Harrison KA, Murphy RC, Hinshaw JC, Prestwich GD, Hilaire AS, Prescott SM, Zimmerman GA, McIntyre TM. Oxidized alkyl phospholipids are specific, high affinity peroxisome proliferator-activated receptor gamma ligands and agonists. J Biol Chem 2001; 276:16015-16023.

164. Lehmann JM, Moore LB, Smith-Oliver TA, Wilkison WO, Willson TM, Kliewer SA. An antidiabetic thiazolidinedione is a high affinity ligand for peroxisome proliferator-activated receptor gamma (PPAR gamma). J Biol Chem 1995; 270:12953-12956.

165. McKenna NJ, Lanz RB, O'Malley BW. Nuclear receptor coregulators: cellular and molecular biology. Endocr Rev 1999; 20:321-344.

166. Barak Y, Nelson MC, Ong ES, Jones YZ, Ruiz-Lozano P, Chien KR, Koder A, Evans RM. PPAR gamma is required for placental, cardiac, and adipose tissue development. Mol Cell 1999; 4:585-595.

167. He W, Barak Y, Hevener A, Olson P, Liao D, Le J, Nelson M, Ong E, Olefsky JM, Evans RM. Adipose-specific peroxisome proliferator-activated receptor gamma knockout causes insulin resistance in fat and liver but not in muscle. Proc Natl Acad Sci U S A 2003; 100:15712-15717.

168. Lehrke M, Lazar MA. The many faces of PPARgamma. Cell 2005; 123:993-999.

169. Desmarais JA, Lopes FL, Zhang H, Das SK, Murphy BD. The Peroxisome Proliferator-Activated Receptor Gamma Regulates Trophoblast Cell Differentiation in Mink (Mustela vison). Biol Reprod 2007; 77:829-839.

170. Campbell FM, Bush PG, Veerkamp JH, Dutta-Roy AK. Detection and cellular localization of plasma membrane-associated and cytoplasmic fatty acid-binding proteins in human placenta. Placenta 1998; 19:409-415.

171. Fitscher BA, Riedel HD, Young KC, Stremmel W. Tissue distribution and cDNA cloning of a human fatty acid transport protein (hsFATP4). Biochim Biophys Acta 1998; 1443:381-385.

172. Schaiff WT, Bildirici I, Cheong M, Chern PL, Nelson DM, Sadovsky Y. Peroxisome proliferator-activated receptor-gamma and retinoid X receptor signaling regulate fatty acid uptake by primary human placental trophoblasts. J Clin Endocrinol Metab 2005; 90:4267-4275.

173. Stahl A. A current review of fatty acid transport proteins (SLC27). Pflugers Arch 2004; 447:722-727.

174. Gimeno RE, Hirsch DJ, Punreddy S, Sun Y, Ortegon AM, Wu H, Daniels T, Stricker-Krongrad A, Lodish HF, Stahl A. Targeted deletion of fatty acid transport protein-4 results in early embryonic lethality. J Biol Chem 2003; 278:49512-49516.

175. Forman BM, Chen J, Evans RM. Hypolipidemic drugs, polyunsaturated fatty acids, and eicosanoids are ligands for peroxisome proliferator-activated receptors alpha and delta. Proc Natl Acad Sci U S A 1997; 94:4312-4317.

176. Yu K, Bayona W, Kallen CB, Harding HP, Ravera CP, McMahon G, Brown M, Lazar MA. Differential activation of peroxisome proliferator-activated receptors by eicosanoids. J Biol Chem 1995; 270:23975-23983.

177. Amri EZ, Bonino F, Ailhaud G, Abumrad NA, Grimaldi PA. Cloning of a protein that mediates transcriptional effects of fatty acids in preadipocytes. Homology to peroxisome proliferator-activated receptors. J Biol Chem 1995; 270:2367-2371.

178. Oliver WR, Jr., Shenk JL, Snaith MR, Russell CS, Plunket KD, Bodkin NL, Lewis MC, Winegar DA, Sznaidman ML, Lambert MH, Xu HE, Sternbach DD, et al. A selective peroxisome proliferator-activated receptor delta agonist promotes reverse cholesterol transport. Proc Natl Acad Sci U S A 2001; 98:5306-5311.

179. Bastie C, Holst D, Gaillard D, Jehl-Pietri C, Grimaldi PA. Expression of peroxisome proliferator-activated receptor PPARdelta promotes induction of PPARgamma and adipocyte differentiation in 3T3C2 fibroblasts. J Biol Chem 1999; 274:21920-21925.

180. Brun RP, Tontonoz P, Forman BM, Ellis R, Chen J, Evans RM, Spiegelman BM. Differential activation of adipogenesis by multiple PPAR isoforms. Genes Dev 1996; 10:974-984.

181. Barak Y, Sadovsky Y, Shalom-Barak T. PPAR Signaling in Placental Development and Function. PPAR Res 2008; 2008:142082.

182. Barak Y, Liao D, He W, Ong ES, Nelson MC, Olefsky JM, Boland R, Evans RM. Effects of peroxisome proliferator-activated receptor delta on placentation, adiposity, and colorectal cancer. Proc Natl Acad Sci U S A 2002; 99:303-308.

183. Nadra K, Anghel SI, Joye E, Tan NS, Basu-Modak S, Trono D, Wahli W, Desvergne B. Differentiation of trophoblast giant cells and their metabolic functions are dependent on peroxisome proliferator-activated receptor beta/delta. Mol Cell Biol 2006; 26:3266-3281.

184. Lim H, Paria BC, Das SK, Dinchuk JE, Langenbach R, Trzaskos JM, Dey SK. Multiple female reproductive failures in cyclooxygenase 2-deficient mice. Cell 1997; 91:197-208.

185. Tan NS, Icre G, Montagner A, Bordier-ten-Heggeler B, Wahli W, Michalik L. The nuclear hormone receptor peroxisome proliferator-activated receptor beta/delta potentiates cell chemotactism, polarization, and migration. Mol Cell Biol 2007; 27:7161-7175.

186. Whirledge S, Cidlowski JA. A role for glucocorticoids in stress-impaired reproduction: beyond the hypothalamus and pituitary. Endocrinology 2013; 154:4450-4468.

187. Busillo JM, Cidlowski JA. The five Rs of glucocorticoid action during inflammation: ready, reinforce, repress, resolve, and restore. Trends Endocrinol Metab 2013; 24:109-119.

188. Sala GB, Hayashi K, Catt KJ, Dufau ML. Adrenocorticotropin action in isolated adrenal cells. The intermediate role of cyclic AMP in stimulation of corticosterone synthesis. J Biol Chem 1979; 254:3861-3865.

189. Simpson ER, Waterman MR. Regulation of the synthesis of steroidogenic enzymes in adrenal cortical cells by ACTH. Annu Rev Physiol 1988; 50:427-440.

190. Chrousos GP, Gold PW. The concepts of stress and stress system disorders. Overview of physical and behavioral homeostasis. JAMA 1992; 267:1244-1252.

191. Bush IE, Ferguson KA. The secretion of the adrenal cortex in the sheep. J Endocrinol 1953; 10:1-8.

192. Simmons RM, Satterfield MC, Welsh TH, Jr., Bazer FW, Spencer TE. HSD11B1, HSD11B2, PTGS2, and NR3C1 expression in the peri-implantation ovine uterus: effects of pregnancy, progesterone, and interferon tau. Biol Reprod 2010; 82:35-43.

193. Wachter R, Masarik L, Burzle M, Mallik A, von Mandach U. Differential expression and activity of 11beta-hydroxysteroid dehydrogenase in human placenta and fetal membranes from pregnancies with intrauterine growth restriction. Fetal Diagn Ther 2009; 25:328-335.

194. Wyrwoll CS, Seckl JR, Holmes MC. Altered placental function of 11beta-hydroxysteroid dehydrogenase 2 knockout mice. Endocrinology 2009; 150:1287-1293.

195. Shams M, Kilby MD, Somerset DA, Howie AJ, Gupta A, Wood PJ, Afnan M, Stewart PM. 11Beta-hydroxysteroid dehydrogenase type 2 in human pregnancy and reduced expression in intrauterine growth restriction. Hum Reprod 1998; 13:799-804.

196. Brooks K, Burns G, Moraes JGN, Spencer TE. Analysis of the Uterine Epithelial Transcriptome and Luminal Fluid Proteome During the Peri-implantation Period of Pregnancy in Sheep. Biol Reprod 2016; In review.

197. Michael AE, Thurston LM, Rae MT. Glucocorticoid metabolism and reproduction: a tale of two enzymes. Reproduction 2003; 126:425-441.

198. Evans RM, Hollenberg SM. Cooperative and positional independent trans-activation domains of the human glucocorticoid receptor. Cold Spring Harb Symp Quant Biol 1988; 53 Pt 2:813-818.

199. Giguere V, Hollenberg SM, Rosenfeld MG, Evans RM. Functional domains of the human glucocorticoid receptor. Cell 1986; 46:645-652.

200. Hollenberg SM, Evans RM. Multiple and cooperative trans-activation domains of the human glucocorticoid receptor. Cell 1988; 55:899-906.

201. Kumar R, Thompson EB. The structure of the nuclear hormone receptors. Steroids 1999; 64:310-319.

202. Kumar R, Thompson EB. Gene regulation by the glucocorticoid receptor: structure:function relationship. J Steroid Biochem Mol Biol 2005; 94:383-394.

203. Pratt WB, Toft DO. Steroid receptor interactions with heat shock protein and immunophilin chaperones. Endocr Rev 1997; 18:306-360.

204. Dittmar KD, Pratt WB. Folding of the glucocorticoid receptor by the reconstituted Hsp90-based chaperone machinery. The initial hsp90.p60.hsp70-dependent step is sufficient for creating the steroid binding conformation. J Biol Chem 1997; 272:13047-13054.

205. Dittmar KD, Demady DR, Stancato LF, Krishna P, Pratt WB. Folding of the glucocorticoid receptor by the heat shock protein (hsp) 90-based chaperone machinery. The role of p23 is to stabilize receptor.hsp90 heterocomplexes formed by hsp90.p60.hsp70. J Biol Chem 1997; 272:21213-21220.

206. Hawle P, Siepmann M, Harst A, Siderius M, Reusch HP, Obermann WM. The middle domain of Hsp90 acts as a discriminator between different types of client proteins. Mol Cell Biol 2006; 26:8385-8395.

207. Starr DB, Matsui W, Thomas JR, Yamamoto KR. Intracellular receptors use a common mechanism to interpret signaling information at response elements. Genes Dev 1996; 10:1271-1283.

208. Smirnov AN. Nuclear receptors: nomenclature, ligands, mechanisms of their effects on gene expression. Biochemistry (Mosc) 2002; 67:957-977.

209. Jenkins BD, Pullen CB, Darimont BD. Novel glucocorticoid receptor coactivator effector mechanisms. Trends Endocrinol Metab 2001; 12:122-126.

210. Deroo BJ, Archer TK. Glucocorticoid receptor-mediated chromatin remodeling in vivo. Oncogene 2001; 20:3039-3046.

211. Morrison N, Eisman J. Role of the negative glucocorticoid regulatory element in glucocorticoid repression of the human osteocalcin promoter. J Bone Miner Res 1993; 8:969-975.

212. Sakai DD, Helms S, Carlstedt-Duke J, Gustafsson JA, Rottman FM, Yamamoto KR. Hormone-mediated repression: a negative glucocorticoid response element from the bovine prolactin gene. Genes Dev 1988; 2:1144-1154.

213. Diamond MI, Miner JN, Yoshinaga SK, Yamamoto KR. Transcription factor interactions: selectors of positive or negative regulation from a single DNA element. Science 1990; 249:1266-1272.

214. Drouin J, Trifiro MA, Plante RK, Nemer M, Eriksson P, Wrange O. Glucocorticoid receptor binding to a specific DNA sequence is required for hormone-dependent repression of pro-opiomelanocortin gene transcription. Mol Cell Biol 1989; 9:5305-5314.

215. Drouin J, Sun YL, Nemer M. Glucocorticoid repression of pro-opiomelanocortin gene transcription. J Steroid Biochem 1989; 34:63-69.

216. Malkoski SP, Handanos CM, Dorin RI. Localization of a negative glucocorticoid response element of the human corticotropin releasing hormone gene. Mol Cell Endocrinol 1997; 127:189-199.

217. Webster JC, Cidlowski JA. Mechanisms of Glucocorticoid-receptor-mediated Repression of Gene Expression. Trends Endocrinol Metab 1999; 10:396-402.

218. Konig H, Ponta H, Rahmsdorf HJ, Herrlich P. Interference between pathway-specific transcription factors: glucocorticoids antagonize phorbol ester-induced AP-1 activity without altering AP-1 site occupation in vivo. EMBO J 1992; 11:2241-2246.

219. Schule R, Rangarajan P, Kliewer S, Ransone LJ, Bolado J, Yang N, Verma IM, Evans RM. Functional antagonism between oncoprotein c-Jun and the glucocorticoid receptor. Cell 1990; 62:1217-1226.

220. McKay LI, Cidlowski JA. Molecular control of immune/inflammatory responses: interactions between nuclear factor-kappa B and steroid receptor-signaling pathways. Endocr Rev 1999; 20:435-459.

221. Quenby S, Kalumbi C, Bates M, Farquharson R, Vince G. Prednisolone reduces preconceptual endometrial natural killer cells in women with recurrent miscarriage. Fertil Steril 2005; 84:980-984.

222. Quenby S, Farquharson R. Uterine natural killer cells, implantation failure and recurrent miscarriage. Reprod Biomed Online 2006; 13:24-28.

223. Langdown ML, Sugden MC. Enhanced placental GLUT1 and GLUT3 expression in dexamethasone-induced fetal growth retardation. Mol Cell Endocrinol 2001; 185:109-117.

224. Jones HN, Ashworth CJ, Page KR, McArdle HJ. Cortisol stimulates system A amino acid transport and SNAT2 expression in a human placental cell line (BeWo). Am J Physiol Endocrinol Metab 2006; 291:E596-603.

225. Mandl M, Ghaffari-Tabrizi N, Haas J, Nohammer G, Desoye G. Differential glucocorticoid effects on proliferation and invasion of human trophoblast cell lines. Reproduction 2006; 132:159-167.

226. Gharraee Z, Beharry KD, Valencia AM, Cho S, Guajardo L, Nageotte MP, Modanlou HD. Effects of antenatal betamethasone on maternal and fetoplacental matrix metalloproteinases 2 and 9 activities in human singleton pregnancies. J Investig Med 2006; 54:245-254.

227. Imseis HM, Zimmerman PD, Samuels P, Kniss DA. Tumour necrosis factor-alpha induces cyclo-oxygenase-2 gene expression in first trimester trophoblasts: suppression by glucocorticoids and NSAIDs. Placenta 1997; 18:521-526.

228. Librach CL, Feigenbaum SL, Bass KE, Cui TY, Verastas N, Sadovsky Y, Quigley JP, French DL, Fisher SJ. Interleukin-1 beta regulates human cytotrophoblast metalloproteinase activity and invasion in vitro. J Biol Chem 1994; 269:17125-17131.

229. Ma Y, Ryu JS, Dulay A, Segal M, Guller S. Regulation of plasminogen activator inhibitor (PAI)-1 expression in a human trophoblast cell line by glucocorticoid (GC) and transforming growth factor (TGF)-beta. Placenta 2002; 23:727-734.

230. Crocker IP, Barratt S, Kaur M, Baker PN. The in-vitro characterization of induced apoptosis in placental cytotrophoblasts and syncytiotrophoblasts. Placenta 2001; 22:822-830.

231. Gur C, Diav-Citrin O, Shechtman S, Arnon J, Ornoy A. Pregnancy outcome after first trimester exposure to corticosteroids: a prospective controlled study. Reprod Toxicol 2004; 18:93-101.

232. Michael AE, Papageorghiou AT. Potential significance of physiological and pharmacological glucocorticoids in early pregnancy. Hum Reprod Update 2008; 14:497-517.

233. Boomsma CM, Keay SD, Macklon NS. Peri-implantation glucocorticoid administration for assisted reproductive technology cycles. Cochrane Database Syst Rev 2007:CD005996.

234. Boomsma CM, Keay SD, Macklon NS. Peri-implantation glucocorticoid administration for assisted reproductive technology cycles. Cochrane Database Syst Rev 2012; 6:CD005996.

235. Braun T, Li S, Moss TJ, Newnham JP, Challis JR, Gluckman PD, Sloboda DM. Maternal betamethasone administration reduces binucleate cell number and placental lactogen in sheep. J Endocrinol 2007; 194:337-347.

236. Deshaies Y, Dagnault A, Lalonde J, Richard D. Interaction of corticosterone and gonadal steroids on lipid deposition in the female rat. Am J Physiol 1997; 273:E355-362.

237. Mittelstadt PR, Galon J, Franchimont D, O'Shea JJ, Ashwell JD. Glucocorticoid-inducible genes that regulate T-cell function. Ernst Schering Res Found Workshop 2002:319-339.

238. Galon J, Franchimont D, Hiroi N, Frey G, Boettner A, Ehrhart-Bornstein M, O'Shea JJ, Chrousos GP, Bornstein SR. Gene profiling reveals unknown enhancing and suppressive actions of glucocorticoids on immune cells. FASEB J 2002; 16:61-71.

239. Whirledge SD, Oakley RH, Myers PH, Lydon JP, DeMayo F, Cidlowski JA. Uterine glucocorticoid receptors are critical for fertility in mice through control of embryo implantation and decidualization. Proc Natl Acad Sci U S A 2015; 112:15166-15171.

240. Summerton J, Weller D. Morpholino antisense oligomers: design, preparation, and properties. Antisense Nucleic Acid Drug Dev 1997; 7:187-195.

241. Summerton JE. Morpholino, siRNA, and S-DNA compared: impact of structure and mechanism of action on off-target effects and sequence specificity. Curr Top Med Chem 2007; 7:651-660.

242. Morcos PA. Achieving efficient delivery of morpholino oligos in cultured cells. Genesis 2001; 30:94-102.

243. Li YF, Morcos PA. Design and synthesis of dendritic molecular transporter that achieves efficient in vivo delivery of morpholino antisense oligo. Bioconjug Chem 2008; 19:1464-1470.

244. Dunlap KA, Palmarini M, Varela M, Burghardt RC, Hayashi K, Farmer JL, Spencer TE. Endogenous retroviruses regulate periimplantation placental growth and differentiation. Proc Natl Acad Sci U S A 2006; 103:14390-14395.

245. Wang X, Frank JW, Little DR, Dunlap KA, Satterfield MC, Burghardt RC, Hansen TR, Wu G, Bazer FW. Functional role of arginine during the peri-implantation period of pregnancy. I. Consequences of loss of function of arginine transporter SLC7A1 mRNA in ovine conceptus trophectoderm. FASEB J 2014; 28:2852-2863.

246. Gullapalli R, Wong A, Brigham E, Kwong G, Wadsworth A, Willits C, Quinn K, Goldbach E, Samant B. Development of ALZET(R) osmotic pump compatible solvent compositions to solubilize poorly soluble compounds for preclinical studies. Drug Deliv 2012; 19:239-246.

247. Theeuwes F, Yum SI. Principles of the design and operation of generic osmotic pumps for the delivery of semisolid or liquid drug formulations. Ann Biomed Eng 1976; 4:343-353.

248. Summerton JE. Endo-Porter: a novel reagent for safe, effective delivery of substances into cells. Ann N Y Acad Sci 2005; 1058:62-75.

249. Meister G, Tuschl T. Mechanisms of gene silencing by double-stranded RNA. Nature 2004; 431:343-349.

250. Hannon GJ, Rossi JJ. Unlocking the potential of the human genome with RNA interference. Nature 2004; 431:371-378.

251. Matranga C, Tomari Y, Shin C, Bartel DP, Zamore PD. Passenger-strand cleavage facilitates assembly of siRNA into Ago2-containing RNAi enzyme complexes. Cell 2005; 123:607-620.

252. Smart N, Scambler PJ, Riley PR. A rapid and sensitive assay for quantification of siRNA efficiency and specificity. Biol Proced Online 2005; 7:1-7.

253. Birmingham A, Anderson E, Sullivan K, Reynolds A, Boese Q, Leake D, Karpilow J, Khvorova A. A protocol for designing siRNAs with high functionality and specificity. Nat Protoc 2007; 2:2068-2078.

254. Manjunath N, Wu H, Subramanya S, Shankar P. Lentiviral delivery of short hairpin RNAs. Adv Drug Deliv Rev 2009; 61:732-745.

255. Van den Haute C, Eggermont K, Nuttin B, Debyser Z, Baekelandt V. Lentiviral vector-mediated delivery of short hairpin RNA results in persistent knockdown of gene expression in mouse brain. Hum Gene Ther 2003; 14:1799-1807.

256. Georgiades P, Cox B, Gertsenstein M, Chawengsaksophak K, Rossant J. Trophoblast-specific gene manipulation using lentivirus-based vectors. Biotechniques 2007; 42:317-318, 320, 322-315.

257. Lois C, Hong EJ, Pease S, Brown EJ, Baltimore D. Germline transmission and tissue-specific expression of transgenes delivered by lentiviral vectors. Science 2002; 295:868-872.

258. Hofmann A, Kessler B, Ewerling S, Weppert M, Vogg B, Ludwig H, Stojkovic M, Boelhauve M, Brem G, Wolf E, Pfeifer A. Efficient transgenesis in farm animals by lentiviral vectors. EMBO Rep 2003; 4:1054-1060.

259. Sliva K, Schnierle BS. Selective gene silencing by viral delivery of short hairpin RNA. Virol J 2010; 7:248.

260. Lee DS, Rumi MA, Konno T, Soares MJ. In vivo genetic manipulation of the rat trophoblast cell lineage using lentiviral vector delivery. Genesis 2009; 47:433-439.

261. Marraffini LA, Sontheimer EJ. CRISPR interference: RNA-directed adaptive immunity in bacteria and archaea. Nat Rev Genet 2010; 11:181-190.

262. Bolotin A, Quinquis B, Sorokin A, Ehrlich SD. Clustered regularly interspaced short palindrome repeats (CRISPRs) have spacers of extrachromosomal origin. Microbiology 2005; 151:2551-2561.

263. Jinek M, Chylinski K, Fonfara I, Hauer M, Doudna JA, Charpentier E. A programmable dual-RNA-guided DNA endonuclease in adaptive bacterial immunity. Science 2012; 337:816-821.

264. Porteus MH, Baltimore D. Chimeric nucleases stimulate gene targeting in human cells. Science 2003; 300:763.

265. Miller JC, Holmes MC, Wang J, Guschin DY, Lee YL, Rupniewski I, Beausejour CM, Waite AJ, Wang NS, Kim KA, Gregory PD, Pabo CO, et al. An improved zinc-finger nuclease architecture for highly specific genome editing. Nat Biotechnol 2007; 25:778-785.

266. Christian M, Cermak T, Doyle EL, Schmidt C, Zhang F, Hummel A, Bogdanove AJ, Voytas DF. Targeting DNA double-strand breaks with TAL effector nucleases. Genetics 2010; 186:757-761.

267. Sanjana NE, Cong L, Zhou Y, Cunniff MM, Feng G, Zhang F. A transcription activator-like effector toolbox for genome engineering. Nat Protoc 2012; 7:171-192.

268. Gasiunas G, Barrangou R, Horvath P, Siksnys V. Cas9-crRNA ribonucleoprotein complex mediates specific DNA cleavage for adaptive immunity in bacteria. Proc Natl Acad Sci U S A 2012; 109:E2579-2586.

269. Garneau JE, Dupuis ME, Villion M, Romero DA, Barrangou R, Boyaval P, Fremaux C, Horvath P, Magadan AH, Moineau S. The CRISPR/Cas bacterial immune system cleaves bacteriophage and plasmid DNA. Nature 2010; 468:67-71.

270. Urnov FD, Rebar EJ, Holmes MC, Zhang HS, Gregory PD. Genome editing with engineered zinc finger nucleases. Nat Rev Genet 2010; 11:636-646.

271. Sander JD, Joung JK. CRISPR-Cas systems for editing, regulating and targeting genomes. Nat Biotechnol 2014; 32:347-355.

272. Perez EE, Wang J, Miller JC, Jouvenot Y, Kim KA, Liu O, Wang N, Lee G, Bartsevich VV, Lee YL, Guschin DY, Rupniewski I, et al. Establishment of HIV-1 resistance in CD4+ T cells by genome editing using zinc-finger nucleases. Nat Biotechnol 2008; 26:808-816.

273. Cong L, Ran FA, Cox D, Lin S, Barretto R, Habib N, Hsu PD, Wu X, Jiang W, Marraffini LA, Zhang F. Multiplex genome engineering using CRISPR/Cas systems. Science 2013; 339:819-823.

274. Chen F, Pruett-Miller SM, Huang Y, Gjoka M, Duda K, Taunton J, Collingwood TN, Frodin M, Davis GD. High-frequency genome editing using ssDNA oligonucleotides with zinc-finger nucleases. Nat Methods 2011; 8:753-755.

275. Saleh-Gohari N, Helleday T. Conservative homologous recombination preferentially repairs DNA double-strand breaks in the S phase of the cell cycle in human cells. Nucleic Acids Res 2004; 32:3683-3688.

276. Sapranauskas R, Gasiunas G, Fremaux C, Barrangou R, Horvath P, Siksnys V. The Streptococcus thermophilus CRISPR/Cas system provides immunity in Escherichia coli. Nucleic Acids Res 2011; 39:9275-9282.

277. Hsu PD, Scott DA, Weinstein JA, Ran FA, Konermann S, Agarwala V, Li Y, Fine EJ, Wu X, Shalem O, Cradick TJ, Marraffini LA, et al. DNA targeting specificity of RNA-guided Cas9 nucleases. Nat Biotechnol 2013; 31:827-832.

278. Fu Y, Foden JA, Khayter C, Maeder ML, Reyon D, Joung JK, Sander JD. High-frequency off-target mutagenesis induced by CRISPR-Cas nucleases in human cells. Nat Biotechnol 2013; 31:822-826.

279. Tan W, Proudfoot C, Lillico SG, Whitelaw CB. Gene targeting, genome editing: from Dolly to editors. Transgenic Res 2016.

280. DeMayo FJ, Spencer TE, Editors-in-Chief BoR. CRISPR bacon: a sizzling technique to generate genetically engineered pigs. Biol Reprod 2014; 91:79.

281. Terns RM, Terns MP. CRISPR-based technologies: prokaryotic defense weapons repurposed. Trends Genet 2014; 30:111-118.

282. Ran FA, Hsu PD, Wright J, Agarwala V, Scott DA, Zhang F. Genome engineering using the CRISPR-Cas9 system. Nat Protoc 2013; 8:2281-2308.

283. Farin CE, Imakawa K, Hansen TR, McDonnell JJ, Murphy CN, Farin PW, Roberts RM. Expression of trophoblastic interferon genes in sheep and cattle. Biol Reprod 1990; 43:210-218.

284. Anthony RV, Helmer SD, Sharif SF, Roberts RM, Hansen PJ, Thatcher WW, Bazer FW. Synthesis and processing of ovine trophoblast protein-1 and bovine trophoblast protein-1, conceptus secretory proteins involved in the maternal recognition of pregnancy. Endocrinology 1988; 123:1274-1280.

285. Marcus GJ. Prostaglandin formation by the sheep embryo and endometrium as an indication of maternal recognition of pregnancy. Biol Reprod 1981; 25:56-64.

286. Roberts RM, Xie S, Mathialagan N. Maternal recognition of pregnancy. Biol Reprod 1996; 54:294-302.

287. Thatcher WW, Hansen PJ, Gross TS, Helmer SD, Plante C, Bazer FW. Antiluteolytic effects of bovine trophoblast protein-1. J Reprod Fertil Suppl 1989; 37:91-99.

288. Bazer FW, Spencer TE, Johnson GA. Interferons and uterine receptivity. Semin Reprod Med 2009; 27:90-102.

289. Bauersachs S, Mitko K, Ulbrich SE, Blum H, Wolf E. Transcriptome studies of bovine endometrium reveal molecular profiles characteristic for specific stages of estrous cycle and early pregnancy. Exp Clin Endocrinol Diabetes 2008; 116:371-384.

290. Hansen TR, Austin KJ, Perry DJ, Pru JK, Teixeira MG, Johnson GA. Mechanism of action of interferon-tau in the uterus during early pregnancy. J Reprod Fertil 1999; 54:329-339.

291. Bazan JF. Structural design and molecular evolution of a cytokine receptor superfamily. Proc Natl Acad Sci U S A 1990; 87:6934-6938.

292. Stewart MD, Johnson GA, Vyhlidal CA, Burghardt RC, Safe SH, Yu-Lee LY, Bazer FW, Spencer TE. Interferon-tau activates multiple signal transducer and activator of transcription proteins and has complex effects on interferon-responsive gene transcription in ovine endometrial epithelial cells. Endocrinology 2001; 142:98-107.

293. Han CS, Mathialagan N, Klemann SW, Roberts RM. Molecular cloning of ovine and bovine type I interferon receptor subunits from uteri, and endometrial expression of messenger ribonucleic acid for ovine receptors during the estrous cycle and pregnancy. Endocrinology 1997; 138:4757-4767.

294. Imakawa K, Tamura K, Lee RS, Ji Y, Kogo H, Sakai S, Christenson RK. Temporal expression of type I interferon receptor in the peri-implantation ovine extra-embryonic membranes: demonstration that human IFNalpha can bind to this receptor. Endocr J 2002; 49:195-205.

295. Wang XL, Wang K, Han GC, Zeng SM. A potential autocrine role for interferon tau in ovine trophectoderm. Reprod Domest Anim 2013; 48:819-825.

296. Bazer FW, Roberts RM, Basha SM, Zavy MT, Caton D, Barron DH. Method for obtaining ovine uterine secretions from unilaterally pregnant ewes. J Anim Sci 1979; 49:1522-1527.

297. Summerton J, Stein D, Huang SB, Matthews P, Weller D, Partridge M. Morpholino and phosphorothioate antisense oligomers compared in cell-free and in-cell systems. Antisense Nucleic Acid Drug Dev 1997; 7:63-70.

298. Wang X, Frank JW, Little DR, Dunlap KA, Carey Satterfield M, Burghardt RC, Hansen TR, Wu G, Bazer FW. Functional role of arginine during the peri-implantation period of pregnancy. I. Consequences of loss of function of arginine transporter SLC7A1 mRNA in ovine conceptus trophectoderm. FASEB J 2014.

299. Gerdes J, Schwab U, Lemke H, Stein H. Production of a mouse monoclonal antibody reactive with a human nuclear antigen associated with cell proliferation. Int J Cancer 1983; 31:13-20.

300. Li X, Traganos F, Melamed MR, Darzynkiewicz Z. Single-step procedure for labeling DNA strand breaks with fluorescein- or BODIPY-conjugated deoxynucleotides: detection of apoptosis and bromodeoxyuridine incorporation. Cytometry 1995; 20:172-180.

301. Gavrieli Y, Sherman Y, Ben-Sasson SA. Identification of programmed cell death in situ via specific labeling of nuclear DNA fragmentation. J Cell Biol 1992; 119:493-501.

302. Wang X, Ying W, Dunlap KA, Lin G, Satterfield MC, Burghardt RC, Wu G, Bazer FW. Arginine Decarboxylase and Agmatinase: An Alternative Pathway for De Novo Biosynthesis of Polyamines for Development of Mammalian Conceptuses. Biol Reprod 2014.

303. Leese HJ, Baumann CG, Brison DR, McEvoy TG, Sturmey RG. Metabolism of the viable mammalian embryo: quietness revisited. Mol Hum Reprod 2008; 14:667-672.

304. Young LE, Sinclair KD, Wilmut I. Large offspring syndrome in cattle and sheep. Rev Reprod 1998; 3:155-163.

305. Rizos D, Ward F, Duffy P, Boland MP, Lonergan P. Consequences of bovine oocyte maturation, fertilization or early embryo development in vitro versus in vivo: implications for blastocyst yield and blastocyst quality. Molecular reproduction and development 2002; 61:234-248.

306. Reik W, Romer I, Barton SC, Surani MA, Howlett SK, Klose J. Adult phenotype in the mouse can be affected by epigenetic events in the early embryo. Development 1993; 119:933-942.

307. Schwartzman RA, Cidlowski JA. Apoptosis: the biochemistry and molecular biology of programmed cell death. Endocr Rev 1993; 14:133-151.

308. Bortner CD, Oldenburg NB, Cidlowski JA. The role of DNA fragmentation in apoptosis. Trends Cell Biol 1995; 5:21-26.

309. Hernandez-Ledezma JJ, Sikes JD, Murphy CN, Watson AJ, Schultz GA, Roberts RM. Expression of bovine trophoblast interferon in conceptuses derived by in vitro techniques. Biol Reprod 1992; 47:374-380.

310. Hernandez-Ledezma JJ, Mathialagan N, Villanueva C, Sikes JD, Roberts RM. Expression of bovine trophoblast interferons by in vitro-derived blastocysts is correlated with their morphological quality and stage of development. Mol Reprod Dev 1993; 36:1-6.

311. Bartol FF, Roberts RM, Bazer FW, Lewis GS, Godkin JD, Thatcher WW. Characterization of proteins produced in vitro by periattachment bovine conceptuses. Biol Reprod 1985; 32:681-693.

312. Kubisch HM, Larson MA, Roberts RM. Relationship between age of blastocyst formation and interferon-tau secretion by in vitro-derived bovine embryos. Mol Reprod Dev 1998; 49:254-260.

313. Kubisch HM, Sirisathien S, Bosch P, Hernandez-Fonseca HJ, Clements G, Liukkonen JR, Brackett BG. Effects of developmental stage, embryonic interferon-tau secretion and recipient synchrony on pregnancy rate after transfer of in vitro produced bovine blastocysts. Reprod Domest Anim 2004; 39:120-124.

314. Bauersachs S, Ulbrich SE, Reichenbach HD, Reichenbach M, Buttner M, Meyer HH, Spencer TE, Minten M, Sax G, Winter G, Wolf E. Comparison of the effects of early pregnancy with human interferon, alpha 2 (IFNA2), on gene expression in bovine endometrium. Biol Reprod 2012; 86:46.

315. Bazer FW, Wu G, Spencer TE, Johnson GA, Burghardt RC, Bayless K. Novel pathways for implantation and establishment and maintenance of pregnancy in mammals. Mol Hum Reprod 2010; 16:135-152.

316. Bauersachs S, Ulbrich SE, Zakhartchenko V, Minten M, Reichenbach M, Reichenbach HD, Blum H, Spencer TE, Wolf E. The endometrium responds differently to cloned versus fertilized embryos. Proc Natl Acad Sci U S A 2009; 106:5681-5686.

317. Mansouri-Attia N, Sandra O, Aubert J, Degrelle S, Everts RE, Giraud-Delville C, Heyman Y, Galio L, Hue I, Yang X, Tian XC, Lewin HA, et al. Endometrium as an early sensor of in vitro embryo manipulation technologies. Proc Natl Acad Sci U S A 2009; 106:5687-5692.

318. Forde N, Carter F, Spencer TE, Bazer FW, Sandra O, Mansouri-Attia N, Okumu LA, McGettigan PA, Mehta JP, McBride R, O'Gaora P, Roche JF, et al. Conceptus-induced changes in the endometrial transcriptome: how soon does the cow know she is pregnant? Biol Reprod 2011; 85:144-156.

319. Ott TL, Gifford CA. Effects of early conceptus signals on circulating immune cells: lessons from domestic ruminants. Am J Reprod Immunol 2010; 64:245-254.

320. Johnson GA, Spencer TE, Hansen TR, Austin KJ, Burghardt RC, Bazer FW. Expression of the interferon tau inducible ubiquitin cross-reactive protein in the ovine uterus. Biol Reprod 1999; 61:312-318.

321. Johnson GA, Spencer TE, Burghardt RC, Joyce MM, Bazer FW. Interferon-tau and progesterone regulate ubiquitin cross-reactive protein expression in the ovine uterus. Biol Reprod 2000; 62:622-627.

322. Spencer TE, Forde N, Dorniak P, Hansen TR, Romero JJ, Lonergan P. Conceptus-derived prostaglandins regulate gene expression in the endometrium prior to pregnancy recognition in ruminants. Reproduction 2013; 146:377-387.

323. Hansen TR, Austin KJ, Perry DJ, Pru JK, Teixeira MG, Johnson GA. Mechanism of action of interferon-tau in the uterus during early pregnancy. J Reprod Fertil Suppl 1999; 54:329-339.

324. Bauersachs S, Wolf E. Immune aspects of embryo-maternal cross-talk in the bovine uterus. J Reprod Immunol 2013; 97:20-26.

325. Hansen TR, Pru JK. ISGylation: A Conserved Pathway in Mammalian Pregnancy. Adv Exp Med Biol 2014; 759:13-31.

326. Imakawa K, Imai M, Sakai A, Suzuki M, Nagaoka K, Sakai S, Lee SR, Chang KT, Echternkamp SE, Christenson RK. Regulation of conceptus adhesion by endometrial CXC chemokines during the implantation period in sheep. Mol Reprod Dev 2006.

327. Johnson GA, Austin KJ, Collins AM, Murdoch WJ, Hansen TR. Endometrial ISG17 mRNA and a related mRNA are induced by interferon-tau and localized to glandular epithelial and stromal cells from pregnant cows. Endocrine 1999; 10:243-252.

328. Uze G, Lutfalla G, Mogensen KE. Alpha and beta interferons and their receptor and their friends and relations. J Interferon Cytokine Res 1995; 15:3-26.

329. Lamken P, Gavutis M, Peters I, Van der Heyden J, Uze G, Piehler J. Functional cartography of the ectodomain of the type I interferon receptor subunit ifnar1. J Mol Biol 2005; 350:476-488.

330. de Weerd NA, Vivian JP, Nguyen TK, Mangan NE, Gould JA, Braniff SJ, Zaker-Tabrizi L, Fung KY, Forster SC, Beddoe T, Reid HH, Rossjohn J, et al. Structural basis of a unique interferon-beta signaling axis mediated via the receptor IFNAR1. Nat Immunol 2013; 14:901-907.

331. Kim S, Choi Y, Bazer FW, Spencer TE. Identification of genes in the ovine endometrium regulated by interferon tau independent of signal transducer and activator of transcription 1. Endocrinology 2003; 144:5203-5214.

332. Choi Y, Johnson GA, Spencer TE, Bazer FW. Pregnancy and interferon tau regulate MHC class I and beta-2-microglobulin expression in the ovine uterus. Biol Reprod 2003; 68:1703-1710.

333. Lee J, Stanley JA, McCracken JA, Banu SK, Arosh JA. Intrauterine Co-Administration of ERK1/2 Inhibitor U0126 Inhibits Interferon TAU Action in the Endometrium and Restores Luteolytic PGF2alpha Pulses in Sheep. Biol Reprod 2014.

334. Johnson GA, Burghardt RC, Newton GR, Bazer FW, Spencer TE. Development and characterization of immortalized ovine endometrial cell lines. Biol Reprod 1999; 61:1324-1330.

335. Johnson GA, Stewart MD, Gray CA, Choi Y, Burghardt RC, Yu-Lee LY, Bazer FW, Spencer TE. Effects of the estrous cycle, pregnancy, and interferon tau on 2',5'-oligoadenylate synthetase expression in the ovine uterus. Biol Reprod 2001; 64:1392-1399.

336. Arnaud F, Black SG, Murphy L, Griffiths DJ, Neil SJ, Spencer TE, Palmarini M. Interplay between ovine bone marrow stromal cell antigen 2/tetherin and endogenous retroviruses. J Virol 2010; 84:4415-4425.

337. Joyce MM, White FJ, Burghardt RC, Muniz JJ, Spencer TE, Bazer FW, Johnson GA. Interferon stimulated gene 15 conjugates to endometrial cytosolic proteins and is expressed at the uterine-placental interface throughout pregnancy in sheep. Endocrinology 2005; 146:675-684.

338. Hue I, Degrelle SA, Turenne N. Conceptus elongation in cattle: genes, models and questions. Anim Reprod Sci 2012; 134:19-28.

339. Wang J, Guillomot M, Hue I. Cellular organization of the trophoblastic epithelium in elongating conceptuses of ruminants. Comptes rendus biologies 2009; 332:986-997.

340. Simmons RM, Erikson DW, Kim J, Burghardt RC, Bazer FW, Johnson GA, Spencer TE. Insulin-like growth factor binding protein-1 in the ruminant uterus: potential endometrial marker and regulator of conceptus elongation. Endocrinology 2009; 150:4295-4305.

341. Desmarais JA, Lopes FL, Zhang H, Das SK, Murphy BD. The peroxisome proliferator-activated receptor gamma regulates trophoblast cell differentiation in mink (Mustela vison). Biol Reprod 2007; 77:829-839.

342. Barak Y, Liao D, He W, Ong ES, Nelson MC, Olefsky JM, Boland R, Evans RM. Effects of peroxisome proliferator-activated receptor Î´ on placentation, adiposity, and colorectal cancer. Proc Natl Acad Sci U S A 2002; 99:303-308.

343. Nadra K, Anghel SI, Joye E, Tan NS, Basu-Modak S, Trono D, Wahli W, Desvergne B. Differentiation of Trophoblast Giant Cells and Their Metabolic Functions Are Dependent on Peroxisome Proliferator-Activated Receptor {beta}/{delta}. Mol. Cell. Biol. 2006; 26:3266-3281.

344. Van Heeke G, Ott TL, Strauss A, Ammaturo D, Bazer FW. High yield expression and secretion of the ovine pregnancy recognition hormone interferon-tau by Pichia pastoris. J Interferon Cytokine Res 1996; 16:119-126.

345. Zhang Y, Liu T, Meyer CA, Eeckhoute J, Johnson DS, Bernstein BE, Nusbaum C, Myers RM, Brown M, Li W, Liu XS. Model-based analysis of ChIP-Seq (MACS). Genome Biol 2008; 9:R137.

346. Bailey TL, Boden M, Buske FA, Frith M, Grant CE, Clementi L, Ren J, Li WW, Noble WS. MEME SUITE: tools for motif discovery and searching. Nucleic Acids Res 2009; 37:W202-208.

347. Chen J, Bardes EE, Aronow BJ, Jegga AG. ToppGene Suite for gene list enrichment analysis and candidate gene prioritization. Nucleic Acids Res 2009; 37:W305-311.

348. Summerton J, Weller D. Morpholino antisense oligomers: design, preparation, and properties. Antisense Nucleic Acid Drug Dev 1997; 7:187-195.

349. Tontonoz P, Hu E, Graves RA, Budavari AI, Spiegelman BM. mPPAR gamma 2: tissue-specific regulator of an adipocyte enhancer. Genes Dev 1994; 8:1224-1234.

350. Chen F, Law SW, O'Malley BW. Identification of two mPPAR related receptors and evidence for the existence of five subfamily members. Biochem Biophys Res Commun 1993; 196:671-677.

351. Xie SC, Low BG, Nagel RJ, Kramer KK, Anthony RV, Zoli AP, Beckers JF, Roberts RM. Identification of the major pregnancy-specific antigens of cattle and sheep as inactive members of the aspartic proteinase family. Proc Natl Acad Sci U S A 1991; 88:10247-10251.

352. Desvergne B, Wahli W. Peroxisome proliferator-activated receptors: nuclear control of metabolism. Endocr Rev 1999; 20:649-688.

353. Sinclair KD, Rooke JA, McEvoy TG. Regulation of nutrient uptake and metabolism in pre-elongation ruminant embryos. Reprod Suppl 2003; 61:371-385.

354. Petters RM, Johnson BH, Reed ML, Archibong AE. Glucose, glutamine and inorganic phosphate in early development of the pig embryo in vitro. J Reprod Fertil 1990; 89:269-275.

355. Riley JK, Moley KH. Glucose utilization and the PI3-K pathway: mechanisms for cell survival in preimplantation embryos. Reproduction 2006; 131:823-835.

356. Wales RG, Waugh EE. Catabolic utilization of glucose by the sheep conceptus between days 13 and 19 of pregnancy. Reprod Fertil Dev 1993; 5:111-122.

357. Bazer FW, Kim J, Ka H, Johnson GA, Wu G, Song G. Select nutrients in the uterine lumen of sheep and pigs affect conceptus development. J Reprod Dev 2012; 58:180-188.

358. Gao H, Wu G, Spencer TE, Johnson GA, Bazer FW. Select Nutrients in the Ovine Uterine Lumen. IV. Expression of Neutral and Acidic Amino Acid Transporters in Ovine Uteri and Periimplantation Conceptuses. Biol Reprod 2009.

359. Foretz M, Pacot C, Dugail I, Lemarchand P, Guichard C, Le Liepvre X, Berthelier-Lubrano C, Spiegelman B, Kim JB, Ferre P, Foufelle F. ADD1/SREBP-1c is required in the activation of hepatic lipogenic gene expression by glucose. Mol Cell Biol 1999; 19:3760-3768.

360. Foretz M, Guichard C, Ferre P, Foufelle F. Sterol regulatory element binding protein-1c is a major mediator of insulin action on the hepatic expression of glucokinase and lipogenesis-related genes. Proc Natl Acad Sci U S A 1999; 96:12737-12742.

361. Rosen ED, Sarraf P, Troy AE, Bradwin G, Moore K, Milstone DS, Spiegelman BM, Mortensen RM. PPAR gamma is required for the differentiation of adipose tissue in vivo and in vitro. Mol Cell 1999; 4:611-617.

362. Kim JB, Wright HM, Wright M, Spiegelman BM. ADD1/SREBP1 activates PPARgamma through the production of endogenous ligand. Proc Natl Acad Sci U S A 1998; 95:4333-4337.

363. Sapin V, Dolle P, Hindelang C, Kastner P, Chambon P. Defects of the chorioallantoic placenta in mouse RXRalpha null fetuses. Dev Biol 1997; 191:29-41.

364. Carnegie JA, McCully ME, Robertson HA. The early development of the sheep trophoblast and the involvement of cell death. Am J Anat 1985; 174:471-488.

365. Carnegie JA, McCully ME, Robertson HA. The early development of the sheep trophoblast and the involvement of cell death. Am J Anat 1985; 174:471-488.

366. Galhardo M, Sinkkonen L, Berninger P, Lin J, Sauter T, Heinaniemi M. Integrated analysis of transcript-level regulation of metabolism reveals disease-relevant nodes of the human metabolic network. Nucleic Acids Res 2014; 42:1474-1496.

367. McEvoy TG, Coull GD, Broadbent PJ, Hutchinson JS, Speake BK. Fatty acid composition of lipids in immature cattle, pig and sheep oocytes with intact zona pellucida. J Reprod Fertil 2000; 118:163-170.

368. Dennis EA. Diversity of group types, regulation, and function of phospholipase A2. J Biol Chem 1994; 269:13057-13060.

369. Wang H, Dey SK. Lipid signaling in embryo implantation. Prostaglandins Other Lipid Mediat 2005; 77:84-102.

370. Eto M, Shindou H, Koeberle A, Harayama T, Yanagida K, Shimizu T. Lysophosphatidylcholine acyltransferase 3 is the key enzyme for incorporating arachidonic acid into glycerophospholipids during adipocyte differentiation. Int J Mol Sci 2012; 13:16267-16280.

371. Yen CL, Stone SJ, Cases S, Zhou P, Farese RV, Jr. Identification of a gene encoding MGAT1, a monoacylglycerol acyltransferase. Proc Natl Acad Sci U S A 2002; 99:8512-8517.

372. Fournier T, Guibourdenche J, Handschuh K, Tsatsaris V, Rauwel B, Davrinche C, Evain-Brion D. PPARgamma and human trophoblast differentiation. J Reprod Immunol 2011; 90:41-49.

373. Santos JE, Thatcher WW, Chebel RC, Cerri RL, Galvao KN. The effect of embryonic death rates in cattle on the efficacy of estrus synchronization programs. Anim Reprod Sci 2004; 82-83:513-535.

374. Tan W, Carlson DF, Lancto CA, Garbe JR, Webster DA, Hackett PB, Fahrenkrug SC. Efficient nonmeiotic allele introgression in livestock using custom endonucleases. Proc Natl Acad Sci U S A 2013; 110:16526-16531.

375. Hai T, Teng F, Guo R, Li W, Zhou Q. One-step generation of knockout pigs by zygote injection of CRISPR/Cas system. Cell Res 2014; 24:372-375.

376. Spencer TE, Bazer FW. Uterine and placental factors regulating conceptus growth in domestic animals. J Anim Sci 2004; 82 E-Suppl:E4-13.

377. A I, Jeannin E, Wahli W, Desvergne B. Polarity and specific sequence requirements of peroxisome proliferator-activated receptor (PPAR)/retinoid X receptor heterodimer binding to DNA. A functional analysis of the malic enzyme gene PPAR response element. J Biol Chem 1997; 272:20108-20117.

378. Satterfield MC, Song G, Kochan KJ, Riggs PK, Simmons RM, Elsik CG, Adelson DL, Bazer FW, Zhou H, Spencer TE. Discovery of candidate genes and pathways in the endometrium regulating ovine blastocyst growth and conceptus elongation. Physiological genomics 2009; 39:85-99.

379. Wang H, Yang H, Shivalila CS, Dawlaty MM, Cheng AW, Zhang F, Jaenisch R. One-step generation of mice carrying mutations in multiple genes by CRISPR/Cas-mediated genome engineering. Cell 2013; 153:910-918.

380. Brooks K, Spencer TE. Biological Roles of Interferon Tau (IFNT) and Type I IFN Receptors in Elongation of the Ovine Conceptus. Biol Reprod 2015; 92:47.

381. Brooks KE, Burns GW, Spencer TE. Peroxisome Proliferator Activator Receptor Gamma (PPARG) Regulates Conceptus Elongation in Sheep. Biol Reprod 2015; 92:42.

382. Choi Y, Johnson GA, Spencer TE, Bazer FW. Pregnancy and interferon tau regulate major histocompatibility complex class I and beta2-microglobulin expression in the ovine uterus. Biol Reprod 2003; 68:1703-1710.

383. Ott TL, Yin J, Wiley AA, Kim HT, Gerami-Naini B, Spencer TE, Bartol FF, Burghardt RC, Bazer FW. Effects of the estrous cycle and early pregnancy on uterine expression of Mx protein in sheep (Ovis aries). Biol Reprod 1998; 59:784-794.

384. Wiedenheft B, Sternberg SH, Doudna JA. RNA-guided genetic silencing systems in bacteria and archaea. Nature 2012; 482:331-338.

385. Terns MP, Terns RM. CRISPR-based adaptive immune systems. Curr Opin Microbiol 2011; 14:321-327.

386. Sapolsky RM, Romero LM, Munck AU. How do glucocorticoids influence stress responses? Integrating permissive, suppressive, stimulatory, and preparative actions. Endocr Rev 2000; 21:55-89.

387. Hayashi R, Wada H, Ito K, Adcock IM. Effects of glucocorticoids on gene transcription. Eur J Pharmacol 2004; 500:51-62.

388. Buckingham JC. Glucocorticoids: exemplars of multi-tasking. Br J Pharmacol 2006; 147 Suppl 1:S258-268.

389. Reichardt HM, Kaestner KH, Wessely O, Gass P, Schmid W, Schutz G. Analysis of glucocorticoid signalling by gene targeting. J Steroid Biochem Mol Biol 1998; 65:111-115.

390. Fowden AL, Szemere J, Hughes P, Gilmour RS, Forhead AJ. The effects of cortisol on the growth rate of the sheep fetus during late gestation. J Endocrinol 1996; 151:97-105.

391. Waddell BJ, Hisheh S, Dharmarajan AM, Burton PJ. Apoptosis in rat placenta is zone-dependent and stimulated by glucocorticoids. Biol Reprod 2000; 63:1913-1917.

392. Alfaidy N, Li W, MacIntosh T, Yang K, Challis J. Late gestation increase in 11beta-hydroxysteroid dehydrogenase 1 expression in human fetal membranes: a novel intrauterine source of cortisol. J Clin Endocrinol Metab 2003; 88:5033-5038.

393. Wei C, Liu J, Yu Z, Zhang B, Gao G, Jiao R. TALEN or Cas9 - rapid, efficient and specific choices for genome modifications. J Genet Genomics 2013; 40:281-289.

394. Huang WL, Beazley LD, Quinlivan JA, Evans SF, Newnham JP, Dunlop SA. Effect of corticosteroids on brain growth in fetal sheep. Obstet Gynecol 1999; 94:213-218.

395. Hardy DB, Yang K. The expression of 11 beta-hydroxysteroid dehydrogenase type 2 is induced during trophoblast differentiation: effects of hypoxia. J Clin Endocrinol Metab 2002; 87:3696-3701.

396. Edwards CR, Benediktsson R, Lindsay RS, Seckl JR. 11 beta-Hydroxysteroid dehydrogenases: key enzymes in determining tissue-specific glucocorticoid effects. Steroids 1996; 61:263-269.

397. Krozowski Z. The 11beta-hydroxysteroid dehydrogenases: functions and physiological effects. Mol Cell Endocrinol 1999; 151:121-127.

398. Benediktsson R, Edwards CR. 11 beta-Hydroxysteroid dehydrogenases: tissue-specific dictators of glucocorticoid action. Essays Biochem 1996; 31:23-36.

399. Burton PJ, Waddell BJ. Dual function of 11beta-hydroxysteroid dehydrogenase in placenta: modulating placental glucocorticoid passage and local steroid action. Biol Reprod 1999; 60:234-240.

400. Benediktsson R, Calder AA, Edwards CR, Seckl JR. Placental 11 beta-hydroxysteroid dehydrogenase: a key regulator of fetal glucocorticoid exposure. Clin Endocrinol (Oxf) 1997; 46:161-166.

401. Arcuri F, Sestini S, Paulesu L, Bracci L, Carducci A, Manzoni F, Cardone C, Cintorino M. 11Beta-hydroxysteroid dehydrogenase expression in first trimester human trophoblasts. Mol Cell Endocrinol 1998; 141:13-20.

402. Robert F, Hardy J. Cushing's disease: a correlation of radiological, surgical and pathological findings with therapeutic results. Pathol Res Pract 1991; 187:617-621.

403. Khatchadourian A, Maysinger D. Lipid droplets: their role in nanoparticle-induced oxidative stress. Mol Pharm 2009; 6:1125-1137.

404. Edwards CR, Benediktsson R, Lindsay RS, Seckl JR. Dysfunction of placental glucocorticoid barrier: link between fetal environment and adult hypertension? Lancet 1993; 341:355-357.

405. Holmes MC, Abrahamsen CT, French KL, Paterson JM, Mullins JJ, Seckl JR. The mother or the fetus? 11beta-hydroxysteroid dehydrogenase type 2 null mice provide evidence for direct fetal programming of behavior by endogenous glucocorticoids. J Neurosci 2006; 26:3840-3844.

406. Kajantie E, Dunkel L, Turpeinen U, Stenman UH, Andersson S. Placental 11beta-HSD2 activity, early postnatal clinical course, and adrenal function in extremely low birth weight infants. Pediatr Res 2006; 59:575-578.

407. Field T, Hernandez-Reif M, Diego M, Figueiredo B, Schanberg S, Kuhn C. Prenatal cortisol, prematurity and low birthweight. Infant Behav Dev 2006; 29:268-275.

408. Fire A, Xu S, Montgomery MK, Kostas SA, Driver SE, Mello CC. Potent and specific genetic interference by double-stranded RNA in Caenorhabditis elegans. Nature 1998; 391:806-811.

409. Hannon GJ. RNA interference. Nature 2002; 418:244-251.

410. Park F. Lentiviral vectors: are they the future of animal transgenesis? Physiol Genomics 2007; 31:159-173.

411. Okada Y, Ueshin Y, Isotani A, Saito-Fujita T, Nakashima H, Kimura K, Mizoguchi A, Oh-Hora M, Mori Y, Ogata M, Oshima RG, Okabe M, et al. Complementation of placental defects and embryonic lethality by trophoblast-specific lentiviral gene transfer. Nat Biotechnol 2007; 25:233-237.

412. Baker CM, Goetzmann LN, Cantlon JD, Jeckel KM, Winger QA, Anthony RV. The Development of Ovine Chorionic Somatomammotropin Hormone Deficienct Pregnancies. Am J Physiol Regul Integr Comp Physiol 2016:ajpregu 00311 02015.

413. Yuan B, Latek R, Hossbach M, Tuschl T, Lewitter F. siRNA Selection Server: an automated siRNA oligonucleotide prediction server. Nucleic Acids Res 2004; 32:W130-134.

414. Kiem HP, Wu RA, Sun G, von Laer D, Rossi JJ, Trobridge GD. Foamy combinatorial anti-HIV vectors with MGMTP140K potently inhibit HIV-1 and SHIV replication and mediate selection in vivo. Gene Ther 2010; 17:37-49.

415. Hofmann A, Zakhartchenko V, Weppert M, Sebald H, Wenigerkind H, Brem G, Wolf E, Pfeifer A. Generation of transgenic cattle by lentiviral gene transfer into oocytes. Biol Reprod 2004; 71:405-409.

416. Purcell SH, Cantlon JD, Wright CD, Henkes LE, Seidel GE, Jr., Anthony RV. The involvement of proline-rich 15 in early conceptus development in sheep. Biol Reprod 2009; 81:1112-1121.

417. Baker CM, Goetzmann LN, Cantlon JD, Jeckel KM, Winger QA, Anthony RV. Development of ovine chorionic somatomammotropin hormone-deficient pregnancies. Am J Physiol Regul Integr Comp Physiol 2016; 310:R837-846.

418. Dann CT, Alvarado AL, Hammer RE, Garbers DL. Heritable and stable gene knockdown in rats. Proc Natl Acad Sci U S A 2006; 103:11246-11251.

419. van den Brandt J, Wang D, Kwon SH, Heinkelein M, Reichardt HM. Lentivirally generated eGFP-transgenic rats allow efficient cell tracking in vivo. Genesis 2004; 39:94-99.

420. Hewlett IK, Geyer SJ, Hawthorne CA, Ruta M, Epstein JS. Kinetics of early HIV-1 gene expression in infected H9 cells assessed by PCR. Oncogene 1991; 6:491-493.

421. Van Maele B, De Rijck J, De Clercq E, Debyser Z. Impact of the central polypurine tract on the kinetics of human immunodeficiency virus type 1 vector transduction. J Virol 2003; 77:4685-4694.

422. Zhang B, Metharom P, Jullie H, Ellem KA, Cleghorn G, West MJ, Wei MQ. The significance of controlled conditions in lentiviral vector titration and in the use of multiplicity of infection (MOI) for predicting gene transfer events. Genet Vaccines Ther 2004; 2:6.

423. Kissler S, Stern P, Takahashi K, Hunter K, Peterson LB, Wicker LS. In vivo RNA interference demonstrates a role for Nramp1 in modifying susceptibility to type 1 diabetes. Nat Genet 2006; 38:479-483.

424. Punzon I, Criado LM, Serrano A, Serrano F, Bernad A. Highly efficient lentiviral-mediated human cytokine transgenesis on the NOD/scid background. Blood 2004; 103:580-582.

425. Szulc J, Wiznerowicz M, Sauvain MO, Trono D, Aebischer P. A versatile tool for conditional gene expression and knockdown. Nat Methods 2006; 3:109-116.

426. Mohamedali A, Moreau-Gaudry F, Richard E, Xia P, Nolta J, Malik P. Self-inactivating lentiviral vectors resist proviral methylation but do not confer position-independent expression in hematopoietic stem cells. Mol Ther 2004; 10:249-259.

427. Pion M, Jordan A, Biancotto A, Dequiedt F, Gondois-Rey F, Rondeau S, Vigne R, Hejnar J, Verdin E, Hirsch I. Transcriptional suppression of in vitro-integrated human immunodeficiency virus type 1 does not correlate with proviral DNA methylation. J Virol 2003; 77:4025-4032.

428. Pannell D, Ellis J. Silencing of gene expression: implications for design of retrovirus vectors. Rev Med Virol 2001; 11:205-217.

429. Pannell D, Osborne CS, Yao S, Sukonnik T, Pasceri P, Karaiskakis A, Okano M, Li E, Lipshitz HD, Ellis J. Retrovirus vector silencing is de novo methylase independent and marked by a repressive histone code. EMBO J 2000; 19:5884-5894.

430. Jaenisch R, Harbers K, Jahner D, Stewart C, Stuhlmann H. DNA methylation, retroviruses, and embryogenesis. J Cell Biochem 1982; 20:331-336.

431. Hamra FK, Gatlin J, Chapman KM, Grellhesl DM, Garcia JV, Hammer RE, Garbers DL. Production of transgenic rats by lentiviral transduction of male germ-line stem cells. Proc Natl Acad Sci U S A 2002; 99:14931-14936.

432. McGrew MJ, Sherman A, Ellard FM, Lillico SG, Gilhooley HJ, Kingsman AJ, Mitrophanous KA, Sang H. Efficient production of germline transgenic chickens using lentiviral vectors. EMBO Rep 2004; 5:728-733.

433. Chapman SC, Lawson A, Macarthur WC, Wiese RJ, Loechel RH, Burgos-Trinidad M, Wakefield JK, Ramabhadran R, Mauch TJ, Schoenwolf GC. Ubiquitous GFP expression in transgenic chickens using a lentiviral vector. Development 2005; 132:935-940.

434. Hanna C, Long C, Westhusin M, Kraemer D. TRANSFECTION OF BOVINE OOCYTES AND PREIMPLANTATION EMBRYOS WITH COMMERCIAL TRANSFECTION REAGENTS: COMPARISON OF EMBRYONIC STAGE AND ZONA INTEGRITY ON TRANSFECTION EFFICIENCY. Biology of Reproduction 2007; 77:112.

435. Spencer TE. Biological roles of uterine glands in pregnancy. Semin Reprod Med 2014; 32:346-357.

436. Bazer FW, Song G, Kim J, Erikson DW, Johnson GA, Burghardt RC, Gao H, Carey Satterfield M, Spencer TE, Wu G. Mechanistic mammalian target of rapamycin (MTOR) cell signaling: effects of select nutrients and secreted phosphoprotein 1 on development of mammalian conceptuses. Mol Cell Endocrinol 2012; 354:22-33.

437. Koch JM, Ramadoss J, Magness RR. Proteomic profile of uterine luminal fluid from early pregnant ewes. J Proteome Res 2010; 9:3878-3885.

438. Burns G, Brooks K, Wildung M, Navakanitworakul R, Christenson LK, Spencer TE. Extracellular vesicles in luminal fluid of the ovine uterus. PLoS One 2014; 9:e90913.

439. Bazer FW, Spencer TE, Thatcher WW. Growth and development of the ovine conceptus. J Anim Sci 2012; 90:159-170.

440. Cummings M, McGinley CV, Wilkinson N, Field SL, Duffy SR, Orsi NM. A robust RNA integrity-preserving staining protocol for laser capture microdissection of endometrial cancer tissue. Analytical biochemistry 2011; 416:123-125.

441. Cunningham F, Amode MR, Barrell D, Beal K, Billis K, Brent S, Carvalho-Silva D, Clapham P, Coates G, Fitzgerald S, Gil L, Girón CG, et al. Ensembl 2015. Nucleic Acids Res 2015; 43:D662-669.

442. Li H, Handsaker B, Wysoker A, Fennell T, Ruan J, Homer N, Marth G, Abecasis G, Durbin R, 1000 Genome Project Data Processing Subgroup. The Sequence Alignment/Map format and SAMtools. Bioinformatics 2009; 25:2078-2079.

443. Quinlan AR. BEDTools: The Swiss-Army Tool for Genome Feature Analysis. Curr Protoc Bioinformatics 2014; 47:11.12.11-34.

444. Tabb DL. What's driving false discovery rates? J Proteome Res 2008; 7:45-46.

445. Bazer FW, Spencer TE, Johnson GA, Burghardt RC. Uterine receptivity to implantation of blastocysts in mammals. Front Biosci (Schol Ed) 2011; 3:745-767.

446. Satterfield MC, Song G, Kochan KJ, Riggs PK, Simmons RM, Elsik CG, Adelson DL, Bazer FW, Zhou H, Spencer TE. Discovery of candidate genes and pathways in the endometrium regulating ovine blastocyst growth and conceptus elongation. Physiol Genomics 2009; 39:85-99.

447. Ing NH, Roberts RM. The major progesterone-modulated proteins secreted into the sheep uterus are members of the serpin superfamily of serine protease inhibitors. J Biol Chem 1989; 264:3372-3379.

448. Stephenson DC, Leslie MV, Low BG, Newton GR, Hansen PJ, Bazer FW. Secretion of the major progesterone-induced proteins of the sheep uterus by caruncular and intercaruncular endometrium of the pregnant ewe from days 20-140 of gestation. Domest Anim Endocrinol 1989; 6:349-362.

449. Ing NH, Francis H, McDonnell JJ, Amann JF, Roberts RM. Progesterone induction of the uterine milk proteins: major secretory proteins of sheep endometrium. Biol Reprod 1989; 41:643-654.

450. Johnson GA, Burghardt RC, Bazer FW. Osteopontin: a leading candidate adhesion molecule for implantation in pigs and sheep. J Anim Sci Biotechnol 2014; 5:56.

451. Spencer TE, Hansen TR. Implantation and Establishment of Pregnancy in Ruminants. Adv Anat Embryol Cell Biol 2015; 216:105-135.

452. Thomas G. Furin at the cutting edge: from protein traffic to embryogenesis and disease. Nat Rev Mol Cell Biol 2002; 3:753-766.

453. Laursen LS, Overgaard MT, Soe R, Boldt HB, Sottrup-Jensen L, Giudice LC, Conover CA, Oxvig C. Pregnancy-associated plasma protein-A (PAPP-A) cleaves insulin-like growth factor binding protein (IGFBP)-5 independent of IGF: implications for the mechanism of IGFBP-4 proteolysis by PAPP-A. FEBS Lett 2001; 504:36-40.

454. Chiu WW, Chamley LW. Human seminal plasma prolactin-inducible protein is an immunoglobulin G-binding protein. J Reprod Immunol 2003; 60:97-111.

455. Hassan MI, Waheed A, Yadav S, Singh TP, Ahmad F. Prolactin inducible protein in cancer, fertility and immunoregulation: structure, function and its clinical implications. Cell Mol Life Sci 2009; 66:447-459.

456. Caputo E, Camarca A, Moharram R, Tornatore P, Thatcher B, Guardiola J, Martin BM. Structural study of GCDFP-15/gp17 in disease versus physiological conditions using a proteomic approach. Biochemistry 2003; 42:6169-6178.

457. Caputo E, Manco G, Mandrich L, Guardiola J. A novel aspartyl proteinase from apocrine epithelia and breast tumors. J Biol Chem 2000; 275:7935-7941.

458. Johnson GA, Bazer FW, Jaeger LA, Ka H, Garlow JE, Pfarrer C, Spencer TE, Burghardt RC. Muc-1, integrin, and osteopontin expression during the implantation cascade in sheep. Biol Reprod 2001; 65:820-828.

459. Mansouri-Attia N, Aubert J, Reinaud P, Giraud-Delville C, Taghouti G, Galio L, Everts RE, Degrelle S, Richard C, Hue I, Yang X, Tian XC, et al. Gene expression profiles of bovine caruncular and intercaruncular endometrium at implantation. Physiol Genomics 2009; 39:14-27.

460. Murray A, Sienerth AR, Hemberger M. Plet1 is an epigenetically regulated cell surface protein that provides essential cues to direct trophoblast stem cell differentiation. Sci Rep 2016; 6:25112.

461. Spencer TE, Bazer FW. Biology of progesterone action during pregnancy recognition and maintenance of pregnancy. Front Biosci 2002; 7:d1879-1898.

462. Bazer FW, Burghardt RC, Johnson GA, Spencer TE, Wu G. Interferons and progesterone for establishment and maintenance of pregnancy: interactions among novel cell signaling pathways. Reproductive biology 2008; 8:179-211.

463. Spencer TE, Bazer FW. Conceptus signals for establishment and maintenance of pregnancy. Reprod Biol Endocrinol 2004; 2:49.

464. Spencer TE, Ott TL, Bazer FW. Expression of interferon regulatory factors one and two in the ovine endometrium: effects of pregnancy and ovine interferon tau. Biol Reprod 1998; 58:1154-1162.

465. Sterchi EE, Stocker W, Bond JS. Meprins, membrane-bound and secreted astacin metalloproteinases. Mol Aspects Med 2008; 29:309-328.

466. Forde N, Lonergan P. Transcriptomic analysis of the bovine endometrium: What is required to establish uterine receptivity to implantation in cattle? J Reprod Dev 2012; 58:189-195.

467. Wagner L, Oliyarnyk O, Gartner W, Nowotny P, Groeger M, Kaserer K, Waldhausl W, Pasternack MS. Cloning and expression of secretagogin, a novel neuroendocrine- and pancreatic islet of Langerhans-specific Ca2+-binding protein. J Biol Chem 2000; 275:24740-24751.

468. Zelensky AN, Gready JE. The C-type lectin-like domain superfamily. FEBS J 2005; 272:6179-6217.

469. Brigstock DR. Regulation of angiogenesis and endothelial cell function by connective tissue growth factor (CTGF) and cysteine-rich 61 (CYR61). Angiogenesis 2002; 5:153-165.

470. Balmain N. Calbindin-D9k. A vitamin-D-dependent, calcium-binding protein in mineralized tissues. Clin Orthop Relat Res 1991:265-276.

471. Welt C, Sidis Y, Keutmann H, Schneyer A. Activins, inhibins, and follistatins: from endocrinology to signaling. A paradigm for the new millennium. Exp Biol Med (Maywood) 2002; 227:724-752.

472. O'Connell AR, McNatty KP, Hurst PR, Spencer TE, Bazer FW, Reader KL, Johnstone PD, Davis GH, Juengel JL. Activin A and follistatin during the oestrous cycle and early pregnancy in ewes. J Endocrinol 2016; 228:193-203.

473. Soleimanpour SA, Gupta A, Bakay M, Ferrari AM, Groff DN, Fadista J, Spruce LA, Kushner JA, Groop L, Seeholzer SH, Kaufman BA, Hakonarson H, et al. The diabetes susceptibility gene Clec16a regulates mitophagy. Cell 2014; 157:1577-1590.

474. Blomberg Le A, Garrett WM, Guillomot M, Miles JR, Sonstegard TS, Van Tassell CP, Zuelke KA. Transcriptome profiling of the tubular porcine conceptus

identifies the differential regulation of growth and developmentally associated genes. Mol Reprod Dev 2006; 73:1491-1502.

475. Glaser C, Heinrich J, Koletzko B. Role of FADS1 and FADS2 polymorphisms in polyunsaturated fatty acid metabolism. Metabolism 2010; 59:993-999.

476. Avis JM, Clarke PR. Ran, a GTPase involved in nuclear processes: its regulators and effectors. J Cell Sci 1996; 109 (Pt 10):2423-2427.

477. Cordin O, Banroques J, Tanner NK, Linder P. The DEAD-box protein family of RNA helicases. Gene 2006; 367:17-37.

478. Sowden J, Putt W, Morrison K, Beddington R, Edwards Y. The embryonic RNA helicase gene (ERH): a new member of the DEAD box family of RNA helicases. Biochem J 1995; 308 (Pt 3):839-846.

479. Mizuuchi M, Cindrova-Davies T, Olovsson M, Charnock-Jones DS, Burton GJ, Yung HW. Placental endoplasmic reticulum stress negatively regulates transcription of placental growth factor via ATF4 and ATF6beta: implications for the pathophysiology of human pregnancy complications. J Pathol 2016; 238:550-561.

480. Strumpf D, Mao CA, Yamanaka Y, Ralston A, Chawengsaksophak K, Beck F, Rossant J. Cdx2 is required for correct cell fate specification and differentiation of trophectoderm in the mouse blastocyst. Development 2005; 132:2093-2102.

481. Imakawa K, Kim MS, Matsuda-Minehata F, Ishida S, Iizuka M, Suzuki M, Chang KT, Echternkamp SE, Christenson RK. Regulation of the ovine interferon-tau gene by a blastocyst-specific transcription factor, Cdx2. Mol Reprod Dev 2006; 73:559-567.

482. Cross JC. Genetic insights into trophoblast differentiation and placental morphogenesis. Semin Cell Dev Biol 2000; 11:105-113.

483. Harris JR. Placental endogenous retrovirus (ERV): structural, functional, and evolutionary significance. Bioessays 1998; 20:307-316.

484. Mi S, Lee X, Li X, Veldman GM, Finnerty H, Racie L, LaVallie E, Tang XY, Edouard P, Howes S, Keith JC, Jr., McCoy JM. Syncytin is a captive retroviral envelope protein involved in human placental morphogenesis. Nature 2000; 403:785-789.

485. Frendo JL, Olivier D, Cheynet V, Blond JL, Bouton O, Vidaud M, Rabreau M, Evain-Brion D, Mallet F. Direct involvement of HERV-W Env glycoprotein in human trophoblast cell fusion and differentiation. Mol Cell Biol 2003; 23:3566-3574.

486. Dupressoir A, Vernochet C, Bawa O, Harper F, Pierron G, Opolon P, Heidmann T. Syncytin-A knockout mice demonstrate the critical role in placentation of a fusogenic, endogenous retrovirus-derived, envelope gene. Proc Natl Acad Sci U S A 2009; 106:12127-12132.

487. Dupressoir A, Vernochet C, Harper F, Guegan J, Dessen P, Pierron G, Heidmann T. A pair of co-opted retroviral envelope syncytin genes is required for formation of the two-layered murine placental syncytiotrophoblast. Proc Natl Acad Sci U S A 2011; 108:E1164-1173.

488. Cornelis G, Heidmann O, Degrelle SA, Vernochet C, Lavialle C, Letzelter C, Bernard-Stoecklin S, Hassanin A, Mulot B, Guillomot M, Hue I, Heidmann T, et al. Captured retroviral envelope syncytin gene associated with the unique placental structure of higher ruminants. Proc Natl Acad Sci U S A 2013; 110:E828-837.

489. Black SG, Arnaud F, Palmarini M, Spencer TE. Endogenous retroviruses in trophoblast differentiation and placental development. Am J Reprod Immunol 2010; 64:255-264.

490. Spencer TE, Mura M, Gray CA, Griebel PJ, Palmarini M. Receptor usage and fetal expression of ovine endogenous betaretroviruses: implications for coevolution of endogenous and exogenous retroviruses. J Virol 2003; 77:749-753.

491. Dunlap KA, Palmarini M, Adelson DL, Spencer TE. Sheep endogenous betaretroviruses (enJSRVs) and the hyaluronidase 2 (HYAL2) receptor in the ovine uterus and conceptus. Biol Reprod 2005; 73:271-279.

492. Armezzani A, Varela M, Spencer TE, Palmarini M, Arnaud F. "Menage a Trois": the evolutionary interplay between JSRV, enJSRVs and domestic sheep. Viruses 2014; 6:4926-4945.

493. Palmarini M, Mura M, Spencer TE. Endogenous betaretroviruses of sheep: teaching new lessons in retroviral interference and adaptation. J Gen Virol 2004; 85:1-13.

494. Dunlap KA, Palmarini M, Spencer TE. Ovine endogenous betaretroviruses (enJSRVs) and placental morphogenesis. Placenta 2006; 27 Suppl A:S135-140.

495. Diskin MG, Sreenan JM. Fertilization and embryonic mortality rates in beef heifers after artificial insemination. J Reprod Fertil %R 10.1530/jrf.0.0590463 1980; 59:463-468.

496. Spencer TE, Ott TL, Bazer FW. tau-Interferon: pregnancy recognition signal in ruminants. Proc Soc Exp Biol Med 1996; 213:215-229.

497. Bazer FW, Gao H, Johnson GA, Wu G, Bailey DW, Burghardt RC. Select nutrients and glucose transporters in pig uteri and conceptuses. Soc Reprod Fertil Suppl 2009; 66:335-336.

498. Ezashi T, Ealy AD, Ostrowski MC, Roberts RM. Control of interferon-tau gene expression by Ets-2. Proc Natl Acad Sci U S A 1998; 95:7882-7887.

499. Ezashi T, Ghosh D, Roberts RM. Repression of Ets-2-induced transactivation of the tau interferon promoter by Oct-4. Mol Cell Biol 2001; 21:7883-7891.

500. Yamaguchi H, Ikeda Y, Moreno JI, Katsumura M, Miyazawa T, Takahashi E, Imakawa K, Sakai S, Christenson RK. Identification of a functional transcriptional factor AP-1 site in the sheep interferon tau gene that mediates a response to PMA in JEG3 cells. Biochem J 1999; 340 (Pt 3):767-773.

501. Ezashi T, Das P, Gupta R, Walker A, Roberts RM. The role of homeobox protein distal-less 3 and its interaction with ETS2 in regulating bovine interferon-tau gene expression-synergistic transcriptional activation with ETS2. Biol Reprod 2008; 79:115-124.

502. Nishioka N, Yamamoto S, Kiyonari H, Sato H, Sawada A, Ota M, Nakao K, Sasaki H. Tead4 is required for specification of trophectoderm in pre-implantation mouse embryos. Mech Dev 2008; 125:270-283.

503. Russ AP, Wattler S, Colledge WH, Aparicio SA, Carlton MB, Pearce JJ, Barton SC, Surani MA, Ryan K, Nehls MC, Wilson V, Evans MJ. Eomesodermin is required for mouse trophoblast development and mesoderm formation. Nature 2000; 404:95-99.

504. Ellinwood WE, Nett TM, Niswender GD. Maintenance of the corpus luteum of early pregnancy in the ewe. II. Prostaglandin secretion by the endometrium in vitro and in vivo. Biol Reprod 1979; 21:845-856.

505. Kim S, Choi Y, Spencer TE, Bazer FW. Effects of the estrous cycle, pregnancy and interferon tau on expression of cyclooxygenase two (COX-2) in ovine endometrium. Reprod Biol Endocrinol 2003; 1:58.

506. El-Sayed A, Hoelker M, Rings F, Salilew D, Jennen D, Tholen E, Sirard M-A, Schellander K, Tesfaye D. Large-scale transcriptional analysis of bovine embryo biopsies in relation to pregnancy success after transfer to recipients. Physiol. Genomics 2006; 28:84-96.

507. Innis SM. Essential fatty acids in growth and development. Prog Lipid Res 1991; 30:39-103.

508. Nafikov RA, Beitz DC. Carbohydrate and lipid metabolism in farm animals. J Nutr 2007; 137:702-705.

509. Ribeiro ES, Gomes G, Greco LF, Cerri RL, Vieira-Neto A, Monteiro PL, Jr., Lima FS, Bisinotto RS, Thatcher WW, Santos JE. Carryover effect of postpartum inflammatory diseases on developmental biology and fertility in lactating dairy cows. J Dairy Sci 2016; 99:2201-2220.

510. Boshier DP, Fairclough RJ, Holloway H. Assessment of sheep blastocyst effects on neutral lipids in the uterine caruncular epithelium. J Reprod Fertil 1987; 79:569-573.

511. Burns PD, Engle TE, Harris MA, Enns RM, Whittier JC. Effect of fish meal supplementation on plasma and endometrial fatty acid composition in nonlactating beef cows. J Anim Sci 2003; 81:2840-2846.

512. Bilby TR, Jenkins T, Staples CR, Thatcher WW. Pregnancy, bovine somatotropin, and dietary n-3 fatty acids in lactating dairy cows: III. Fatty acid distribution. J Dairy Sci 2006; 89:3386-3399.

513. Wang JC, Derynck MK, Nonaka DF, Khodabakhsh DB, Haqq C, Yamamoto KR. Chromatin immunoprecipitation (ChIP) scanning identifies primary glucocorticoid receptor target genes. Proc Natl Acad Sci U S A 2004; 101:15603-15608.

514. Yamamoto KR. Steroid receptor regulated transcription of specific genes and gene networks. Annu Rev Genet 1985; 19:209-252.

515. Shang H, Meng W, Sloboda DM, Li S, Ehrlich L, Plagemann A, Dudenhausen JW, Henrich W, Newnham JP, Challis JR, Braun T. Effects of maternal dexamethasone treatment early in pregnancy on glucocorticoid receptors in the ovine placenta. Reprod Sci 2015; 22:534-544.

516. Lan ZJ, Gu P, Xu X, Cooney AJ. Expression of the orphan nuclear receptor, germ cell nuclear factor, in mouse gonads and preimplantation embryos. Biol Reprod 2003; 68:282-289.

VITA

Kelsey Brooks grew up outside of Seattle, WA with her parents Liz and Ron Brooks. She became interested in pursuing a career in science during high school and declared her major in Genetics and Cell Biology soon after enrolling at Washington State University (WSU) as an undergraduate. While at WSU she conducted undergraduate research in the lab of Dr. Kwan Hee Kim studying the effects of retinoic acid on testis development. Following graduate with a B.S. in 2010, Kelsey remained in Pullman, WA to work as a technician for Dr. John Nilson and Dr. Mary Hunzicker-Dunn. In 2012, Kelsey began work towards a PhD in the lab of Dr. Thomas Spencer in the department of Animal Science. Dr. Spencer relocated to the University of Missouri (MU) in the spring of 2015, and shortly after the lab at WSU joined him in Columbia, MO. There, Kelsey finished her studies and the requirements to earn a PhD from MU. Following completion of her PhD she will begin a postdoctoral position at the Oregon National Primate Research Center in Portland, OR. There she will have the opportunity to continue working on early embryonic development with Dr. Shawn Chavez, as well as remain close to her husband, Benjamin Holmesmith, and parents in the pacific northwest.